A&A 464, 211–227 (2007)
DOI: 10.1051/0004-6361:20066101
© ESO 2007

Astronomy & Astrophysics

Unveiling the Cygnus OB2 stellar population with Chandra⋆

J. F. Albacete Colombo[1], E. Flaccomio[1], G. Micela[1], S. Sciortino[1], and F. Damiani[1]

INAF – Osservatorio Astronomico di Palermo, Piazza del Parlamento 1, 90134 Palermo, Italy
e-mail: facundo@astropa.unipa.it

Received 25 July 2006 / Accepted 10 October 2006

ABSTRACT

Aims. The aim of this work is to identify the so far unknown low mass stellar population of the ∼2 Myr old Cygnus OB2 star forming region, and to investigate the X-ray and near-IR stellar properties of its members.
Methods. We analyzed a 97.7 ks *Chandra* ACIS-I observation pointed at the core of the Cygnus OB2 region. Sources were detected using the PWDETECT code and were positionally correlated with optical and near-IR catalogs from the literature. Source events were extracted with the Acis EXTRACT package. X-ray variability was characterized through the Kolmogorov-Smirnov test and spectra were fitted using absorbed thermal plasma models.
Results. We detected 1003 X-ray sources. Of these, 775 have near-IR counterparts and are expected to be almost all associated with Cygnus OB2 members. From near-IR color–color and color–magnitude diagrams we estimate a typical absorption toward Cygnus OB2 of $A_v \approx 7.0$ mag. Although the region is young, very few stars (∼4.4%) show disk-induced excesses in the near-IR. X-ray variability is detected in ∼13% of the sources, but this fraction increases, up to 50%, with increasing source statistics. Flares account for at least 60% of the variability. Despite being generally bright, all but 2 of the 26 detected O- that early B-type stars are not significantly variable. Typical X-ray spectral parameters are $\log N_H \sim 22.25$ (cm^{-2}) and $kT \sim 1.35$ keV with 1σ dispersion of 0.2 dex and 0.4 keV, respectively. Variable and flaring sources have harder spectra with median $kT = 3.3$ and 3.8 keV, respectively. OB stars are typically softer ($kT \sim 0.75$ keV). X-ray luminosities range between 10^{30} and 10^{31} erg s^{-1} for intermediate- and low-mass stars, and 2.5×10^{30} and between 6.3×10^{33} erg s^{-1} for OB stars.
Conclusions. The Cygnus OB2 region has a very rich population of low-mass X-ray emitting stars. Circumstellar disks seem to be very scarce. X-ray variability is related to the magnetic activity of low-mass stars ($M/M_\odot \sim 0.5$ to 3.0) display X-ray activity levels comparable to those of Orion Nebular Cluster (ONC) sources in the same mass range.

Key words. stars: formation – stars: early-type – stars: pre-main-sequence – X-rays: stars –
Galaxy: open clusters and associations: individual: Cygnus OB2

1. Introduction

The Cygnus OB2 association is one of the richest star forming regions in the Galaxy, containing a large population of O- and B-type stars, some of which are among the most massive stars known (Torres-Dodgen et al. 1991). For its richness Cygnus OB2 has been in the past considered a "young globular cluster" (Knödlseder 2000), although uncertainties remain on the real size of total cluster population (Hanson 2003). At a distance of 1.45 kpc (DM = 10.80, Hanson 2003), Cygnus OB2 lies behind the Great Cygnus Rift and is affected by large and non-uniform extinction, A_v: 5 to 15. Its distance and absorption have so far hindered optical studies of intermediate- and low- mass stars in the region. The position of known massive OB stars in the HR diagram of Cygnus OB2 suggests an age between 1 and 3 Myr, with ∼2 Myr as the most probable value (Massey & Thompson 1991; Knödlseder et al. 2002) .

The Cygnus OB2 region played a remarkable role in the history of stellar X-ray astronomy as an early X-ray observation, performed with the *Einstein* satellite and analyzed by Harnden et al. (1979), first revealed that early-type stars are intense X-ray emitters. This work was also the first to suggest the idea that X-rays in OB stars are produced in shocks within stellar winds, the starting point for the X-ray emission model of Lucy & White (1980). Subsequent *ROSAT*, *ASCA*, and *Chandra*-HETG observations of massive stars in the Cygnus OB2 region have improved our understanding of the mechanisms responsible for the X-ray emission of O-type stars (Waldron et al. 2004, 1998; Kitamoto & Mukai 1996).

These latter studies of the region have focused on the four most known OB-type stars of the region, Cyg#5, 8, 9, and 12, but have left the X-ray properties of the other high-, intermediate-, and low-mass stars in the region unexplored. Indeed the intermediate/low-mass population has not even been identified yet. Because of the much higher X-ray luminosity of young stars (e.g. $\log(L_x) \sim 30$–31 erg/s, for $M = 1.0$–$3.0\ M_\odot$) with respect to older field stars (e.g. Getman et al. 2005a), X-ray observations have proved an efficient tool to select likely members of young Star Forming Regions (SFR). Thanks to its high sensitivity and spatial resolution, the Advanced CCD Imaging Spectrometer (ACIS) camera on board the *Chandra* satellite (Garmire et al. 2003) is particularly suited for this kind of study in crowded stellar fields such as Cygnus OB2.

In this paper we present the analysis of a deep (∼97.7 ks) *Chandra* ACIS observation of Cygnus OB2. In Sect. 2 we introduce our X-ray observation and describe our data calibration and reduction procedure. In Sect. 3 we describe source detection, photon extraction and first characterization of X-ray spectra via hardness ratios. In Sect. 4 we characterize our sources by cross-identifying them with available optical and near-IR

⋆ Tables 1–3 are only available in electronic form at
http://www.aanda.org

Article published by EDP Sciences and available at http://www.aanda.org or http://dx.doi.org/10.1051/0004-6361:20066101

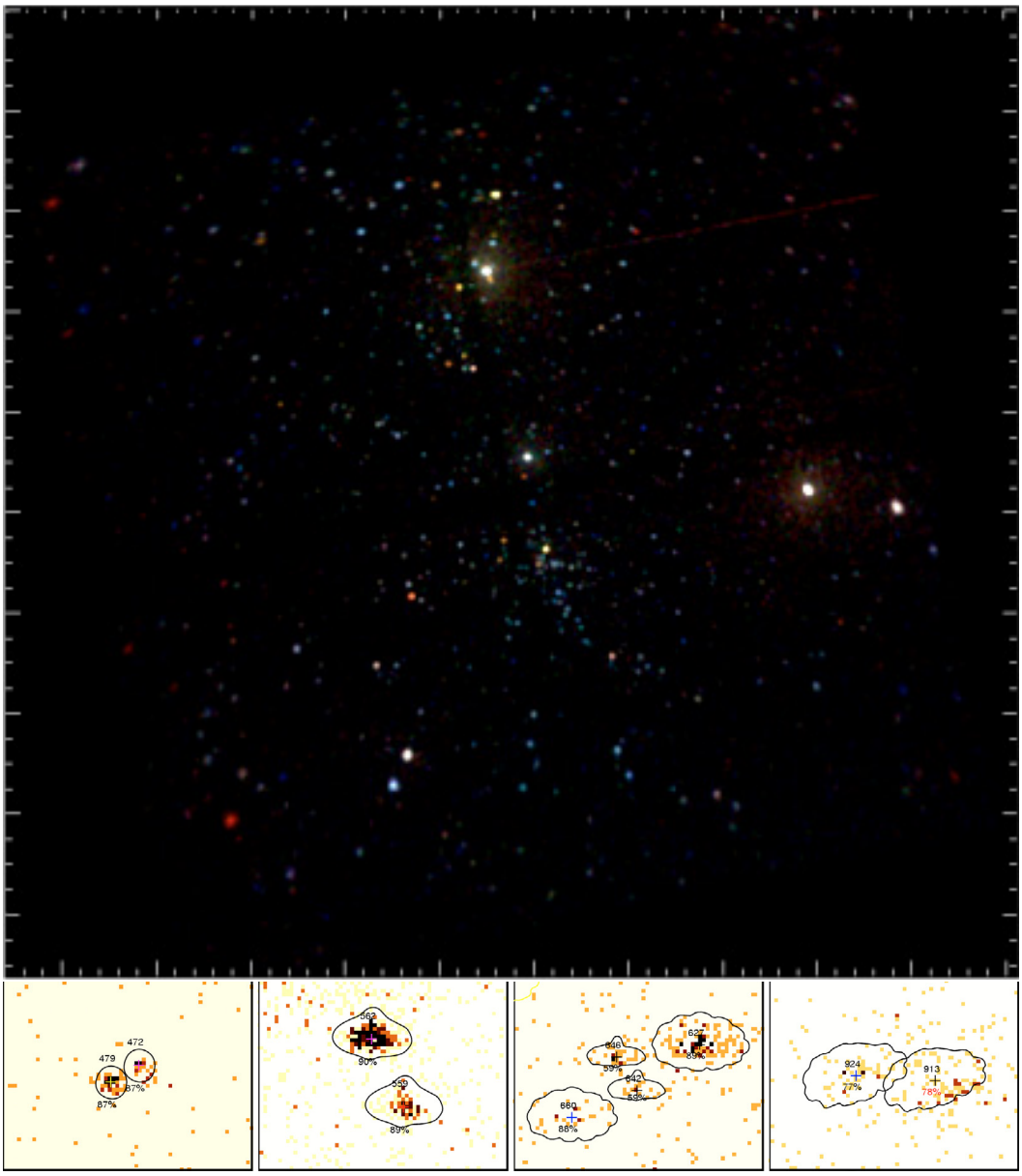

Fig. 1. *Upper panel*: color-coded ACIS-I image of the $17' \times 17'$ field in Cygnus OB2 (see color version in the electronic edition). Kernel smoothing was applied to highlight point sources. Energy bands for the RGB image are [0.5:1.7], [1.7:2.8], and [2.8:8.0] keV for the red, green, and blue colors, respectively. The four panels at the bottom show four $30'' \times 20''$ areas of the ACIS field at four different distances from the optical axis: *from left to right*: 0.7, 4.7, 5.4, and 7 arcmin. They illustrate the dependence of the PSF quality on off-axis and show (black continuous lines) the source photon extraction regions established with ACIS EXTRACT. Figures next to these contours indicate the source identification numbers (from Table 1) and the encircled energy fractions.

catalogs. Section 5 deals with X-ray variability while in Sect. 6 the results of the X-ray spectral analysis is presented. In Sect. 7 we discuss out results concerning the X-ray characteristics of high-, intermediate- and low-mass stars of the region. Finally, in Sect. 8 we summarize our results and draw our conclusions.

2. The X-ray observation

Cygnus OB2 was observed with the ACIS detector on board the *Chandra X-ray Observatory* (CXO) (Weisskopf et al. 2002) on 2004 January 16 (Obs.Id. 4511; PI: E. Flaccomio). The total exposure time was 97.7 ks. The data were acquired in VERY FAINT mode, to ease filtering of background events, with six CCD turned on, the four comprising the ACIS-I array [0, 1, 2, 3], plus CCDs 6 and 7, part of ACIS-S. However, data from the latter two CCDs will not be used in the following because of the much degraded point spread function (PSF) and reduced effective area resulting from their large distance from the optical axis. The ACIS-I $17' \times 17'$ field of view (FOV) is covered by 4 chips each with 1024×1024 pixels (scale $0.49''$ px^{-1}). The observation was pointed toward RA = $20^{\rm h}33^{\rm m}12.2^{\rm s}$ and Dec = $+41°15'00.7''$, chosen to maximize the number of stars in the FOV and to keep two source-dense regions close to the optical axis, where the PSF is sharper. Figure 1 shows Cygnus OB2 as seen in X-rays by our ACIS-I observation.

2.1. Data reduction

Data reduction, starting with the Level 1 event list provided by the pipeline processing at the CXO, was performed using

CIAO 3.2.2[1] and the CALDB 3.1.0 set of calibration files. We produced a level 2 event file using the ACIS_PROCESS_EVENT CIAO task, taking advantage of the VF-mode enhanced background filtering, and retaining only events with grades = 0, 2, 3, 4, 6 and status = 0. Photon energies were corrected for the time dependence of the energy gain using the CORR_TGAIN CIAO task. Intervals of background flaring were searched for, but none were found. We will hereafter assume a constant background. To improve the sensitivity to faint sources, given the spectrum of the background and that of typical sources, we filtered out events outside the [500:8000] eV energy band.

An exposure map, needed by the source detection algorithm and to renormalizes source count-rates, was calculated with the CIAO tool MKEXPMAP assuming a monochromatic spectrum (kT = 2.0 keV)[2].

3. Analysis

In this section we describe the first steps taken for the analysis of the ACIS-I data. We discuss the detection of X-ray point sources (Sect. 3.1), the definition of source and background event lists (Sect. 3.2), and a first spectral characterization of source spectra through hardness ratios (Sect. 3.3).

3.1. X-ray source detection

Source detection was performed with the Palermo Wavelet Detection code, PWDetect[3] (Damiani et al. 1997b), on the level 2 event list restricted to the [500:8000] eV energy band. PWDetect analyzes the data at different spatial scales, allowing the detection of both point-like and moderately extended sources, and efficiently resolving close sources pairs. The most important input parameter is the detection threshold (*SNR*), which we establish from the relationship between threshold, background level of the observation, and expected number of spurious detections due to Poisson noise, as determined from extensive simulations of source-free fields (cf. Damiani et al. 1997a). The background level was determined with the BACKGROUND command in the XIMAGE[4] package. The method amounts to dividing the image into equal-size boxes, discarding those that, according to several statistical criteria, are contaminated by sources, and finally computing the mean level of the remaining ones. We obtain that our ACIS-I observation comprises a total of about 1.58×10^5 background photons. This background level translates into a *SNR* threshold of 5.2 if we accept one spurious detection in the FOV, or into *SNR* > 4.5 if we accept 10 spurious detections. The first choice results in the detection of 868 sources and the second one in 1054 sources. By accepting an extra ∼9 spurious detections in the FOV we thus gain about 177 new reliable sources. Considering moreover that 10 spurious sources amounts to only ∼1% of the total number of detections, we decided to adopt the second less conservative criterion.

After a careful visual inspection of the initial source list, we rejected a total of 51 detections which we considered spurious: 39 were produced by different instrumental artifacts (i.e. out-of-time events, CCD gaps, detector edges, etc.) that were not included in the simulations of source-free fields used to establish the *SNR* threshold, but that are easily recognized. The remaining 12 were multiple detections of the same sources with different spatial scales[5]. In total, our final list of X-ray sources in the Cygnus OB2 region contains 1003 X-ray detections, 99% of which are expected to be real. The first 7 columns of Table 1 list, for each source: a running source number, name (according to CXC naming convention[6]), sky position (RA and Dec) with relative uncertainty, off-axis angle (θ), significance of the detection (Sig.).

3.2. Photon extraction

For further analysis of the detected sources, we used ACIS EXTRACT[7] (AE) v3.79 (Broos et al. 2002), an IDL based package that makes use of TARA[8], CIAO and FTOOLS[9].

The optimal extraction of point source photons is complicated by the non-Gaussian shape of the PSF and by its strong non-uniformity across the ACIS field of view. In particular the width and asymmetry of the PSF depend significantly on the off-axis distance (θ). The PSF is narrow and nearly circular in the inner $\theta \lesssim 5'$ but becomes rapidly broader and more asymmetric at larger off-axis, as demonstrated in the bottom panel of Fig. 1 where we show sources detected in our data at four different off-axis angles.

Extraction from circular regions containing a large fraction (e.g. 99%) of the PSF would guarantee to collect almost all source photons. However, given the extended wings of the PSF, very large regions would be needed, incurring in the risk of contamination from nearby sources, especially in crowded fields like ours. Moreover the resulting inclusion of a large number of background events would reduce the signal to noise of weak sources. On the other hand, extraction from regions that are too small may reduce the photon statistic for further spectral and timing analysis.

In order to tackle this problem, AE begins with calculating the shape of the model PSF at each source position using the CIAO task MKPSF. It then refines the initial source positions (in our case estimated by PWDetect assuming a symmetric PSF) by correlating the source images with the model PSFs. Following AE science hints[10], this last procedure was only used for those sources lying at off-axis larger than 5 arcmin (464 sources), while for the rest of the source (539 sources) we simply adopt data-mean positions. Coordinates listed in Table 1, as well as their 1σ uncertainties, are the result of this process. We verified that these positions are an improvement over those computed by PWDetect, especially at large off-axis angles, comparing the offsets between X-ray sources and counterparts in the 2MASS catalog (see Sect. 4.2).

After re-computing positions, AE defines source extraction regions as polygonal contours of the model PSF containing a specified fraction of source events ($f_{\rm PSF}$). Generally, we chose

[1] http://cxc.harvard.edu/ciao/

[2] http://asc.harvard.edu/ciao/download/doc/expmap_intro.ps

[3] See http://www.astropa.unipa.it/progetti_ricerca/PWDetect

[4] http://heasarc.nasa.gov/xanadu/ximage/ximage.html

[5] This effect occurred for only 3 sources at large off-axis angles, where the PSF is particularly elongated and thus significantly different from the symmetric PSF assumed by PWDetect. Note that, quite obviously, this effect is also not included in the simulations of source-free fields.

[6] http://cxc.harvard.edu/cdo/scipubs.html

[7] http://www.astro.psu.edu/xray/docs/TARA/ae_users_guide.html

[8] http://www.astro.psu.edu/xray/docs/TARA/

[9] http://heasarc.gsfc.nasa.gov/docs/software/ftools/

[10] http://www.astro.psu.edu/xray/docs/TARA/ae_users_guide/node35

Table 1. Cygnus OB2 X-ray source catalog: first 35 rows. The complete table, containing 1003 rows is available in the electronic edition of the journal.

N_x	NAME	RA	Dec	Error	θ	Sig.	Area	PSF	Cts	Exp. Time	Count Rates ($\times 10^{-3}$ ctn s^{-1})				$\overline{E}_x$	Var.
#	CXOCYG J+	[h:m:s]	[d:m:s]	($''$)	($'$)	(σ)	(px.)	(%)	(ph.)	(ks)	Tot.	Soft	Med.	Hard	(keV)	log(P_{ks})
1	203225.09+411019.6	20:32:25.09	41:10:19.60	0.62	10.03	6.55	1170	0.90	67	87.8255	0.855	0.135	0.233	0.487	3.23	−4.00 †
2	203225.55+410847.3	20:32:25.55	41:08:47.36	0.70	10.76	6.66	1429	0.89	72	92.9360	0.871	0.620	0.059	0.192	1.35	−0.65
3	203225.97+411054.7	20:32:25.97	41:10:54.77	0.75	9.62	4.28	973	0.90	35	90.9414	0.434	0.099	0.153	0.182	2.37	−0.32
4	203227.51+411358.3	20:32:27.52	41:13:58.37	0.88	8.47	2.30	630	0.89	14	92.5496	0.173	0.004	0.060	0.109	3.18	−0.17
5	203227.62+410831.4	20:32:27.63	41:08:31.46	0.76	10.61	5.92	1420	0.91	55	96.8402	0.637	0.160	0.198	0.278	2.36	−0.00
6	203227.70+411317.0	20:32:27.71	41:13:17.07	0.26	8.55	13.38	618	0.89	216	96.5481	2.521	0.529	0.862	1.130	2.61	−4.00 †
7	203228.88+410807.5	20:32:28.89	41:08:07.59	0.80	10.67	5.09	1623	0.90	49	96.6863	0.571	0.136	0.167	0.268	2.75	−2.37 †
8	203229.12+411400.7	20:32:29.12	41:14:00.78	0.55	8.16	4.09	545	0.89	33	92.8669	0.400	0.130	0.078	0.192	2.62	−0.59
9	203229.26+410850.1	20:32:29.26	41:08:50.17	0.59	10.17	6.70	834	0.82	64	92.6690	0.842	0.364	0.202	0.276	2.02	−0.44
10	203229.84+411454.2	20:32:29.85	41:14:54.27	0.50	7.97	5.56	525	0.90	50	93.3914	0.605	0.249	0.185	0.171	2.24	−0.67
11	203229.91+411056.0	20:32:29.92	41:10:56.06	0.72	8.94	2.77	751	0.90	19	92.9014	0.227	0.080	0.058	0.089	2.30	−0.97
12	203230.63+410829.1	20:32:30.64	41:08:29.11	0.58	10.19	8.52	1205	0.90	99	94.5473	1.173	0.320	0.478	0.375	2.14	−0.08
13	203230.63+410854.8	20:32:30.63	41:08:54.82	0.66	9.92	5.21	784	0.83	44	96.4507	0.552	0.067	0.180	0.305	2.93	−1.14 †
14	203230.88+411029.5	20:32:30.89	41:10:29.53	0.46	8.99	7.08	761	0.90	75	96.5167	0.867	0.063	0.176	0.628	3.42	−0.07
15	203231.39+410955.9	20:32:31.40	41:09:55.98	0.57	9.21	6.16	821	0.90	60	94.7546	0.714	0.259	0.168	0.287	2.27	−0.01
16	203231.42+411335.0	20:32:31.43	41:13:35.01	0.55	7.80	3.85	480	0.90	30	93.4071	0.357	0.039	0.098	0.220	3.01	−0.33
17	203231.53+411407.9	20:32:31.53	41:14:07.98	0.05	7.70	55.14	431	0.89	3173	97.6726	36.534	14.545	13.742	8.247	1.85	−2.83
18	203231.58+411712.5	20:32:31.58	41:17:12.52	0.73	7.95	2.01	517	0.90	12	92.8637	0.145	0.007	0.049	0.089	3.10	−0.04
19	203232.32+411507.3	20:32:32.32	41:15:07.30	0.56	7.50	3.55	418	0.89	25	94.0133	0.306	0.031	0.097	0.177	3.23	−0.02
20	203232.44+411312.3	20:32:32.45	41:13:12.36	0.43	7.69	5.60	413	0.89	49	93.2124	0.592	0.112	0.202	0.278	2.64	−2.69 †
21	203233.28+411058.8	20:32:33.29	41:10:58.88	0.75	8.36	2.82	575	0.90	18	88.3312	0.230	0.162	0.034	0.034	1.15	−0.44
22	203233.47+411218.0	20:32:33.48	41:12:18.04	0.49	7.77	4.49	459	0.90	34	91.7675	0.415	0.177	0.127	0.111	1.82	−0.04
23	203233.53+411405.7	20:32:33.54	41:14:05.74	0.38	7.33	5.47	364	0.90	50	95.7566	0.593	0.199	0.201	0.193	1.92	−0.49
24	203234.33+411506.3	20:32:34.34	41:15:06.33	0.54	7.12	3.71	350	0.90	26	94.3211	0.311	0.074	0.056	0.181	3.52	−0.44
25	203234.45+411154.7	20:32:34.45	41:11:54.74	0.58	7.75	3.96	446	0.90	27	94.8080	0.326	0.061	0.203	0.062	2.06	−0.26
26	203235.17+411143.4	20:32:35.18	41:11:43.48	0.47	7.70	4.97	430	0.90	39	91.6010	0.475	0.196	0.159	0.120	1.96	−0.03
27	203235.65+411509.5	20:32:35.65	41:15:09.50	0.33	6.88	7.09	312	0.90	70	96.3691	0.815	0.228	0.368	0.219	2.10	−1.17
28	203235.86+411248.4	20:32:35.87	41:12:48.42	0.37	7.18	5.22	340	0.90	43	93.8249	0.519	0.083	0.289	0.147	2.04	−2.14 †
29	203235.96+412135.6	20:32:35.97	41:21:35.64	0.78	9.47	4.51	669	0.83	33	95.8351	0.413	0.190	0.064	0.159	1.85	−0.11
30	203236.32+411900.7	20:32:36.32	41:19:00.76	0.47	7.84	4.96	489	0.90	41	94.6415	0.484	0.209	0.129	0.146	1.76	−0.44
31	203236.38+411831.0	20:32:36.39	41:18:31.08	0.62	7.59	3.81	403	0.89	26	90.0839	0.333	0.242	0.060	0.032	1.41	−1.46
32	203236.50+411810.3	20:32:36.50	41:18:10.36	0.67	7.42	3.78	376	0.89	26	91.6356	0.320	0.115	0.112	0.093	1.90	−1.55
33	203236.62+412214.5	20:32:36.63	41:22:14.52	0.26	9.85	14.02	689	0.81	232	97.5187	2.949	1.112	0.835	1.002	1.93	−4.00 †
34	203236.86+411944.6	20:32:36.86	41:19:44.62	0.40	8.16	7.22	544	0.90	74	97.0381	0.859	0.295	0.288	0.277	1.86	−0.83
35	203236.84+412146.1	20:32:36.85	41:21:46.11	0.56	9.48	5.65	660	0.83	46	95.1661	0.592	0.278	0.162	0.153	1.82	−1.24

Notes – †: flare-like sources.

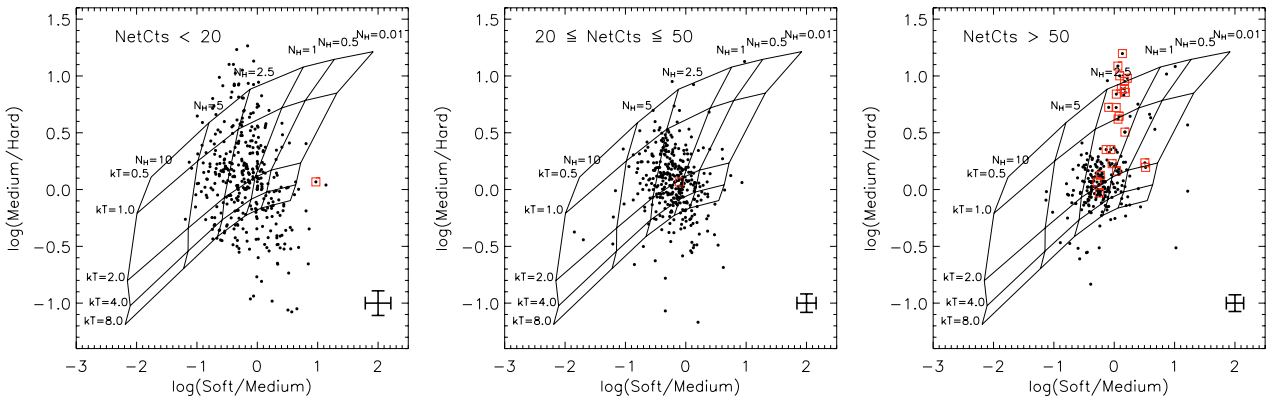

Fig. 2. X-ray color–color diagrams for our ACIS sources. The three panels refer to sources in three ranges of detected counts, as indicated in the upper-left corners. Colors are defined for three energy bands: *Soft* (0.5−1.7 keV), *Medium* (1.7−2.8 keV) and *Hard* (2.8−8.0 keV) keV. The grids refer to predicted colors for Raymond-Smith thermal emission models with different temperatures (kT = 0.5, 1.0, 2.0, 4.0, and 8.0 keV) and affected by varying amounts of absorption, $N_{\rm H}$ = 0.01, 0.5, 1.0, 2.5, 5, and 10×10^{22} cm^{-2}. Boxes refer to known O- and early B-type stars. Note that the dispersion of points is larger for low-statistics sources. Typical 1σ error bars are plotted in the right-bottom part of each panel.

$f_{\rm PSF}$ = 90%, and computed the contours from the PSF for a mono-energetic source with E = 1.49 keV. For ∼8% of the sources in the denser parts of the Cygnus OB2 field this fraction was reduced to avoid contamination with other nearby sources, in the most extreme cases down to $f_{\rm PSF} \sim 40\%$. The four panels at the bottom of Fig. 1 show examples of extraction regions. Otherwise, we have detected only six sources: Id.# 17, 60, 488, 544, 568, 729 that suffers of a pile-up fraction ($f_{\rm pile-up}$) of 3.96%, 17.7%, 11.6%, 2.39%, 15.6% and 4.6%, respectively. In these cases, we extracted events in annular regions that exclude the PSF cores for all sources that exhibits a $f_{\rm pile-up}$ greater than 2%. The inner radii was fixed at 2 arcsec[11], while the outer circles were choosen as the smallest that inscribe the $f_{\rm PSF}$ = 99% contours.

Although the ACIS-I instrumental background level is spatially quite uniform, the actual observed background varies substantially across the crowded Cygnus OB2 field due to the extended PSF wings of bright sources and to their readout trails. The background was therefore estimated locally for each source, adopting once again the automated procedure implemented in AE, which defines background extraction regions as circular annuli with inner radii 1.1 times the maximum distance between the source and the 99% PSF contour, and outer radii defined so that the regions contain more than 100 "background" events. In order to exclude contamination of the regions by nearby sources, background events are defined from a "swiss cheese" image that excludes events within the inner annuli radii of all the 1003 sources.

Results of the photon extraction procedure are listed in Cols. 8−16 of Table 1. We give: the source extraction area (Col. 8); the PSF fraction within the extraction area, assuming E = 1.49 keV (9); the background-corrected extracted source counts in the 0.5−8.0 keV band (10); the exposure time (11), the count rates (CR) in four spectral bands computed as the ratio between the source photons (corrected for $f_{\rm PSF}$) and the exposure time (12−15); the median photon energy ($\overline{E_{\rm x}}$), (16).

In summary, our 1003 X-ray detections span a wide count range, from 4 to ∼15 000 photons. Most sources are faint (e.g. 42% have less than 20 photons). The lower envelope of the counts vs. off-axis plot (not shown) indicates that the minimum number of photons necessary for detection ranges from 4 on axis to ∼20 close to the detector corners (θ = 10 arcmin).

3.3. X-ray hardness ratios

In order to characterize the X-ray spectra of low-statistic sources it is common practice to use the ratios of source counts in different spectral bands, i.e. X-ray hardness ratios (XHR), or the logarithm of these values which can be considered "X-ray colors" (Schulz et al. 1989; Prestwich et al. 2003).

We use this method, dividing the full energy range into three bands: Soft ($S_{\rm x}$: 0.5−1.7 keV), Medium ($M_{\rm x}$: 1.7−2.8 keV) and Hard ($H_{\rm x}$: 2.8−8.0 keV). Figure 2 shows, separately for sources in three detected counts ranges, the "Hard X-ray color" ($\log[M_{\rm x}/H_{\rm x}]$) vs. the "Soft X-ray color" ($\log[S_{\rm x}/M_{\rm x}]$). For reference we also plot the predicted loci for absorbed thermal sources with plasma temperatures between 0.5 and 8.0 keV and $N_{\rm H}$ between 10^{20} and 10^{23} cm^{-2}. The grid was calculated with the *Portable Interactive Multi-Mission Simulator* (PIMMS[12]) for a Raymond-Smith (RS) emission model (Raymond & Smith 1977).

A comparison of the three panels in Fig. 2 shows that the position of sources with respect to the $kT - N_{\rm H}$ grid is significantly affected, other than by the source spectra, by the source statistic. The positions of individual sources with less than 20 counts (left panel) are, for example, considerably spread out because of large statistical uncertainties. Sources with higher statistics (20 ≤ NetCnts ≤ 50, central panel) are more concentrated around $kT \sim 2.0$ keV and $N_{\rm H} \sim 2.3 \times 10^{22}$ cm^{-2}. Sources with more than 50 photons (right panel) are even more concentrated around these same values of kT and $N_{\rm H}$. A separate group of soft-spectrum sources however becomes visible in the upper part of the grid, with typical $kT \sim 0.8$ keV. Most of these sources are associated with known early type stars, indicated by squares in Fig. 2. Others, with somewhat smaller $N_{\rm H}$, are likely foreground stars as also argued in Sect. 4.2.

4. Optical and near-IR counterparts

Cygnus OB2 has been the target of numerous optical studies for more than 50 years (Johnson & Morgan 1954; Schulte 1958).

[11] http://www.astro.msfc.nasa.gov/Ch4/Ch4_15-03_Tsujimoto.pdf

[12] http://heasarc.gsfc.nasa.gov/docs/software/tools/pimms.html

Table 2. Near-IR counterparts of Cygnus OB2 X-ray sources and near-IR stellar parameters: first rows. The complete version is available in the electronic edition of the journal.

N_x	X-ray – 2MASS counterpart		Off.	2MASS photometry				$A_v^{\ddagger}$
#	CXOAC J+	2MASS J+	($''$)	J	H	K_s	Ph. qual†	(mag)
1	203225.09+411019.6	–	–	–	–	–	–	–
2	203225.55+410847.3	20322545+4108473	1.56	14.76 ± 0.06	14.23 ± 0.07	13.95 ± 0.07	AAA	8.54
3	203225.97+411054.7	20322597+4110547	0.24	15.24 ± 0.05	13.65 ± 0.03	12.69 ± 0.03	AAA	7.71
4	203227.51+411358.3	20322756+4114001	1.61	16.00 ± 0.06	14.46 ± 0.04	13.90 ± 0.06	AAA	0.16
5	203227.62+410831.4	20322754+4108336	2.41	15.91 ± 0.06	14.39 ± 0.03	13.82 ± 0.05	AAA	N/A
6	203227.70+411317.0	20322768+4113169	0.58	14.96 ± 0.03	13.49 ± 0.02	12.88 ± 0.03	AAA	2.21
7	203228.88+410807.5	–	–	–	–	–	–	–
8	203229.12+411400.7	20322913+4114012	0.26	16.74 ± 0.16	15.36 ± 0.08	14.72 ± 0.11	CAB	9.01
9	203229.26+410850.1	20322928+4108494	1.03	12.26 ± 0.01	11.49 ± 0.01	11.07 ± 0.01	AAA	8.52
10	203229.84+411454.2	20322985+4114536	0.83	17.44	15.43 ± 0.10	14.37 ± 0.09	UAA	N/A
11	203229.91+411056.0	20322994+4110575	1.29	15.26 ± 0.05	14.04 ± 0.04	13.53 ± 0.04	AAA	N/A
12	203230.63+410829.1	20323051+4108284	2.19	15.47 ± 0.07	13.71	13.09	AUU	4.19
13	203230.63+410854.8	20323064+4108565	1.49	15.31 ± 0.05	13.68 ± 0.03	13.01 ± 0.03	AAA	5.43
14	203230.88+411029.5	–	–	–	–	–	–	–
15	203231.39+410955.9	20323143+4109558	0.58	14.52 ± 0.05	13.04	12.46	AUU	9.69

† 2MASS photometric quality flags for the J, H and, K_s bands: "A" to "D" indicate decreasing quality of the measurements, "U" that the value is an upper limit. See 2MASS documentation for details. ‡N/A indicates stars with unconstrained A_v (see text).

Massey & Thompson (1991) identified 120 candidate massive members in an area of about 0.35 deg^2, on the basis of UBV photometry, and gave optical spectral classifications for over 70 OB stars. More recently, Hanson (2003) published new spectral classification for 14 more OB candidates, improving the massive star census of Cygnus OB2, and the estimates for its distance (1450 pc) and age (∼2 Myr). A total of 33 OB stars from the catalog of Hanson (2003) lie in the 0.0823 deg^2 FOV of our X-ray observation and were thus cross identified with our X-ray source list (Sect. 3.2). Due to the high and variable absorption in the Cygnus OB2 line of sight, and to the relative shallowness of the available optical catalogs, the correlation between X-ray sources and optical catalogs is of limited use for the study of intermediate- and low-mass stars. We thus decided to base our characterization of the X-ray sources mostly on near-IR data, for which the impact of dust extinction is reduced and is comparable to that in the X-ray band. We made use of J (1.25 μm), H (1.65 μm) and K_s (2.17 μm) photometry from the *Two Micron All Sky Survey* (2MASS) Point Source Catalog (PSC)[13]. 2MASS is complete to magnitudes of 15.8, 15.1 and 14.3 mag in the J, H and K_s bands, respectively. We limited our analysis to 2MASS sources for which the quality flag for at least one of the three magnitudes is equal to A, B, C or D (cf. the 2MASS All-Sky Data Release User's Guide). With this restriction 11 sources were removed from our initial list of 5061 2MASS point sources in the ACIS FOV, leaving a total of 5050 objects.

4.1. Cross-identification

We began by cross identifying our X-ray source list with the 2MASS catalog. Identification radii, R_{id}, were chosen to limit the number of spurious identifications due to chance alignments, N_{chance}, and at the same time to include a large number of the true physical associations, N_{true}. First we estimated, as a function of R_{id}, the number of chance identifications expected in a given sky area, A_{search}, assuming (i) uncorrelated NIR and X-ray positions and (ii) a uniform surface source density of the N_{2MASS} 2MASS sources lying in the search area: $N_{chance}(R_{id}) = N_X A_{id} N_{2MASS}/A_{search}$, where $A_{id} = \pi R_{id}^2$ is the area of identification circles. $N_{true}(R_{id})$ can instead be estimated from the observed total number of identifications at any given R_{id} as $N_{id}(R_{id}) - N_{chance}(R_{id})$. We chose the identification radius as the largest for which $N_{true} > N_{chance}$.

Because the *Chandra* PSF, and therefore the position uncertainty of X-ray sources, depends mainly on the off-angles, we perform this analysis in four different ranges of off-angles: [0−2), [2−4), [4−7) and >7 arcmin. Our identification radii in these four regions are 1.0, 1.5, 2.1, and 2.7 arcsec, respectively.

Before performing the final identifications we searched for possible systematic differences between the X-ray and 2MASS positions. We first performed a preliminary cross-identification and compared the coordinates of identified pairs. A small systematic offset between the two catalogs was found. We thus shifted the *Chandra* coordinates and performed a new cross-identification, repeating this process iteratively until the offset was reduced to ∼0.01 arcsec, i.e. much smaller than the statistical errors on source positions. In the end the offset between the two catalogs was: $\Delta(RA_{x-2MASS}) = +0.12'' \pm 0.10''$ and $\Delta(Dec_{x-2MASS}) = +0.49'' \pm 0.17''$. The result of the final identification is shown in Table 2, where we list, in the first 7 columns, the X-ray and near-IR identifiers of cross-identified sources, the offset between the two positions, and the J, H, K_s magnitudes from 2MASS. A total of 775 X-ray sources out of the 1003 in our list were identified with 2MASS objects. Three X-ray sources (#12, #148, and #449) were identified with two 2MASS objects but, after checking the positions visually, we adopted the closer of the counterparts. The fraction of identified X-ray sources appears to increase as we move to larger off-angles. In the four annular regions defined above, these fractions are: 76/116 (65%), 227/304 (74%), 294/374 (79%) and 178/209 (85%), in order of increasing off-angles. This trend can be attributed to the already mentioned (3.2) dependence of the ACIS-I sensitivity on the off-axis angle and to the fact that more intense X-ray sources are more likely to have a near-IR counterpart than fainter ones.

With respect to the expected number of chance identifications we estimate, for off-axis ranges [0:2), [2:4), [4:7), and >7 arcmin, and with the formula given above, no more than 1.6, 7.9, 16.4, and 12.5, respectively for a total of ≤39. Note however

[13] See `http://www.ipac.caltech.edu/2mass`

that the assumption that X-ray and 2MASS source lists are fully uncorrelated is not true (other than for the 10 expected spurious detections), so that this number should be considered as a loose upper limit (cf. Damiani et al. 2003).

We estimate the expected number of extragalactic sources in our detection list following Flaccomio et al. (2006). We consider the ACIS count-rates of non-stellar sources in the *Chandra Deep Field North* (CDFN, Alexander et al. 2003; Barger et al. 2003) and estimate absorption corrected count-rates assuming $N_{\rm H} = 1.54 \times 10^{22}$ (from $A_{\rm v} = 7.0$, see Sect. 4.2) using PIMMS and assuming power-law spectra with index Γ. We then compare these count rates with upper limits taken at random positions in the ACIS FOV. For Γ between 1 and 2 we obtain 61 to 87 expected extragalactic sources. Given the intrinsic near-IR fluxes of these sources and the absorption toward Cygnus OB2, they are expected to be among the 228 without NIR counterparts (cf. Flaccomio et al. 2006).

We identified our X-ray source list with the 33 early type stars listed by Hanson (2003) and lying in our ACIS FOV. Of these, all the 20 O-type stars associated with an X-ray source, while of the 13 B-type stars only 6 are detected.

4.2. Near-IR properties of the X-ray sources

We now investigate the NIR properties of the X-ray sources with 2MASS counterparts. For this purpose we restrict our analysis to sources with high quality photometry, i.e. those for which the *quality flag* (see 2MASS documentation) is "*AAA*", or for which uncertainties on the J, H and $K_{\rm s}$ magnitudes are all lower than 0.1 mag. With these requirements the total number of IR sources in the ACIS FOV is reduced from 5050 to 2187. Counterparts of X-ray sources were selected only on the basis of their magnitude errors (<0.1 mag), yielding 519 sources out of the original 775.

Figure 3 shows the $J - H$ vs. $H - K_{\rm s}$ color–color (CC) diagram for all the selected 2MASS objects in the ACIS FOV, both X-ray detected and undetected. We also plot for comparison the MS (Kenyon & Hartmann 1995), the Classical T-Tauri Stars (CTTS) locus of Meyer et al. (1997), and three reddening vectors starting from these loci and with slope ($A_{\rm Ks}/E(H - K_{\rm s}) = 0.125$) taken from the extinction law given by Hanson (2003). Cygnus OB2 members with purely photospheric emission should lie in this reddening band. However, as the line of sight toward Cygnus OB2 is not far from that to the Galactic center, many field interlopers are also expected in the same band. Young stellar objects (YSOs), such as Classical T Tauri and Herbig Ae/Be stars, because of the NIR excess emission originating in the inner parts of their circumstellar disks, are often found to the right of this band, i.e. in the CTTS locus.

However, very few X-ray sources, i.e. likely Cygnus OB2 members, have colors consistent with the (reddened) CTTS locus. If we neglect the uncertainties on data points, 23 sources lie in the reddening band of the CTTS locus. We do not include here the peculiar supergiant B5 Ie Cyg#12 and discuss its nature in Sect. 7.1. A total of 23 stars in the CTTS reddening band means a fraction of 23/519 ~ 4.4% of all the X-ray sources in the CC diagram. We compare this fraction with the one observed in the ONC, adopting Chandra Orion Ultradeep Project (COUP) sources in the same mass range[14] that we reach in Cygnus OB2 (i.e. $M \geq 1\ M_{\odot}$, cf. Sect. 7): 19/92 ~ 20.6%. The difference between the two fractions of

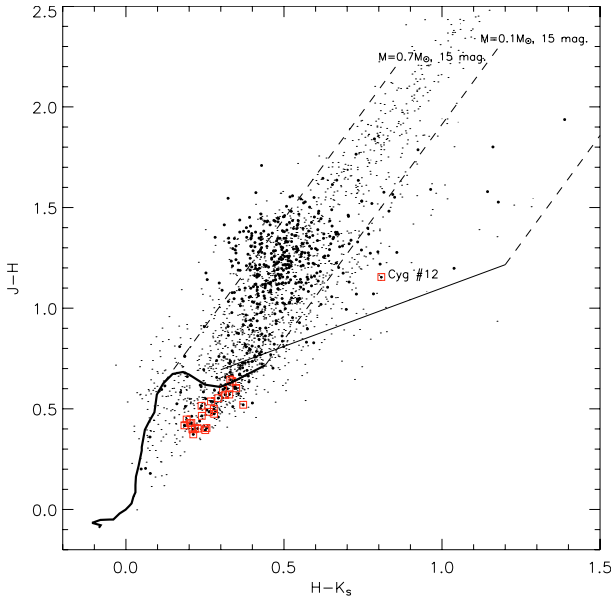

Fig. 3. $JHK_{\rm s}$ color–color diagram of objects in the 17′ × 17′ Cygnus OB2 FOV with high quality 2MASS photometry. Filled circles and small points refer to X-ray detected and undetected 2MASS sources, respectively. Detected known O- and B-type stars are indicated by squares. We also show for reference the main-sequence from Kenyon & Hartmann (1995), the CTTS locus of Meyer et al. (1997) and reddening vectors (*dashed lines*) with length corresponding to $A_{\rm v} = 15$ mag. Note: i) the low number of X-ray sources lying in the CTTS loci; ii) the peculiar position of Cyg #12 (labeled), one of most intrinsically luminous stars in the Galaxy, indicative of a high reddening.

stars with near-IR detected disks is significant, a factor of ~4.7. It could be for two different reasons:

- Cygnus OB2 is older than the ONC (~2 vs. ~1 Myr) and its disks might have dissipated. According to Hillenbrand (2005), the fraction of stars with disks detectable in the near-IR should decrease between 1 and 2 Myr by a factor of 2–3. This, together with the statistical uncertainties in the disk fractions might explain the observed difference[15].
- The effect of disk photo-evaporation by the intense UV radiation field of the hot massive OB stars. This mechanism, predicted theoretically (e.g. Adams et al. 2004) and observed, e.g., in the ONC proplyds (e.g. Bally et al. 2000), is thought to be effective in massive star forming regions, such as Cygnus OB2, having a large number of UV emitting O- and B-type stars. A shortening of the disk lifetime with decreasing distance from O- stars has been recently observed in the massive star forming region NGC 6611 (Guarcello et al. 2006, in prep.).

Figure 4 shows the $K_{\rm s}$ vs. $H - K_{\rm s}$ color magnitude (CM) diagram for the same stars plotted in Fig. 3. We also show for reference the expected cluster locus: the intrinsic $K_{\rm s}$ magnitudes and $H-K_{\rm s}$ colors for stars earlier than B5V were taken from the MS calibration of Knödlseder (2000) and Bessell & Brett (1989). For later spectral types (masses between 0.1 and 7 $M_{\odot}$), we adopted

[14] We only consider COUP sources for which mass estimates are given by Getman et al. (2005a).

[15] A direct comparison with the results of Hillenbrand (2005) is however not possible because her estimate of disk lifetime (i) refers to star in the 0.3–1.0 $M_{\odot}$, i.e. less massive than the ones we observe in Cygnus OB2, (ii) is based on a different, and more efficient, indicator of disks presence than the one we can use here, i.e. the $H - K$ color excess measured with respect to the photospheric value as determined from spectral types.

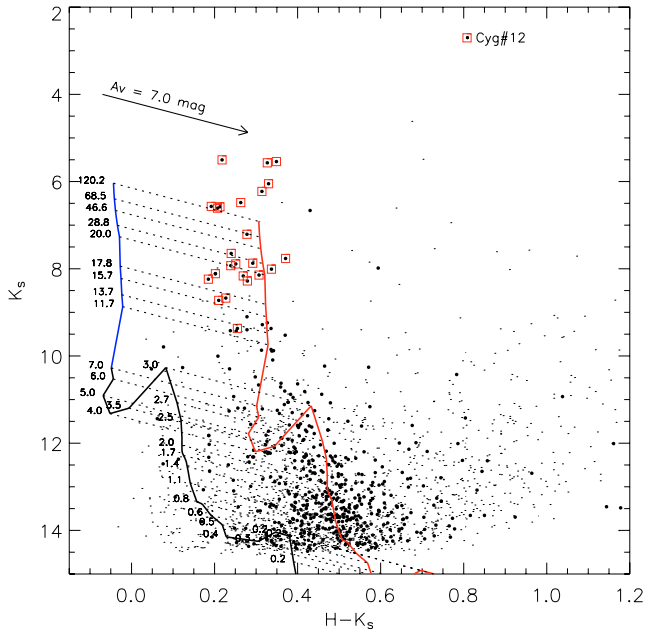

Fig. 4. CM diagrams of the Cygnus OB2 region. Symbols as in Fig. 3. The two parallel curves indicate the expected cluster loci for the assumed distance and for a mean reddening of A_V = 0.0 and 7.0 mag. They represent the MS for (un-reddened) K_{s0} < 10.3 and the 2 Myr isochrone for fainter magnitudes.

the 2 Myr isochrone from Siess et al. (2000), converted to the observational plane using the calibration given by Kenyon & Hartmann (1995). The adopted MS and 2 Myr isochrone overlap satisfactorily.

In order to estimate the typical visual absorption of cluster members we calculated the distance of each X-ray source to the cluster locus along the reddening direction. Resulting A_v values for individual sources are listed in the last column of Table 2. Note that for 10.25 < K_{s0} < 11.35 the absorption cannot be constrained because the reddening vector intersects the cluster locus more than once. We computed median absorption values in two luminosity ranges: for K_{s0} > 11.35 we obtained A_v =7.0 mag, while for K_{s0} < 10.25, considering only the known OB stars, we obtained A_v = 5.63 mag. We note that the above estimations depend on the reliability of the assumed cluster locus and on the assumption that the H and K magnitudes are not significantly affected by disk-induced excesses. As observed above, given the paucity of stars with excesses, the latter appears to be a good approximation for Cygnus OB2 stars. It is comforting that our estimate for the OB type stars is in fairly good agreement with the median of the extinctions computed by Hanson (2003) using photometric and spectroscopic data: A_v = 5.7 mag. The lower extinction derived for high mass stars than to lower mass ones may indicate that the strong winds and radiation field of massive stars may have cleared their surrounding environment.

In both the CC and CM diagrams, some X-ray sources, of the order of 15−20, lie close to the un-reddened cluster loci. These are likely to be foreground MS stars and thus to contaminate the sample of X-ray detected cluster members. This conclusion is corroborated by the X-ray hardness-ratio analysis: eight of these stars have soft and relatively unabsorbed spectra (the stars to the right of the OB stars, in the upper-right corner of Fig. 2-right), as expected from foreground field stars.

In the following (Sect. 7) we will correlate the X-ray properties of our sources with stellar parameters derived from the available optical and near-IR data. We obtain an estimate of stellar masses for 682 2MASS counterparts from the J-band magnitudes (limited to *quality flags* "A" to "D") and the mass vs. J mag. relationship appropriate for the cluster age, distance and extinction, obtained as described above for the cluster locus in the H, $H-K$ diagram[16]. The relation is degenerate in two ranges of J, corresponding to 0.2−0.4 $M_\odot$ and 2.8−5.3 $M_\odot$. Four and 28 X-ray detected stars lie in these ranges, respectively.

5. Temporal variability

The temporal variability of young low mass sources is often complex: the most common phenomena are magnetic flares with rapid rise and slower decays, superposed on an apparently constant or, sometimes, rotationally modulated emission (Flaccomio et al. 2005; Wolk et al. 2005). Other forms of variability, with less clear physical origin, are often observed.

We first investigated X-ray variability using the non-binned one-sample Kolmogorov-Smirnov (KS) test (Press et al. 1992). This test compares the distribution of photon arrival times with that expected for a constant source. The test was applied to photons in the source extraction regions, which also contain background photons. Given that the background was found to be low and constant (Sect. 2.1), the results, i.e. the confidence with which we can reject the hypothesis that the flux was constant during our observation, can be attributed to the source photons. Table 1, Col. 17, reports the logarithm of the KS-test significance with values < −4 truncated at that value: sources with $\log(P_{KS}) < -3.0$ can be considered almost definitively variable as we expect at most one of the 1003 sources (i.e. 0.1%) to be erroneously classified as variable. Eighty-five X-ray sources (≈8.5% of the total) fall in this category. Sources with $-2.0 < \log(P_{KS}) < -3.0$ can be considered as likely variable, but up to 9 such sources (on average) might actually be constant. Forty-nine Cygnus OB2 sources fall in this category.

These numbers of sources in which variability is detected are a lower limit to the total number of variable sources in the region for several reasons: i) most of the observed variability is in the form of flares, i.e. events that are shorter than our observation and with a duty-cycle that may be considerably longer (Wolk et al. 2005); ii) the sensitivity of statistical tests to time variability of a given relative amplitude depends critically on photon statistics. This is illustrated in Fig. 5, where we plot the fraction of variable sources as a function of source counts: the clear correlation between the two quantities is most likely due to this statistical bias even though we cannot exclude a real dependence.

Next, we extracted binned light-curves for each of our Cygnus OB2 X-ray sources adopting a bin length of 600 s, a compromise between bins that are long enough to reach a good signal-to-noise ratio per bin for most sources and sufficiently short to resolve the decay phase of typical flares. Since the background of our observation is both low (negligible for many sources) and constant, we did not apply any background subtraction. We inspected the 857 light-curves of sources with >10 photons, finding flare-like events, qualitatively defined as a rapid rise and a slow decay, in 98 sources, i.e. ≈9.8% of the cases. These sources are indicated by a † in the last column of Table 1. Of these 98 sources, 66 (∼65%) have a $\log(P_{KS}) \leq -3.0$, while 13 were classified as probably variable ($-2.0 < \log P_{KS} \leq -3.0$).

[16] The use of the J-band is justified because (i) in the presence of disk excesses the J-band is the most representative of the photospheric emission and (ii) the mass ranges in which the mass-luminosity relationship is degenerate are narrower than for a similar relationship in the H and K bands.

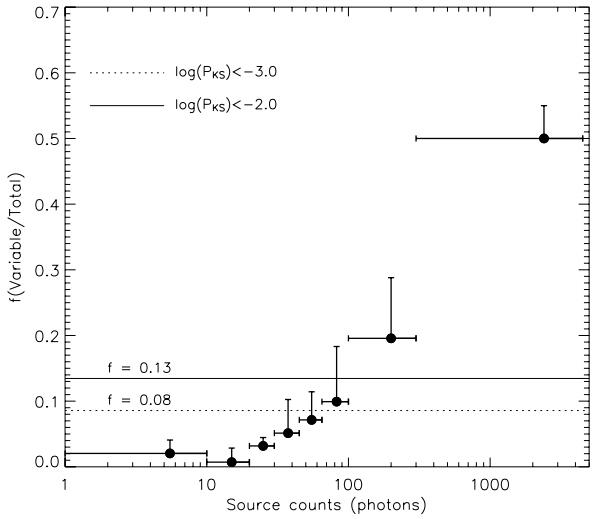

Fig. 5. Fraction of variable sources as a function of source counts. Horizontal bars indicate the range of source counts. Filled circles indicate, for each counts bin, the fraction of sources with $\log(P_{\rm KS}) < -3.0$ (85 sources in total), while the upper tip of the vertical bars indicate the fraction with $\log(P_{\rm KS}) < -2.0$ (134 sources in total). The continuous and dashed horizontal lines indicate the overall (average) variability fractions obtained for the two confidence levels.

The remaining 19 sources were not detected as variable by the KS test ($\log P_{\rm KS} > -2.0$) and may or may not be actually "flaring". Figure 6 shows light-curves for 20 variable sources, 14 of which are classified as flaring. Some of these sources (e.g. #1, #676 and #911) experience "impulsive" flares with very quick rises and decay phases of only a few hours. Others (e.g. #33, #172, and #260) show longer (2 to 10 h) flares. In several instances a second impulsive event is visible during the exponential decay of a previous flare (e.g. sources #6, #52, #439, #600, #796, and #945). Other sources (e.g. #555, #834 and #863) have variable light-curves that bear little resemblance to typical flares and are instead characterized by slow continuous rises or decays that might be explained by rotational modulation of non-homogeneously distributed plasma (Flaccomio et al. 2005).

As expected if flares originate from magnetic reconnection events (Favata & Micela 2003), the median photon energies for flaring sources are generally higher than those of non-flaring sources: the distribution of median energies for the flaring source peaks at $\overline{E}_x \approx 2.6$ keV, with a 1σ dispersion of 0.4 keV, while for non-variable stars it peaks at $\overline{E}_x \approx 2.1$ keV, with a 1σ dispersion of 0.3 keV. A similar conclusion can be drawn from the spectral modeling presented in the next section (Sect. 6): flaring sources often require higher temperature models than non-variable ones.

The variability of massive O and early B-type stars is significantly different from that of low mass members. Among the 26 OB stars detected in our FOV, 24 are classified as non-variable ($\log(P_{\rm KS}) > -2.0$), in spite of their higher than average statistics, having between ∼40 and 15 000 counts, with a median of ∼111 counts. A comparison with Fig. 5 shows that the variabile fraction of OB stars (7.7%) is significantly lower than for the bulk of our sources with similar statistics. This finding agrees with the common view of X-ray emission from O stars, which is believed to be unrelated to solar-like magnetic activity, and rather is explained as the integrated emission from a large number of small shocks occurring in the strong winds of these stars (Feldmeier et al. 1997; Owocki & Cohen 1999). Interestingly however, two of these sources, #60 and #979, are significantly variable, with $\log(P_{\rm KS})$ values lower than −4. Figure 7 shows their light-curves.

Source #60 (Cyg#12) is a B5 Ie star (Hanson 2003). The X-ray light-curve shows a roughly linear decay of the ACIS count rate from ≈0.18 cnt s^{-1} to ≈0.16 cnt s^{-1}. The star was observed by Waldron et al. (1998) who did not report variability during ∼125 ks of non-continuous ROSAT PSPC observation. This kind of variability may be similar to the rotational modulation observed on the O7 star θ Ori C (Gagné et al. 2005) and is attributed to the presence of a rigidly rotating magnetosphere (RRM), which may form in magnetic early-type stars with misaligned magnetic and rotation axe (Owocki et al. 2005). We defer further discussion of the nature of Cyg #12 to Sect. 7.1.

Source #979 is identified as star #646 in Hanson (2003) and there is classified as a B1.5V + ? star, the question mark indicating the presence of an unresolved faint secondary. The observed variable X-ray emission is much fainter than in the previous case and might be due to the magnetic activity of the companion of the B1.5 V primary, presumably a lower mass star.

6. Spectral analysis

In order to characterize the hot plasma responsible for the X-ray emission of Cygnus OB2 stars, and to estimate their intrinsic X-ray luminosities, we analyzed the ACIS spectra of each of our 1003 sources. Reduced source and background spectra in the 0.5−8.0 keV band were produced with AE (see Sect. 3.2), along with individual "redistribution matrices files" (RMF) and "ancillary response files" (ARF). For model fitting, spectra were grouped so to have a specified number of events in each energy bin. Grouping was tuned to the source statistics and we chose 2, 5, 7, 10, and 60 counts per channel for sources with net-counts in the following ranges: [0−40], [40−100], [100−200], [200−500], and [500−16 000]. Spectral fitting of background-subtracted spectra was performed with XSPEC v12.0 (Arnaud 2004) and our own shell and TCL scripts to automate the process as described in Flaccomio et al. (2006). Best fit parameters for the chosen models were found by χ^2 minimization.

We fit our spectra assuming emission by a thermal plasma, in collisional ionization equilibrium, as modeled by the APEC code (Smith et al. 2001). Elemental abundances are not easily constrained with low-statistic spectra and were fixed at $Z = 0.3\ Z_\odot$, with solar abundances taken from Anders & Grevesse (1989). The choice of sub-solar abundances is suggested by several X-ray studies of star forming regions (e.g. Feigelson et al. 2002; Preibisch 2003). Absorption was accounted for using the WABS model, parametrized by the hydrogen column density, $N_{\rm H}$ (Morrison & McCammon 1983).

Except for X-ray sources associated with O- and early B-type stars, which are discussed separately in Sect. 7.1, we fit source spectra with one-temperature (1T) plasma models using an automated procedure. In order to reduce the risk of finding a relative minimum in the χ^2 spaces, our procedure chooses the best fit among several obtained starting from a grid of initial values of the model parameters: $\log(N_{\rm H})$ = 21.0, 21.7, 22.0, 22.4, 22.7 and 23.0 cm^{-2} and kT = 0.5, 0.75, 1.0, 2.0, 5.0 keV. Best fit values of $\log(N_{\rm H}) < 20.8$ cm^{-2} were truncated at 20.8 because, in the 0.5−8.0 keV energy range, ACIS spectra are insensitive to lower column densities. For the same reason, 154 best fit values of kT turned out to be >10 keV and were truncated at that value.

As noted by many authors (e.g. Getman et al. 2002, 2005b; Flaccomio et al. 2006), the spectral fitting of low statistic ACIS sources is problematic because of a degeneracy between plasma

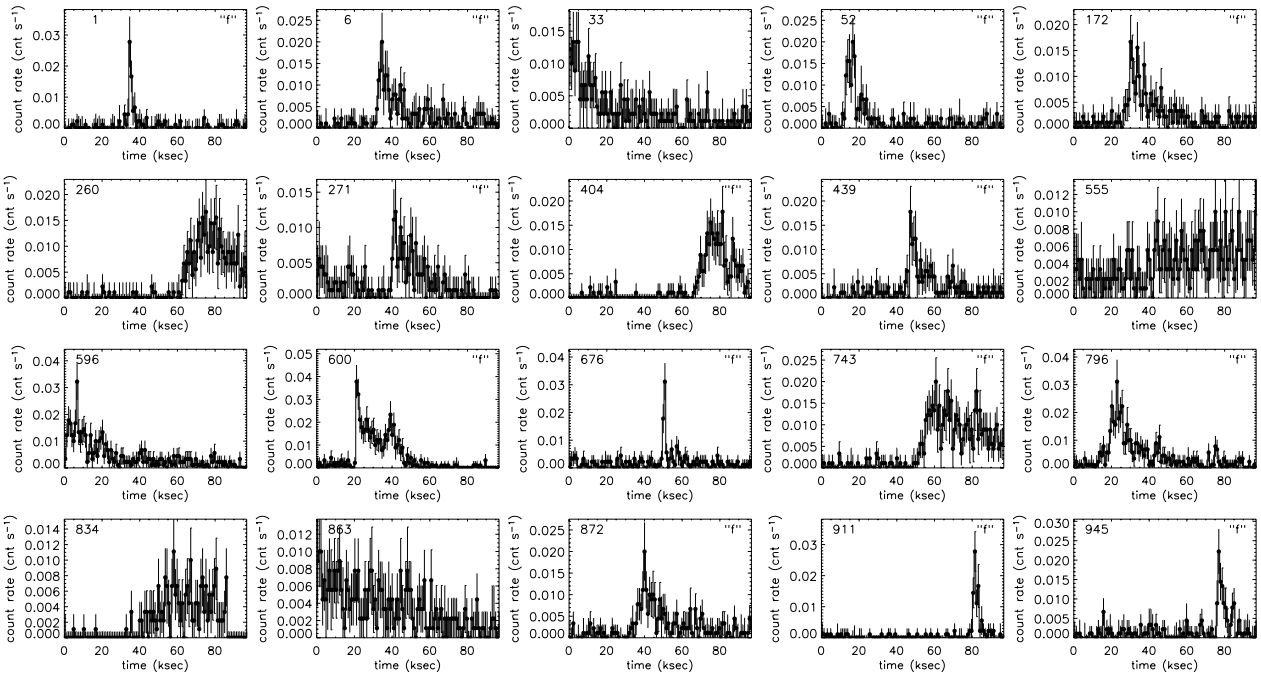

Fig. 6. Light curves (in the 0.5−8.0 keV band) for 20 sources with variable emission during our 97.7 ks *Chandra* observation. The bin length is 600 s. Source numbers are given in the upper-left corner of each panel, followed by an "f" for sources classified as flaring.

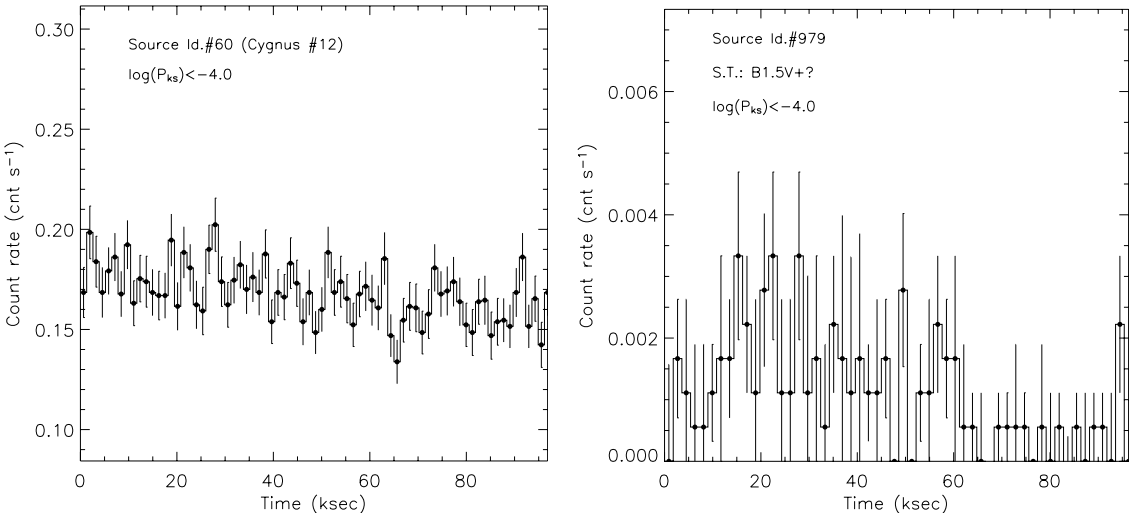

Fig. 7. Light curves in the 0.5−8.0 keV band for the two variable early-type stars: *Left*: source Id. #60, known as a B5Ie, has been recently classified a B5 ± 0.5 Ia+ star by Klochkova & Chentsov (2004). X-ray variability of this star was unknown until now. The time bin-size is 900 s. *Right*: source Id. #979 is probably a B1.5 V+"?" binary system (Massey & Thompson 1991). The time bin size here is 1300 s. Source number and results of the KS test are given in the legend.

temperature and absorption. The degeneracy also results in a systematic bias: kT values are often underestimated by as much as ∼50% while $N_{\rm H}$ values are overestimated. We investigated this issue with our data by considering the distributions of the best fit parameters for source in different count-statistic bins. Figure 8 shows the run of mean kT and $N_{\rm H}$ with source counts for spectra fitted with 1T models. The systematic decrease of $N_{\rm H}$ and the increase of kT with increasing source statistics are hardly explainable as physical effects and rather indicate that the spectral parameters obtained for sources with less than ∼20 photons are ill-constrained.

The uncertainty on the $N_{\rm H}$ is particularly serious as it implies large and systematic uncertainties on the absorption-corrected X-ray luminosities. In order to reduce the risk of erroneous results, we discarded from the following analysis results for source with <20 net photons, a total of 423 sources. Table 3 presents the results of the automated 1T spectral fits for 554 sources (the results of the spectral fitting for the 26 sources associated with known OB stars will be presented in Sect. 7.1, Table 4). We list source numbers (Col. 1) from Tables 1 and 2, background subtracted counts in the spectra (2), the best fit hydrogen column densities and their 1σ errors (3), the plasma temperatures and their 1σ errors (4), and the emission measures (5). Columns (6) and (7) give the reduced χ^2_ν for the spectral fits and the relative degrees of freedom, respectively.

The hydrogen column densities derived from X-ray spectral fitting depend of the interstellar material in the line of sight to the Cygnus OB2 cloud and on the location of stars within

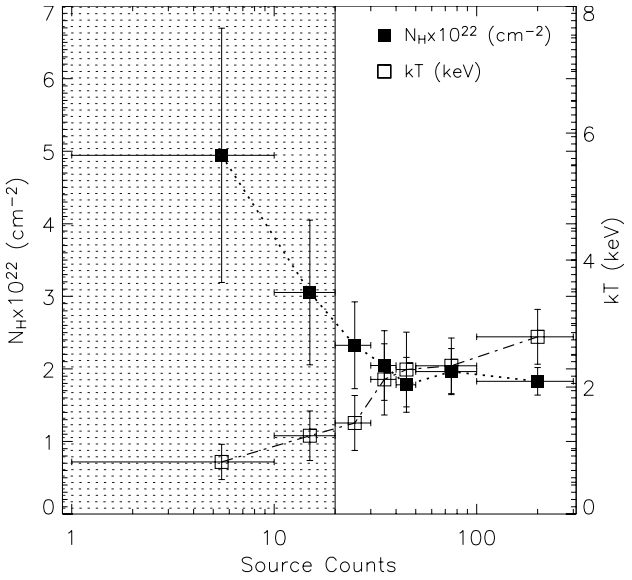

Fig. 8. Median $N_{\rm H}$ and kT vs. source counts for sources fit with one-temperature models. Filled and empty squares indicate the average values of the $N_{\rm H}$ and kT in each considered count range with vertical scales given on the right and left-hand side, respectively. The extent of the count ranges is indicated by the horizontal error bars. Vertical error bars indicate the median of the 1σ uncertainties on the two parameters. For this plot we only considered $N_{\rm H}$ and kT values with formal relative errors smaller than 90%. The hatched area below 20 counts indicates the count-range in which spectral fits were discarded because of strong biases in the best fit parameters.

Table 3. Results of X-ray spectral fits: first rows. The complete version is available in the electronic edition of the Journal.

$N_{\rm x}$ #	Cnts (ph.)	log($N_{\rm H}$) ($\rm cm^{-2}$)	kT (keV)	log(EM) ($\rm cm^{-3}$)	Stat. (χ^2_ν)	d.o.f.
1	67	22.13 ± 0.26	9.99	53.70	0.34	17
2	72	21.05 ± 0.34	0.74 ± 0.12	53.40	1.54	17
3	35	21.75 ± 0.03	9.99	53.40	0.38	9
5	55	22.15 ± 0.27	6.05 ± 8.52	53.40	0.81	14
6	216	22.13 ± 0.68	5.52 ± 3.06	54.10	0.96	19
7	49	21.86 ± 0.04	9.99	53.40	0.78	15
8	33	21.70 ± 0.08	9.99	53.40	0.51	9
9	64	21.44 ± 0.03	9.99	53.40	0.76	14
10	50	21.60 ± 0.10	1.04 ± 0.23	53.40	1.00	12
12	99	22.14 ± 0.47	2.19 ± 0.91	53.88	1.02	24
13	44	22.42 ± 0.29	3.74 ± 3.87	53.70	1.20	10
14	75	22.51 ± 0.30	9.99	53.70	1.10	19
15	60	21.90 ± 0.24	6.85 ± 8.19	53.40	0.66	14
16	30	22.53 ± 0.10	2.72 ± 2.67	53.70	0.82	7
17	3173	22.16 ± 0.25	1.34 ± 0.64	55.65	1.57	252
19	25	22.48 ± 0.15	3.43 ± 4.19	53.40	0.56	6
20	49	22.26 ± 0.30	3.04 ± 1.86	53.70	0.72	11

the cloud material of Cygnus OB2. Figure 9a shows the distribution of log $N_{\rm H}$ values for the 580 sources with more than 20 counts. They appear to be normally distributed with a median log $N_{\rm H} \sim 22.25$ ($\rm cm^{-2}$) and a *FWHM* of ∼0.21 dex. The shaded area in Fig. 9a indicates an apparent excess of relatively unabsorbed sources (log $N_{\rm H} < 21.8$ $\rm cm^{-2}$) with respect to the log-normal distribution of the bulk of the sources. These ∼23 sources are likely associated with foreground stars. Most of these sources seem to be spatially distributed uniformly in the FOV of the Cygnus OB2 region.

Another interesting observation is that the $N_{\rm H}$ distribution of the 106 X-ray sources without near-IR counterparts (dark gray histogram in Fig. 9) seems to be skewed toward higher values than the global distribution. For example, while only 11% of the X-ray sources with counterparts have $N_{\rm H} > 22.5$, this is true for 29 (27%) of the unidentified sources.

According to the relationship between $N_{\rm H}$ and $A_{\rm V}$, $N_{\rm H} = 2.2 \times 10^{21} A_{\rm v}$ $\rm cm^{-2}$ (Ryter 1996), the median $N_{\rm H}$ of all detected sources with more than 20 counts corresponds to $A_{\rm v} \sim 8.1^{12.8}_{5.1}$ mag. If we only consider the sources with near-IR counterparts (and > than 20 counts) we obtain log $N_{\rm H} = 22.23$, which corresponds to $A_{\rm v}$ =7.7 mag, i.e. in reasonable agreement with the value calculated from the NIR CMD ($A_{\rm v} \approx 7.0$ mag).

Figure 9(b) shows the distribution of plasma temperatures: it peaks at ∼1.35 keV, has a median ∼2.4 keV and shows an extended hard tail. Variable sources (log $P_{\rm KS} < -2$) have harder spectra with median $kT = 3.3$ keV and flaring sources (see hatched histogram in Fig. 9b) are even harder with a median $kT = 3.75$ keV.

We derived unabsorbed X-ray luminosities for each of our sources. For O and B-type stars, discussed in detail below (Sect. 7.1), luminosities were derived from individual spectral fits. For the other sources, given the considerable uncertainties in the absorption estimates, especially at the faint end, we preferred not to use the results of spectral fits individually. Rather, we computed a single count-rate to $L_{\rm X}$ conversion factor that takes into consideration the average intrinsic source spectrum and interstellar absorption. This conversion factor, computed as the median ratio between the individual unabsorbed X-ray luminosities (from the best fit spectral models) and the source count-rates is 7.92×10^{33} ergs.

7. Results

We now discuss the implications of our data for the understanding of X-ray emission from young stars and for the study of the Cygnus OB2 stellar population. We split the discussion according to stellar mass and, correspondingly, expected X-ray emission mechanism. We first discuss known O and early B (<B2) stars, i.e. massive stars ($M \gtrsim 12$ $M_\odot$) expected to generate X-rays in their powerful stellar winds. Next, using our mass estimates based on the J-band magnitude (Sect. 4.2), we define and study the properties of two subsamples of intermediate and low-mass X-ray detected stars. We base the distinction between the two groups on the model-predicted thickness of the convective layer, whose presence has been often found to be correlated with solar-like coronal activity. Stars with small or absent convective layers are instead believed to be unable to sustain coronal activity, although the matter is somewhat controversial. Adopting the 2 Myr isochrone from the SDF models, we observe that the thickness of the convective layer relative to the stellar radius, $R_{\rm c}$, decreases rapidly, from ∼5% to <1%, as the stellar mass increases from 3 to 3.3 $M_\odot$. This rather sharp boundary however lies in the 2.8−5.3 $M_\odot$ range in which our mass estimates are degenerate and therefore unconstrained (see Sect. 4.2). In order to resolve this ambiguity, we define the intermediate-mass range as 2.8−10 $M_\odot$, resulting in the selection of 57 stars[17]. Low mass stars are finally defined as stars with $M < 2.8$ $M_\odot$ and are

[17] There are only 28 stars with masses in the 2.8−5.3 $M_\odot$ range and for which this interval formally corresponds to the uncertainty on the mass estimate. We therefore expect a small fraction of the 57 intermediate mass stars to lie in the 2.8−3.0 $M_\odot$ range and to have a substantial model-predicted convective envelope.

Table 4. X-ray spectral parameters of the Cygnus OB2 OB-type stars.

Src.	Optical Parameters		χ^2_ν	Pile-up	$N_{\rm H}[\times10^{22}]$ [cm^{-2}]		kT_1	kT_2	Abundance	Flux [10^{-13}]
#	Hanson#	S.T.		(%)	WABS	ABSORI	[keV]	[keV]	[$Z_\odot$]	[erg s^{-1} cm^{-2}]
60[b]	304	B5 Ie	1.4	∼18	2.15 ± 0.15	0.87 ± 0.12	0.63 ± 0.03	1.56 ± 0.11	0.43 ± 0.04	$235.4^{255.4}_{201.7}$
133	339	O8.5 V	1.1	no	0.24 ± 0.18	–	1.53 ± 0.68	–	(0.3)	$0.11^{0.19}_{0.07}$
253	378	B0 V	1.0	no	3.57 ± 0.09	–	0.43 ± 0.15	–	(0.3)	$2.00^{2.21}_{1.42}$
315	390	O8 V	0.8	no	3.30 ± 0.08	–	0.44 ± 0.10	–	0.15 ± 0.09	$0.64^{0.73}_{0.51}$
433	417	O4 III(f)	1.5	≲2	2.30 ± 0.07	–	0.39 ± 0.06	1.94 ± 0.73	0.60 ± 0.34	$42.1^{45.3}_{34.6}$
456	421	O9.5 V	1.4	no	1.45 ± 0.08	–	1.71 ± 1.02	–	(0.30)	$1.06^{0.88}_{1.09}$
488[b]	431	O5 If	1.3	∼12	2.09 ± 0.07	–	0.79 ± 0.05	2.82 ± 0.61	0.65 ± 0.10	$72.6^{75.5}_{67.5}$
530	448	O6 V	1.4	no	1.97 ± 0.34	–	0.65 ± 0.20	–	(0.1)	$1.18^{1.39}_{0.96}$
537	455	O8 V	1.1	no	2.19 ± 0.07	–	0.61 ± 0.17	–	(0.1)	$1.20^{1.28}_{1.07}$
544	457	O3 If	1.3	≲2	2.12 ± 0.06	0.56 ± 0.09	0.39 ± 0.14	1.32 ± 0.19	0.97 ± 0.3	$88.8^{98.6}_{77.5}$
562	462	O6.5 II	1.0	no	2.52 ± 0.48	–	0.40 ± 0.12	–	0.14 ± 0.1	$8.45^{9.1}_{6.4}$
568[a]	465	O6If + O5.5III(f)	1.4	∼15	2.94 ± 1.25	–	0.91 ± 0.05	2.64 ± 0.07	0.52 ± 0.07	$61.3^{64.9}_{57.1}$
584	470	O9.5 V	0.8	no	1.85 ± 0.07	–	0.44 ± 0.18	–	(0.3)	$3.49^{3.98}_{2.89}$
597	473	O8.5 V	1.0	no	1.88 ± 0.09	–	0.30 ± 0.22	–	1.07	$3.00^{3.78}_{2.38}$
615	480	O7.5 V	1.0	no	2.73 ± 0.06	–	0.50 ± 0.17	–	(0.1)	$4.01^{4.43}_{3.42}$
625	483	O5 If	1.0	no	1.00 ± 0.08	–	0.55 ± 0.06	–	0.60 ± 0.21	$99.4^{107.3}_{86.4}$
626	485	O8 V	1.1	no	1.65 ± 0.04	–	0.88 ± 0.23	–	(0.1)	$0.38^{0.53}_{0.21}$
686	507	O8.5 V	1.1	no	2.39 ± 0.08	–	0.35 ± 0.11	–	(0.3)	$4.16^{5.04}_{3.28}$
729[a]	516	O5.5 V(f)	1.1	≲4	0.81 ± 0.05	0.51 ± 0.32	1.98 ± 0.12	–	0.38 ± 0.09	$11.7^{12.4}_{10.1}$
779	534	O7.5 V	1.2	no	1.16 ± 0.03	–	2.28 ± 0.55	–	(0.1)	$6.05^{7.74}_{4.91}$
817	556	B1 Ib	0.9	no	1.57 ± 0.08	–	0.18 ± 0.07	–	(0.3)	$1.20^{1.53}_{0.94}$
881	588	B0 V	0.9	no	1.84 ± 0.05	–	0.42 ± 0.20	–	(0.3)	$0.81^{1.02}_{0.71}$
895	601	O9.5 III	1.0	no	1.98 ± 0.07	–	0.38 ± 0.21	–	(0.3)	$0.72^{0.92}_{0.50}$
971	642	B1 III	0.9	no	1.73 ± 0.05	–	0.96 ± 0.45	–	(0.3)	$0.14^{0.30}_{0.09}$
979	646	B1.5 V +?	1.5	no	2.90 ± 1.24	–	1.92 ± 1.01	–	(0.3)	$0.22^{0.63}_{0.29}$
1001	696	O9.5 V	0.8	no	0.71 ± 0.02	–	0.54 ± 0.17	–	(0.3)	$0.71^{0.83}_{0.42}$

Notes: (1) Abundance values in parenthesis indicate cases for which abundances were fixed in the spectral fit (see text), (2) Absorption-corrected fluxes are calculated in the 0.5−8.0 keV energy range (3) Three bright sources, #60, #488, and #568, suffer pile-up, and we extracted the spectra from annular rings (see Sect. 3.2) that exclude the central parts of the PSFs. [a] The 6.4+6.7 keV FeK$_\alpha$ complex is observed; [b] The FeI 6.4 keV line is not detected, but the 6.7 keV seems to be present.

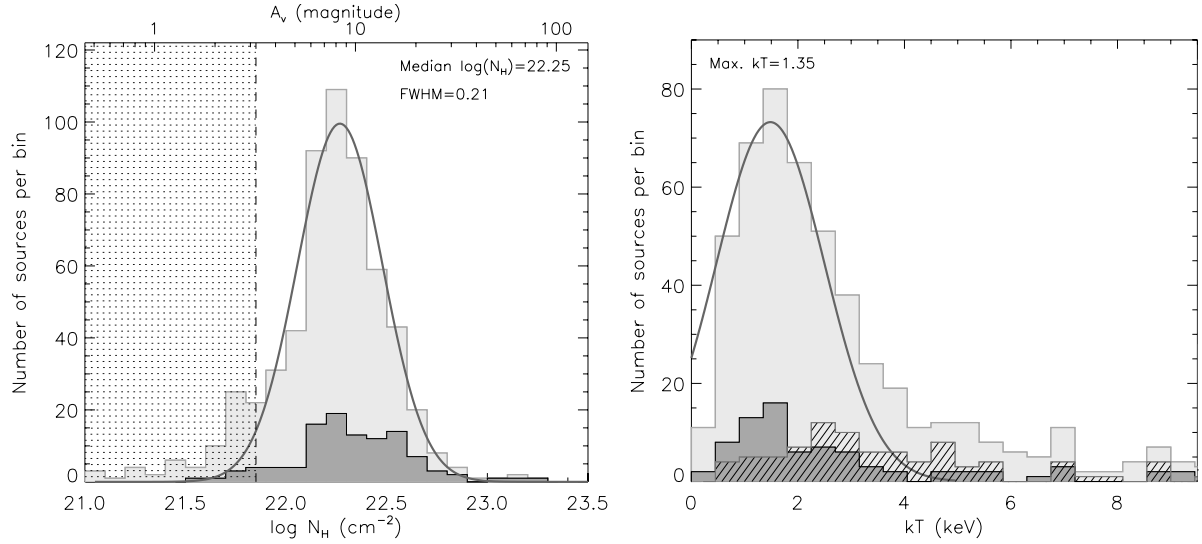

Fig. 9. a) Distributions of absorbing columns, $N_{\rm H}$, with the corresponding visual absorption scale at the top. The light gray area refers to sources with net-counts greater than 20. The maximum of the distribution is at log $N_{\rm H}$ ∼ 22.25 cm^{-2} with a Full Width Half Maximum (*FWHM*) of about 0.21 dex. The shaded area on the left indicates an excess of low-absorption sources with respect to the log-normal distribution that best describes the histogram (the continuous curve), possibly associated with foreground stars. The darker gray histogram refers to the subsample of sources without a 2MASS counterpart. **b)** Same as panel **a)** for plasma temperatures (kT) with, in addition, the distribution for "flaring" sources (hatched histogram). The peak of the overall distribution is at ∼1.35 keV.

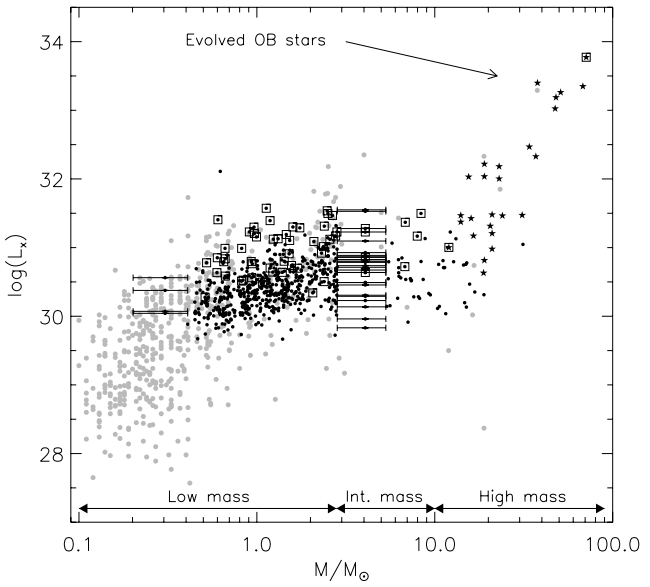

Fig. 10. Log $M/M_\odot$ vs. log L_x for Cygnus OB2 sources with NIR counterparts (black circles and star-symbols) and for ONC sources observed by the COUP project (gray circles). Variable sources are indicated by empty squares, known O- and early B-type stars by star-symbols.

predicted to have substantial convective envelopes ($R_c > 18\%$). 578 counterparts to X-ray sources fall in this category. Because of the sensitivity limit of 2MASS only 25(4) sources of these stars have masses below 0.5(0.4) $M_\odot$, which we may consider as our approximate detection limit. Our *completeness* limit is however probably higher, at ∼1 $M_\odot$, corresponding to $J = 15.8$, i.e. roughly the completeness limit of 2MASS. A histogram of the logarithm of stellar masses also peaks at ∼1 $M_\odot$, confirming the above estimate given that the mass function usually increases towards lower masses.

Figure 10 shows the L_X-mass scatter plot for 683 X-ray sources in all three mass ranges. We distinguish with different symbols stars of low- and intermediate-mass, as determined from the J-band magnitude, and massive stars with known O- and early B- spectral types[18]. Note that stars in the 2.8−5.3 $M_\odot$ and 0.2−0.4 $M_\odot$ ranges are plotted with horizontal error bars spanning the entire range, because the J-band vs. mass relation was found to be degenerate. In the plot we also indicate the position of 57 time-variable X-ray sources. They appear to be brighter than other sources of the same mass, probably because variability is more readily detected in sources with high photon statistics (see Sect. 5).

7.1. High-mass stars

The Cygnus OB2 region is one of the most massive SFR in the Galaxy, with ∼2600 ± 400 OB star members (Knödlseder 2000). The presence of a variety of evolved stars suggests that the star formation process was non-coeval (Massey & Thompson 1991; Hanson 2003). Out of a total of 20 O-type and 13 B-type stars lying in our Cygnus OB2 ACIS FOV, 7 and 3, respectively, are evolved (luminosity class: I−III). While we detect X-ray emission from all O stars regardless of evolutionary status, we have only detected 6 B stars, among which all the evolved ones. The detection fraction of evolved B stars is thus 100% while it is only 33% (3 our of 9[19]) for un-evolved ones.

The most widely accepted explanation for the X-ray emission of single O and early B-type stars invokes multiple small-scale shocks in the inner layers of their radiation-driven stellar winds (e.g. Feldmeier et al. 1997). Recent theoretical and observational results however support, for several OB stars, another physical plasma heating model involving strong magnetic fields: the magnetically channeled wind shock (MCWS) model (Schulz et al. 2003; Owocki et al. 2005; Gagné et al. 2005). Moreover, binary systems in which both components are O- and early B-type stars can produce intense thermal X-ray emission from wind-wind interactions as well as non-thermal X-ray emission from Inverse Compton scattering.

We modeled the spectra of O and B stars with one- or two-temperature thermal plasma emission models (APEC), absorbed by neutral interstellar and circumstellar material (WABS). Because the dense stellar winds of evolved OB stars are affected by the strong stellar UV/EUV ionizing radiation, the additional absorption of X-rays by a partially ionized stellar also wind should be considered. For evolved stars we then decided to model the combined effect of ISM plus wind material with a *warm* absorption model (WABS × ABSORI, see e.g. Waldron et al. 1998). For sources #60, #544, and #729, we found that the inclusion of a warm absorber in the spectral model yields satisfactory fits of the soft part of the spectra (≤1.2 keV), reducing the χ^2_ν from 2.1 to 1.4, from 2.7 to 1.3, and from 2.2 to 1.2, for the three sources respectively. The spectra of other evolved sources did not support the presence of the warm absorber, although in many cases the spectra have too low statistics to be conclusive. Metal abundances were fixed at $Z = 0.3\,Z_\odot$ in fitting faint sources (<100 ph.) and left as a free parameter for brighter sources. When the best fit abundance was lower than $Z = 0.1\,Z_\odot$ we repeated the fit with Z fixed at this value.

Figure 12 shows three notable examples of spectral modeling and the best-fit parameter values for the 26 detected OB stars are presented in Table 4. We list: X-ray source numbers from Table 1 (Col. 1), identification numbers and spectral types from Hanson (2003) (2 and 3), reduced χ^2 of the best fit (4), fraction of pile-up as reported by AE (as discussed Sect. 3.2, if f(Pile-up) > 2% we used an annular photon extraction region that excludes the peak of the PSF), the N_H of the *cold* and *hot* absorption components from WABS and ABSORI, respectively (6 and 7), plasma temperatures of the two components (8 and 9), metal abundances (10). Column (11) finally gives the un-absorbed X-ray flux in the 0.5−8.0 keV energy band.

The median absorption of the 26 OB stars is log N_H = 22.19 cm^{-2}, very similar but slightly lower than the median value of lower mass stars (22.23, see Sect. 7.3). It is tempting to attribute the lower absorption of O stars to the sweeping of the cloud material by strong winds. A two-sided KS test comparing the distribution of N_H for O and B stars with that of lower mass ones gives, however, a null result.

Most of the O- and early B- type stars are well fit by a soft thermal emission model with kT ranging between 0.5 and 0.7 keV (∼5.8−8.1 MK), in agreement with the predictions of the wind shock model (Lucy & White 1980; Owocki et al. 1988). The spectra of some sources, however, require a second (hard) thermal component, which is not predicted by the wind shock model. The presence of this component seems to depend on the stellar evolutionary status: out of the 10 evolved O- and early B-type stars (spectral types B5 Ie,

[18] A number of X-ray detected stars with no spectral type appear to be of high mass but with lower X-ray luminosities than those with spectral types. In the discussion of high mass stars, however, we will only consider stars with spectral types.

[19] One undetected B stars has an unknown luminosity class.

O4 III, O5 If, O3 If, O6 If +O5.5III(f)) 5 (50%) show evidence of a hard thermal emission with kT roughly between 1.3 and 3.0 keV (14−35 MK), while among the 16 class V stars, the hot component is only required in 3 cases (i.e. 23%). Several physical mechanisms have been proposed to explain the hard emission observed in some of our OB stars:

- *Magnetically Confined Wind Shocks* (MCWS). X-ray emission from MCWS is predicted by simulations of radiation-driven winds in the presence of a magnetic field (ud-Doula & Owocki 2002) and it has most likely been observed in O-type stars (e.g. θ^1Orionis C, Gagné et al. 2005). The model predicts that the overall degree of plasma confinement is determined by a single dimensionless parameter $\eta_\star \equiv \frac{B_{\rm eq}^2 R_\star}{\dot{M} v_\infty}$, where $B_{\rm eq}$ is the equatorial dipole magnetic intensity at the stellar surface, $R_\star$ is the stellar radius, $\dot{M}$ is the mass-loss rate, and v_∞ is the terminal wind speed. Simulations with typical parameters for OB stars predict high post-shock temperatures of about 20−30 MK (1.7−2.6 keV). Furthermore, in the case of oblique rotators, i.e. when the rotational and magnetic axes are misaligned, rotational modulation of the X-ray emission can be observed. This might be the case of our source B5 Ie (Id.#60 ≡ Cyg#12) for which $kT_2 = 1.56$ keV and the light-curve shows, during our observation, a gradual decay (cf. Figs. 7 and 12).
- *Highly compressed wind shocks* in evolved O-type stars or *colliding winds* in the case of early-type binary systems (Stevens et al. 1992; Raassen et al. 2003). Our source #568 (Cyg#8) is an O6If + O5.5III(f) supergiant-giant pair, whose X-ray spectrum indicates hot thermal plasma at $kT_2 = 2.64 \pm 0.07$ keV. A colliding wind scenario is moreover suggested by the presence of the FeK$_\alpha$ complex (6.4 + 6.7 keV) in its spectrum[20] (cf. Fig. 12). The other two O-type supergiants, sources #544 (O3 If) and #625 (O5 If, see Fig. 12), although requiring a second thermal component, show rather soft spectra and no FeK$_\alpha$ (6.4+6.7 keV) complex.
- *Inverse Compton scattering* of photospheric UV photons by relativistic particles that are Fermi-accelerated in shocks within the chaotic stellar winds of OB supergiants (cf. Chen & White 1991). The actual production of the needed relativistic electrons by stellar wind shocks is, however, still in doubt. We can likely rule out this possibility for our Cygnus OB2 OB stars, given that all of them are well fit by thermal emission models in which the lines of several elements give a significant contribution.

One of the most intriguing and so far unexplained observational results regarding the X-ray emission of O- and early B- type stars is the existence of a simple proportionality between the X-ray luminosity ($L_{\rm x}$), and the bolometric luminosity ($L_{\rm bol}$) (Berghoefer et al. 1997). We explore this relationship for Cygnus OB2 O- and early B-type stars in Fig. 11. $L_{\rm x}$ values were calculated from our X-ray spectral analysis. Bolometric luminosities with relative uncertainties were estimated form the known spectral types and the calibrations given by Martins et al. (2005).

[20] The temperatures reached by hydrodynamic shocks in the winds of single stars are usually not high enough to produce significant Fe K$_\alpha$ emission. In wide early-type binary systems, however, stellar winds collide with velocities close to v_∞ and are thus heated to sufficiently high temperatures. In such cases, the cooler surrounding wind material, excited by the high energy radiation, can produce the 6.4 keV fluorescent Fe line. The observation of the Fe-complex can thus be a used as diagnostic for colliding-wind binaries (Raassen et al. 2003).

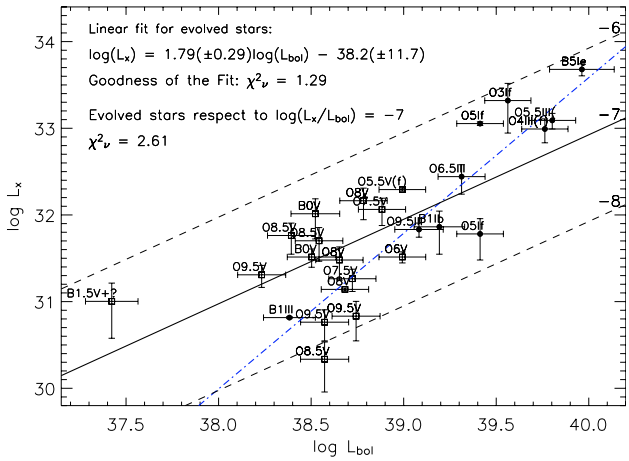

Fig. 11. X-ray versus bolometric luminosity for main-sequence and evolved OB-type stars (open and filled symbols, respectively) in the Cygnus OB2 region. The dotted and continuous lines indicate log $L_{\rm x}/L_{\rm bol} = -6, -7$, and -8. Evolved stars (i.e. giants and supergiants) seems to follow a power-law relation with index ∼1.8 (dashed line).

The proportionality between $L_{\rm x}$ and $L_{\rm bol}$ is retrieved, albeit with a large dispersion. However, when we distinguish between main sequence stars and evolved ones (i.e. giants and supergiants), we discover, for these latter, an apparently tight $L_{\rm x} - L_{\rm bol}$ relationship which is not a simple proportionality. For evolved stars, the χ^2_ν with respect to the $L_{\rm X} = 10^{-7}\ L_{\rm bol}$ relation is 2.61, while if we adopt the best-fit power law (with index $\Gamma \sim 1.8$) the χ^2_ν is reduced to ∼1.3. We test the statistical significance of including this additional degree of freedom in the $L_{\rm x}/L_{\rm bol}$ relation. We used a F$_\chi$-test as described in Bevington et al. 1969. We found that F$_\chi$-test ∼0.6, which does not indicate a significant improvement of the quality of the fit (F$_\chi$ should be greater than 1.1), even when adopting a significance level as high as 0.1. However, this result is affected by the small number of evolved O and B stars in our sample. A similar analysis with more stars from other regions will be needed to confirm, or disprove, this tentative result.

A more detailed study of the physical origins of the X-ray emission from OB stars and on its dependence on stellar wind parameters will be presented in forthcoming paper.

7.1.1. Specific sources

We now discuss the results of our analysis for three noteworthy OB stars in the ACIS FOV that have been the subject of previous investigations.

- **Cygnus OB2 #8** (ACIS source # 568). It has recently been classified as an O6If + O5.5III(f) binary with a 21.9d period and strong evidence of phase-locked X-ray variability (De Becker & Rauw 2005). Our observation only covers ∼5% of the orbital period and we do not detect variability. Cygnus OB2 #8 has also been observed by Waldron et al. (2004) with the *Chandra* High Energy transmission Grating Spectrometer (HETGS). They fit the X-ray spectrum with a a 2T thermal model with $T_1 = 3.98 \pm 1.67$ MK (0.34 ± 0.14 keV) and T_2 13.88 ± 1.80 MK (1.2 ± 0.15 keV) and obtain an $L_{\rm x}/L_{\rm bol}$ ratio of $\sim 1.8 \times 10^{-7}$. The spectral parameters are in rough agreement with those obtained here (see Fig. 12 and results presented in Table 4), but we find a somewhat higher $L_{\rm x}/L_{\rm bol}$, $\sim 4.0 \times 10^{-7}$. The discrepancy is

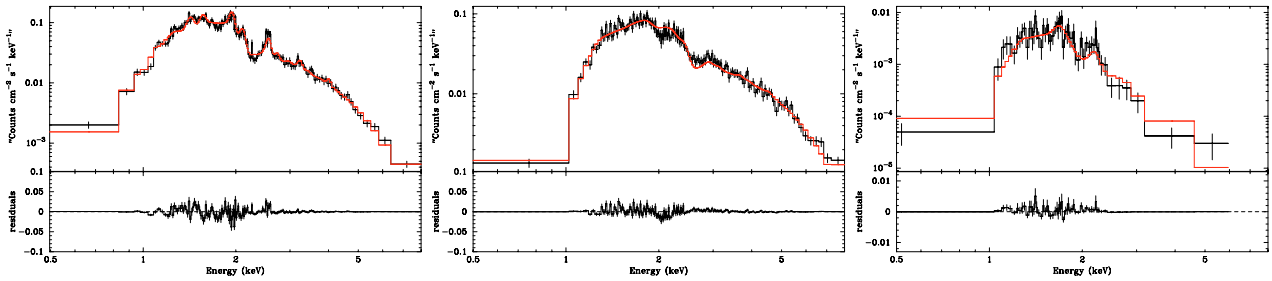

Fig. 12. ACIS-I spectra of three OB stars. The data were fitted with absorbed two temperatures optically thin thermal plasma models. *Left*: Cyg#12 (Src.Id. #60), showing a prominent FeK 6.7 keV emission line, indicative of hot thermal plasma. *Center*: Cyg#8 (Src.Id. #568), a colliding wind binary with a strong FeK$_\alpha$ blend at 6.4+6.7 keV, arguing in favor of the thermal nature of the hard part of the spectrum and consistent with the expected emission from a colliding wind region (Raassen et al. 2003). *Right*: source #625 (O5.5 If), a typical super-giant fit with a 1-T model with a soft temperature model: $KT_1 = 0.55 \pm 0.06$ keV.

however due exclusively to the different adopted bolometric luminosities: Waldron et al. (2004) use $\log L_{\rm bol} = 39.79$ from Bieging et al. (1989), while here we adopt $\log(L_{\rm bol}) = 39.4$ obtained from Herrero et al. (2002).

– **Cygnus OB2 #9** (ACIS source #488). An O5 If super giant, it is the strongest and most variable non-thermal radio emitter in Cygnus OB2 (Van Loo 2005). In X-rays it is however fainter than other evolved stars. Cygnus OB2 #9 has not been indicated as a binary in the literature. However, periodic radio variability has been observed with a period of ∼2.35 yr (Blomme, private communication). Waldron et al. (1998) did not detect variability in *EINSTEIN* and *ROSAT* X-ray data. Rauw et al. (2005) successfully fit the XMM-Newton EPIC X-ray spectrum with an absorbed 2-T thermal model ($kT_1 = 0.63 \pm 0.03$ and $kT_2 \sim 2.4$ keV). These results are roughly consistent with ours (cf. Table 4).
– **Cygnus OB2 #12** (ACIS source # 60) has been variously classified and its spectral type is probably variable. Most investigations however agree with an extremely luminous B supergiant B5 Ie (Hanson 2003), possibly related to the Luminous Blue Variable (LBV) phenomenon. Two-dimensional spectral classification suggests a B5+/−0.5 Ia$^+$ spectral type (Klochkova & Chentsov 2004). In our near-IR color–color diagram (Fig. 3), Cygnus OB2 #12 appears to be highly absorbed and to be affected by a near-IR excess typical of Herbig AeBe stars (Lada & Adams 1992). Klochkova & Chentsov (2004) present evidence of a line radial velocity gradient that can be interpreted as an indication of matter infall. These findings suggest the existence of an accretion disk around the star.
The *XMM-Newton* EPIC spectrum of Cygnus OB2 #12 was also fitted by Rauw et al. (2005), who find temperatures $kT_1 = 0.73 \pm 0.16$ and $kT_2 = 1.8 \pm 0.4$ keV, consistent with our own estimation (see Fig. 12 and Table 4). The temperature of the hard component is significantly higher than expected according to the wind shock emission model, given the low velocity of the stellar wind, ∼150 km s^{-1}. Emission from MCWS might better explain the spectrum (see above). Such a scenario could also explain the observed X-ray variability (see Sect. 5) if the magnetosphere is tilted with respect to the rotation axis as in the case of θ^1 Orionis C (Gagné et al. 2005).

7.2. Intermediate-mass stars

Intermediate-mass stars ($2.8 < M/M_\odot < 10$) are not expected to emit X-rays because, unlike O- and early B stars, they do not drive strong stellar winds nor possess outer convective zones that can sustain a dynamo mechanism such as the one that is ultimately held responsible for X-ray activity in low-mass stars. Several studies have however observed X-ray emission apparently associated with late B- and A-type stars. Although its origin has been often attributed to the coronal activity of unresolved late-type companions (e.g. Stelzer et al. 2006a,b), the matter is controversial. The Cygnus OB2 region has a large number of intermediate mass stars. It is therefore an ideal target to check this hypothesis. We classify 66 ACIS sources as intermediate-mass. The $L_{\rm X}$ vs. mass plot in Fig. 11 does not reveal any dramatic discontinuity at the boundaries with low and high mass stars. Intermediate mass stars, however, do not seem to follow the trend of increasing $L_{\rm X}$ with mass of lower mass stars, and seem to have $L_{\rm X}$ values that span the whole range spanned by these latter. This observation is consistent with the companion scenario.

As further supporting evidence for this conclusion we note that 8 of the X-ray sources associated with intermediate mass stars (about 12% of the sample) are variable, which is almost the same fraction found for low-mass stars (see Sect. 6.3). Moreover, their X-ray spectra are well represented by isothermal models with median $kT = 2.6$ keV, also in agreement with values found for low mass stars (see Sect. 7.3).

At the distance of Cygnus OB2 an offset between IR and X-ray positions of 1″, i.e. roughly the *on-axis Chandra* spatial resolution, corresponds to a projected separation of 1450 AU. X-ray source positions can however be determined with a precision of ∼0.1″ (145 AU) or even better, depending on the source statistics and off-angle. If the intermediate-mass primary of a binary system is X-ray dark we should thus be able to distinguish, at least statistically, whether the observed X-ray emission originates from the low mass secondary in the case of *wide* binary systems, defined as systems with separation >0.001 pc (206 AU) (cf. Close et al. 1990). Figure 13 shows an example of an X-ray source associated with an intermediate-mass counterpart, but with a significant spatial offset. A comparison of the distributions of X-ray-NIR offsets for X-ray sources associated with low and intermediate mass counterparts is however inconclusive. If the companion hypothesis is correct, most X-ray emitting low-mass companions are not in wide systems.

7.3. Low-mass stars

The origin of X-ray activity in low-mass PMS stars has so far eluded full understanding. Although many aspects of MS coronal activity also are not understood, the X-ray activity of MS

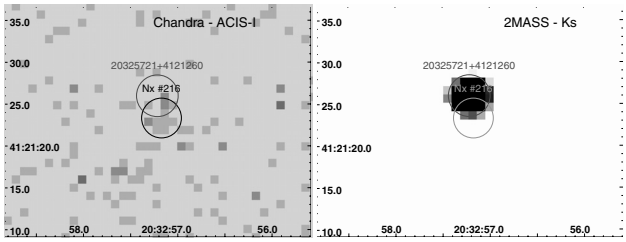

Fig. 13. Example of a possible misidentification of an X-ray source with a intermediate-mass near-IR star. We show the X-ray and K_s-band images of ACIS source #216. The X-ray and 2MASS positions differ by ∼2.5 arcsec (∼1.8×10^{-2} pc at the Cygnus OB2 distance). The X-ray source might be instead associated with a faint near-IR source undetected in 2MASS.

stars correlates well with stellar rotational and convection properties, thus supporting the picture of a solar-like corona that is ultimately powered by a stellar dynamo. For Pre-Main Sequence (PMS) stars, however, no such a correlation has been found and the picture appears somewhat complicated by the presence of accretion disks, which seem to play an important role in the X-ray emission. On one hand plasma heated by shocks due to the accretion process is likely to be a source of soft X-rays (cf. Kastner et al. 2002; Stelzer & Schmitt 2004; Favata et al. 2005; Flaccomio et al. 2006). On the other hand the presence of accretion disks seems to lower the overall activity level, although probably making the X-ray emission harder and more time variable (Flaccomio et al. 2003; Preibisch et al. 2005; Flaccomio et al. 2006).

We have defined the low mass range $M < 2.8\ M_\odot$, based on the presence of a significant convection envelope. The X-ray spectra and luminosities of low mass stars in Cygnus OB2 are typical of T-Tauri stars in other regions: our spectral analysis (Sect. 6) yields a median $kT = 2.38$ keV and $\log N_H = 22.23$. Figure 10 indicates that, although the spread of L_x at any given mass is of the order of 1 dex, a trend of increasing L_x with mass is observed. The same figure shows for comparison the nearly complete sample of Orion Nebular Cluster (ONC) stars as observed by the Chandra Orion Ultra-deep Project (COUP) (Getman et al. 2005b). The sensitivity limits of the two observations are quite different because of the larger distance of Cygnus OB2 (∼1450 pc vs. 470 pc for the ONC), and the longer exposure time of the COUP observation (∼838 vs. ∼97 ks for our data). However, as already discussed, the most severe limit to the completeness of our sample of likely members with near-IR counterparts is likely to be the sensitivity limit of the 2MASS data. The Cygnus OB2 stars in Fig. 10 have a well defined limit of mass, at ∼0.4−0.5 $M_\odot$, rather than X-ray luminosity.

Figure 10 shows that the luminosities of low mass stars in Cygnus OB2 and in the ONC are compatible. The numbers of stars in the 1.0−2.8 $M_\odot$ mass range in the Cygnus OB2 and ONC regions differ considerably. In Cygnus OB2 we count 334 such stars, about 10 times as many as the in a sample of 375 COUP-detected lightly absorbed ($A_v < 2$) ONC stars with mass estimates, in which we find 34 stars in the same range (Getman et al. 2005b). Assuming that the IMFs in the two regions are the same and that the considered sample of lightly absorbed ONC stars is complete, we can estimate the total number of stars in our Cygnus OB2 ACIS FOV as $375/34 \times 334 \sim 3700$. Considering that our FOV contains only one fourth of the 106 OB stars known in Cygnus OB2, we can then scale this number by the number of OB stars to get the total expected Cygnus OB2 population: ∼15 000 stars. The total stellar mass of the cluster can be then estimated by multiplying this number by the average stellar mass in the lightly absorbed COUP sample ($0.84\ M_\odot$): $M_{cl} \sim 1.2 \times 10^4\ M_\odot$, somewhat lower than the estimate of Knödlseder (2000), who derived $4-10 \times 10^4\ M_\odot$.

Deeper and more extended X-ray and near-IR surveys of Cygnus OB2 will be invaluable for the study of young stars of all masses with unprecedented statistic. Such observations has been recently obtained at the TNG observatory, and we will present such results in a forthcoming paper.

8. Summary and conclusions

We have reported the results of a deep *Chandra* X-ray observation pointed toward the ∼2 Myr old star forming region Cygnus OB2. Source detection was performed using PWDdetect, a wavelet-based algorithm, supplemented by visual inspection, identifying 1003 X-ray sources in the $17' \times 17'$ ACIS-I field of view. Data extraction was performed using the semi-automated IDL-based ACIS EXTRACT package, which is well suited to the analysis of observations of crowded fields such as ours.

The X-ray source list was cross-identified with optical and near-IR (2MASS) catalogs: 26 X-ray sources were identified with optically characterized OB members of Cygnus OB2 (out of the 33 lying in the FOV) and 775 with 2MASS sources. Among these latter sources almost all are believed to be Cygnus OB2 members. About ∼80 X-ray sources without an optical/NIR counterpart are estimated to be of extragalactic nature (AGNs) while the remaining X-ray sources with no counterpart are likely associated with members that are fainter than the 2MASS completeness limit.

In order to characterize the previously unidentified likely cluster members with NIR counterparts, we placed them on NIR color–magnitude (K_s vs. $H - K_s$) and color–color ($H - K_s$ vs. $J-H$) diagrams. A first estimate of interstellar extinction was obtained adopting a 2 Myr isochrone for the low- and intermediate-mass stars and assuming that O- and early B-type stars lie on the MS. We find a median visual absorption for OB stars of $A_v \sim 5.6$ mag, while low mass likely members seem to be slightly more absorbed, $A_v \sim 7.0$ mag. We also use the 2 Myr isochrone and the J magnitude to estimate masses of likely members assuming that they share the same distance and absorption. Our sample of X-ray selected members with near-IR counterparts reaches down to $M = 0.4-0.5\ M_\odot$, and is likely complete down to $\sim 1\ M_\odot$. From the $H - K_s$ vs. $J - H$ diagram we estimate the fraction of low-mass stars with NIR excesses (23/519), finding it to be quite low with respect to the 1 Myr old ONC region indicating that either (i) the disk fraction decreases steeply with stellar age, or (ii) the intense photo-evaporating UV-field due to the large population of O stars in the region has reduced the disk lifetime.

At least 85 or 134 X-ray sources, i.e. ∼8.5% and 13% of the total, were found to be variable within our observation with a confidence level of 99.9% or 99%, respectively. The fraction of variable sources increases with increasing source counts, likely as a result of a statistical bias. The light-curves of 97 sources indicate an impulsive, flare-like, behavior while the rest show more gradual variations of the X-ray emission. Only two of the 24 detected O- and early B-type stars are detected as variable during our 97 ks observation, in spite of the high statistic of their light-curves. These exceptions are the B5 Ie star Cygnus#12 (our source #60), showing a rather linear decay of the count rate during the observation, and a B1.5 V+? star (#979), which also shows a slow variability, possibly related to rotational modulation. In this latter case the detected emission may originate

from the primary B1.5 component and/or from its presumably lower mass companion indicated by the spectral type published by Hanson (2003).

We modeled the ACIS X-ray spectra of sources with more than 20 photons assuming absorbed thermal emission models. Median $\log(N_{\rm H})$ and kT values of the sources are 22.25 ($\rm cm^{-2}$) and 2.36 keV, respectively. Variable sources, $P_{\rm KS} < 0.01$ have harder spectra (median kT: 3.3 keV) than non-variable ones (median kT:2.1 keV) and flaring sources are even harder (median kT:3.8). Sources associated with O- and early B-type stars are instead quite soft (median kT: 0.75 keV). Absorption corrected X-ray luminosities of OB stars were calculated from the best fit spectral models. For the other, typically fainter, sources, we adopted a single count-rate to flux conversion factor computed from the results of individual spectral fits. Low mass stars have $L_{\rm x}$ ranging between 10^{30} and 10^{31} erg s^{-1} (median 2.5×10^{30}). Variable low mass stars are on average 0.4 dex brighter, probably because of a selection effect. These X-ray luminosities are consistent with those of similar mass stars in the slightly younger (1 Myr) ONC region. O and B-type stars are the most luminous, with $L_{\rm x} = 2.5 \times 10^{30}$–$6.3 \times 10^{33}$ erg s^{-1}. Their X-ray and bolometric luminosities are in rough agreement with the relation $L_{\rm x}/L_{\rm bol} = 10^{-7}$, albeit with an order of magnitude dispersion. The X-ray luminosities of the 10 *evolved* OB stars in our sample however, seem to obey a better defined and steeper power-law relation with $L_{\rm bol}$: $L_{\rm x} \propto L_{\rm bol}^{1.8}$). Further studies of a larger number of evolved OB-type stars are needed to confirm or disprove this dependence.

Acknowledgements. This publication makes use of data products from the Two Micron All Sky Survey, which is a joint project of the University of Massachusetts and the Infrared Processing and Analysis Center/California Institute of Technology, funded by the National Aeronautics and Space Administration and the National Science Foundation. J.F.A.C acknowledges support by the Marie Curie Fellowship Contract No. MTKD-CT-2004-002769 of the project "*The Influence of Stellar High Energy Radiation on Planetary Atmospheres*", and the host institution INAF - Osservatorio Astronomico di Palermo (OAPA). E. F., G. M., F. D. and S. S. acknowledge financial support from the Ministero dell'Universita' e della Ricerca research grants, and ASI/INAF Contract I/023/05/0.

References

Adams, F. C., Hollenbach, D., Laughlin, G., & Gorti, U. 2004, ApJ, 611, 360
Alexander, D. M., Bauer, F. E., Brandt, W. N., et al. 2003, AJ, 126, 539
Anders, E., & Grevesse, N. 1989, Geochim. Cosmochim. Acta, 53, 197
Arnaud, K. 2004, AAS/High Energy Astrophysics Division, 8
Bally, J., O'Dell, C. R., & McCaughrean, M. J. 2000, AJ, 119, 2919
Barger, A. J., Cowie, L. L., Capak, P., et al. 2003, AJ, 126, 632
Berghoefer, T. W., Schmitt, J. H. M. M., Danner, R., & Cassinelli, J. P. 1997, A&A, 322, 167
Bessell, M. S., & Brett, J. M. 1989, LNP Vol. 341, Infrared Extinction and Standardization, 341, 61
Bevington, P. R. 1969, Data reduction and error analysis for the physical sciences (New York: McGraw-Hill), 1969
Bieging, J. H., Abbott, D. C., & Churchwell, E. B. 1989, ApJ, 340, 518
Broos, P., Townsley, L., Getman, K., & Bauer, F. 2002, ACIS Extract, An ACIS Point Source Extraction Package, `http://www.astro.psu.edu/xray/docs/TARA/`
Chen, W., & White, R. L. 1991, ApJ, 366, 512
Close, L. M., Richer, H. B., & Crabtree, D. R. 1990, AJ, 100, 1968
Damiani, F., Maggio, A., Micela, G., & Sciortino, S. 1997a, ApJ, 483, 350
Damiani, F., Maggio, A., Micela, G., & Sciortino, S. 1997b, ApJ, 483, 370
Damiani, F., Flaccomio, E., Micela, G., et al. 2003, ApJ, 588, 1009
De Becker, M., & Rauw, G. 2005, in Massive Stars and High-Energy Emission in OB Associations, ed. G. Rauw, Y. Nazé, & E. R. Blomme, Gosset, 73
Favata, F., & Micela, G. 2003, Space Sci. Rev., 108, 577
Favata, F., Flaccomio, E., Reale, F., et al. 2005, ApJS, 160, 469
Feigelson, E. D., Broos, P., Gaffney, J. A., et al. 2002, ApJ, 574, 258
Feldmeier, A., Puls, J., & Pauldrach, A. W. A. 1997, A&A, 322, 878
Flaccomio, E., Damiani, F., Micela, G., et al. 2003, ApJ, 582, 382
Flaccomio, E., Micela, G., Sciortino, S., et al. 2005, ApJS, 160, 450
Flaccomio, E., Micela, G., & Sciortino, S. 2006, ArXiv Astrophysics e-prints
Gagné, M., Oksala, M. E., Cohen, D. H., et al. 2005, ApJ, 634, 712
Garmire, G. P., Bautz, M. W., Ford, P. G., Nousek, J. A., & Ricker, G. R. 2003, in X-Ray and Gamma-Ray Telescopes and Instruments for Astronomy, ed. Joachim E. Truemper, & Harvey D. Tananbaum, Proc. SPIE, 4851, 28
Getman, K. V., Feigelson, E. D., Townsley, L., et al. 2002, ApJ, 575, 354
Getman, K. V., Feigelson, E. D., Grosso, N., et al. 2005a, ApJS, 160, 353
Getman, K. V., Flaccomio, E., Broos, P. S., et al. 2005b, ApJS, 160, 319
Guarcello, M., Prisinzano, L., Micela, G., et al. 2006, A&A, in prep.
Hanson, M. M. 2003, ApJ, 597, 957
Harnden, F. R., Branduardi, G., Gorenstein, P., et al. 1979, ApJ, 234, L51
Herrero, A., Puls, J., & Najarro, F. 2002, A&A, 396, 949
Hillenbrand, L. A. 2005, ArXiv Astrophysics e-prints
Johnson, H. L., & Morgan, W. W. 1954, ApJ, 119, 344
Kastner, J. H., Huenemoerder, D. P., Schulz, N. S., Canizares, C. R., & Weintraub, D. A. 2002, ApJ, 567, 434
Kenyon, S. J., & Hartmann, L. 1995, ApJS, 101, 117
Kitamoto, S., & Mukai, K. 1996, PASJ, 48, 813
Klochkova, V. G., & Chentsov, E. L. 2004, Astron. Rep., 48, 1005
Knödlseder, J. 2000, A&A, 360, 539
Knödlseder, J., Cerviño, M., Le Duigou, J.-M., et al. 2002, A&A, 390, 945
Lada, C. J., & Adams, F. C. 1992, ApJ, 393, 278
Lucy, L. B., & White, R. L. 1980, ApJ, 241, 300
Martins, F., Schaerer, D., & Hillier, D. J. 2005, A&A, 436, 1049
Massey, P., & Thompson, A. B. 1991, AJ, 101, 1408
Meyer, M. R., Calvet, N., & Hillenbrand, L. A. 1997, AJ, 114, 288
Morrison, R., & McCammon, D. 1983, ApJ, 270, 119
Owocki, S. P., & Cohen, D. H. 1999, ApJ, 520, 833
Owocki, S. P., Castor, J. I., & Rybicki, G. B. 1988, ApJ, 335, 914
Owocki, S., Townsend, R., & Ud-Doula, A. 2005, in Magnetic Fields in the Universe: From Laboratory and Stars to Primordial Structures, ed. E. M. de Gouveia dal Pino, G. Lugones, & A. Lazarian, AIP Conf. Proc., 784, 239
Preibisch, T. 2003, A&A, 401, 543
Preibisch, T., Kim, Y.-C., Favata, F., et al. 2005, ApJS, 160, 401
Press, W. H., Teukolsky, S. A., Vetterling, W. T., & Flannery, B. P. 1992, Numerical recipes in FORTRAN. The art of scientific computing (Cambridge: University Press), 2nd ed.
Prestwich, A. H., Irwin, J. A., Kilgard, R. E., et al. 2003, ApJ, 595, 719
Raassen, A. J. J., van der Hucht, K. A., Mewe, R., et al. 2003, Adv. Space Res., 32, 1161
Rauw, G., De Becker, M., & Linder, N. 2005, in Massive Stars and High-Energy Emission in OB Associations, ed. G. Rauw, Y. Nazé, & E. R. Blomme, Gosset, 103
Raymond, J. C., & Smith, B. W. 1977, ApJS, 35, 419
Ryter, C. E. 1996, Ap&SS, 236, 285
Schulte, D. H. 1958, ApJ, 128, 41
Schulz, N. S., Hasinger, G., & Truemper, J. 1989, A&A, 225, 48
Schulz, N. S., Canizares, C., Huenemoerder, D., & Tibbets, K. 2003, ApJ, 595, 365
Siess, L., Dufour, E., & Forestini, M. 2000, A&A, 358, 593
Smith, R. K., Brickhouse, N. S., Liedahl, D. A., & Raymond, J. C. 2001, ApJ, 556, L91
Stelzer, B., & Schmitt, J. H. M. M. 2004, A&A, 418, 687
Stelzer, B., Huélamo, N., Micela, G., & Hubrig, S. 2006a, A&A, 452, 1001
Stelzer, B., Micela, G., Hamaguchi, K., & Schmitt, J. H. M. M. 2006b, ArXiv Astrophysics e-prints
Stevens, I. R., Blondin, J. M., & Pollock, A. M. T. 1992, ApJ, 386, 265
Torres-Dodgen, A. V., Carroll, M., & Tapia, M. 1991, MNRAS, 249, 1
ud-Doula, A., & Owocki, S. P. 2002, ApJ, 576, 413
Van Loo, S. 2005, Ph.D. Thesis
Waldron, W. L., Corcoran, M. F., Drake, S. A., & Smale, A. P. 1998, ApJS, 118, 217
Waldron, W. L., Cassinelli, J. P., Miller, N. A., MacFarlane, J. J., & Reiter, J. C. 2004, ApJ, 616, 542
Weisskopf, M. C., Brinkman, B., Canizares, C., et al. 2002, PASP, 114, 1
Wolk, S. J., Harnden, F. R., Flaccomio, E., et al. 2005, ApJS, 160, 423

Online Material

Table 1. Cygnus OB2 source catalog.

N_x	NAME	RA	Dec	Error	θ	Sig.	Area	PSF	Cts	Exp.	Count Rates ($\times10^{-3}$ ctn s^{-1})				$\overline{E_x}$	Var.
#	CXOCYG J+	[h:m:s]	[d:m:s]	($''$)	($'$)	(σ)	(px.)	(%)	(ph.)	(ks)	Tot.	Soft	Med.	Hard	(keV)	log(P_{ks})
1	203225.09+411019.6	20:32:25.09	41:10:19.60	0.62	10.03	6.55	1170	0.90	67	87.8255	0.855	0.135	0.233	0.487	3.23	−4.00 †
2	203225.55+410847.3	20:32:25.55	41:08:47.36	0.70	10.76	6.66	1429	0.89	72	92.9360	0.871	0.620	0.059	0.192	1.35	−0.65
3	203225.97+411054.7	20:32:25.97	41:10:54.77	0.75	9.62	4.28	973	0.90	35	90.9414	0.434	0.099	0.153	0.182	2.37	−0.32
4	203227.51+411358.3	20:32:27.52	41:13:58.37	0.88	8.47	2.30	630	0.89	14	92.5496	0.173	0.004	0.060	0.109	3.18	−0.17
5	203227.62+410831.4	20:32:27.63	41:08:31.46	0.76	10.61	5.92	1420	0.91	55	96.8402	0.637	0.160	0.198	0.278	2.36	−0.00
6	203227.70+411317.0	20:32:27.71	41:13:17.07	0.26	8.55	13.38	618	0.89	216	96.5481	2.521	0.529	0.862	1.130	2.61	−4.00 †
7	203228.88+410807.5	20:32:28.89	41:08: 7.59	0.80	10.67	5.09	1623	0.90	49	96.6863	0.571	0.136	0.167	0.268	2.75	−2.37 †
8	203229.12+411400.7	20:32:29.12	41:14: 0.78	0.55	8.16	4.09	545	0.89	33	92.8669	0.400	0.130	0.078	0.192	2.62	−0.59
9	203229.26+410850.1	20:32:29.26	41:08:50.17	0.59	10.17	6.70	834	0.82	64	92.6690	0.842	0.364	0.202	0.276	2.02	−0.44
10	203229.84+411454.2	20:32:29.85	41:14:54.27	0.50	7.97	5.56	525	0.90	50	93.3914	0.605	0.249	0.185	0.171	2.24	−0.67
11	203229.91+411056.0	20:32:29.92	41:10:56.06	0.72	8.94	2.77	751	0.90	19	92.9014	0.227	0.080	0.058	0.089	2.30	−0.97
12	203230.63+410829.1	20:32:30.64	41:08:29.11	0.58	10.19	8.52	1205	0.90	99	94.5473	1.173	0.320	0.478	0.375	2.14	−0.08
13	203230.63+410854.8	20:32:30.63	41:08:54.82	0.66	9.92	5.21	784	0.83	44	96.4507	0.552	0.067	0.180	0.305	2.93	−1.14 †
14	203230.88+411029.5	20:32:30.89	41:10:29.53	0.46	8.99	7.08	761	0.90	75	96.5167	0.867	0.063	0.176	0.628	3.42	−0.07
15	203231.39+410955.9	20:32:31.40	41:09:55.98	0.57	9.21	6.16	821	0.90	60	94.7546	0.714	0.259	0.168	0.287	2.27	−0.01
16	203231.42+411335.0	20:32:31.43	41:13:35.01	0.55	7.80	3.85	480	0.90	30	93.4071	0.357	0.039	0.098	0.220	3.01	−0.33
17	203231.53+411407.9	20:32:31.53	41:14: 7.98	0.05	7.70	55.14	431	0.89	3173	97.6726	36.534	14.545	13.742	8.247	1.85	−2.83
18	203231.58+411712.5	20:32:31.58	41:17:12.52	0.73	7.95	2.01	517	0.90	12	92.8637	0.145	0.007	0.049	0.089	3.10	−0.04
19	203232.32+411507.3	20:32:32.32	41:15: 7.30	0.56	7.50	3.55	418	0.89	25	94.0133	0.306	0.031	0.097	0.177	3.23	−0.02
20	203232.44+411312.3	20:32:32.45	41:13:12.36	0.43	7.69	5.60	413	0.89	49	93.2124	0.592	0.112	0.202	0.278	2.64	−2.69 †
21	203233.28+411058.8	20:32:33.29	41:10:58.88	0.75	8.36	2.82	575	0.90	18	88.3312	0.230	0.162	0.034	0.034	1.15	−0.44
22	203233.47+411218.0	20:32:33.48	41:12:18.04	0.49	7.77	4.49	459	0.90	34	91.7675	0.415	0.177	0.127	0.111	1.82	−0.04
23	203233.53+411405.7	20:32:33.54	41:14: 5.74	0.38	7.33	5.47	364	0.90	50	95.7566	0.593	0.199	0.201	0.193	1.92	−0.49
24	203234.33+411506.3	20:32:34.34	41:15: 6.33	0.54	7.12	3.71	350	0.90	26	94.3211	0.311	0.074	0.056	0.181	3.52	−0.44
25	203234.45+411154.7	20:32:34.45	41:11:54.74	0.58	7.75	3.96	446	0.90	27	94.8080	0.326	0.061	0.203	0.062	2.06	−0.26
26	203235.17+411143.4	20:32:35.18	41:11:43.48	0.47	7.70	4.97	430	0.90	39	91.6010	0.475	0.196	0.159	0.120	1.96	−0.03
27	203235.65+411509.5	20:32:35.65	41:15: 9.50	0.33	6.88	7.09	312	0.90	70	96.3691	0.815	0.228	0.368	0.219	2.10	−1.17
28	203235.86+411248.4	20:32:35.87	41:12:48.42	0.37	7.18	5.22	340	0.90	43	93.8249	0.519	0.083	0.289	0.147	2.04	−2.14 †
29	203235.96+412135.6	20:32:35.97	41:21:35.64	0.78	9.47	4.51	669	0.83	33	95.8351	0.413	0.190	0.064	0.159	1.85	−0.11
30	203236.32+411900.7	20:32:36.32	41:19: 0.76	0.47	7.84	4.96	489	0.90	41	94.6415	0.484	0.209	0.129	0.146	1.76	−0.44
31	203236.38+411831.0	20:32:36.39	41:18:31.08	0.62	7.59	3.81	403	0.89	26	90.0839	0.333	0.242	0.060	0.032	1.41	−1.46
32	203236.50+411810.3	20:32:36.50	41:18:10.36	0.67	7.42	3.78	376	0.89	26	91.6356	0.320	0.115	0.112	0.093	1.90	−1.55
33	203236.62+412214.5	20:32:36.63	41:22:14.52	0.26	9.85	14.02	689	0.81	232	97.5187	2.949	1.112	0.835	1.002	1.93	−4.00 †
34	203236.86+411944.6	20:32:36.86	41:19:44.62	0.40	8.16	7.22	544	0.90	74	97.0381	0.859	0.295	0.288	0.277	1.86	−0.83
35	203236.84+412146.1	20:32:36.85	41:21:46.11	0.56	9.48	5.65	660	0.83	46	95.1661	0.592	0.278	0.162	0.153	1.82	−1.24
36	203237.55+411150.8	20:32:37.55	41:11:50.86	0.38	7.25	5.53	345	0.90	45	97.5878	0.517	0.345	0.142	0.030	1.31	−0.29
37	203237.53+411712.4	20:32:37.54	41:17:12.41	0.33	6.88	6.04	305	0.90	55	83.4533	0.736	0.058	0.359	0.319	2.68	−4.00 †
38	203237.71+411405.3	20:32:37.72	41:14: 5.36	0.44	6.55	3.92	242	0.90	29	97.2737	0.336	0.093	0.156	0.087	2.18	−0.27
39	203237.83+412208.7	20:32:37.84	41:22: 8.76	0.44	9.62	8.34	650	0.81	91	96.8873	1.159	0.335	0.401	0.422	2.20	−1.56 †
40	203237.87+412119.0	20:32:37.87	41:21:19.02	0.41	9.02	8.98	821	0.91	109	95.6623	1.261	0.622	0.405	0.233	1.70	−0.01
41	203237.94+411502.7	20:32:37.95	41:15: 2.70	0.41	6.44	4.09	243	0.90	31	96.6172	0.368	0.119	0.147	0.103	1.89	−0.43
42	203238.10+410833.1	20:32:38.10	41:08:33.10	0.75	9.11	3.00	797	0.90	23	93.7243	0.276	0.073	0.074	0.130	2.64	−0.99
43	203238.10+411244.4	20:32:38.11	41:12:44.50	0.27	6.80	6.07	263	0.89	53	94.2018	0.635	0.078	0.243	0.315	2.74	−4.00 †
44	203238.07+412313.8	20:32:38.07	41:23:13.89	0.72	10.43	7.14	1564	0.91	83	96.7900	0.952	0.415	0.276	0.261	1.89	−0.17
45	203238.26+411141.7	20:32:38.26	41:11:41.75	0.62	7.20	3.11	337	0.90	18	84.2417	0.247	0.072	0.048	0.127	2.70	−0.01
46	203238.43+411201.1	20:32:38.44	41:12: 1.16	0.57	7.02	3.30	309	0.90	20	91.6764	0.248	0.041	0.126	0.081	2.37	−0.67

Table 1. continued.

N_x	NAME	RA	Dec	Error	θ	Sig.	Area	PSF	Cts	Exp.	Count Rates ($\times 10^{-3}$ ctn s^{-1})				$\overline{E}_x$	Var.
#	CXOCYG J+	[h:m:s]	[d:m:s]	($''$)	($'$)	(σ)	(px.)	(%)	(ph.)	(ks)	Tot.	Soft	Med.	Hard	(keV)	log(P_{ks})
47	203238.56+411422.0	20:32:38.56	41:14:22.10	0.35	6.36	4.79	223	0.90	42	92.4931	0.508	0.179	0.185	0.144	1.98	−0.69
48	203239.41+411906.3	20:32:39.42	41:19: 6.38	0.40	7.40	5.44	362	0.89	45	92.3423	0.556	0.225	0.146	0.185	1.98	−0.00
49	203239.52+411112.5	20:32:39.52	41:11:12.56	0.33	7.23	6.11	338	0.90	53	88.7678	0.668	0.098	0.307	0.263	2.28	−0.01
50	203239.82+412358.2	20:32:39.82	41:23:58.23	0.71	10.83	6.51	1799	0.91	78	94.3745	0.916	0.512	0.204	0.200	1.64	−0.45
51	203239.90+411348.1	20:32:39.91	41:13:48.18	0.36	6.19	4.12	202	0.90	32	92.5936	0.385	0.093	0.168	0.125	1.97	−2.91 †
52	203240.12+411034.7	20:32:40.12	41:10:34.75	0.21	7.49	11.29	386	0.90	156	93.9379	1.853	0.286	0.754	0.814	2.69	−4.00 †
53	203240.07+412201.7	20:32:40.08	41:22: 1.71	0.62	9.26	5.09	882	0.90	43	92.1538	0.527	0.277	0.172	0.078	1.69	−0.79
54	203240.22+412244.7	20:32:40.22	41:22:44.79	0.68	9.79	7.02	1053	0.89	73	94.9776	0.860	0.231	0.225	0.404	2.68	−1.06 †
55	203240.26+411740.9	20:32:40.27	41:17:40.92	0.39	6.57	4.53	250	0.90	33	88.9626	0.417	0.248	0.098	0.071	1.58	−0.03
56	203240.59+411454.8	20:32:40.60	41:14:54.82	0.21	5.95	6.62	123	0.83	62	97.4904	0.768	0.131	0.354	0.283	2.42	−0.00
57	203240.65+411111.6	20:32:40.66	41:11:11.62	0.40	7.06	4.32	306	0.90	30	94.3306	0.359	0.039	0.159	0.161	2.71	−2.31
58	203240.72+412106.1	20:32:40.72	41:21: 6.19	0.51	8.49	5.50	612	0.90	49	93.2061	0.585	0.195	0.164	0.226	2.08	−0.03
59	203240.81+411720.2	20:32:40.82	41:17:20.23	0.56	6.34	2.39	221	0.90	12	91.8900	0.151	0.100	0.024	0.027	1.50	−0.54
60	203240.94+411428.8	20:32:40.95	41:14:28.90	0.02	5.90	121.01	180	0.90	14913	97.7542	169.233	64.017	72.828	32.388	1.89	−4.00
61	203240.96+411551.0	20:32:40.96	41:15:51.09	0.33	5.94	5.18	170	0.89	40	94.3997	0.480	0.108	0.162	0.210	2.65	−0.50
62	203240.97+411449.6	20:32:40.98	41:14:49.67	0.35	5.88	3.40	124	0.84	23	95.2540	0.296	0.127	0.091	0.079	1.88	−0.03
63	203241.06+411955.2	20:32:41.07	41:19:55.23	0.53	7.64	3.41	431	0.90	24	93.3223	0.286	0.131	0.038	0.118	2.00	−0.12
64	203241.33+411849.9	20:32:41.34	41:18:49.97	0.28	6.95	7.59	282	0.89	77	96.2026	0.908	0.210	0.278	0.420	2.49	−3.85
65	203241.55+411154.7	20:32:41.56	41:11:54.70	0.49	6.55	2.45	223	0.89	13	95.1158	0.158	0.026	0.079	0.053	2.30	−0.29
66	203241.61+411549.0	20:32:41.62	41:15:49.02	0.61	5.81	2.38	181	0.91	12	83.6449	0.168	0.062	0.048	0.058	1.72	−0.00
67	203241.66+411406.5	20:32:41.66	41:14: 6.54	0.32	5.82	4.77	166	0.90	40	95.0216	0.478	0.149	0.144	0.184	2.52	−0.25
68	203241.87+411555.9	20:32:41.87	41:15:55.98	0.32	5.78	4.06	178	0.91	27	95.9199	0.315	0.090	0.152	0.073	2.02	−0.10
69	203242.15+411712.2	20:32:42.16	41:17:12.24	0.37	6.06	3.69	193	0.91	22	89.7981	0.280	0.062	0.100	0.118	2.64	−0.01
70	203242.18+411641.4	20:32:42.19	41:16:41.42	0.38	5.89	3.02	184	0.91	17	75.4940	0.255	0.105	0.061	0.089	1.86	−0.00
71	203242.46+412236.6	20:32:42.47	41:22:36.66	0.55	9.43	6.85	866	0.89	68	95.5210	0.801	0.339	0.319	0.143	1.82	−2.00
72	203242.88+412016.5	20:32:42.88	41:20:16.58	0.29	7.62	9.01	416	0.90	107	94.4154	1.266	0.641	0.355	0.270	1.65	−0.19
73	203242.86+412343.1	20:32:42.87	41:23:43.16	0.50	10.31	10.07	1396	0.90	138	97.5501	1.573	0.418	0.699	0.456	2.08	−0.14
74	203242.91+411914.4	20:32:42.91	41:19:14.42	0.29	6.94	8.23	274	0.89	89	97.7071	1.026	0.416	0.351	0.259	1.86	−4.00 †
75	203243.03+411741.1	20:32:43.04	41:17:41.10	0.51	6.10	3.27	197	0.91	19	94.7609	0.224	0.073	0.061	0.091	2.04	−0.02
76	203243.01+412309.3	20:32:43.02	41:23: 9.34	0.81	9.82	4.55	1094	0.91	38	91.2869	0.465	0.159	0.104	0.202	2.01	−0.33
77	203243.09+411359.3	20:32:43.10	41:13:59.34	0.26	5.57	4.77	142	0.90	38	97.5564	0.435	0.225	0.097	0.113	1.64	−0.79
78	203243.10+411750.9	20:32:43.10	41:17:50.96	0.45	6.16	2.88	201	0.91	16	79.7155	0.222	0.022	0.044	0.157	3.34	−0.23
79	203243.34+411514.1	20:32:43.34	41:15:14.19	0.37	5.43	2.76	143	0.90	16	91.6136	0.194	0.051	0.052	0.091	2.53	−0.26
80	203243.34+411657.1	20:32:43.34	41:16:57.12	0.68	5.76	2.67	167	0.90	13	84.9578	0.182	0.052	0.069	0.061	2.56	−1.01
81	203243.40+411102.9	20:32:43.40	41:11: 2.90	0.32	6.71	5.63	245	0.89	47	96.6737	0.545	0.167	0.189	0.189	2.20	−4.00 †
82	203243.95+411709.9	20:32:43.95	41:17: 9.93	0.41	5.73	4.16	163	0.90	27	96.1052	0.314	0.139	0.062	0.113	1.89	−0.10
83	203244.22+411615.7	20:32:44.22	41:16:15.75	0.37	5.41	3.12	141	0.90	18	63.5644	0.320	0.050	0.175	0.094	2.11	−0.96
84	203244.31+411743.8	20:32:44.31	41:17:43.81	0.41	5.91	3.69	176	0.90	22	93.1181	0.271	0.053	0.182	0.037	2.04	−0.26
85	203244.35+411445.3	20:32:44.36	41:14:45.35	0.26	5.25	4.21	109	0.89	29	90.8158	0.365	0.116	0.175	0.075	1.82	−0.17
86	203244.42+411122.9	20:32:44.43	41:11:22.95	0.50	6.36	2.55	204	0.89	13	89.0097	0.175	0.021	0.097	0.058	2.50	−0.02
87	203244.71+410701.4	20:32:44.71	41:07: 1.42	0.71	9.52	5.51	1290	0.90	52	97.3019	0.602	0.112	0.182	0.308	3.00	−0.10
88	203244.74+411305.4	20:32:44.74	41:13: 5.48	0.26	5.51	5.02	135	0.90	37	95.7063	0.434	0.076	0.152	0.205	2.77	−0.32
89	203244.81+411227.4	20:32:44.82	41:12:27.47	0.45	5.75	2.87	152	0.90	15	80.0861	0.217	0.075	0.074	0.069	2.23	−0.00
90	203244.82+411549.0	20:32:44.82	41:15:49.07	0.39	5.21	3.33	125	0.91	19	97.4747	0.226	0.041	0.105	0.081	2.12	−1.19
91	203244.85+411419.1	20:32:44.85	41:14:19.17	0.35	5.19	2.27	104	0.89	12	77.7838	0.179	0.008	0.046	0.125	4.30	−0.24
92	203244.83+411848.1	20:32:44.83	41:18:48.13	0.48	6.39	3.42	218	0.90	21	96.4099	0.252	0.115	0.084	0.053	1.89	−0.12
93	203244.90+411519.8	20:32:44.90	41:15:19.83	0.25	5.15	5.73	105	0.89	45	93.4825	0.544	0.160	0.210	0.174	2.08	−1.52

Table 1. continued.

N_x	NAME	RA	Dec	Error	θ	Sig.	Area	PSF	Cts	Exp.	Count Rates ($\times 10^{-3}$ ctn s^{-1})				$\overline{E}_x$	Var.
#	CXOCYG J+	[h:m:s]	[d:m:s]	($''$)	($'$)	(σ)	(px.)	(%)	(ph.)	(ks)	Tot.	Soft	Med.	Hard	(keV)	log(P_{ks})
94	203244.86+412350.5	20:32:44.87	41:23:50.60	0.63	10.22	7.21	1383	0.90	80	96.3377	0.929	0.440	0.310	0.178	1.77	−0.03
95	203245.08+411247.3	20:32:45.08	41:12:47.34	0.42	5.57	2.21	138	0.90	10	91.3906	0.127	0.049	0.041	0.037	2.14	−0.13
96	203245.08+411725.6	20:32:45.08	41:17:25.62	0.38	5.64	2.65	82	0.80	13	94.9650	0.173	0.043	0.072	0.058	2.20	−0.56
97	203245.24+411221.2	20:32:45.25	41:12:21.21	0.37	5.73	3.63	150	0.90	22	90.5676	0.275	0.128	0.054	0.093	1.74	−0.06
98	203245.30+411721.1	20:32:45.31	41:17:21.12	0.41	5.57	2.54	79	0.80	12	86.4278	0.177	0.063	0.065	0.049	2.23	−0.72
99	203245.49+411546.9	20:32:45.49	41:15:46.94	0.29	5.08	3.09	101	0.89	17	94.5724	0.208	0.111	0.048	0.049	1.61	−0.41
100	203245.59+411659.2	20:32:45.59	41:16:59.20	0.32	5.38	4.25	129	0.90	28	95.0750	0.328	0.094	0.142	0.092	2.14	−1.19
101	203245.64+411647.1	20:32:45.64	41:16:47.13	0.41	5.30	2.05	125	0.90	9	75.4940	0.142	0.026	0.074	0.043	1.96	−1.39
102	203245.76+411349.7	20:32:45.76	41:13:49.73	0.22	5.11	4.99	109	0.90	37	95.4739	0.437	0.126	0.135	0.175	2.61	−0.18
103	203245.81+411502.9	20:32:45.81	41:15: 2.95	0.33	4.96	3.20	93	0.89	18	93.3129	0.223	0.087	0.050	0.086	1.92	−0.12
104	203245.79+412108.2	20:32:45.80	41:21: 8.21	0.33	7.88	7.49	429	0.89	77	97.0538	0.892	0.389	0.233	0.270	1.92	−1.19
105	203245.91+411238.7	20:32:45.92	41:12:38.70	0.29	5.48	3.94	131	0.90	24	90.3635	0.304	0.125	0.178	0.001	1.86	−0.16
106	203246.14+411040.1	20:32:46.14	41:10:40.14	0.34	6.55	6.12	224	0.90	53	94.5724	0.627	0.100	0.271	0.257	2.59	−0.12
107	203246.27+410713.3	20:32:46.27	41:07:13.30	0.77	9.19	4.02	1086	0.89	33	94.6949	0.400	0.090	0.194	0.116	2.17	−1.40
108	203246.31+411107.8	20:32:46.32	41:11: 7.83	0.49	6.23	3.29	189	0.90	19	90.6210	0.243	0.107	0.072	0.064	1.82	−0.02
109	203246.36+411652.9	20:32:46.37	41:16:52.97	0.42	5.21	2.97	102	0.89	15	94.8488	0.188	0.133	0.039	0.015	1.44	−0.12
110	203246.41+411301.8	20:32:46.41	41:13: 1.82	0.47	5.24	1.64	116	0.90	6	86.0069	0.087	0.015	0.071	0.001	1.83	−0.42
111	203246.66+411808.5	20:32:46.66	41:18: 8.52	0.45	5.73	3.26	151	0.90	19	96.4916	0.221	0.088	0.057	0.075	2.10	−0.29
112	203246.70+411316.3	20:32:46.71	41:13:16.32	0.49	5.10	1.96	107	0.90	8	75.3306	0.132	0.055	0.064	0.013	1.76	−0.03
113	203246.86+411742.8	20:32:46.86	41:17:42.86	0.41	5.48	1.68	134	0.90	7	79.9385	0.103	−0.004	0.071	0.037	2.34	−0.04
114	203246.91+412118.7	20:32:46.91	41:21:18.75	0.55	7.89	5.26	479	0.90	43	96.9219	0.499	0.151	0.124	0.224	2.36	−0.18
115	203247.40+411251.1	20:32:47.41	41:12:51.16	0.34	5.14	3.39	107	0.91	19	91.3026	0.236	0.063	0.067	0.106	2.07	−0.06
116	203247.47+411211.7	20:32:47.48	41:12:11.70	0.42	5.44	2.84	126	0.91	15	82.3916	0.208	0.079	0.068	0.061	1.95	−1.57
117	203247.81+411334.8	20:32:47.81	41:13:34.90	0.42	4.81	2.50	89	0.90	12	89.3709	0.158	0.022	0.013	0.123	3.50	−1.50
118	203247.87+411632.3	20:32:47.88	41:16:32.38	0.47	4.82	2.28	84	0.89	10	84.8102	0.142	0.028	0.058	0.056	2.43	−0.17
119	203247.98+411653.9	20:32:47.99	41:16:53.97	0.35	4.93	2.12	87	0.89	9	71.2473	0.152	0.046	0.101	0.006	1.74	−0.00
120	203248.18+411352.1	20:32:48.19	41:13:52.10	0.42	4.66	1.91	71	0.89	8	82.3916	0.116	0.040	0.019	0.057	2.90	−0.23
121	203248.25+411229.1	20:32:48.25	41:12:29.20	0.26	5.17	3.97	95	0.89	24	88.9060	0.314	0.066	0.108	0.140	2.62	−0.00
122	203248.43+411439.4	20:32:48.44	41:14:39.48	0.15	4.49	7.07	77	0.90	66	93.4888	0.783	0.175	0.297	0.311	2.27	−0.76
123	203248.47+411608.2	20:32:48.47	41:16: 8.22	0.19	4.60	5.40	85	0.91	41	95.2509	0.481	0.151	0.143	0.188	2.30	−0.03
124	203248.53+412336.2	20:32:48.53	41:23:36.21	0.56	9.68	6.53	823	0.83	63	93.3820	0.815	0.330	0.304	0.181	1.89	−1.46 †
125	203248.63+410811.6	20:32:48.63	41:08:11.61	0.33	8.14	9.62	546	0.90	121	97.1512	1.385	0.324	0.487	0.574	2.23	−1.33
126	203248.87+411519.8	20:32:48.87	41:15:19.87	0.31	4.40	3.15	75	0.90	16	83.6354	0.222	0.127	0.062	0.034	1.64	−0.01
127	203248.91+410930.4	20:32:48.91	41:09:30.49	0.70	7.04	2.83	317	0.90	16	89.1228	0.208	0.077	0.073	0.058	1.96	−0.05
128	203249.02+410746.8	20:32:49.03	41:07:46.88	0.44	8.45	6.41	582	0.89	63	96.3879	0.734	0.127	0.328	0.279	2.26	−3.61 †
129	203249.39+411230.6	20:32:49.39	41:12:30.64	0.29	4.97	2.45	97	0.91	11	91.2398	0.143	0.074	0.054	0.015	1.67	−0.00
130	203249.38+411606.8	20:32:49.38	41:16: 6.85	0.32	4.43	2.91	76	0.90	15	93.7903	0.179	0.050	0.041	0.087	2.69	−0.01
131	203249.34+412224.5	20:32:49.34	41:22:24.54	0.64	8.55	4.35	514	0.86	31	96.1241	0.386	0.133	0.163	0.090	1.98	−0.06
132	203249.51+411532.8	20:32:49.52	41:15:32.84	0.12	4.30	8.31	70	0.90	87	94.2112	1.027	0.213	0.391	0.422	2.23	−0.14
133	203249.85+412342.2	20:32:49.86	41:23:42.22	0.59	9.65	7.19	871	0.84	72	91.7267	0.930	0.624	0.194	0.113	1.45	−0.34
134	203249.92+411511.1	20:32:49.93	41:15:11.19	0.38	4.19	2.00	57	0.89	8	70.0914	0.132	0.043	0.077	0.012	1.85	−0.20
135	203250.08+411626.7	20:32:50.08	41:16:26.79	0.33	4.40	2.72	57	0.87	13	80.1301	0.193	0.065	0.051	0.077	2.18	−1.48
136	203250.11+411458.1	20:32:50.11	41:14:58.16	0.35	4.16	2.44	56	0.90	11	89.8515	0.142	0.017	0.045	0.080	2.84	−0.00
137	203250.16+411836.1	20:32:50.16	41:18:36.14	0.28	5.48	3.84	132	0.91	24	77.1022	0.345	0.173	0.089	0.082	1.73	−0.00
138	203250.25+412216.6	20:32:50.26	41:22:16.68	0.74	8.36	2.90	477	0.86	17	84.6217	0.238	0.135	0.086	0.017	1.55	−0.31
139	203250.39+411038.2	20:32:50.39	41:10:38.21	0.58	6.00	2.80	173	0.90	15	96.4633	0.176	0.034	0.081	0.061	2.20	−0.00
140	203250.41+411749.5	20:32:50.41	41:17:49.52	0.22	4.97	5.48	97	0.90	42	96.1555	0.489	0.094	0.187	0.208	2.27	−0.59

Table 1. continued.

N_x	NAME	RA	Dec	Error	θ	Sig.	Area	PSF	Cts	Exp.	Count Rates ($\times 10^{-3}$ ctn s^{-1})				$\overline{E_x}$	Var.
#	CXOCYG J+	[h:m:s]	[d:m:s]	($''$)	($'$)	(σ)	(px.)	(%)	(ph.)	(ks)	Tot.	Soft	Med.	Hard	(keV)	log(P_{ks})
141	203250.42+411629.6	20:32:50.43	41:16:29.61	0.14	4.36	6.47	55	0.87	55	96.4162	0.660	0.257	0.197	0.206	2.02	−0.06
142	203250.69+410825.3	20:32:50.69	41:08:25.30	0.22	7.74	12.31	453	0.90	186	97.2517	2.128	0.800	0.708	0.619	1.95	−1.48
143	203250.69+411609.1	20:32:50.70	41:16: 9.12	0.23	4.20	4.40	56	0.89	28	86.7827	0.372	0.123	0.151	0.098	2.01	−0.75
144	203250.87+411145.6	20:32:50.87	41:11:45.66	0.38	5.17	2.18	95	0.89	9	70.2799	0.160	0.072	0.055	0.033	2.01	−0.02
145	203250.98+411245.6	20:32:50.98	41:12:45.61	0.29	4.58	2.99	66	0.89	15	80.5667	0.217	0.020	0.093	0.104	2.49	−2.98 †
146	203251.13+411253.5	20:32:51.13	41:12:53.58	0.24	4.50	4.27	72	0.91	27	86.5409	0.352	0.081	0.085	0.185	3.19	−0.59 †
147	203251.14+411237.7	20:32:51.14	41:12:37.77	0.25	4.62	3.74	78	0.91	22	95.3325	0.259	0.040	0.146	0.073	1.88	−0.01
148	203251.15+412026.1	20:32:51.16	41:20:26.16	0.40	6.71	4.24	246	0.90	29	92.2010	0.359	0.121	0.145	0.094	1.91	−0.06
149	203251.15+412245.8	20:32:51.15	41:22:45.81	0.77	8.70	4.36	665	0.90	33	95.5807	0.395	0.151	0.110	0.134	1.99	−0.12
150	203251.35+411123.7	20:32:51.36	41:11:23.79	0.33	5.34	2.99	120	0.90	16	86.9178	0.207	0.067	0.079	0.061	1.83	−0.34
151	203251.34+411617.2	20:32:51.34	41:16:17.29	0.34	4.13	2.55	54	0.90	11	84.9421	0.157	−0.004	0.049	0.112	3.88	−0.02
152	203251.36+411409.0	20:32:51.36	41:14: 9.06	0.14	4.01	6.31	50	0.89	53	91.9120	0.653	0.164	0.250	0.238	2.04	−0.11
153	203251.55+411300.7	20:32:51.56	41:13: 0.70	0.28	4.37	3.47	67	0.90	19	84.1506	0.259	0.164	0.101	−0.006	1.67	−0.00
154	203251.52+412037.7	20:32:51.53	41:20:37.72	0.56	6.83	2.73	259	0.89	15	67.0227	0.259	0.088	0.027	0.145	2.59	−0.11
155	203251.70+411710.9	20:32:51.71	41:17:10.97	0.52	4.42	2.28	61	0.89	10	71.5237	0.164	0.009	0.042	0.113	3.28	−0.46
156	203252.00+411600.7	20:32:52.00	41:16: 0.77	0.23	3.93	3.81	49	0.90	22	88.8589	0.285	0.057	0.121	0.107	2.40	−0.94
157	203252.11+411313.5	20:32:52.12	41:13:13.54	0.38	4.18	1.96	60	0.90	8	91.3183	0.102	0.041	0.044	0.017	2.08	−0.46
158	203252.12+411828.6	20:32:52.13	41:18:28.62	0.41	5.13	3.66	106	0.90	21	95.8759	0.253	0.040	0.121	0.092	2.27	−0.61
159	203252.17+411815.7	20:32:52.18	41:18:15.74	0.22	4.98	3.67	95	0.90	21	79.3825	0.307	0.117	0.103	0.086	1.79	−2.12
160	203252.41+411029.8	20:32:52.41	41:10:29.82	0.41	5.85	3.64	161	0.90	22	84.7160	0.290	0.082	0.068	0.140	2.50	−0.00
161	203252.47+411541.3	20:32:52.47	41:15:41.32	0.17	3.77	4.83	45	0.90	33	89.6976	0.419	0.019	0.096	0.304	4.47	−0.38
162	203252.52+411736.5	20:32:52.52	41:17:36.53	0.30	4.52	3.20	64	0.89	17	81.1321	0.240	0.063	0.091	0.086	1.98	−0.06
163	203252.59+411255.2	20:32:52.60	41:12:55.22	0.35	4.24	2.39	54	0.89	10	95.0938	0.129	0.008	0.032	0.089	3.58	−0.54
164	203252.60+412102.5	20:32:52.60	41:21: 2.52	0.29	7.07	7.98	319	0.90	85	93.6867	1.008	0.363	0.438	0.207	2.04	−1.34 †
165	203252.69+411019.4	20:32:52.70	41:10:19.49	0.18	5.95	9.25	172	0.90	106	96.2811	1.225	0.419	0.509	0.297	2.05	−0.28
166	203252.84+411955.0	20:32:52.84	41:19:55.02	0.30	6.11	4.77	181	0.90	35	96.7271	0.406	0.119	0.196	0.091	1.95	−0.13
167	203253.12+411559.0	20:32:53.12	41:15:59.08	0.27	3.72	2.40	44	0.90	10	70.8547	0.173	0.073	0.059	0.041	1.77	−0.89
168	203253.37+411927.7	20:32:53.37	41:19:27.76	0.52	5.69	2.37	144	0.90	11	79.1627	0.165	0.050	0.103	0.012	1.80	−0.00
169	203253.55+410714.1	20:32:53.55	41:07:14.19	0.65	8.53	4.71	809	0.90	41	92.3517	0.497	0.008	0.122	0.367	4.04	−0.24
170	203253.53+411545.3	20:32:53.54	41:15:45.32	0.14	3.59	5.29	40	0.89	39	96.6235	0.453	0.112	0.241	0.100	2.18	−0.01
171	203253.56+412019.4	20:32:53.57	41:20:19.47	0.49	6.36	2.16	207	0.90	11	66.5233	0.191	−0.017	0.043	0.165	3.85	−0.89
172	203253.77+411513.3	20:32:53.77	41:15:13.32	0.06	3.47	13.82	38	0.89	219	95.0718	2.589	0.552	0.955	1.083	2.42	−4.00 †
173	203253.88+411216.0	20:32:53.88	41:12:16.10	0.51	4.41	1.49	60	0.89	5	86.7702	0.073	0.021	0.023	0.029	2.33	−0.01
174	203253.90+411536.7	20:32:53.91	41:15:36.79	0.15	3.50	1.17	38	0.89	3	66.6521	0.067	−0.005	0.079	−0.007	1.80	−0.18
175	203253.95+411702.7	20:32:53.95	41:17: 2.72	0.33	3.99	3.00	49	0.90	15	94.7703	0.184	0.030	0.054	0.100	2.84	−1.06
176	203254.09+411726.5	20:32:54.10	41:17:26.56	0.49	4.19	2.02	54	0.90	8	69.7616	0.138	0.041	0.059	0.039	2.24	−0.14
177	203254.17+411128.1	20:32:54.18	41:11:28.17	0.20	4.91	6.18	82	0.89	51	89.2798	0.653	0.029	0.157	0.468	3.98	−0.45
178	203254.22+410818.2	20:32:54.22	41:08:18.20	0.30	7.51	8.88	414	0.90	103	95.6435	1.199	0.302	0.477	0.420	2.15	−1.41
179	203254.19+411242.4	20:32:54.20	41:12:42.41	0.15	4.10	5.73	49	0.90	44	96.9250	0.517	0.123	0.238	0.156	2.14	−0.58
180	203254.21+411025.4	20:32:54.21	41:10:25.42	0.35	5.70	4.04	151	0.90	25	87.7564	0.325	0.145	0.081	0.100	1.79	−0.95
181	203254.28+411433.5	20:32:54.29	41:14:33.51	0.19	3.40	1.42	34	0.89	5	40.9367	0.140	0.074	0.021	0.045	2.23	−0.26
182	203254.28+412333.2	20:32:54.29	41:23:33.28	0.68	9.18	4.96	959	0.90	42	94.5504	0.498	0.171	0.195	0.132	2.01	−0.57
183	203254.33+411458.5	20:32:54.33	41:14:58.56	0.16	3.36	4.44	35	0.89	28	95.4425	0.337	0.105	0.140	0.092	1.98	−0.23
184	203254.39+410640.9	20:32:54.40	41:06:40.93	0.56	8.98	6.28	1066	0.90	65	93.0616	0.780	0.146	0.291	0.342	2.28	−1.88
185	203254.43+411550.0	20:32:54.43	41:15:50.00	0.33	3.44	2.13	37	0.89	9	76.9451	0.133	0.039	0.070	0.023	1.91	−0.06
186	203254.56+410840.2	20:32:54.57	41:08:40.27	0.59	7.16	2.59	323	0.89	14	91.6230	0.177	0.030	0.067	0.080	2.46	−0.01
187	203254.55+411446.5	20:32:54.56	41:14:46.54	0.11	3.33	6.06	33	0.89	49	92.8072	0.595	0.154	0.191	0.250	2.45	−1.47

Table 1. continued.

N_x	NAME	RA	Dec	Error	θ	Sig.	Area	PSF	Cts	Exp.	Count Rates ($\times 10^{-3}$ ctn s^{-1})				$\overline{E_x}$	Var.
#	CXOCYG J+	[h:m:s]	[d:m:s]	($''$)	($'$)	(σ)	(px.)	(%)	(ph.)	(ks)	Tot.	Soft	Med.	Hard	(keV)	log(P_{ks})
188	203254.61+411341.4	20:32:54.62	41:13:41.45	0.15	3.56	4.30	36	0.90	27	87.5303	0.352	0.045	0.211	0.096	2.23	−0.06
189	203254.60+411932.8	20:32:54.61	41:19:32.84	0.37	5.61	3.89	137	0.90	24	90.7121	0.302	0.118	0.076	0.108	1.92	−1.80
190	203254.79+411203.0	20:32:54.80	41:12: 3.06	0.14	4.42	7.05	69	0.90	64	95.9199	0.745	0.181	0.261	0.303	2.37	−0.75
191	203254.89+411517.8	20:32:54.89	41:15:17.90	0.18	3.27	2.55	33	0.89	12	76.5117	0.176	0.069	0.069	0.039	1.88	−0.09
192	203255.02+411038.8	20:32:55.03	41:10:38.90	0.76	5.43	1.24	130	0.91	4	89.9803	0.058	0.017	0.017	0.023	2.05	−0.15
193	203255.12+411314.8	20:32:55.13	41:13:14.80	0.11	3.67	6.69	39	0.89	58	91.1770	0.723	0.180	0.255	0.288	2.08	−0.59
194	203255.15+411651.9	20:32:55.15	41:16:51.99	0.17	3.71	3.85	42	0.89	23	81.2326	0.317	0.051	0.161	0.105	2.26	−2.17
195	203255.27+410832.0	20:32:55.28	41:08:32.06	0.36	7.22	6.52	332	0.90	59	84.1694	0.790	0.101	0.298	0.390	2.71	−4.00 †
196	203255.26+411747.5	20:32:55.26	41:17:47.54	0.27	4.23	3.39	55	0.89	18	75.9337	0.277	−0.007	0.070	0.214	4.30	−0.00
197	203255.33+411821.9	20:32:55.33	41:18:21.93	0.50	4.62	1.92	69	0.89	8	85.6897	0.107	0.032	0.059	0.016	1.98	−0.02
198	203255.34+411852.5	20:32:55.35	41:18:52.53	0.31	5.00	2.89	84	0.89	15	87.6465	0.193	0.057	0.084	0.053	2.04	−1.62
199	203255.67+411519.0	20:32:55.67	41:15:19.01	0.17	3.13	3.66	30	0.90	21	86.5723	0.272	0.073	0.113	0.086	1.91	−0.54
200	203255.78+411012.2	20:32:55.78	41:10:12.26	0.32	5.72	4.16	154	0.90	27	85.4195	0.359	0.108	0.131	0.120	2.26	−0.02
201	203255.72+412246.6	20:32:55.73	41:22:46.70	0.78	8.36	2.61	586	0.90	16	81.1886	0.220	0.078	0.035	0.107	2.55	−0.92
202	203255.86+412233.4	20:32:55.87	41:22:33.46	0.65	8.15	3.50	537	0.90	24	93.3757	0.290	0.106	0.117	0.067	1.97	−0.03
203	203256.28+411317.6	20:32:56.29	41:13:17.65	0.25	3.45	2.84	34	0.89	14	84.0375	0.189	0.037	0.104	0.048	2.04	−0.02
204	203256.35+411436.7	20:32:56.36	41:14:36.78	0.20	3.01	2.72	28	0.90	13	89.2861	0.164	0.071	0.059	0.034	1.77	−0.00
205	203256.40+411206.6	20:32:56.40	41:12: 6.69	0.29	4.15	2.76	59	0.90	13	92.5873	0.164	−0.004	0.056	0.112	3.67	−0.75
206	203256.49+411053.1	20:32:56.49	41:10:53.11	0.16	5.08	7.43	105	0.90	71	95.9419	0.826	0.157	0.386	0.284	2.26	−1.15 †
207	203256.55+411314.8	20:32:56.56	41:13:14.88	0.27	3.43	3.10	34	0.89	16	94.6415	0.192	0.021	0.045	0.126	3.35	−0.12
208	203256.61+411401.9	20:32:56.62	41:14: 1.96	0.33	3.09	1.80	29	0.89	7	94.4625	0.084	0.056	0.021	0.007	1.47	−0.50
209	203256.66+412015.9	20:32:56.66	41:20:15.97	0.43	6.01	3.71	173	0.90	23	91.6136	0.282	0.072	0.158	0.052	2.07	−0.26
210	203256.71+411044.8	20:32:56.71	41:10:44.80	0.44	5.17	2.73	112	0.91	13	76.9294	0.200	0.052	0.106	0.042	2.14	−0.00
211	203256.69+412025.4	20:32:56.70	41:20:25.40	0.49	6.15	3.13	186	0.90	18	93.9128	0.214	0.094	0.070	0.050	2.11	−1.11
212	203256.74+411215.8	20:32:56.74	41:12:15.88	0.19	4.00	2.66	53	0.90	12	88.3941	0.162	0.008	0.047	0.106	2.97	−1.06
213	203256.85+411441.0	20:32:56.85	41:14:41.04	0.17	2.91	3.24	27	0.90	17	88.7113	0.217	0.072	0.073	0.072	2.17	−0.00
214	203257.07+410903.8	20:32:57.08	41:09: 3.85	0.54	6.59	2.65	249	0.89	14	81.3142	0.204	0.013	0.050	0.141	3.28	−0.54
215	203257.06+411313.9	20:32:57.06	41:13:13.98	0.32	3.36	2.31	33	0.89	10	75.1704	0.153	0.012	0.041	0.100	2.85	−0.04
216	203257.17+412123.3	20:32:57.17	41:21:23.33	0.64	6.98	2.98	282	0.89	17	91.9308	0.214	0.086	0.036	0.092	2.10	−0.38
217	203257.25+411445.4	20:32:57.25	41:14:45.46	0.21	2.83	2.80	26	0.90	13	91.1173	0.166	0.047	0.072	0.047	2.15	−0.23
218	203257.32+412047.5	20:32:57.33	41:20:47.51	0.27	6.42	6.08	215	0.90	52	93.7872	0.620	0.069	0.331	0.220	2.15	−3.18 †
219	203257.36+411333.3	20:32:57.36	41:13:33.32	0.08	3.15	8.14	29	0.89	83	92.7538	1.002	0.226	0.346	0.430	2.47	−0.86
220	203257.56+411234.7	20:32:57.56	41:12:34.70	0.14	3.68	5.56	38	0.89	42	87.0403	0.545	0.164	0.165	0.215	2.12	−2.63
221	203257.73+411029.4	20:32:57.74	41:10:29.49	0.43	5.28	2.24	106	0.89	10	93.7086	0.123	0.055	0.030	0.038	1.72	−0.81
222	203257.80+410937.9	20:32:57.80	41:09:37.98	0.41	6.02	3.16	185	0.90	18	84.5463	0.245	0.020	0.093	0.132	3.13	−0.90
223	203257.82+411359.1	20:32:57.82	41:13:59.16	0.17	2.89	2.86	27	0.89	14	78.1638	0.204	0.025	0.082	0.096	2.50	−0.50
224	203257.91+411619.0	20:32:57.92	41:16:19.06	0.10	2.99	4.19	28	0.90	26	86.7827	0.336	0.100	0.164	0.073	2.04	−0.48
225	203257.94+412156.9	20:32:57.95	41:21:56.92	0.58	7.44	3.79	333	0.88	25	93.8249	0.305	0.041	0.078	0.186	3.29	−0.14
226	203258.03+411058.1	20:32:58.04	41:10:58.12	0.17	4.84	7.38	93	0.90	70	97.3993	0.798	0.110	0.288	0.400	2.73	−3.05 †
227	203258.09+410713.6	20:32:58.10	41:07:13.68	0.62	8.22	4.66	649	0.90	39	95.4833	0.460	0.085	0.148	0.227	2.77	−2.11
228	203258.16+411735.0	20:32:58.16	41:17:35.08	0.26	3.69	2.53	39	0.90	11	88.9186	0.149	0.020	0.085	0.043	2.30	−0.35
229	203258.22+411250.6	20:32:58.23	41:12:50.65	0.19	3.41	3.69	33	0.89	21	79.6181	0.300	0.053	0.124	0.123	2.34	−2.72
230	203258.27+411617.8	20:32:58.27	41:16:17.86	0.20	2.92	2.16	28	0.90	9	92.3266	0.112	0.022	0.034	0.056	2.45	−0.22
231	203258.27+412147.8	20:32:58.27	41:21:47.81	0.51	7.27	3.77	287	0.87	24	88.8684	0.311	0.089	0.169	0.053	2.07	−0.24
232	203258.37+412000.9	20:32:58.37	41:20: 0.96	0.38	5.64	3.07	142	0.90	17	73.4617	0.269	−0.003	0.028	0.244	4.32	−0.06
233	203258.39+411543.2	20:32:58.40	41:15:43.23	0.08	2.69	7.23	25	0.90	67	96.8402	0.774	0.043	0.170	0.561	3.72	−0.49

Table 1. continued.

N_x	NAME	RA	Dec	Error	θ	Sig.	Area	PSF	Cts	Exp.	Count Rates ($\times 10^{-3}$ ctn s^{-1})				$\overline{E_x}$	Var.
#	CXOCYG J+	[h:m:s]	[d:m:s]	($''$)	($'$)	(σ)	(px.)	(%)	(ph.)	(ks)	Tot.	Soft	Med.	Hard	(keV)	log(P_{ks})
234	203258.44+411105.4	20:32:58.45	41:11: 5.50	0.36	4.70	1.62	75	0.89	6	43.8201	0.165	0.092	0.013	0.060	1.45	−4.00
235	203258.45+411403.9	20:32:58.45	41:14: 3.92	0.18	2.76	2.19	25	0.89	9	58.1085	0.181	0.016	0.112	0.053	2.30	−0.11
236	203258.52+411234.8	20:32:58.52	41:12:34.82	0.32	3.54	2.35	35	0.90	10	82.6397	0.140	0.065	0.052	0.024	1.85	−0.03
237	203258.54+411525.2	20:32:58.55	41:15:25.24	0.21	2.60	2.17	24	0.89	9	91.6042	0.113	0.022	0.046	0.045	2.23	−0.39
238	203258.73+411226.6	20:32:58.73	41:12:26.64	0.10	3.61	7.25	37	0.90	67	95.3797	0.786	0.208	0.266	0.312	2.55	−3.71 †
239	203258.74+411110.0	20:32:58.75	41:11:10.00	0.14	4.61	7.63	71	0.89	74	96.5984	0.866	0.158	0.378	0.329	2.31	−4.00 †
240	203258.93+411202.8	20:32:58.94	41:12: 2.84	0.21	3.88	3.23	44	0.89	17	85.6928	0.230	0.060	0.061	0.109	2.53	−0.39
241	203258.93+411840.7	20:32:58.94	41:18:40.78	0.35	4.44	2.26	61	0.89	10	72.4598	0.160	0.069	0.038	0.052	2.01	−0.66
242	203259.00+411051.8	20:32:59.00	41:10:51.89	0.14	4.84	8.66	94	0.90	93	96.8277	1.067	0.236	0.394	0.437	2.34	−0.90
243	203259.04+411758.7	20:32:59.04	41:17:58.78	0.12	3.87	6.43	44	0.90	54	91.5445	0.667	0.178	0.239	0.250	2.10	−3.36
244	203259.17+411937.4	20:32:59.17	41:19:37.44	0.20	5.22	7.19	111	0.91	68	96.2811	0.786	0.684	0.093	0.009	1.09	−0.20
245	203259.20+411229.5	20:32:59.21	41:12:29.60	0.17	3.51	3.72	35	0.90	21	75.1736	0.318	0.116	0.161	0.041	1.76	−0.01
246	203259.21+412049.0	20:32:59.22	41:20:49.02	0.42	6.30	4.54	202	0.90	32	93.6458	0.382	0.132	0.094	0.156	2.36	−0.26
247	203259.24+412137.4	20:32:59.25	41:21:37.47	0.60	7.05	3.61	293	0.89	22	92.0156	0.271	0.060	0.109	0.101	2.42	−0.37
248	203259.24+412238.4	20:32:59.25	41:22:38.42	0.52	8.01	5.12	506	0.90	42	93.5893	0.499	0.133	0.145	0.221	2.30	−0.49
249	203259.31+411037.4	20:32:59.32	41:10:37.41	0.31	5.01	3.01	105	0.91	16	78.5847	0.226	0.061	0.147	0.017	2.05	−0.10
250	203259.38+411223.5	20:32:59.38	41:12:23.51	0.37	3.56	1.69	36	0.90	6	69.0518	0.103	−0.003	0.030	0.076	3.34	−0.20
251	203259.45+410941.4	20:32:59.46	41:09:41.46	0.55	5.84	3.64	171	0.90	22	90.1970	0.277	0.027	0.089	0.161	3.70	−0.46
252	203259.57+411055.1	20:32:59.58	41:10:55.20	0.37	4.73	2.14	89	0.90	9	91.6481	0.114	0.042	0.055	0.017	1.73	−0.15
253	203259.63+411514.6	20:32:59.63	41:15:14.61	0.10	2.38	5.18	22	0.89	37	84.2888	0.498	0.197	0.251	0.050	1.73	−0.46
254	203259.63+411941.0	20:32:59.63	41:19:41.08	0.15	5.24	8.08	111	0.91	83	91.8492	1.007	0.251	0.482	0.274	2.24	−0.02
255	203259.75+411300.0	20:32:59.75	41:13: 0.08	0.19	3.09	2.98	28	0.89	15	87.7533	0.194	0.048	0.074	0.072	1.91	−0.88
256	203259.75+411419.4	20:32:59.76	41:14:19.46	0.09	2.44	6.36	21	0.89	53	92.6910	0.646	0.179	0.252	0.214	2.21	−0.85
257	203259.77+411345.4	20:32:59.77	41:13:45.48	0.14	2.66	1.46	23	0.89	5	81.2671	0.072	0.010	0.053	0.010	1.92	−0.65
258	203259.85+412036.5	20:32:59.85	41:20:36.57	0.45	6.06	3.13	179	0.90	17	83.6574	0.236	0.093	0.067	0.076	2.58	−0.05
259	203259.94+411027.9	20:32:59.94	41:10:27.95	0.32	5.10	3.57	97	0.89	21	85.7462	0.275	0.109	0.097	0.069	1.82	−0.64
260	203259.98+410848.6	20:32:59.99	41:08:48.62	0.14	6.61	15.90	261	0.90	289	94.7138	3.414	0.449	1.156	1.808	2.93	−4.00 †
261	203300.01+411107.2	20:33: 0.01	41:11: 7.23	0.39	4.52	2.93	68	0.89	14	75.7515	0.221	0.158	0.025	0.038	1.37	−0.00
262	203300.16+411217.6	20:33: 0.16	41:12:17.64	0.29	3.54	2.50	36	0.89	11	87.0089	0.147	0.062	0.024	0.061	1.98	−0.05
263	203300.29+411656.6	20:33: 0.29	41:16:56.61	0.23	2.96	2.01	28	0.89	8	52.7688	0.175	0.080	0.081	0.015	1.70	−0.38
264	203300.38+411730.6	20:33: 0.38	41:17:30.69	0.33	3.35	1.75	34	0.90	6	78.7543	0.098	0.024	0.039	0.034	2.21	−0.10
265	203300.38+411651.7	20:33: 0.39	41:16:51.79	0.34	2.89	1.83	28	0.89	7	83.6323	0.097	0.010	0.051	0.036	2.26	−0.16
266	203300.42+411124.4	20:33: 0.42	41:11:24.44	0.28	4.23	3.14	58	0.90	16	92.0376	0.202	0.056	0.092	0.054	2.24	−0.30
267	203300.41+412030.8	20:33: 0.42	41:20:30.88	0.37	5.93	2.55	48	0.66	12	84.0281	0.217	0.049	0.013	0.156	4.14	−3.55
268	203300.46+411147.5	20:33: 0.47	41:11:47.55	0.31	3.91	2.65	53	0.90	12	85.1683	0.167	0.049	0.074	0.044	2.11	−0.10
269	203300.52+411550.1	20:33: 0.53	41:15:50.15	0.15	2.35	3.13	22	0.89	16	88.7930	0.206	0.047	0.124	0.035	1.91	−1.39
270	203300.52+412214.0	20:33: 0.52	41:22:14.06	0.42	7.55	7.24	384	0.89	71	95.9545	0.838	0.284	0.270	0.284	2.11	−0.00
271	203300.59+411859.3	20:33: 0.59	41:18:59.32	0.08	4.54	12.63	65	0.89	186	97.7071	2.135	0.371	0.878	0.886	2.39	−4.00 †
272	203300.73+410929.4	20:33: 0.74	41:09:29.41	0.29	5.93	5.19	179	0.90	39	96.9250	0.457	0.119	0.182	0.157	2.28	−0.30
273	203300.77+411627.1	20:33: 0.78	41:16:27.19	0.15	2.59	3.90	23	0.89	23	93.0239	0.281	0.058	0.106	0.117	2.10	−0.13
274	203300.77+412032.1	20:33: 0.78	41:20:32.13	0.31	5.93	1.38	48	0.66	4	65.3611	0.115	0.015	0.063	0.037	2.62	−1.95
275	203300.84+412133.8	20:33: 0.84	41:21:33.80	0.62	6.89	2.56	273	0.90	13	83.1046	0.184	0.048	0.081	0.055	2.02	−0.22
276	203300.88+411115.6	20:33: 0.89	41:11:15.69	0.18	4.31	3.17	61	0.90	16	87.5554	0.215	0.085	0.098	0.033	1.85	−0.13
277	203300.90+411736.7	20:33: 0.90	41:17:36.78	0.17	3.36	3.66	34	0.90	21	81.3771	0.289	0.051	0.134	0.104	2.31	−0.27
278	203300.95+411423.8	20:33: 0.96	41:14:23.81	0.13	2.21	3.49	19	0.90	19	80.2589	0.270	0.052	0.123	0.095	2.52	−0.17
279	203300.95+412119.9	20:33: 0.96	41:21:19.98	0.52	6.67	3.82	247	0.90	24	92.2795	0.299	0.095	0.108	0.096	1.88	−0.42
280	203301.09+411755.7	20:33: 1.09	41:17:55.75	0.08	3.59	9.36	39	0.90	106	92.4114	1.293	0.238	0.564	0.491	2.37	−2.23 †
281	203301.15+411321.8	20:33: 1.16	41:13:21.82	0.20	2.65	2.04	23	0.90	8	54.9707	0.171	0.058	0.118	−0.005	1.95	−0.10

Table 1. continued.

N_x	NAME	RA	Dec	Error	θ	Sig.	Area	PSF	Cts	Exp.	Count Rates ($\times 10^{-3}$ ctn s^{-1})				$\overline{E}_x$	Var.
#	CXOCYG J+	[h:m:s]	[d:m:s]	($''$)	($'$)	(σ)	(px.)	(%)	(ph.)	(ks)	Tot.	Soft	Med.	Hard	(keV)	log(P_{ks})
282	203301.16+411152.7	20:33: 1.16	41:11:52.72	0.38	3.76	2.10	48	0.90	8	88.5009	0.112	0.021	0.047	0.044	1.99	−0.15
283	203301.20+410918.2	20:33: 1.20	41:09:18.28	0.11	6.07	17.51	192	0.90	346	96.7146	3.964	0.605	1.557	1.801	2.64	−3.61 †
284	203301.21+410858.0	20:33: 1.22	41:08:58.01	0.37	6.39	3.86	231	0.89	25	92.5465	0.310	0.072	0.121	0.117	2.34	−0.34
285	203301.25+411459.5	20:33: 1.26	41:14:59.53	0.17	2.06	2.68	19	0.89	12	78.3774	0.180	0.013	0.098	0.069	2.17	−1.18
286	203301.26+411256.8	20:33: 1.27	41:12:56.84	0.12	2.92	1.02	26	0.89	3	53.1206	0.069	0.061	−0.006	0.014	1.37	−0.00
287	203301.35+411055.5	20:33: 1.36	41:10:55.60	0.41	4.57	2.55	81	0.90	12	84.4490	0.161	−0.008	0.100	0.069	2.41	−1.83
288	203301.35+411223.6	20:33: 1.36	41:12:23.61	0.20	3.32	3.13	32	0.90	16	82.5204	0.221	0.037	0.106	0.078	2.56	−4.00 †
289	203301.35+411331.2	20:33: 1.36	41:13:31.30	0.27	2.53	2.35	22	0.89	10	86.7702	0.134	0.011	0.088	0.036	2.12	−0.00
290	203301.38+412158.5	20:33: 1.38	41:21:58.56	0.54	7.26	3.47	358	0.90	21	94.6792	0.256	0.039	0.129	0.087	2.42	−0.44
291	203301.43+411200.2	20:33: 1.44	41:12: 0.25	0.29	3.63	2.44	44	0.90	11	88.3375	0.140	0.022	0.073	0.045	2.52	−0.70
292	203301.49+411211.5	20:33: 1.49	41:12:11.55	0.11	3.47	3.24	4	0.39	16	80.1269	0.547	0.161	0.226	0.160	2.08	−0.13
293	203301.49+411211.6	20:33: 1.49	41:12:11.64	0.10	3.47	3.36	4	0.39	17	80.1269	0.579	0.193	0.226	0.160	1.98	−0.13
294	203301.58+412302.9	20:33: 1.58	41:23: 2.97	0.70	8.28	4.80	679	0.91	40	95.6906	0.471	0.130	0.164	0.177	2.20	−1.67
295	203301.67+411248.2	20:33: 1.68	41:12:48.27	0.16	2.97	3.46	27	0.89	19	92.0345	0.235	0.034	0.046	0.154	3.37	−0.61
296	203301.66+411959.0	20:33: 1.66	41:19:59.09	0.49	5.35	2.77	121	0.90	14	80.4473	0.204	0.095	0.003	0.106	2.81	−0.03
297	203301.68+411751.4	20:33: 1.68	41:17:51.40	0.17	3.47	4.08	37	0.89	25	95.9890	0.293	0.102	0.172	0.019	1.86	−0.06
298	203301.72+411147.0	20:33: 1.72	41:11:47.08	0.34	3.78	2.22	49	0.90	9	50.9062	0.213	0.058	0.125	0.031	2.04	−1.00
299	203301.72+411500.5	20:33: 1.72	41:15: 0.58	0.07	1.97	7.15	18	0.89	65	95.7848	0.766	0.279	0.244	0.243	1.96	−0.44
300	203301.77+411110.5	20:33: 1.77	41:11:10.58	0.07	4.31	15.46	61	0.89	270	94.2866	3.212	1.573	0.981	0.658	1.70	−4.00 †
301	203301.80+411103.9	20:33: 1.81	41:11: 3.92	0.20	4.41	4.27	64	0.89	27	92.0690	0.336	0.019	0.142	0.175	2.81	−0.97
302	203301.83+411317.3	20:33: 1.84	41:13:17.33	0.15	2.60	3.83	22	0.89	22	84.6845	0.297	0.078	0.143	0.076	2.01	−0.42
303	203301.94+411059.0	20:33: 1.94	41:10:59.02	0.21	4.47	3.64	67	0.89	21	77.9251	0.308	0.007	0.110	0.192	2.99	−0.00
304	203301.93+411739.3	20:33: 1.93	41:17:39.30	0.41	3.28	1.27	33	0.89	4	60.2758	0.080	0.015	0.052	0.013	2.37	−0.07
305	203301.97+410644.4	20:33: 1.97	41:06:44.42	0.76	8.49	4.07	859	0.89	33	94.0918	0.394	0.076	0.182	0.136	2.11	−0.07
306	203301.95+411946.8	20:33: 1.96	41:19:46.88	0.28	5.15	3.64	107	0.90	22	84.7693	0.289	0.041	0.174	0.074	1.95	−0.04
307	203302.18+411848.8	20:33: 2.19	41:18:48.84	0.23	4.24	3.70	56	0.89	22	82.2691	0.301	0.114	0.144	0.044	1.74	−0.09
308	203302.26+411533.4	20:33: 2.26	41:15:33.44	0.10	1.95	5.17	18	0.89	37	94.8802	0.441	0.115	0.187	0.139	2.17	−0.54
309	203302.31+411324.2	20:33: 2.31	41:13:24.28	0.10	2.46	5.11	21	0.89	36	88.3564	0.462	0.176	0.175	0.112	1.88	−0.70
310	203302.35+411828.1	20:33: 2.35	41:18:28.15	0.37	3.92	1.77	47	0.90	7	78.4497	0.104	0.035	0.021	0.048	3.45	−0.14 †
311	203302.40+411738.4	20:33: 2.40	41:17:38.48	0.31	3.21	2.18	32	0.89	9	67.5252	0.155	0.079	0.030	0.046	1.54	−0.16
312	203302.63+411355.7	20:33: 2.64	41:13:55.77	0.26	2.10	2.05	19	0.89	8	66.4793	0.142	0.048	0.082	0.013	1.83	−0.02
313	203302.87+410705.9	20:33: 2.88	41:07: 5.96	0.59	8.11	5.01	630	0.90	41	95.0279	0.482	0.070	0.211	0.201	2.45	−2.29
314	203302.87+411514.0	20:33: 2.88	41:15:14.01	0.11	1.77	2.76	17	0.89	13	94.2929	0.159	0.021	0.082	0.056	2.64	−0.50
315	203302.90+411742.9	20:33: 2.91	41:17:42.97	0.08	3.22	9.39	29	0.88	107	96.4821	1.258	0.607	0.525	0.126	1.72	−0.30
316	203303.03+411329.2	20:33: 3.04	41:13:29.28	0.13	2.30	4.31	20	0.89	27	91.6984	0.335	0.084	0.181	0.071	2.24	−0.29
317	203303.03+411740.1	20:33: 3.03	41:17:40.19	0.18	3.17	3.60	29	0.88	20	75.9306	0.303	0.072	0.131	0.101	2.14	−1.08
318	203303.07+411243.4	20:33: 3.08	41:12:43.48	0.14	2.86	3.04	26	0.89	15	89.9080	0.193	0.073	0.061	0.059	1.86	−0.28
319	203303.22+411629.4	20:33: 3.22	41:16:29.46	0.10	2.25	3.58	20	0.89	20	84.2982	0.269	−0.003	0.050	0.223	3.57	−0.04
320	203303.53+411253.6	20:33: 3.54	41:12:53.64	0.14	2.67	4.29	26	0.90	27	70.4841	0.429	0.091	0.076	0.262	3.51	−2.02 †
321	203303.64+411236.6	20:33: 3.64	41:12:36.62	0.17	2.89	3.17	26	0.89	16	80.8023	0.229	0.053	0.109	0.066	2.27	−0.00
322	203303.66+411334.2	20:33: 3.66	41:13:34.25	0.15	2.16	2.90	19	0.89	14	84.9358	0.190	−0.002	0.024	0.169	3.73	−0.01
323	203303.66+411218.2	20:33: 3.67	41:12:18.25	0.24	3.15	2.31	29	0.90	10	69.7082	0.164	0.013	0.077	0.074	2.30	−0.57
324	203303.88+411736.2	20:33: 3.89	41:17:36.24	0.10	3.03	5.93	29	0.90	47	96.2654	0.548	0.113	0.252	0.183	2.28	−0.28
325	203304.06+411124.5	20:33: 4.06	41:11:24.54	0.25	3.92	3.25	49	0.90	17	81.9676	0.241	0.037	0.089	0.115	2.65	−0.15
326	203304.10+410755.3	20:33: 4.11	41:07:55.31	0.40	7.25	5.40	397	0.90	47	93.2846	0.568	0.182	0.238	0.148	2.01	−0.17
327	203304.16+410651.5	20:33: 4.16	41:06:51.52	0.43	8.29	8.63	773	0.90	97	96.0707	1.127	0.293	0.421	0.413	2.40	−0.94
328	203304.22+411411.7	20:33: 4.23	41:14:11.76	0.17	1.71	1.76	16	0.89	6	79.7437	0.094	−0.002	−0.001	0.097	5.16	−0.06

Table 1. continued.

N_x	NAME	RA	Dec	Error	θ	Sig.	Area	PSF	Cts	Exp.	Count Rates ($\times 10^{-3}$ ctn s^{-1})				$\overline{E_x}$	Var.
#	CXOCYG J+	[h:m:s]	[d:m:s]	($''$)	($'$)	(σ)	(px.)	(%)	(ph.)	(ks)	Tot.	Soft	Med.	Hard	(keV)	log(P_{ks})
329	203304.26+410723.1	20:33: 4.26	41:07:23.16	0.60	7.77	3.40	487	0.90	23	90.2033	0.290	0.039	0.116	0.135	2.75	−0.01
330	203304.24+411254.6	20:33: 4.25	41:12:54.62	0.08	2.58	7.26	22	0.89	67	97.2517	0.780	0.137	0.322	0.321	2.66	−2.40
331	203304.28+411235.2	20:33: 4.28	41:12:35.22	0.19	2.85	2.80	25	0.89	13	87.8098	0.173	0.024	0.088	0.061	2.38	−0.02
332	203304.30+411613.4	20:33: 4.31	41:16:13.48	0.23	1.92	2.37	18	0.89	10	92.6784	0.127	0.058	0.047	0.022	1.80	−0.01
333	203304.32+411420.4	20:33: 4.32	41:14:20.48	0.19	1.63	1.74	16	0.89	6	80.1615	0.092	0.026	0.026	0.040	2.12	−0.49
334	203304.38+411405.3	20:33: 4.39	41:14: 5.38	0.23	1.74	2.38	18	0.90	10	75.1390	0.156	0.027	0.058	0.071	2.68	−0.28
335	203304.42+411830.8	20:33: 4.42	41:18:30.81	0.07	3.80	10.90	43	0.90	141	94.4656	1.669	0.324	0.727	0.619	2.33	−4.00 †
336	203304.48+411128.1	20:33: 4.48	41:11:28.10	0.13	3.83	7.67	47	0.89	74	93.3160	0.897	0.069	0.391	0.438	2.74	−4.00 †
337	203304.49+411157.6	20:33: 4.50	41:11:57.63	0.27	3.38	1.99	34	0.89	8	83.0795	0.111	−0.003	0.051	0.063	2.81	−0.08
338	203304.57+411612.9	20:33: 4.57	41:16:12.98	0.11	1.88	3.05	18	0.89	15	82.2314	0.212	0.052	0.080	0.079	2.23	−0.62
339	203304.67+411205.9	20:33: 4.67	41:12: 5.98	0.27	3.24	2.33	31	0.89	10	88.0925	0.131	0.049	0.023	0.059	2.21	−1.22
340	203304.70+411506.2	20:33: 4.70	41:15: 6.26	0.17	1.42	2.34	17	0.90	10	90.1153	0.128	0.010	0.096	0.022	2.24	−0.08
341	203304.75+411312.4	20:33: 4.75	41:13:12.40	0.12	2.29	4.67	19	0.89	31	96.3534	0.365	0.067	0.173	0.125	2.45	−0.40
342	203304.75+411650.4	20:33: 4.75	41:16:50.41	0.20	2.31	3.13	21	0.89	16	86.6320	0.211	0.049	0.114	0.049	2.10	−0.13
343	203304.78+410857.2	20:33: 4.79	41:08:57.23	0.59	6.22	2.75	217	0.90	15	94.4436	0.185	−0.003	0.031	0.156	4.02	−0.25
344	203304.86+411238.7	20:33: 4.86	41:12:38.70	0.24	2.74	2.78	24	0.89	13	63.5582	0.238	0.086	0.103	0.049	1.96	−0.62
345	203304.95+411129.5	20:33: 4.95	41:11:29.50	0.24	3.78	3.84	46	0.89	22	90.2598	0.284	0.058	0.070	0.156	3.00	−0.40
346	203305.01+411256.2	20:33: 5.02	41:12:56.22	0.25	2.48	1.72	21	0.89	6	61.1490	0.120	0.053	0.053	0.015	2.04	−0.10
347	203305.03+411421.5	20:33: 5.04	41:14:21.55	0.13	1.50	1.24	2	0.42	3	43.5845	0.215	−0.001	0.163	0.053	2.19	−0.09
348	203305.03+411831.4	20:33: 5.03	41:18:31.43	0.20	3.76	2.72	42	0.90	13	93.8029	0.161	0.053	0.089	0.018	1.89	−0.52
349	203305.04+411146.6	20:33: 5.05	41:11:46.64	0.14	3.50	2.15	7	0.47	8	88.1585	0.215	0.072	0.072	0.071	2.01	−0.35
350	203305.03+411421.4	20:33: 5.04	41:14:21.44	0.13	1.50	1.24	2	0.42	3	43.5845	0.215	−0.001	0.163	0.053	2.19	−0.09
351	203305.05+411144.8	20:33: 5.05	41:11:44.88	0.09	3.53	5.16	7	0.47	36	93.9442	0.837	0.090	0.476	0.271	2.24	−2.41
352	203305.17+411233.2	20:33: 5.18	41:12:33.26	0.08	2.79	7.31	25	0.89	68	94.7043	0.809	0.188	0.281	0.340	2.47	−1.64
353	203305.20+411335.6	20:33: 5.21	41:13:35.65	0.15	1.94	3.04	17	0.89	15	91.2398	0.190	0.072	0.072	0.047	1.80	−0.04
354	203305.25+411604.5	20:33: 5.25	41:16: 4.52	0.11	1.69	4.69	17	0.89	31	94.1609	0.376	0.212	0.070	0.094	1.63	−0.86
355	203305.26+412138.7	20:33: 5.27	41:21:38.74	0.45	6.76	4.22	261	0.89	30	92.4397	0.372	0.128	0.121	0.122	2.10	−1.29
356	203305.28+411258.6	20:33: 5.29	41:12:58.68	0.11	2.42	4.86	21	0.89	33	91.5194	0.411	0.084	0.182	0.145	2.33	−0.67
357	203305.30+411303.6	20:33: 5.30	41:13: 3.68	0.15	2.34	3.04	20	0.89	15	86.6320	0.201	0.075	0.102	0.023	1.83	−0.00
358	203305.36+411311.8	20:33: 5.36	41:13:11.83	0.13	2.23	4.01	19	0.89	24	79.7720	0.342	0.095	0.124	0.123	2.27	−1.55
359	203305.41+411153.6	20:33: 5.41	41:11:53.63	0.10	3.37	6.95	35	0.89	62	94.2772	0.745	0.118	0.261	0.367	2.72	−0.27
360	203305.47+411610.5	20:33: 5.47	41:16:10.56	0.14	1.72	3.05	17	0.89	15	72.5728	0.241	0.044	0.075	0.122	3.18	−0.21
361	203305.59+411348.2	20:33: 5.60	41:13:48.29	0.08	1.73	6.77	18	0.90	59	94.6729	0.699	0.198	0.315	0.186	2.02	−0.33
362	203305.72+411136.7	20:33: 5.72	41:11:36.78	0.28	3.61	2.43	42	0.89	11	64.6952	0.193	0.013	0.065	0.115	2.83	−0.29
363	203305.79+411634.7	20:33: 5.79	41:16:34.78	0.32	1.98	1.88	19	0.89	7	88.1302	0.095	−0.003	0.024	0.074	3.66	−0.20
364	203305.89+411905.0	20:33: 5.90	41:19: 5.05	0.30	4.24	2.01	57	0.90	8	80.0767	0.124	0.019	0.057	0.048	1.95	−0.17
365	203305.92+412057.5	20:33: 5.93	41:20:57.52	0.67	6.06	2.17	186	0.90	10	95.0687	0.127	0.055	0.053	0.018	1.77	−0.18
366	203306.07+411256.7	20:33: 6.07	41:12:56.73	0.06	2.37	10.15	21	0.89	123	94.8237	1.463	0.378	0.555	0.531	2.18	−0.26
367	203306.13+411012.6	20:33: 6.14	41:10:12.61	0.58	4.94	1.56	96	0.89	6	83.3716	0.083	0.035	0.033	0.014	1.76	−1.01
368	203306.19+411453.8	20:33: 6.20	41:14:53.81	0.28	1.14	1.03	16	0.90	3	14.3889	0.254	−0.016	0.132	0.137	2.97	−0.48
369	203306.21+411715.3	20:33: 6.21	41:17:15.37	0.20	2.51	1.47	23	0.90	5	80.8745	0.073	0.039	0.010	0.024	1.66	−0.20
370	203306.20+412242.9	20:33: 6.20	41:22:42.96	0.69	7.79	2.92	527	0.90	19	81.9142	0.262	0.035	0.172	0.056	2.14	−0.65
371	203306.24+410948.3	20:33: 6.24	41:09:48.34	0.58	5.33	2.55	139	0.90	12	76.3169	0.184	0.011	0.063	0.110	3.50	−0.27
372	203306.26+411235.1	20:33: 6.27	41:12:35.13	0.08	2.67	7.18	24	0.89	66	95.5587	0.779	0.163	0.408	0.208	2.08	−0.26
373	203306.27+411100.4	20:33: 6.28	41:11: 0.42	0.33	4.16	2.12	59	0.89	9	82.9381	0.127	0.021	0.061	0.045	2.21	−0.00
374	203306.27+412019.0	20:33: 6.28	41:20:19.03	0.46	5.42	2.31	114	0.89	11	92.9297	0.139	0.093	0.036	0.009	1.60	−0.10
375	203306.32+412215.2	20:33: 6.32	41:22:15.28	0.62	7.33	3.41	350	0.89	21	94.4028	0.255	0.104	0.045	0.105	2.00	−0.35

Table 1. continued.

N_x	NAME	RA	Dec	Error	θ	Sig.	Area	PSF	Cts	Exp.	Count Rates ($\times 10^{-3}$ ctn s^{-1})				$\overline{E}_x$	Var.
#	CXOCYG J+	[h:m:s]	[d:m:s]	($''$)	($'$)	(σ)	(px.)	(%)	(ph.)	(ks)	Tot.	Soft	Med.	Hard	(keV)	log(P_{ks})
376	203306.35+411353.1	20:33: 6.35	41:13:53.11	0.21	1.58	1.51	18	0.90	5	88.3061	0.068	0.048	0.022	−0.002	1.42	−0.13
377	203306.38+411330.7	20:33: 6.39	41:13:30.79	0.14	1.86	3.14	17	0.89	16	82.1340	0.224	0.052	0.093	0.079	2.20	−0.07
378	203306.47+411206.8	20:33: 6.47	41:12: 6.87	0.08	3.09	9.30	30	0.90	105	95.9230	1.225	0.208	0.498	0.519	2.64	−0.06
379	203306.61+412158.3	20:33: 6.61	41:21:58.36	0.33	7.04	7.15	305	0.89	69	95.3859	0.817	0.029	0.305	0.483	3.38	−0.00
380	203306.64+411817.7	20:33: 6.64	41:18:17.78	0.49	3.45	1.13	36	0.90	3	40.3870	0.106	0.044	0.015	0.046	2.02	−0.12
381	203306.71+411200.0	20:33: 6.72	41:12: 0.00	0.08	3.18	8.48	32	0.89	89	97.4307	1.027	0.124	0.504	0.398	2.34	−1.43
382	203306.73+411527.5	20:33: 6.74	41:15:27.58	0.12	1.12	1.84	16	0.90	7	56.2836	0.144	−0.004	0.015	0.133	3.89	−0.21
383	203306.79+411727.8	20:33: 6.80	41:17:27.85	0.14	2.66	4.30	25	0.89	27	88.1711	0.347	0.086	0.124	0.137	2.08	−0.39
384	203306.84+411224.3	20:33: 6.84	41:12:24.38	0.12	2.80	5.08	26	0.89	36	95.7503	0.424	0.033	0.161	0.230	3.19	−4.00 †
385	203306.85+411503.4	20:33: 6.86	41:15: 3.49	0.19	1.01	2.02	15	0.90	8	94.2929	0.098	0.033	0.044	0.021	1.86	−0.20
386	203306.91+411647.2	20:33: 6.91	41:16:47.28	0.22	2.04	1.71	19	0.89	6	74.0742	0.098	0.012	0.012	0.073	4.11	−0.17
387	203306.93+411858.9	20:33: 6.94	41:18:58.96	0.17	4.09	4.55	53	0.90	31	89.5185	0.391	0.137	0.214	0.039	1.76	−0.26
388	203307.00+411649.6	20:33: 7.01	41:16:49.70	0.10	2.06	5.26	19	0.89	38	94.2426	0.458	0.188	0.141	0.129	2.20	−0.30
389	203307.06+411300.1	20:33: 7.07	41:13: 0.15	0.08	2.23	6.76	20	0.89	59	93.5704	0.714	0.118	0.358	0.238	2.43	−0.00
390	203307.07+411604.3	20:33: 7.08	41:16: 4.36	0.10	1.44	4.21	17	0.90	26	91.5413	0.320	0.033	0.131	0.156	2.55	−4.00 †
391	203307.13+411625.7	20:33: 7.13	41:16:25.72	0.17	1.71	1.84	19	0.90	7	69.4067	0.116	0.027	0.045	0.044	2.68	−0.09
392	203307.14+411141.2	20:33: 7.15	41:11:41.20	0.17	3.46	5.74	39	0.89	45	85.8907	0.589	0.101	0.245	0.243	2.46	−1.78
393	203307.14+412006.9	20:33: 7.14	41:20: 6.93	0.19	5.19	6.98	101	0.89	65	97.0067	0.755	0.309	0.312	0.134	1.82	−1.76
394	203307.15+411318.7	20:33: 7.16	41:13:18.78	0.14	1.95	2.27	18	0.89	10	93.8406	0.120	0.021	0.020	0.080	3.22	−0.00
395	203307.16+411730.4	20:33: 7.16	41:17:30.44	0.24	2.67	2.47	25	0.89	11	96.1523	0.131	0.067	0.067	−0.002	1.66	−0.32
396	203307.17+411520.2	20:33: 7.17	41:15:20.20	0.08	1.00	5.64	15	0.90	43	76.0311	0.635	0.100	0.158	0.378	3.12	−1.84
397	203307.25+411000.4	20:33: 7.26	41:10: 0.44	0.49	5.09	3.14	105	0.89	16	89.1165	0.211	0.022	0.109	0.080	2.05	−2.18 †
398	203307.32+411214.6	20:33: 7.32	41:12:14.62	0.10	2.92	6.82	28	0.90	60	91.4377	0.737	0.157	0.327	0.253	2.34	−0.03
399	203307.34+411341.5	20:33: 7.35	41:13:41.60	0.12	1.61	3.72	16	0.89	21	82.9915	0.291	0.038	0.092	0.160	3.50	−0.57
400	203307.36+411800.0	20:33: 7.36	41:18: 0.04	0.13	3.13	4.78	31	0.90	32	93.0302	0.395	0.078	0.153	0.164	2.26	−1.44
401	203307.40+411151.3	20:33: 7.40	41:11:51.39	0.23	3.28	2.87	34	0.89	14	81.9142	0.195	−0.003	0.065	0.133	3.41	−1.00
402	203307.45+411226.4	20:33: 7.46	41:12:26.47	0.05	2.72	12.52	26	0.89	182	95.6938	2.134	0.291	0.711	1.132	2.93	−4.00 †
403	203307.47+411254.5	20:33: 7.47	41:12:54.51	0.14	2.29	1.09	23	0.90	3	46.7067	0.082	−0.004	0.066	0.019	2.28	−0.06
404	203307.50+412032.3	20:33: 7.50	41:20:32.32	0.12	5.60	13.60	143	0.90	216	88.3312	2.709	0.279	0.969	1.460	2.91	−4.00 †
405	203307.55+411821.2	20:33: 7.56	41:18:21.24	0.23	3.46	2.77	37	0.90	13	86.0949	0.178	0.058	0.085	0.035	1.89	−1.72
406	203307.57+411947.6	20:33: 7.57	41:19:47.61	0.12	4.86	9.41	94	0.91	110	96.7680	1.264	0.300	0.556	0.408	2.05	−0.11
407	203307.59+411300.7	20:33: 7.60	41:13: 0.80	0.06	2.18	9.21	19	0.89	103	95.6906	1.215	0.233	0.561	0.421	2.17	−2.85
408	203307.73+410828.5	20:33: 7.73	41:08:28.53	0.33	6.59	5.61	276	0.90	46	92.9517	0.562	0.071	0.261	0.230	2.45	−1.10
409	203307.83+411243.0	20:33: 7.84	41:12:43.10	0.18	2.44	3.50	25	0.90	19	93.1213	0.231	0.010	0.140	0.081	2.50	−1.84
410	203307.86+411216.3	20:33: 7.87	41:12:16.30	0.10	2.86	7.13	27	0.90	65	93.6615	0.779	0.058	0.343	0.378	2.80	−0.03
411	203307.91+411254.3	20:33: 7.91	41:12:54.36	0.19	2.26	2.67	20	0.89	12	94.4531	0.149	0.058	0.057	0.034	2.14	−0.26
412	203307.91+411606.9	20:33: 7.92	41:16: 6.99	0.15	1.37	2.34	16	0.90	10	74.3695	0.155	0.056	0.072	0.027	1.79	−0.05
413	203307.97+411257.7	20:33: 7.98	41:12:57.71	0.13	2.20	4.15	20	0.89	25	96.1084	0.299	0.069	0.162	0.069	2.20	−0.06
414	203307.98+411300.7	20:33: 7.98	41:13: 0.70	0.05	2.15	10.86	19	0.89	139	97.7511	1.604	0.320	0.699	0.585	2.31	−3.35
415	203307.99+411659.4	20:33: 8.00	41:16:59.49	0.13	2.13	4.13	20	0.89	25	78.6538	0.363	0.040	0.126	0.197	2.97	−1.57
416	203308.02+411801.5	20:33: 8.03	41:18: 1.59	0.14	3.12	3.18	31	0.90	16	88.5417	0.213	0.055	0.035	0.123	3.06	−0.11
417	203308.03+411436.9	20:33: 8.03	41:14:36.96	0.23	0.88	1.77	16	0.90	6	79.3197	0.094	0.026	0.069	−0.001	1.89	−0.01
418	203308.04+411642.9	20:33: 8.04	41:16:42.96	0.16	1.88	3.27	18	0.89	17	90.4891	0.216	0.035	0.109	0.072	2.23	−0.33
419	203308.05+412217.4	20:33: 8.06	41:22:17.48	0.53	7.32	4.90	351	0.90	36	91.2021	0.443	0.098	0.180	0.166	2.17	−0.14
420	203308.09+411109.6	20:33: 8.09	41:11: 9.60	0.16	3.93	5.18	52	0.90	37	86.5157	0.486	0.087	0.226	0.173	2.21	−3.65 †
421	203308.09+411526.9	20:33: 8.09	41:15:26.96	0.16	0.89	2.30	15	0.90	10	86.1608	0.132	0.022	0.074	0.036	2.20	−0.45
422	203308.21+410626.4	20:33: 8.21	41:06:26.46	0.50	8.60	7.12	954	0.90	76	96.2529	0.880	0.232	0.428	0.220	2.04	−0.36

Table 1. continued.

N_x	NAME	RA	Dec	Error	θ	Sig.	Area	PSF	Cts	Exp.	Count Rates ($\times10^{-3}$ ctn s^{-1})				$\overline{E_x}$	Var.
#	CXOCYG J+	[h:m:s]	[d:m:s]	($''$)	($'$)	(σ)	(px.)	(%)	(ph.)	(ks)	Tot.	Soft	Med.	Hard	(keV)	log(P_{ks})
423	203308.21+411304.0	20:33: 8.21	41:13: 4.08	0.11	2.08	4.25	19	0.89	26	94.4593	0.317	0.023	0.141	0.153	2.62	−0.11
424	203308.23+411823.1	20:33: 8.23	41:18:23.15	0.09	3.46	7.37	37	0.90	70	93.7715	0.836	0.205	0.374	0.257	2.12	−0.41
425	203308.25+411513.1	20:33: 8.25	41:15:13.14	0.25	0.77	1.44	15	0.90	5	91.4942	0.063	0.009	0.057	−0.003	1.82	−0.00
426	203308.29+411543.0	20:33: 8.29	41:15:43.02	0.15	1.02	2.87	16	0.90	14	92.3172	0.172	0.141	0.022	0.009	1.37	−0.00
427	203308.33+411421.1	20:33: 8.33	41:14:21.19	0.18	0.98	2.23	16	0.90	9	59.2361	0.179	0.035	0.072	0.072	2.33	−0.02
428	203308.50+411734.6	20:33: 8.50	41:17:34.66	0.23	2.66	2.11	25	0.89	9	75.5065	0.134	0.008	0.041	0.084	3.69	−0.29
429	203308.53+411328.1	20:33: 8.54	41:13:28.13	0.12	1.69	3.74	17	0.89	21	90.9571	0.267	0.010	0.109	0.147	2.93	−0.05
430	203308.56+411435.9	20:33: 8.56	41:14:35.91	0.12	0.80	3.65	16	0.90	20	52.4453	0.438	0.061	0.210	0.168	2.43	−3.90
431	203308.59+411915.1	20:33: 8.59	41:19:15.20	0.22	4.30	3.31	60	0.90	19	84.5181	0.256	0.010	0.101	0.145	3.09	−0.90
432	203308.63+411514.4	20:33: 8.64	41:15:14.43	0.05	0.71	9.69	15	0.90	113	97.3302	1.304	0.179	0.476	0.649	2.80	−4.00 †
433	203308.76+411318.5	20:33: 8.77	41:13:18.56	0.01	1.82	34.24	8	0.73	1240	97.5564	17.503	8.308	7.729	1.466	1.73	−1.24
434	203308.80+411257.4	20:33: 8.80	41:12:57.49	0.08	2.15	5.97	19	0.89	47	96.1712	0.557	0.127	0.185	0.244	2.40	−0.01
435	203308.84+411214.8	20:33: 8.84	41:12:14.86	0.13	2.84	3.92	27	0.90	23	96.2937	0.271	0.056	0.090	0.125	2.77	−0.07
436	203308.84+411317.1	20:33: 8.85	41:13:17.16	0.02	1.84	18.18	8	0.73	366	97.4213	5.173	2.876	2.001	0.295	1.63	−0.52
437	203308.89+411327.7	20:33: 8.90	41:13:27.80	0.21	1.67	2.25	17	0.89	9	82.2660	0.132	0.026	0.067	0.040	2.49	−0.70
438	203308.90+411243.5	20:33: 8.91	41:12:43.59	0.11	2.37	4.42	24	0.90	28	76.9734	0.411	0.056	0.185	0.170	2.68	−3.83
439	203308.91+412227.3	20:33: 8.91	41:22:27.38	0.26	7.47	11.04	400	0.90	148	91.9434	1.803	0.292	0.722	0.790	2.55	−4.00 †
440	203308.95+411705.7	20:33: 8.96	41:17: 5.71	0.13	2.17	3.70	19	0.89	21	26.9309	0.888	0.158	0.282	0.447	2.81	−4.00 †
441	203308.96+411101.9	20:33: 8.96	41:11: 1.92	0.44	4.03	2.04	56	0.90	8	79.0056	0.118	0.040	0.053	0.025	1.83	−0.01
442	203308.97+411537.5	20:33: 8.98	41:15:37.52	0.22	0.87	1.64	16	0.90	6	58.7273	0.118	0.013	0.032	0.072	3.16	−0.88
443	203309.01+411331.0	20:33: 9.02	41:13:31.08	0.11	1.61	4.26	17	0.89	26	96.3345	0.311	0.080	0.139	0.092	2.24	−0.41
444	203309.06+411227.8	20:33: 9.06	41:12:27.89	0.16	2.62	3.49	24	0.89	19	92.4648	0.235	0.034	0.094	0.106	2.75	−3.05
445	203309.12+411308.6	20:33: 9.13	41:13: 8.61	0.07	1.96	8.20	18	0.89	83	89.4777	1.048	0.124	0.449	0.475	2.49	−4.00
446	203309.15+411343.2	20:33: 9.16	41:13:43.20	0.08	1.41	6.46	18	0.90	54	94.2897	0.645	0.128	0.317	0.199	2.20	−0.02
447	203309.26+411302.1	20:33: 9.27	41:13: 2.10	0.08	2.05	6.26	19	0.89	51	93.6741	0.619	0.154	0.226	0.239	2.20	−4.00
448	203309.30+411618.6	20:33: 9.31	41:16:18.69	0.13	1.41	4.01	17	0.90	24	86.0320	0.315	0.074	0.166	0.075	2.14	−1.04
449	203309.32+411250.6	20:33: 9.32	41:12:50.62	0.11	2.24	5.60	20	0.89	42	96.7114	0.496	0.138	0.185	0.173	1.92	−0.09
450	203309.32+411428.9	20:33: 9.32	41:14:28.94	0.14	0.76	3.32	16	0.90	17	81.3142	0.242	0.012	0.122	0.108	2.78	−0.14
451	203309.38+411347.0	20:33: 9.38	41:13:47.06	0.19	1.34	1.90	17	0.90	7	76.9011	0.109	0.012	0.070	0.026	2.23	−0.00
452	203309.42+411320.3	20:33: 9.43	41:13:20.31	0.15	1.75	2.82	17	0.89	13	85.3284	0.180	0.011	0.077	0.091	3.28	−0.65
453	203309.45+411258.3	20:33: 9.46	41:12:58.33	0.15	2.10	3.20	19	0.89	16	86.6006	0.217	0.089	0.076	0.051	1.96	−0.19
454	203309.53+412109.9	20:33: 9.54	41:21: 9.94	0.32	6.17	4.96	204	0.91	37	88.8118	0.465	0.069	0.236	0.160	2.23	−0.08
455	203309.59+411308.0	20:33: 9.59	41:13: 8.08	0.08	1.94	5.98	18	0.89	47	93.0333	0.575	0.131	0.216	0.228	2.26	−0.48
456	203309.60+411300.4	20:33: 9.60	41:13: 0.48	0.06	2.06	9.38	19	0.89	106	93.8657	1.275	0.632	0.525	0.119	1.70	−0.00
457	203309.60+411429.9	20:33: 9.61	41:14:29.98	0.15	0.71	1.59	16	0.90	5	44.7561	0.143	0.023	0.048	0.072	2.94	−0.41
458	203309.63+412130.4	20:33: 9.64	41:21:30.50	0.40	6.51	4.64	239	0.90	34	92.7192	0.413	0.143	0.188	0.082	1.91	−0.59
459	203309.67+412214.3	20:33: 9.68	41:22:14.34	0.46	7.24	5.23	342	0.90	40	92.8417	0.488	0.057	0.236	0.195	2.47	−2.22
460	203309.73+411250.6	20:33: 9.73	41:12:50.69	0.15	2.22	3.76	20	0.89	21	96.2748	0.253	0.069	0.045	0.139	3.18	−0.76
461	203309.78+410902.2	20:33: 9.79	41:09: 2.20	0.23	5.99	6.39	79	0.71	54	96.4350	0.809	0.126	0.418	0.265	2.28	−0.73
462	203309.85+411247.8	20:33: 9.85	41:12:47.85	0.18	2.26	2.27	20	0.89	9	83.4344	0.131	0.012	0.039	0.080	3.01	−0.00
463	203309.92+411139.5	20:33: 9.92	41:11:39.56	0.33	3.38	1.70	37	0.89	6	75.5568	0.096	0.013	0.071	0.011	2.24	−1.12
464	203309.92+411756.2	20:33: 9.92	41:17:56.29	0.13	2.96	4.59	28	0.90	30	97.3271	0.353	0.052	0.144	0.157	2.61	−0.35
465	203309.93+411325.9	20:33: 9.93	41:13:25.97	0.18	1.64	2.70	17	0.89	12	95.9325	0.149	0.046	0.093	0.011	1.82	−0.35
466	203309.95+410856.9	20:33: 9.95	41:08:56.97	0.34	6.08	3.89	82	0.70	24	87.7062	0.390	0.058	0.154	0.178	2.68	−0.22
467	203310.02+412042.2	20:33:10.03	41:20:42.21	0.28	5.71	5.28	159	0.90	41	92.8197	0.500	0.064	0.113	0.324	3.42	−0.06
468	203310.03+411429.6	20:33:10.03	41:14:29.69	0.10	0.66	1.16	15	0.90	3	48.8049	0.084	−0.002	−0.002	0.089	4.12	−0.12
469	203310.04+411743.2	20:33:10.05	41:17:43.23	0.24	2.74	2.28	26	0.90	10	79.2537	0.142	0.036	0.025	0.081	4.23	−0.01

Table 1. continued.

N_x	NAME	RA	Dec	Error	θ	Sig.	Area	PSF	Cts	Exp.	Count Rates ($\times 10^{-3}$ ctn s^{-1})				$\overline{E_x}$	Var.
#	CXOCYGJ+	[h:m:s]	[d:m:s]	($''$)	($'$)	(σ)	(px.)	(%)	(ph.)	(ks)	Tot.	Soft	Med.	Hard	(keV)	log(P_{ks})
470	203310.05+411301.6	20:33:10.06	41:13: 1.66	0.13	2.03	1.39	18	0.89	4	76.1756	0.069	0.028	−0.002	0.043	2.81	−0.23
471	203310.07+411000.8	20:33:10.08	41:10: 0.84	0.13	5.01	11.10	102	0.90	147	96.9564	1.697	0.374	0.657	0.665	2.33	−0.64
472	203310.10+411414.4	20:33:10.10	41:14:14.42	0.10	0.87	4.04	13	0.88	24	96.2466	0.290	0.010	0.022	0.258	4.50	−2.88
473	203310.11+411337.1	20:33:10.11	41:13:37.16	0.16	1.45	2.96	15	0.88	14	84.9076	0.197	0.092	0.039	0.066	1.77	−0.54
474	203310.12+411239.7	20:33:10.13	41:12:39.75	0.18	2.38	2.96	22	0.89	14	76.7818	0.215	0.072	0.086	0.057	2.10	−0.56
475	203310.17+411545.3	20:33:10.17	41:15:45.32	0.07	0.84	6.88	16	0.90	61	97.5501	0.701	0.180	0.283	0.238	2.15	−1.18
476	203310.18+411339.4	20:33:10.18	41:13:39.40	0.09	1.41	5.53	15	0.88	41	91.4691	0.519	0.073	0.322	0.123	2.21	−0.34
477	203310.21+411322.4	20:33:10.22	41:13:22.44	0.23	1.68	2.42	17	0.89	10	93.5296	0.129	0.011	0.059	0.059	2.65	−0.17
478	203310.23+411533.1	20:33:10.24	41:15:33.15	0.10	0.66	4.71	15	0.90	32	62.8514	0.568	0.083	0.223	0.262	2.49	−3.40
479	203310.26+411413.3	20:33:10.26	41:14:13.35	0.07	0.87	6.63	13	0.88	57	94.5379	0.692	0.022	0.299	0.371	2.94	−4.00
480	203310.29+412205.1	20:33:10.29	41:22: 5.20	0.20	7.08	11.42	321	0.90	158	95.9230	1.840	0.434	0.865	0.541	2.08	−0.54
481	203310.45+410925.5	20:33:10.46	41:09:25.59	0.14	5.59	12.14	162	0.90	176	97.2360	2.010	0.286	0.777	0.947	2.68	−4.00 †
482	203310.56+411328.4	20:33:10.57	41:13:28.46	0.12	1.57	3.77	16	0.89	21	83.3559	0.293	0.080	0.134	0.080	1.98	−0.20
483	203310.57+412102.3	20:33:10.58	41:21: 2.30	0.32	6.03	5.85	192	0.90	48	97.1983	0.555	0.064	0.226	0.264	2.58	−3.08
484	203310.58+411538.7	20:33:10.58	41:15:38.74	0.07	0.71	5.85	15	0.90	46	92.0596	0.560	0.130	0.287	0.143	2.15	−0.04
485	203310.60+411323.8	20:33:10.61	41:13:23.88	0.13	1.64	4.17	17	0.89	25	91.2869	0.317	0.024	0.097	0.196	3.25	−0.31
486	203310.64+411748.8	20:33:10.64	41:17:48.87	0.23	2.82	2.41	27	0.90	11	81.4336	0.151	0.063	0.037	0.051	1.88	−0.98
487	203310.71+411339.6	20:33:10.72	41:13:39.69	0.20	1.38	2.27	17	0.90	9	88.9657	0.121	0.036	0.074	0.011	1.86	−0.35
488	203310.72+411507.9	20:33:10.72	41:15: 7.99	0.01	0.31	97.67	15	0.90	9736	97.7511	111.002	24.209	46.683	40.111	2.24	−0.14
489	203310.73+411502.2	20:33:10.74	41:15: 2.24	0.15	0.28	2.81	15	0.90	14	94.9713	0.168	−0.005	0.051	0.122	4.04	−0.26
490	203310.81+411256.4	20:33:10.82	41:12:56.42	0.11	2.09	5.24	19	0.89	37	88.8715	0.478	0.063	0.265	0.151	2.37	−0.26
491	203310.93+410953.3	20:33:10.94	41:09:53.36	0.35	5.13	3.23	108	0.89	18	95.7220	0.215	0.053	0.093	0.069	2.40	−0.04
492	203310.99+411241.8	20:33:10.99	41:12:41.88	0.12	2.33	4.63	22	0.89	30	92.0282	0.376	0.097	0.207	0.072	1.82	−2.18
493	203311.05+411032.0	20:33:11.06	41:10:32.06	0.46	4.48	1.61	84	0.91	6	41.1597	0.172	0.041	0.121	0.010	1.76	−0.56
494	203311.07+411318.0	20:33:11.07	41:13:18.05	0.20	1.72	1.99	17	0.89	7	87.8098	0.101	0.012	0.063	0.025	2.55	−0.08
495	203311.09+411445.4	20:33:11.10	41:14:45.46	0.06	0.33	8.06	15	0.90	81	96.5607	0.945	0.723	0.180	0.042	1.35	−0.31
496	203311.13+411640.6	20:33:11.13	41:16:40.66	0.17	1.68	2.05	17	0.89	8	51.0947	0.186	−0.003	0.039	0.150	3.32	−0.33
497	203311.22+410833.9	20:33:11.22	41:08:33.97	0.20	6.45	10.76	247	0.90	143	94.0856	1.697	0.161	0.762	0.775	2.56	−4.00 †
498	203311.29+411711.4	20:33:11.29	41:17:11.46	0.14	2.19	1.00	20	0.89	3	26.1520	0.137	0.032	0.033	0.072	5.29	−0.30
499	203311.32+411729.0	20:33:11.32	41:17:29.07	0.14	2.48	4.44	23	0.89	29	89.7761	0.362	0.033	0.208	0.121	2.21	−0.16
500	203311.44+411256.7	20:33:11.45	41:12:56.71	0.12	2.07	5.00	19	0.89	34	93.9285	0.416	0.035	0.202	0.179	2.58	−0.69
501	203311.47+411348.0	20:33:11.48	41:13:48.04	0.10	1.22	4.80	17	0.90	32	88.9971	0.409	0.036	0.186	0.186	2.36	−0.64
502	203311.51+411238.8	20:33:11.51	41:12:38.81	0.10	2.37	6.25	22	0.89	51	91.8617	0.633	0.109	0.268	0.256	2.52	−0.22
503	203311.52+410718.9	20:33:11.52	41:07:18.92	0.43	7.70	6.21	457	0.89	58	95.3074	0.689	0.166	0.319	0.203	1.99	−0.23
504	203311.59+411243.0	20:33:11.59	41:12:43.01	0.15	2.30	2.82	24	0.90	13	94.0636	0.161	0.011	0.046	0.105	2.97	−0.05
505	203311.60+411615.8	20:33:11.60	41:16:15.89	0.24	1.26	1.51	17	0.90	5	62.5122	0.097	0.014	0.032	0.050	3.19	−0.08
506	203311.63+411646.4	20:33:11.63	41:16:46.42	0.11	1.77	3.83	18	0.89	22	93.7809	0.269	0.070	0.142	0.058	2.07	−0.73
507	203311.79+411149.9	20:33:11.79	41:11:49.95	0.09	3.18	9.31	33	0.89	105	96.3157	1.231	0.183	0.517	0.530	2.50	−4.00 †
508	203311.87+411245.3	20:33:11.87	41:12:45.32	0.14	2.26	3.97	21	0.89	23	90.8566	0.293	0.098	0.110	0.085	1.93	−0.19
509	203311.89+411213.9	20:33:11.89	41:12:13.93	0.14	2.78	4.24	27	0.89	26	96.8308	0.311	0.066	0.169	0.077	2.14	−0.09
510	203312.04+412023.1	20:33:12.04	41:20:23.18	0.18	5.37	8.03	132	0.91	85	96.5984	0.972	0.192	0.438	0.342	2.28	−0.04
511	203312.05+411649.2	20:33:12.06	41:16:49.26	0.09	1.81	5.42	18	0.89	40	95.2697	0.477	0.139	0.163	0.175	2.01	−1.60
512	203312.20+411014.2	20:33:12.21	41:10:14.27	0.43	4.77	1.88	87	0.89	8	77.0017	0.117	0.037	0.065	0.015	1.88	−0.20
513	203312.25+411104.6	20:33:12.25	41:11: 4.67	0.21	3.93	4.22	53	0.90	26	95.1755	0.314	0.008	0.055	0.251	4.07	−0.01
514	203312.50+411502.0	20:33:12.50	41:15: 2.02	0.16	0.06	3.43	15	0.90	19	91.9811	0.231	0.093	0.094	0.044	1.83	−0.04
515	203312.50+411150.1	20:33:12.51	41:11:50.14	0.15	3.18	4.53	33	0.89	30	91.4785	0.368	0.022	0.240	0.106	2.12	−0.38
516	203312.57+411453.3	20:33:12.58	41:14:53.38	0.21	0.14	2.04	15	0.90	8	70.1731	0.133	0.012	0.076	0.045	2.46	−0.13

Table 1. continued.

N_x	NAME	RA	Dec	Error	θ	Sig.	Area	PSF	Cts	Exp.	Count Rates ($\times10^{-3}$ ctn s^{-1})				$\overline{E_x}$	Var.
#	CXOCYG J+	[h:m:s]	[d:m:s]	($''$)	($'$)	(σ)	(px.)	(%)	(ph.)	(ks)	Tot.	Soft	Med.	Hard	(keV)	log(P_{ks})
517	203312.60+411539.4	20:33:12.61	41:15:39.41	0.16	0.65	2.82	15	0.90	14	89.7478	0.174	0.096	0.045	0.033	1.69	−0.01
518	203312.62+411635.1	20:33:12.63	41:16:35.12	0.13	1.58	3.49	18	0.90	19	87.2005	0.247	0.023	0.138	0.087	2.53	−0.47
519	203312.66+411913.6	20:33:12.66	41:19:13.62	0.27	4.22	3.32	59	0.90	20	86.1137	0.271	0.126	0.112	0.033	1.91	−0.56
520	203312.73+411132.6	20:33:12.74	41:11:32.67	0.11	3.47	7.91	39	0.89	78	94.2395	0.942	0.213	0.425	0.305	2.21	−0.09
521	203312.74+411439.3	20:33:12.74	41:14:39.37	0.22	0.37	2.12	15	0.90	8	79.8725	0.122	−0.001	0.096	0.027	2.53	−0.00
522	203312.86+412115.8	20:33:12.87	41:21:15.87	0.52	6.25	2.08	215	0.90	10	87.5114	0.139	0.009	0.066	0.063	2.49	−0.28
523	203312.87+411154.4	20:33:12.88	41:11:54.50	0.13	3.11	6.12	31	0.90	50	90.5802	0.616	0.096	0.266	0.254	2.33	−1.94
524	203312.97+411257.5	20:33:12.98	41:12:57.56	0.27	2.06	1.91	19	0.89	7	52.2820	0.162	−0.003	0.104	0.061	2.30	−0.12
525	203313.03+411539.0	20:33:13.04	41:15:39.03	0.09	0.66	4.84	15	0.90	33	91.0890	0.408	0.095	0.192	0.120	2.24	−0.93
526	203313.04+411311.5	20:33:13.04	41:13:11.54	0.14	1.83	3.84	18	0.89	22	85.5232	0.296	0.025	0.182	0.090	2.23	−0.02
527	203313.08+411030.1	20:33:13.08	41:10:30.11	0.25	4.51	3.96	83	0.91	24	96.4287	0.280	0.064	0.110	0.105	2.20	−0.54
528	203313.16+411338.6	20:33:13.16	41:13:38.60	0.27	1.38	1.91	18	0.90	7	78.2675	0.108	0.055	0.055	−0.002	1.54	−0.00
529	203313.23+411319.1	20:33:13.23	41:13:19.13	0.12	1.70	4.14	17	0.89	25	73.8952	0.389	0.074	0.180	0.135	2.12	−2.79
530	203313.24+411328.4	20:33:13.25	41:13:28.46	0.05	1.55	10.76	19	0.90	137	93.8783	1.628	0.922	0.625	0.081	1.63	−0.09
531	203313.25+411727.2	20:33:13.26	41:17:27.24	0.18	2.45	2.09	23	0.89	8	89.8578	0.112	0.008	0.057	0.046	2.50	−0.02
532	203313.38+411110.8	20:33:13.39	41:11:10.89	0.31	3.84	1.91	49	0.89	7	48.6887	0.181	0.016	0.131	0.034	1.92	−2.03
533	203313.40+411233.6	20:33:13.40	41:12:33.66	0.22	2.46	2.35	23	0.89	10	89.1008	0.131	0.048	0.023	0.061	1.73	−0.23
534	203313.54+411948.8	20:33:13.55	41:19:48.83	0.28	4.81	3.61	87	0.89	23	93.9788	0.274	0.063	0.153	0.058	2.12	−0.38
535	203313.60+412004.8	20:33:13.61	41:20: 4.88	0.27	5.08	4.18	101	0.90	29	97.1606	0.335	0.068	0.179	0.088	2.26	−2.49
536	203313.62+411749.2	20:33:13.62	41:17:49.27	0.15	2.82	4.33	28	0.90	28	97.2517	0.324	0.096	0.152	0.076	1.98	−0.58
537	203313.67+411305.4	20:33:13.67	41:13: 5.46	0.06	1.94	9.60	18	0.89	111	97.3428	1.286	0.736	0.483	0.067	1.63	−0.07
538	203313.78+411028.0	20:33:13.78	41:10:28.06	0.40	4.55	1.79	85	0.91	7	92.2575	0.089	0.020	0.031	0.037	2.26	−0.45
539	203313.85+411715.1	20:33:13.86	41:17:15.14	0.09	2.26	6.14	21	0.89	50	92.1853	0.613	0.022	0.289	0.302	2.65	−2.98
540	203313.87+411259.0	20:33:13.87	41:12:59.04	0.23	2.05	2.38	19	0.89	10	84.0563	0.140	0.025	0.052	0.064	2.05	−0.11
541	203313.88+411345.4	20:33:13.89	41:13:45.44	0.21	1.29	2.07	17	0.90	8	88.2904	0.108	−0.002	0.061	0.048	2.21	−0.26 †
542	203314.05+411626.9	20:33:14.06	41:16:26.94	0.16	1.48	1.35	18	0.90	4	59.4529	0.086	0.016	−0.002	0.072	4.81	−0.76
543	203314.09+410925.6	20:33:14.10	41:09:25.70	0.40	5.59	2.59	158	0.90	13	96.4036	0.160	0.045	0.105	0.010	1.99	−2.05
544	203314.11+412021.6	20:33:14.11	41:20:21.69	0.04	5.36	41.78	136	0.91	1834	97.6537	20.735	8.399	10.375	1.961	1.77	−0.16
545	203314.13+411446.6	20:33:14.14	41:14:46.61	0.16	0.43	1.92	15	0.90	7	84.9955	0.100	0.012	0.050	0.038	2.36	−0.02
546	203314.15+411450.2	20:33:14.16	41:14:50.28	0.17	0.40	2.66	15	0.90	12	93.2689	0.150	0.058	0.021	0.070	2.74	−1.34
547	203314.16+412054.9	20:33:14.17	41:20:55.00	0.29	5.92	5.37	188	0.91	42	95.6278	0.495	0.032	0.284	0.178	2.36	−2.14
548	203314.22+410852.7	20:33:14.22	41:08:52.80	0.50	6.14	2.92	209	0.91	17	92.1758	0.206	0.010	0.119	0.077	2.40	−0.25
549	203314.24+411227.8	20:33:14.25	41:12:27.87	0.13	2.58	4.22	24	0.89	26	86.5754	0.343	0.076	0.128	0.140	2.28	−0.12
550	203314.25+411236.7	20:33:14.25	41:12:36.79	0.22	2.43	1.53	22	0.89	5	53.1175	0.117	0.018	0.061	0.038	1.86	−0.14
551	203314.31+411221.2	20:33:14.32	41:12:21.28	0.18	2.69	3.32	15	0.80	17	83.4219	0.266	0.014	0.134	0.118	2.71	−0.04
552	203314.32+411932.8	20:33:14.33	41:19:32.89	0.17	4.55	6.48	75	0.89	58	91.1016	0.719	0.294	0.382	0.042	1.80	−0.15
553	203314.38+411223.5	20:33:14.38	41:12:23.51	0.16	2.65	1.77	14	0.80	6	69.2905	0.121	0.071	0.034	0.016	1.64	−0.03
554	203314.39+411901.0	20:33:14.39	41:19: 1.10	0.27	4.03	3.40	55	0.91	21	89.8232	0.263	0.061	0.153	0.049	1.91	−0.32
555	203314.42+411923.5	20:33:14.42	41:19:23.52	0.07	4.40	17.41	68	0.89	343	97.1418	3.970	0.713	1.759	1.498	2.28	−4.00 †
556	203314.44+410633.3	20:33:14.44	41:06:33.34	0.50	8.47	6.38	678	0.87	60	95.6247	0.718	0.197	0.280	0.241	2.17	−4.00 †
557	203314.47+411856.2	20:33:14.48	41:18:56.28	0.10	3.95	10.23	53	0.91	130	97.1669	1.478	0.371	0.633	0.474	2.12	−0.20
558	203314.50+411253.9	20:33:14.50	41:12:53.93	0.14	2.16	3.17	19	0.89	16	82.6021	0.224	0.025	0.120	0.079	2.55	−0.15
559	203314.58+411837.1	20:33:14.58	41:18:37.12	0.09	3.63	9.26	44	0.90	108	97.4307	1.241	0.517	0.436	0.289	1.95	−0.93
560	203314.69+410944.1	20:33:14.69	41:09:44.13	0.51	5.30	2.55	116	0.89	12	81.4524	0.175	0.047	0.114	0.014	1.96	−0.06
561	203314.76+412012.5	20:33:14.77	41:20:12.59	0.34	5.22	4.08	112	0.89	27	88.9532	0.342	0.094	0.135	0.114	2.34	−0.07
562	203314.76+411841.4	20:33:14.77	41:18:41.47	0.06	3.71	15.91	47	0.90	290	96.9973	3.331	1.904	1.284	0.143	1.64	−0.04
563	203314.81+411421.0	20:33:14.82	41:14:21.06	0.20	0.82	1.40	16	0.90	4	89.1950	0.059	−0.001	0.024	0.036	3.76	−2.17

Table 1. continued.

N_x	NAME	RA	Dec	Error	θ	Sig.	Area	PSF	Cts	Exp.	Count Rates ($\times 10^{-3}$ ctn s^{-1})				$\overline{E}_x$	Var.
#	CXOCYG J+	[h:m:s]	[d:m:s]	($''$)	($'$)	(σ)	(px.)	(%)	(ph.)	(ks)	Tot.	Soft	Med.	Hard	(keV)	log(P_{ks})
564	203314.84+410831.4	20:33:14.85	41:08:31.41	0.52	6.51	3.80	245	0.89	25	94.6886	0.303	0.089	0.134	0.080	2.07	−0.00
565	203314.87+410957.6	20:33:14.88	41:09:57.67	0.62	5.07	1.87	102	0.89	7	79.6935	0.112	0.050	0.049	0.014	1.86	−0.33
566	203314.92+411719.4	20:33:14.93	41:17:19.50	0.19	2.37	2.21	22	0.89	9	72.9215	0.145	0.028	0.074	0.044	2.49	−0.07
567	203314.97+411556.8	20:33:14.98	41:15:56.84	0.11	1.07	3.86	16	0.90	22	89.9237	0.281	0.048	0.147	0.085	2.17	−0.11
568	203315.07+411850.3	20:33:15.07	41:18:50.33	0.01	3.86	113.60	51	0.90	13138	97.7700	148.642	37.373	63.566	47.702	2.17	−0.44
569	203315.11+411310.5	20:33:15.12	41:13:10.56	0.11	1.91	4.23	18	0.89	26	72.7425	0.410	−0.002	0.106	0.306	4.40	−3.94 †
570	203315.12+411903.3	20:33:15.12	41:19: 3.36	0.22	4.08	4.77	57	0.90	36	88.9029	0.449	0.089	0.287	0.073	2.10	−0.07
571	203315.18+411530.8	20:33:15.18	41:15:30.88	0.09	0.75	4.96	16	0.90	34	93.5013	0.413	0.106	0.141	0.165	2.07	−0.67
572	203315.21+411327.5	20:33:15.22	41:13:27.55	0.12	1.65	4.03	19	0.90	24	90.1216	0.302	0.047	0.121	0.133	2.50	−1.56
573	203315.28+411522.6	20:33:15.29	41:15:22.69	0.16	0.68	2.66	16	0.90	12	67.2143	0.208	0.031	0.063	0.113	3.42	−0.77
574	203315.31+411855.6	20:33:15.31	41:18:55.66	0.17	3.96	2.76	9	0.48	13	90.8660	0.308	0.134	0.155	0.018	1.73	−0.03
575	203315.33+411029.9	20:33:15.34	41:10:30.00	0.36	4.55	3.56	84	0.91	20	86.3304	0.263	0.060	0.136	0.067	2.20	−0.08
576	203315.38+411751.5	20:33:15.38	41:17:51.51	0.26	2.91	2.00	29	0.90	8	57.4521	0.165	0.029	0.123	0.013	1.93	−0.44
577	203315.39+411338.4	20:33:15.40	41:13:38.45	0.15	1.49	3.62	18	0.90	20	84.1537	0.271	0.077	0.077	0.117	2.55	−0.00
578	203315.40+411329.6	20:33:15.40	41:13:29.61	0.20	1.63	2.79	19	0.90	13	89.1448	0.168	0.048	0.073	0.047	1.80	−0.01
579	203315.43+411816.0	20:33:15.44	41:18:16.05	0.09	3.31	8.63	36	0.89	94	94.2834	1.124	0.250	0.456	0.418	2.24	−2.96
580	203315.45+411856.7	20:33:15.45	41:18:56.77	0.12	3.98	3.07	9	0.47	16	88.7553	0.387	0.162	0.158	0.067	1.76	−0.67
581	203315.55+412133.3	20:33:15.56	41:21:33.36	0.37	6.57	5.86	267	0.90	50	94.2458	0.591	0.511	0.087	−0.007	1.28	−1.01
582	203315.63+411851.4	20:33:15.64	41:18:51.48	0.17	3.90	7.44	52	0.91	75	95.5241	0.871	0.253	0.430	0.188	2.12	−1.49
583	203315.68+411319.4	20:33:15.68	41:13:19.49	0.26	1.81	1.72	20	0.90	6	74.0617	0.097	0.028	0.013	0.057	2.85	−0.00
584	203315.70+412017.0	20:33:15.70	41:20:17.05	0.21	5.31	6.26	108	0.87	53	94.1264	0.654	0.351	0.268	0.035	1.60	−0.04
585	203315.76+410633.1	20:33:15.77	41:06:33.19	0.71	8.48	4.16	661	0.87	31	90.7498	0.399	0.122	0.093	0.184	2.78	−0.41
586	203315.80+411510.2	20:33:15.81	41:15:10.30	0.08	0.69	5.41	16	0.90	40	94.3588	0.478	0.093	0.245	0.140	2.17	−0.03
587	203315.82+411225.8	20:33:15.83	41:12:25.81	0.26	2.67	2.04	25	0.89	8	70.0318	0.135	0.046	0.046	0.044	1.92	−1.19
588	203315.84+412115.0	20:33:15.84	41:21:15.04	0.42	6.28	3.94	229	0.90	26	93.8186	0.318	0.078	0.166	0.074	1.95	−4.00 †
589	203315.89+411623.3	20:33:15.89	41:16:23.37	0.21	1.54	1.52	18	0.90	5	51.9051	0.117	−0.004	0.081	0.039	2.18	−0.09
590	203315.90+412025.3	20:33:15.91	41:20:25.38	0.25	5.46	6.55	148	0.91	58	94.5002	0.689	0.114	0.357	0.218	2.36	−0.26
591	203316.17+411245.3	20:33:16.18	41:12:45.39	0.29	2.37	1.90	21	0.89	7	38.6877	0.218	0.054	0.170	−0.006	1.96	−1.03
592	203316.21+411721.8	20:33:16.22	41:17:21.83	0.14	2.47	3.50	24	0.89	19	95.0624	0.229	0.045	0.080	0.104	2.59	−0.07
593	203316.21+411440.3	20:33:16.22	41:14:40.35	0.06	0.82	7.14	16	0.90	65	96.4382	0.757	0.183	0.287	0.288	2.36	−2.75
594	203316.22+412015.5	20:33:16.22	41:20:15.58	0.22	5.30	7.55	109	0.88	74	85.6488	0.995	0.159	0.559	0.277	2.15	−0.87
595	203316.29+412143.7	20:33:16.30	41:21:43.78	0.32	6.76	6.52	295	0.90	60	94.0227	0.714	0.124	0.425	0.165	2.20	−0.19
596	203316.34+411858.9	20:33:16.34	41:18:58.96	0.05	4.05	17.05	27	0.77	327	93.4511	4.545	0.529	1.927	2.089	2.55	−4.00 †
597	203316.36+411902.1	20:33:16.36	41:19: 2.14	0.12	4.10	7.08	30	0.79	66	96.7805	0.869	0.448	0.390	0.032	1.61	−4.00
598	203316.44+411659.2	20:33:16.44	41:16:59.30	0.23	2.13	2.08	20	0.89	8	56.2553	0.171	0.017	0.037	0.117	3.13	−0.28
599	203316.45+410924.9	20:33:16.46	41:09:24.92	0.25	5.65	6.00	158	0.90	50	95.7880	0.584	0.046	0.233	0.305	2.85	−0.05
600	203316.50+411653.9	20:33:16.50	41:16:53.97	0.03	2.05	19.72	19	0.89	428	89.9112	5.343	2.467	1.906	0.971	1.76	−4.00 †
601	203316.52+410703.7	20:33:16.52	41:07: 3.80	0.45	7.99	5.56	502	0.89	48	92.2732	0.595	0.191	0.247	0.158	1.89	−0.00
602	203316.57+411703.9	20:33:16.57	41:17: 3.98	0.21	2.21	2.38	21	0.89	10	66.0050	0.179	0.083	0.082	0.015	1.76	−0.08
603	203316.60+411258.8	20:33:16.60	41:12:58.82	0.09	2.19	6.38	20	0.89	53	95.0750	0.632	0.164	0.282	0.186	2.08	−4.00
604	203316.64+411542.2	20:33:16.65	41:15:42.23	0.14	1.08	2.64	16	0.90	12	92.7349	0.150	0.022	0.033	0.094	3.20	−0.60
605	203316.66+411404.4	20:33:16.67	41:14: 4.49	0.16	1.25	2.28	17	0.90	9	85.0426	0.128	0.052	0.051	0.025	1.86	−0.77
606	203316.72+411833.1	20:33:16.73	41:18:33.12	0.12	3.64	6.37	45	0.90	55	96.2120	0.639	0.129	0.285	0.225	2.26	−2.75
607	203316.73+411129.3	20:33:16.74	41:11:29.36	0.39	3.62	2.10	42	0.89	8	86.6382	0.116	0.011	0.034	0.072	3.67	−0.01
608	203316.83+411056.8	20:33:16.84	41:10:56.88	0.18	4.15	5.09	59	0.90	36	96.7931	0.424	0.077	0.203	0.144	2.36	−0.92
609	203317.08+411659.7	20:33:17.09	41:16:59.74	0.19	2.18	2.64	20	0.89	12	87.9606	0.159	0.010	0.100	0.048	2.36	−0.60
610	203317.12+411506.6	20:33:17.12	41:15: 6.62	0.12	0.93	3.84	16	0.90	22	84.5809	0.298	0.051	0.130	0.117	2.14	−0.02

Table 1. continued.

N_x	NAME	RA	Dec	Error	θ	Sig.	Area	PSF	Cts	Exp.	Count Rates ($\times 10^{-3}$ ctn s^{-1})				$\overline{E_x}$	Var.
#	CXOCYG J+	[h:m:s]	[d:m:s]	($''$)	($'$)	(σ)	(px.)	(%)	(ph.)	(ks)	Tot.	Soft	Med.	Hard	(keV)	log(P_{ks})
611	203317.31+411342.0	20:33:17.31	41:13:42.07	0.15	1.62	1.85	18	0.90	7	80.1081	0.102	0.024	0.067	0.010	1.95	−0.15
612	203317.38+411653.9	20:33:17.39	41:16:53.97	0.06	2.12	9.91	20	0.89	118	92.7475	1.431	0.251	0.735	0.444	2.17	−4.00 †
613	203317.40+411453.8	20:33:17.40	41:14:53.88	0.14	0.98	3.51	16	0.90	19	84.2448	0.259	0.038	0.170	0.051	2.34	−0.17
614	203317.40+411238.4	20:33:17.41	41:12:38.44	0.18	2.56	3.16	23	0.89	16	93.0302	0.199	0.058	0.107	0.034	1.96	−0.27
615	203317.47+411709.0	20:33:17.48	41:17: 9.06	0.06	2.36	10.66	22	0.89	135	97.2046	1.564	0.760	0.702	0.101	1.70	−1.85
616	203317.51+410724.3	20:33:17.51	41:07:24.38	0.45	7.67	6.06	464	0.90	55	80.4253	0.759	0.150	0.236	0.372	2.75	−3.75 †
617	203317.53+411800.7	20:33:17.53	41:18: 0.75	0.20	3.16	3.22	33	0.90	17	90.7121	0.216	0.116	0.042	0.057	1.64	−0.32
618	203317.55+412041.1	20:33:17.56	41:20:41.17	0.35	5.76	5.29	179	0.91	41	95.3263	0.484	0.066	0.181	0.237	2.66	−4.00 †
619	203317.63+412022.0	20:33:17.64	41:20:22.05	0.30	5.45	3.78	149	0.91	24	96.6329	0.280	0.044	0.149	0.087	2.04	−0.14
620	203317.74+411304.7	20:33:17.75	41:13: 4.72	0.08	2.19	7.33	20	0.89	68	95.9953	0.801	0.232	0.291	0.278	2.21	−0.04
621	203317.76+411753.0	20:33:17.77	41:17:53.05	0.22	3.06	2.99	31	0.90	15	78.3429	0.221	0.021	0.106	0.094	2.37	−0.11
622	203317.83+411323.3	20:33:17.83	41:13:23.38	0.05	1.93	10.84	21	0.90	139	95.5053	1.623	0.382	0.697	0.544	2.14	−0.90
623	203317.95+411917.9	20:33:17.95	41:19:17.90	0.19	4.42	4.71	71	0.89	33	95.0090	0.397	0.128	0.147	0.122	2.08	−1.25
624	203317.97+410749.6	20:33:17.97	41:07:49.62	0.53	7.27	3.82	353	0.89	25	93.5233	0.304	0.062	0.163	0.079	2.15	−0.66
625	203317.99+411830.9	20:33:18.00	41:18:30.92	0.05	3.67	19.72	46	0.90	430	97.3459	4.931	2.605	2.115	0.211	1.67	−0.46
626	203318.06+412136.3	20:33:18.06	41:21:36.40	0.25	6.69	9.79	288	0.90	120	95.3231	1.407	0.751	0.499	0.156	1.67	−0.30
627	203318.06+412136.4	20:33:18.06	41:21:36.40	0.25	6.69	9.78	288	0.90	120	95.3231	1.405	0.751	0.499	0.156	1.67	−0.30
628	203318.06+411714.4	20:33:18.06	41:17:14.50	0.22	2.49	2.33	24	0.89	10	87.6182	0.132	0.049	0.060	0.022	2.01	−0.03
629	203318.08+411731.1	20:33:18.08	41:17:31.20	0.11	2.74	5.67	27	0.90	44	90.6744	0.543	0.145	0.291	0.107	2.04	−1.26
630	203318.08+411731.2	20:33:18.08	41:17:31.20	0.09	2.74	3.46	4	0.39	18	75.1013	0.644	0.238	0.203	0.203	2.07	−0.29
631	203318.14+411101.1	20:33:18.15	41:11: 1.10	0.46	4.15	2.24	57	0.90	9	80.0893	0.138	0.038	0.093	0.007	2.01	−1.46
632	203318.17+410920.5	20:33:18.18	41:09:20.55	0.43	5.78	3.95	167	0.90	25	95.9764	0.300	0.056	0.125	0.119	2.08	−0.52
633	203318.28+411739.0	20:33:18.28	41:17:39.08	0.06	2.87	11.05	29	0.90	144	94.4028	1.709	0.349	0.809	0.551	2.26	−1.49
634	203318.30+412209.5	20:33:18.30	41:22: 9.55	0.53	7.24	4.66	386	0.90	36	93.5202	0.434	0.059	0.179	0.196	2.26	−2.01
635	203318.42+411240.4	20:33:18.43	41:12:40.43	0.12	2.61	4.84	23	0.89	33	90.9226	0.411	0.084	0.146	0.181	2.26	−1.47 †
636	203318.46+411452.9	20:33:18.46	41:14:52.92	0.13	1.18	3.29	17	0.90	17	69.7554	0.281	0.094	0.109	0.077	1.92	−0.25
637	203318.46+411119.2	20:33:18.46	41:11:19.22	0.17	3.87	4.62	48	0.89	31	76.4991	0.455	0.069	0.200	0.185	2.72	−1.06
638	203318.52+411534.9	20:33:18.52	41:15:34.92	0.14	1.31	3.52	17	0.90	19	83.9653	0.260	0.011	0.118	0.131	2.81	−0.03
639	203318.66+411912.0	20:33:18.67	41:19:12.04	0.36	4.36	2.48	68	0.89	12	85.6520	0.162	0.067	0.073	0.021	1.83	−0.00
640	203318.66+411723.6	20:33:18.67	41:17:23.65	0.21	2.67	2.59	26	0.89	12	91.6858	0.149	0.021	0.057	0.070	2.49	−0.00
641	203318.74+411704.1	20:33:18.74	41:17: 4.16	0.25	2.39	1.52	22	0.89	5	81.5624	0.075	0.011	0.039	0.025	2.27	−0.02
642	203318.77+412130.5	20:33:18.78	41:21:30.52	0.41	6.61	2.78	71	0.60	14	82.7026	0.286	0.071	0.188	0.026	2.01	−0.00
643	203318.87+411436.8	20:33:18.87	41:14:36.82	0.06	1.31	8.71	17	0.90	93	96.0989	1.086	0.126	0.404	0.555	2.81	−2.77 †
644	203318.91+411319.2	20:33:18.91	41:13:19.24	0.22	2.11	1.11	20	0.89	3	44.1750	0.090	0.047	0.048	−0.005	1.19	−0.01
645	203318.94+411332.6	20:33:18.95	41:13:32.66	0.34	1.94	1.90	21	0.90	7	60.0120	0.139	0.089	0.035	0.015	1.42	−0.19
646	203319.01+412134.8	20:33:19.01	41:21:34.81	0.32	6.69	4.26	73	0.59	27	86.6728	0.534	0.148	0.243	0.144	2.05	−0.16
647	203318.99+410759.1	20:33:18.99	41:07:59.13	0.62	7.14	3.01	332	0.89	18	93.4165	0.221	0.086	0.106	0.030	1.80	−0.86
648	203319.06+411354.1	20:33:19.06	41:13:54.12	0.26	1.70	1.58	19	0.90	5	66.2846	0.095	0.015	0.049	0.031	1.92	−0.02
649	203319.11+410658.4	20:33:19.12	41:06:58.47	0.51	8.14	4.97	566	0.90	41	92.4334	0.497	0.118	0.219	0.159	2.62	−0.21
650	203319.13+411659.2	20:33:19.13	41:16:59.27	0.06	2.36	9.95	22	0.89	119	97.0098	1.380	0.934	0.379	0.067	1.41	−0.62
651	203319.16+411906.7	20:33:19.16	41:19: 6.78	0.33	4.30	2.84	66	0.89	15	85.9535	0.201	0.025	0.122	0.055	2.21	−0.71
652	203319.21+411756.4	20:33:19.22	41:17:56.44	0.06	3.21	13.58	34	0.90	212	96.7177	2.447	0.213	1.052	1.181	2.68	−4.00 †
653	203319.29+411702.1	20:33:19.30	41:17: 2.11	0.24	2.42	2.20	22	0.89	9	83.3622	0.127	0.024	0.091	0.011	1.94	−0.19
654	203319.42+411741.4	20:33:19.42	41:17:41.50	0.26	3.00	2.17	30	0.90	9	91.6701	0.117	0.006	0.054	0.056	2.72	−0.07
655	203319.44+411349.8	20:33:19.45	41:13:49.84	0.19	1.80	1.35	20	0.90	4	86.8801	0.059	0.037	0.011	0.011	1.69	−0.08
656	203319.46+412008.5	20:33:19.46	41:20: 8.55	0.28	5.31	4.18	122	0.89	27	91.7298	0.335	0.026	0.122	0.188	2.90	−0.65
657	203319.48+411517.6	20:33:19.48	41:15:17.65	0.25	1.39	1.54	18	0.90	5	53.7174	0.115	0.018	0.038	0.059	2.84	−0.03

Table 1. continued.

N_x	NAME	RA	Dec	Error	θ	Sig.	Area	PSF	Cts	Exp.	Count Rates ($\times 10^{-3}$ ctn s^{-1})				$\overline{E}_x$	Var.
#	CXOCYG J+	[h:m:s]	[d:m:s]	($''$)	($'$)	(σ)	(px.)	(%)	(ph.)	(ks)	Tot.	Soft	Med.	Hard	(keV)	log(P_{ks})
658	203319.48+411225.7	20:33:19.48	41:12:25.74	0.20	2.92	2.88	27	0.89	14	83.3873	0.192	0.105	0.051	0.036	1.48	−0.04
659	203319.48+410737.0	20:33:19.48	41:07:37.06	0.37	7.52	6.97	396	0.90	67	96.4476	0.774	0.336	0.298	0.140	1.98	−0.04
660	203319.52+412127.0	20:33:19.53	41:21:27.08	0.63	6.58	3.51	246	0.88	21	88.8181	0.273	0.024	0.151	0.099	2.50	−0.20
661	203319.58+411906.4	20:33:19.58	41:19: 6.45	0.24	4.32	4.52	66	0.89	31	85.1745	0.414	0.078	0.244	0.093	2.05	−0.83
662	203319.59+411803.9	20:33:19.60	41:18: 3.92	0.21	3.35	3.39	37	0.89	19	86.5000	0.248	0.018	0.145	0.085	2.28	−1.41
663	203319.59+411042.3	20:33:19.60	41:10:42.32	0.37	4.52	3.17	70	0.90	17	80.7489	0.238	0.090	0.076	0.072	1.80	−0.14
664	203319.73+412103.1	20:33:19.74	41:21: 3.17	0.48	6.20	4.67	225	0.90	33	93.1998	0.396	0.045	0.201	0.151	2.31	−4.00 †
665	203319.88+411124.6	20:33:19.89	41:11:24.61	0.26	3.88	2.66	47	0.89	12	91.5508	0.157	0.044	0.020	0.093	3.34	−0.81
666	203319.91+410716.8	20:33:19.91	41:07:16.86	0.66	7.86	4.52	490	0.90	34	94.8740	0.401	0.098	0.199	0.104	2.18	−0.10
667	203320.02+412011.6	20:33:20.02	41:20:11.68	0.29	5.39	4.83	127	0.89	35	93.0647	0.432	0.080	0.198	0.154	2.10	−0.33
668	203320.03+411831.6	20:33:20.03	41:18:31.68	0.18	3.81	4.80	50	0.90	34	95.7880	0.398	0.148	0.150	0.100	1.83	−0.32
669	203320.09+411632.8	20:33:20.10	41:16:32.85	0.28	2.13	1.70	20	0.89	6	37.5978	0.193	−0.005	0.025	0.173	4.83	−0.42
670	203320.12+411943.2	20:33:20.13	41:19:43.22	0.16	4.94	7.98	100	0.90	82	96.0110	0.958	0.173	0.467	0.318	2.30	−0.41
671	203320.19+411716.4	20:33:20.19	41:17:16.44	0.11	2.71	5.86	26	0.89	46	96.5889	0.537	0.148	0.240	0.149	2.05	−1.38
672	203320.23+411432.3	20:33:20.24	41:14:32.32	0.06	1.58	8.35	19	0.90	86	96.3753	1.000	0.184	0.391	0.425	2.62	−0.09
673	203320.31+411647.1	20:33:20.31	41:16:47.10	0.22	2.34	1.89	21	0.89	7	54.8199	0.153	0.038	0.078	0.037	2.22	−1.20
674	203320.39+411840.8	20:33:20.40	41:18:40.89	0.29	3.98	3.36	55	0.90	19	85.3818	0.246	0.172	0.040	0.034	1.37	−0.19
675	203320.40+411929.0	20:33:20.41	41:19:29.10	0.19	4.73	6.94	87	0.89	64	91.3246	0.795	0.081	0.007	0.707	4.15	−0.07
676	203320.47+412033.0	20:33:20.47	41:20:33.04	0.13	5.75	12.60	179	0.91	186	96.7114	2.129	1.275	0.696	0.158	1.51	−4.00 †
677	203320.49+412144.8	20:33:20.49	41:21:44.82	0.64	6.91	2.25	322	0.90	10	83.5947	0.141	0.033	0.084	0.023	1.79	−0.12
678	203320.55+411815.6	20:33:20.56	41:18:15.69	0.31	3.61	2.80	43	0.89	14	94.4562	0.173	0.038	0.036	0.099	3.37	−0.15
679	203320.58+411451.3	20:33:20.58	41:14:51.36	0.22	1.58	2.52	18	0.90	11	63.3163	0.203	0.033	0.050	0.120	3.86	−0.36
680	203320.58+411704.4	20:33:20.59	41:17: 4.49	0.24	2.59	2.36	24	0.89	10	89.6630	0.131	0.035	0.085	0.010	1.96	−0.00
681	203320.58+411653.6	20:33:20.59	41:16:53.65	0.17	2.45	3.04	22	0.89	15	87.4266	0.199	0.024	0.075	0.100	3.76	−0.01
682	203320.68+411418.4	20:33:20.68	41:14:18.48	0.18	1.74	2.67	20	0.90	12	82.3728	0.170	0.066	0.093	0.011	1.92	−0.40
683	203320.76+411723.1	20:33:20.76	41:17:23.16	0.12	2.87	4.54	28	0.89	30	89.5876	0.376	0.047	0.183	0.147	2.56	−0.58
684	203320.83+411013.4	20:33:20.84	41:10:13.48	0.47	5.05	2.34	110	0.90	11	88.5448	0.146	0.012	0.014	0.120	4.91	−0.01
685	203320.93+411207.9	20:33:20.94	41:12: 7.93	0.14	3.31	4.98	34	0.89	35	77.6832	0.508	0.141	0.185	0.182	2.27	−0.01
686	203321.01+411739.8	20:33:21.01	41:17:39.88	0.13	3.12	5.05	32	0.90	36	86.0163	0.466	0.254	0.189	0.023	1.66	−0.01
687	203321.04+411708.8	20:33:21.05	41:17: 8.88	0.08	2.70	8.60	26	0.89	91	93.3003	1.099	0.154	0.418	0.527	2.68	−4.00 †
688	203321.04+410647.3	20:33:21.05	41:06:47.35	0.51	8.39	4.76	620	0.90	39	96.8088	0.457	0.104	0.194	0.159	2.39	−0.41
689	203321.10+411659.2	20:33:21.10	41:16:59.30	0.22	2.59	1.53	24	0.89	5	85.3065	0.072	0.010	0.051	0.011	2.04	−0.22
690	203321.11+411756.6	20:33:21.12	41:17:56.62	0.20	3.37	3.67	36	0.90	21	88.7490	0.276	0.043	0.078	0.155	2.90	−3.07
691	203321.14+411242.1	20:33:21.14	41:12:42.12	0.28	2.85	1.71	26	0.89	6	90.6399	0.080	0.023	0.035	0.022	1.89	−0.53
692	203321.15+411325.4	20:33:21.15	41:13:25.46	0.15	2.31	3.30	21	0.89	17	90.5676	0.218	0.098	0.085	0.035	1.74	−0.14
693	203321.21+411845.9	20:33:21.21	41:18:45.91	0.28	4.12	3.87	58	0.91	23	93.4605	0.277	0.029	0.158	0.090	2.11	−0.64
694	203321.25+411839.4	20:33:21.25	41:18:39.49	0.14	4.02	5.81	55	0.90	46	93.6301	0.548	0.158	0.181	0.209	2.20	−4.00 †
695	203321.27+411250.3	20:33:21.28	41:12:50.34	0.14	2.76	4.76	25	0.89	32	97.6600	0.371	0.101	0.147	0.123	2.01	−0.04
696	203321.29+411312.8	20:33:21.30	41:13:12.87	0.26	2.48	1.74	22	0.89	6	66.7054	0.110	0.015	0.031	0.064	2.84	−0.20
697	203321.59+411229.1	20:33:21.60	41:12:29.16	0.23	3.08	2.91	29	0.89	14	66.7180	0.243	0.031	0.115	0.097	1.95	−0.53
698	203321.64+411127.0	20:33:21.64	41:11:27.03	0.37	3.98	1.89	50	0.89	7	86.1922	0.101	0.007	0.009	0.085	3.20	−0.64
699	203321.69+412026.3	20:33:21.69	41:20:26.31	0.47	5.71	3.32	174	0.91	19	95.3639	0.230	0.066	0.089	0.076	1.88	−0.08
700	203321.73+411511.1	20:33:21.74	41:15:11.16	0.08	1.80	6.65	20	0.90	57	94.5724	0.678	0.093	0.363	0.222	2.40	−1.00
701	203321.81+411332.2	20:33:21.81	41:13:32.28	0.08	2.33	7.15	21	0.89	65	93.7118	0.785	0.166	0.310	0.309	2.25	−0.21
702	203321.85+412136.1	20:33:21.86	41:21:36.18	0.38	6.84	5.30	310	0.90	42	93.1370	0.506	0.122	0.233	0.151	2.34	−0.56
703	203321.83+410944.6	20:33:21.83	41:09:44.61	0.35	5.57	3.47	130	0.89	20	89.5405	0.260	0.048	0.115	0.097	2.53	−0.04
704	203321.90+411316.5	20:33:21.91	41:13:16.54	0.18	2.51	3.40	23	0.89	18	95.8445	0.217	0.057	0.104	0.056	2.20	−0.26

Table 1. continued.

N_x	NAME	RA	Dec	Error	θ	Sig.	Area	PSF	Cts	Exp.	Count Rates ($\times 10^{-3}$ ctn s^{-1})				$\overline{E_x}$	Var.
#	CXOCYG J+	[h:m:s]	[d:m:s]	($''$)	($'$)	(σ)	(px.)	(%)	(ph.)	(ks)	Tot.	Soft	Med.	Hard	(keV)	log(P_{ks})
705	203321.92+411731.3	20:33:21.93	41:17:31.38	0.12	3.10	6.05	32	0.90	49	95.7503	0.572	0.056	0.287	0.229	2.24	−0.81
706	203321.97+412037.2	20:33:21.97	41:20:37.21	0.52	5.90	2.72	193	0.91	14	89.8703	0.178	0.024	0.072	0.082	2.50	−0.26
707	203322.00+411431.3	20:33:22.00	41:14:31.34	0.19	1.90	3.04	20	0.90	15	72.4409	0.238	0.059	0.106	0.073	2.11	−2.42
708	203322.01+411217.5	20:33:22.02	41:12:17.57	0.09	3.28	8.89	33	0.89	97	94.8300	1.153	0.317	0.531	0.304	2.02	−0.04
709	203322.06+412153.8	20:33:22.07	41:21:53.86	0.47	7.13	4.21	346	0.89	28	79.1312	0.407	0.013	0.194	0.199	2.77	−2.86 †
710	203322.06+411003.9	20:33:22.06	41:10: 3.90	0.20	5.28	7.96	126	0.91	81	94.9964	0.950	0.174	0.418	0.357	2.31	−2.48
711	203322.12+411245.1	20:33:22.13	41:12:45.10	0.15	2.93	4.42	27	0.89	28	87.3575	0.366	0.152	0.152	0.062	1.85	−0.24
712	203322.25+411744.3	20:33:22.25	41:17:44.30	0.06	3.31	13.48	35	0.90	209	97.1260	2.392	0.397	1.209	0.786	2.26	−3.43 †
713	203322.34+411815.8	20:33:22.35	41:18:15.80	0.25	3.77	3.25	47	0.89	18	86.2268	0.234	0.032	0.027	0.175	3.50	−0.58
714	203322.37+411551.4	20:33:22.38	41:15:51.44	0.18	2.09	1.24	2	0.40	3	42.7742	0.228	−0.001	0.115	0.114	3.37	−0.01
715	203322.40+411551.4	20:33:22.40	41:15:51.40	0.22	2.09	1.00	3	0.41	2	42.7742	0.168	−0.001	0.056	0.113	3.37	−0.08
716	203322.44+411736.5	20:33:22.44	41:17:36.60	0.26	3.23	2.29	34	0.90	10	46.9674	0.240	0.114	0.038	0.088	1.82	−1.16
717	203322.57+411340.2	20:33:22.57	41:13:40.30	0.27	2.36	1.74	21	0.89	6	78.7323	0.094	0.013	0.027	0.055	3.03	−0.48
718	203322.91+411859.8	20:33:22.92	41:18:59.87	0.19	4.46	5.06	71	0.89	37	92.2072	0.454	0.085	0.207	0.162	2.28	−1.06
719	203323.02+411612.0	20:33:23.02	41:16:12.00	0.22	2.35	2.20	21	0.89	9	88.3438	0.120	0.036	0.049	0.035	1.77	−0.33
720	203323.02+410932.5	20:33:23.02	41:09:32.58	0.49	5.83	2.58	148	0.89	14	91.7926	0.172	0.026	0.092	0.054	1.98	−0.43
721	203323.02+411222.0	20:33:23.03	41:12:22.10	0.04	3.33	18.74	34	0.89	389	97.6600	4.477	3.402	0.883	0.192	1.28	−0.57
722	203323.02+411222.1	20:33:23.03	41:12:22.10	0.03	3.33	11.77	4	0.39	161	96.5355	4.259	3.340	0.710	0.209	1.25	−0.32
723	203323.22+411909.2	20:33:23.23	41:19: 9.29	0.28	4.63	2.70	29	0.69	13	89.9457	0.210	0.091	0.058	0.061	1.73	−0.14
724	203323.34+411236.2	20:33:23.35	41:12:36.28	0.07	3.19	11.88	31	0.89	165	96.4193	1.920	0.496	0.730	0.694	2.21	−2.72 †
725	203323.38+411912.1	20:33:23.39	41:19:12.15	0.18	4.69	4.71	30	0.69	32	94.6164	0.490	0.117	0.132	0.242	2.43	−0.03
726	203323.37+411347.3	20:33:23.37	41:13:47.40	0.27	2.43	1.93	25	0.90	7	74.4040	0.114	0.058	0.043	0.012	1.69	−0.02
727	203323.38+411747.8	20:33:23.39	41:17:47.83	0.14	3.49	3.85	16	0.73	22	85.8844	0.362	0.078	0.062	0.222	3.12	−1.97
728	203323.43+412039.8	20:33:23.43	41:20:39.83	0.39	6.03	4.20	178	0.89	28	95.5304	0.333	0.298	0.032	0.002	1.28	−0.59
729	203323.48+410912.2	20:33:23.48	41:09:12.28	0.03	6.18	59.99	200	0.90	3731	97.7574	42.504	15.599	16.900	10.006	1.93	−1.56
730	203323.57+411746.8	20:33:23.58	41:17:46.86	0.18	3.50	2.80	15	0.71	13	83.7799	0.229	0.082	0.082	0.065	2.06	−2.47
731	203323.67+412151.0	20:33:23.68	41:21:51.01	0.43	7.17	4.07	130	0.67	25	97.5187	0.390	0.117	0.205	0.068	1.89	−0.35
732	203323.73+411537.3	20:33:23.74	41:15:37.32	0.12	2.25	4.87	19	0.89	33	97.0727	0.389	0.068	0.195	0.125	1.99	−0.16
733	203323.77+412006.4	20:33:23.77	41:20: 6.46	0.23	5.54	6.70	153	0.90	61	96.6769	0.704	0.134	0.384	0.185	2.18	−0.03
734	203323.84+411310.6	20:33:23.84	41:13:10.67	0.12	2.85	6.61	27	0.89	57	94.6761	0.680	0.223	0.295	0.162	2.02	−0.42
735	203323.83+411106.4	20:33:23.83	41:11: 6.43	0.31	4.47	3.22	67	0.89	17	93.3129	0.211	0.032	0.055	0.123	3.37	−0.04
736	203323.89+412207.8	20:33:23.90	41:22: 7.89	0.41	7.45	6.53	459	0.90	59	96.4790	0.686	0.129	0.360	0.197	1.98	−1.87
737	203323.94+411640.2	20:33:23.94	41:16:40.26	0.24	2.76	2.01	25	0.89	8	59.3210	0.156	0.071	0.033	0.052	1.89	−0.30
738	203324.01+412145.9	20:33:24.02	41:21:45.93	0.46	7.11	3.61	129	0.68	21	92.5088	0.338	0.040	0.229	0.069	2.30	−0.15
739	203324.25+411700.1	20:33:24.25	41:17: 0.14	0.12	3.01	5.13	29	0.89	37	88.0643	0.471	0.124	0.237	0.110	2.07	−0.25
740	203324.31+412106.7	20:33:24.32	41:21: 6.76	0.46	6.51	4.08	257	0.90	28	75.8772	0.425	0.066	0.145	0.214	3.15	−4.00 †
741	203324.32+411752.5	20:33:24.32	41:17:52.56	0.28	3.66	2.02	42	0.90	8	54.9738	0.175	0.154	0.011	0.010	1.16	−0.53
742	203324.38+411416.6	20:33:24.39	41:14:16.68	0.32	2.40	1.05	25	0.90	3	53.4033	0.070	0.017	0.038	0.015	2.22	−0.45
743	203324.41+412032.8	20:33:24.41	41:20:32.82	0.11	5.99	19.34	198	0.91	417	97.4150	4.721	0.760	1.826	2.134	2.64	−4.00 †
744	203324.39+410812.3	20:33:24.40	41:08:12.34	0.47	7.18	4.59	354	0.90	35	95.5179	0.407	0.164	0.149	0.095	1.95	−0.01
745	203324.48+411532.7	20:33:24.48	41:15:32.80	0.07	2.37	4.57	4	0.53	29	90.5614	0.626	0.167	0.293	0.167	2.32	−1.16
746	203324.53+411534.0	20:33:24.54	41:15:34.02	0.04	2.38	8.70	4	0.53	92	94.4876	1.865	0.381	0.762	0.722	2.39	−4.00
747	203324.55+411046.3	20:33:24.56	41:10:46.38	0.42	4.83	2.43	84	0.89	11	78.2895	0.164	0.037	0.096	0.031	1.86	−0.24
748	203324.58+411907.9	20:33:24.59	41:19: 7.94	0.38	4.73	2.72	82	0.89	13	87.8884	0.177	0.056	0.067	0.054	2.09	−0.03
749	203324.60+411553.8	20:33:24.61	41:15:53.89	0.21	2.49	1.92	25	0.90	7	46.6250	0.180	−0.003	0.116	0.068	2.56	−1.52
750	203324.62+411059.4	20:33:24.62	41:10:59.46	0.13	4.65	9.14	75	0.89	102	93.6333	1.229	0.259	0.463	0.507	2.11	−4.00 †
751	203324.77+412223.1	20:33:24.77	41:22:23.12	0.51	7.74	5.85	551	0.90	50	97.4778	0.583	0.157	0.239	0.187	2.15	−2.42

Table 1. continued.

N_x	NAME	RA	Dec	Error	θ	Sig.	Area	PSF	Cts	Exp.	Count Rates ($\times 10^{-3}$ ctn s^{-1})				$\overline{E}_x$	Var.
#	CXOCYG J+	[h:m:s]	[d:m:s]	($''$)	($'$)	(σ)	(px.)	(%)	(ph.)	(ks)	Tot.	Soft	Med.	Hard	(keV)	log(P_{ks})
752	203324.89+412001.6	20:33:24.89	41:20: 1.64	0.43	5.55	1.87	153	0.90	8	82.9978	0.118	0.012	0.025	0.081	3.12	−0.07
753	203324.96+410836.3	20:33:24.96	41:08:36.38	0.07	6.84	36.48	278	0.89	1416	97.3868	16.256	2.229	5.395	8.632	2.97	−0.14
754	203325.01+411537.0	20:33:25.02	41:15:37.08	0.12	2.48	5.04	24	0.90	35	94.8174	0.416	0.069	0.127	0.220	2.96	−0.00
755	203325.12+411818.6	20:33:25.12	41:18:18.65	0.32	4.09	1.93	56	0.90	8	69.7931	0.132	0.036	0.008	0.088	3.10	−0.94
756	203325.10+411050.1	20:33:25.11	41:10:50.16	0.37	4.83	2.89	84	0.89	14	85.8687	0.192	0.047	0.036	0.109	3.41	−0.51
757	203325.10+410724.8	20:33:25.11	41:07:24.89	0.68	7.97	2.74	472	0.89	17	72.3812	0.269	0.055	0.057	0.157	3.36	−0.60
758	203325.23+411146.1	20:33:25.24	41:11:46.17	0.51	4.06	1.91	53	0.90	7	74.2187	0.118	0.010	0.041	0.067	4.33	−0.00
759	203325.27+410918.4	20:33:25.28	41:09:18.44	0.40	6.21	3.67	203	0.90	24	90.4294	0.301	0.064	0.113	0.123	2.44	−1.74
760	203325.42+411039.4	20:33:25.42	41:10:39.47	0.28	5.01	4.41	93	0.89	29	79.9793	0.411	0.092	0.233	0.086	2.04	−0.06
761	203325.50+410932.1	20:33:25.50	41:09:32.18	0.35	6.02	4.54	186	0.90	32	92.5402	0.393	0.184	0.112	0.098	1.80	−0.17
762	203325.66+411555.6	20:33:25.66	41:15:55.69	0.13	2.69	5.11	27	0.90	36	95.9042	0.422	0.044	0.160	0.218	2.81	−0.30
763	203325.82+411853.6	20:33:25.83	41:18:53.64	0.12	4.65	9.83	77	0.89	117	95.0310	1.390	0.252	0.511	0.627	2.52	−0.36
764	203325.91+411322.2	20:33:25.91	41:13:22.29	0.11	3.05	6.22	30	0.89	51	95.0122	0.604	0.210	0.245	0.150	2.02	−0.28
765	203325.92+411333.2	20:33:25.92	41:13:33.24	0.18	2.96	2.52	29	0.89	11	39.7368	0.325	0.108	0.108	0.108	1.86	−2.71
766	203325.93+411718.6	20:33:25.94	41:17:18.63	0.37	3.45	1.39	37	0.90	4	79.7720	0.070	0.009	0.051	0.010	2.01	−0.15
767	203325.94+411316.5	20:33:25.95	41:13:16.58	0.18	3.11	2.63	31	0.89	12	80.8965	0.171	0.053	0.094	0.024	1.91	−0.64
768	203326.03+411901.1	20:33:26.04	41:19: 1.12	0.39	4.77	2.11	82	0.89	9	78.7480	0.138	0.047	0.033	0.058	2.80	−0.17
769	203326.08+411229.6	20:33:26.08	41:12:29.62	0.20	3.62	4.55	40	0.90	30	93.0773	0.362	0.106	0.129	0.127	2.43	−0.18
770	203326.11+411549.0	20:33:26.12	41:15:49.02	0.08	2.73	7.08	28	0.90	64	90.2567	0.792	0.182	0.256	0.354	2.30	−0.46
771	203326.28+412146.7	20:33:26.29	41:21:46.73	0.66	7.26	3.45	387	0.90	22	92.0094	0.274	0.001	0.081	0.192	4.15	−0.16
772	203326.33+411806.0	20:33:26.33	41:18: 6.06	0.21	4.07	3.97	53	0.89	24	97.5187	0.281	0.029	0.132	0.120	2.11	−0.13
773	203326.33+411238.4	20:33:26.34	41:12:38.41	0.15	3.56	5.22	39	0.90	38	88.5951	0.480	0.187	0.197	0.096	1.93	−1.07
774	203326.33+410819.1	20:33:26.33	41:08:19.11	0.57	7.20	3.35	325	0.89	23	88.6956	0.291	0.185	0.074	0.033	1.47	−0.07
775	203326.44+411048.5	20:33:26.45	41:10:48.58	0.30	4.98	4.45	105	0.91	29	72.9592	0.452	0.084	0.143	0.225	2.74	−3.07
776	203326.55+411503.6	20:33:26.56	41:15: 3.64	0.25	2.69	1.92	25	0.89	7	80.7143	0.106	−0.002	0.082	0.026	2.68	0.00
777	203326.60+411547.3	20:33:26.60	41:15:47.31	0.07	2.81	10.06	26	0.89	121	95.7534	1.426	0.315	0.726	0.385	2.10	−0.09
778	203326.68+411555.4	20:33:26.69	41:15:55.44	0.40	2.87	1.70	27	0.89	6	59.7199	0.121	0.035	0.091	−0.004	2.10	−0.90
779	203326.74+411059.3	20:33:26.75	41:10:59.30	0.08	4.86	17.18	98	0.91	331	97.5218	3.753	1.477	1.350	0.926	1.82	−0.14
780	203326.81+412046.9	20:33:26.81	41:20:46.96	0.57	6.39	2.12	236	0.90	11	50.1021	0.247	−0.004	0.123	0.127	2.76	−1.31
781	203326.79+411217.6	20:33:26.79	41:12:17.64	0.17	3.86	4.34	47	0.89	28	88.4977	0.355	0.099	0.160	0.095	2.08	−0.31
782	203326.85+411741.3	20:33:26.85	41:17:41.35	0.24	3.84	3.35	45	0.90	18	83.0355	0.250	0.035	0.129	0.086	2.42	−0.07
783	203326.87+411319.1	20:33:26.87	41:13:19.13	0.19	3.23	3.01	33	0.90	15	75.7170	0.226	0.027	0.115	0.084	2.14	−0.28
784	203327.11+411822.5	20:33:27.11	41:18:22.51	0.18	4.37	5.67	65	0.90	44	95.7157	0.521	0.096	0.260	0.166	2.15	−1.48
785	203327.19+411709.8	20:33:27.19	41:17: 9.88	0.17	3.54	4.15	39	0.89	26	80.8085	0.360	0.037	0.218	0.105	2.12	−0.36
786	203327.23+412008.8	20:33:27.23	41:20: 8.84	0.15	5.86	11.29	177	0.90	153	97.1952	1.751	0.432	0.713	0.605	2.10	−0.86
787	203327.30+411525.6	20:33:27.30	41:15:25.62	0.15	2.86	3.83	27	0.89	22	94.5253	0.266	0.034	0.116	0.116	2.45	−0.41
788	203327.31+410751.3	20:33:27.31	41:07:51.38	0.63	7.70	2.90	444	0.90	18	91.1707	0.224	0.091	0.044	0.089	1.72	−0.51
789	203327.45+411626.5	20:33:27.46	41:16:26.54	0.21	3.20	2.88	31	0.89	14	67.2488	0.238	0.046	0.114	0.078	2.14	−4.00 †
790	203327.59+411507.0	20:33:27.59	41:15: 7.06	0.29	2.89	2.26	28	0.89	9	76.4771	0.141	0.042	0.057	0.042	2.27	−0.43
791	203327.61+412015.7	20:33:27.62	41:20:15.72	0.43	5.99	4.13	190	0.90	28	91.8743	0.340	0.153	0.125	0.061	1.80	−0.77
792	203327.91+411509.4	20:33:27.92	41:15: 9.46	0.19	2.95	2.93	28	0.90	14	72.7268	0.224	0.059	0.106	0.059	2.05	−0.08
793	203328.32+412126.7	20:33:28.32	41:21:26.79	0.69	7.11	3.09	338	0.90	18	83.2554	0.252	0.029	0.150	0.073	2.43	−0.35
794	203328.32+410933.9	20:33:28.32	41:09:33.95	0.33	6.23	5.59	207	0.91	46	92.9705	0.550	0.168	0.284	0.098	2.02	−0.78
795	203328.36+411501.3	20:33:28.37	41:15: 1.38	0.14	3.03	3.94	30	0.90	23	85.7619	0.306	0.089	0.076	0.140	2.41	−0.23
796	203328.43+411937.1	20:33:28.43	41:19:37.20	0.09	5.52	18.22	127	0.89	370	95.9011	4.338	0.690	1.686	1.961	2.47	−4.00 †
797	203328.49+411915.4	20:33:28.49	41:19:15.42	0.22	5.23	5.11	107	0.89	38	77.9031	0.550	0.130	0.234	0.186	2.04	−3.21 †
798	203328.54+410716.7	20:33:28.54	41:07:16.72	0.30	8.32	10.50	592	0.90	139	92.4868	1.673	0.319	0.698	0.655	2.26	−4.00 †

Table 1. continued.

N_x	NAME	RA	Dec	Error	θ	Sig.	Area	PSF	Cts	Exp.	Count Rates ($\times 10^{-3}$ ctn s^{-1})				$\overline{E_x}$	Var.
#	CXOCYG J+	[h:m:s]	[d:m:s]	($''$)	($'$)	(σ)	(px.)	(%)	(ph.)	(ks)	Tot.	Soft	Med.	Hard	(keV)	log(P_{ks})
799	203328.58+411409.4	20:33:28.59	41:14: 9.45	0.22	3.19	2.64	34	0.89	12	64.6544	0.216	0.050	0.085	0.081	2.23	−0.25
800	203328.74+411611.3	20:33:28.75	41:16:11.38	0.31	3.32	1.85	34	0.90	7	75.7201	0.108	0.011	0.042	0.055	2.64	−0.00
801	203328.74+411424.0	20:33:28.74	41:14:24.01	0.16	3.16	4.65	32	0.89	31	95.8068	0.366	0.080	0.221	0.066	2.17	−0.06
802	203329.20+411425.8	20:33:29.21	41:14:25.80	0.23	3.24	2.84	34	0.89	14	74.1151	0.214	0.072	0.118	0.024	1.92	−0.34
803	203329.26+412138.2	20:33:29.27	41:21:38.23	0.61	7.36	3.96	395	0.90	27	93.6427	0.321	0.107	0.114	0.100	2.12	−0.04
804	203329.31+411605.8	20:33:29.31	41:16: 5.85	0.18	3.39	3.37	35	0.90	18	91.7675	0.222	0.059	0.119	0.045	1.99	−0.33
805	203329.41+411806.2	20:33:29.41	41:18: 6.23	0.35	4.47	2.46	67	0.89	11	96.0832	0.139	0.038	0.063	0.039	2.17	−0.05
806	203329.45+412034.8	20:33:29.46	41:20:34.84	0.48	6.44	3.41	235	0.90	21	91.5194	0.255	0.056	0.066	0.133	2.85	−0.42
807	203329.48+411858.7	20:33:29.49	41:18:58.79	0.53	5.12	2.05	115	0.91	9	77.8057	0.137	0.039	0.074	0.025	2.11	−0.42
808	203329.57+412005.5	20:33:29.58	41:20: 5.50	0.39	6.04	4.49	191	0.90	31	89.1165	0.396	0.080	0.185	0.131	2.02	−0.30
809	203329.72+411557.2	20:33:29.73	41:15:57.28	0.15	3.42	6.27	36	0.90	52	95.3891	0.611	0.208	0.231	0.172	1.88	−0.71
810	203329.95+411218.5	20:33:29.96	41:12:18.50	0.27	4.29	3.01	63	0.90	15	91.0231	0.192	0.069	0.069	0.055	2.20	−0.01
811	203330.25+411608.5	20:33:30.26	41:16: 8.54	0.16	3.57	4.83	39	0.90	33	88.8150	0.418	0.098	0.236	0.084	1.99	−0.03
812	203330.32+411406.2	20:33:30.33	41:14: 6.29	0.20	3.52	3.22	42	0.89	17	92.8260	0.208	0.034	0.094	0.080	2.30	−0.05
813	203330.47+412016.4	20:33:30.48	41:20:16.48	0.29	6.28	6.85	217	0.90	63	97.4998	0.719	0.192	0.304	0.223	2.15	−1.61
814	203330.47+410935.7	20:33:30.48	41:09:35.71	0.54	6.41	3.27	224	0.90	19	90.3509	0.246	0.131	0.048	0.067	1.69	−0.73
815	203330.51+411722.0	20:33:30.51	41:17:22.03	0.27	4.17	3.16	54	0.90	16	90.2378	0.208	0.082	0.119	0.006	1.89	−0.09
816	203330.57+411012.0	20:33:30.58	41:10:12.08	0.58	5.92	2.52	174	0.90	13	96.1680	0.152	0.069	0.019	0.064	2.07	−0.05
817	203330.74+411522.7	20:33:30.75	41:15:22.78	0.22	3.50	2.16	37	0.89	9	78.1324	0.133	0.111	0.012	0.010	1.39	−0.15
818	203331.06+412025.5	20:33:31.07	41:20:25.58	0.17	6.47	11.91	238	0.90	168	95.1347	1.958	0.383	0.743	0.833	2.33	−4.00 †
819	203331.14+411317.4	20:33:31.14	41:13:17.40	0.29	3.95	1.86	53	0.90	7	88.8935	0.096	0.009	0.022	0.066	3.06	−0.01
820	203331.20+411610.4	20:33:31.20	41:16:10.49	0.13	3.75	3.56	10	0.55	19	94.8928	0.377	0.132	0.132	0.113	1.83	−1.30
821	203331.27+412131.4	20:33:31.27	41:21:31.47	0.61	7.43	4.38	374	0.89	30	97.6946	0.352	0.100	0.125	0.128	2.20	−0.08
822	203331.33+411602.8	20:33:31.33	41:16: 2.90	0.18	3.74	3.65	43	0.89	21	95.3011	0.248	0.056	0.149	0.043	2.26	−0.35
823	203331.36+411609.6	20:33:31.36	41:16: 9.62	0.14	3.78	1.97	10	0.55	7	86.6602	0.163	0.040	0.061	0.061	2.10	−1.95
824	203331.36+411529.3	20:33:31.37	41:15:29.31	0.16	3.63	4.88	41	0.89	34	88.7239	0.431	0.110	0.162	0.159	1.92	−1.16
825	203331.35+410912.5	20:33:31.36	41:09:12.60	0.65	6.83	3.20	274	0.90	19	75.9714	0.281	0.082	0.158	0.042	1.96	−1.25
826	203331.35+410912.6	20:33:31.36	41:09:12.60	0.65	6.83	3.21	274	0.90	19	75.9714	0.282	0.082	0.158	0.042	1.96	−1.25
827	203331.72+411532.9	20:33:31.73	41:15:32.95	0.20	3.70	3.21	43	0.89	17	78.5941	0.244	0.096	0.083	0.066	1.73	−0.42
828	203331.77+412047.2	20:33:31.77	41:20:47.29	0.17	6.84	13.98	285	0.89	228	96.7460	2.641	0.616	1.265	0.760	2.14	−0.36
829	203331.87+411003.3	20:33:31.87	41:10: 3.40	0.49	6.18	2.65	201	0.90	14	81.0064	0.199	0.067	0.079	0.053	1.74	−0.03
830	203331.91+411642.9	20:33:31.91	41:16:42.93	0.20	4.07	4.21	52	0.89	26	92.7758	0.324	0.055	0.129	0.140	2.26	−0.34
831	203332.11+412122.2	20:33:32.12	41:21:22.24	0.37	7.38	7.35	372	0.90	72	95.6184	0.843	0.184	0.427	0.232	2.28	−1.05
832	203332.11+412019.7	20:33:32.12	41:20:19.76	0.59	6.50	2.89	240	0.90	16	90.5174	0.201	0.080	0.072	0.050	1.79	−0.06
833	203332.05+410558.7	20:33:32.05	41:05:58.77	0.83	9.77	4.27	1255	0.91	36	96.6486	0.417	0.038	0.024	0.355	5.02	−0.38
834	203332.16+411801.9	20:33:32.16	41:18: 1.91	0.10	4.81	12.17	81	0.89	173	69.7020	2.795	0.407	1.069	1.319	2.66	−4.00 †
835	203332.28+411639.2	20:33:32.29	41:16:39.22	0.29	4.11	1.70	53	0.89	6	87.3701	0.087	0.007	0.047	0.032	2.01	−0.02
836	203332.38+411155.8	20:33:32.38	41:11:55.83	0.42	4.88	2.19	101	0.91	10	77.5168	0.142	0.035	0.063	0.045	1.88	−0.05
837	203332.47+411543.1	20:33:32.48	41:15:43.16	0.19	3.87	4.79	47	0.89	33	89.1762	0.416	0.034	0.223	0.158	2.27	−0.38
838	203332.68+411100.1	20:33:32.68	41:11: 0.17	0.40	5.56	3.82	147	0.91	23	96.2937	0.275	0.083	0.107	0.085	2.17	−0.35
839	203332.74+411251.8	20:33:32.75	41:12:51.87	0.38	4.42	1.80	69	0.89	7	86.0791	0.097	0.059	0.019	0.019	1.54	−0.22
840	203332.81+410519.6	20:33:32.81	41:05:19.68	0.78	10.43	5.73	1807	0.91	59	97.3522	0.675	0.269	0.171	0.236	2.12	−0.05
841	203332.92+412147.2	20:33:32.93	41:21:47.24	0.67	7.81	2.87	286	0.79	15	92.2355	0.214	0.030	0.098	0.086	2.26	−0.80
842	203332.93+411040.4	20:33:32.94	41:10:40.43	0.26	5.83	6.22	170	0.90	53	95.8759	0.618	0.174	0.222	0.223	2.18	−0.07
843	203333.01+411428.5	20:33:33.02	41:14:28.54	0.24	3.94	2.69	53	0.90	13	68.3074	0.212	0.095	0.109	0.008	1.74	−0.01
844	203333.09+411730.0	20:33:33.09	41:17:30.02	0.35	4.64	3.15	82	0.91	17	91.2712	0.207	0.066	0.102	0.039	1.95	−0.01
845	203333.09+411132.4	20:33:33.09	41:11:32.46	0.50	5.24	2.42	125	0.91	11	80.1364	0.161	0.032	0.063	0.067	1.98	−0.12

Table 1. continued.

N_x	NAME	RA	Dec	Error	θ	Sig.	Area	PSF	Cts	Exp.	Count Rates ($\times 10^{-3}$ ctn s^{-1})				$\overline{E_x}$	Var.
#	CXOCYG J+	[h:m:s]	[d:m:s]	($''$)	($'$)	(σ)	(px.)	(%)	(ph.)	(ks)	Tot.	Soft	Med.	Hard	(keV)	log(P_{ks})
846	203333.43+411917.2	20:33:33.44	41:19:17.28	0.46	5.84	2.43	146	0.89	12	91.9214	0.148	0.025	0.089	0.034	2.24	−0.01
847	203333.44+410803.1	20:33:33.44	41:08: 3.15	0.52	8.02	4.55	512	0.90	34	92.0282	0.420	0.095	0.190	0.135	2.39	−0.08
848	203333.72+412152.1	20:33:33.73	41:21:52.12	0.38	7.96	4.08	157	0.63	25	97.2862	0.421	0.137	0.203	0.081	1.98	−0.25
849	203333.78+411937.0	20:33:33.79	41:19:37.06	0.30	6.13	6.62	195	0.90	59	94.5347	0.703	0.187	0.279	0.237	2.08	−0.31
850	203333.96+411129.5	20:33:33.97	41:11:29.54	0.37	5.39	2.97	137	0.91	15	83.7579	0.209	0.071	0.126	0.011	1.74	−0.50 †
851	203334.06+412145.9	20:33:34.06	41:21:45.90	0.45	7.90	3.98	153	0.64	24	94.2206	0.415	0.023	0.075	0.317	4.35	−0.24
852	203334.26+411851.4	20:33:34.26	41:18:51.48	0.46	5.65	2.67	151	0.90	14	92.5653	0.175	0.090	0.048	0.037	1.69	−1.38
853	203334.27+411422.2	20:33:34.27	41:14:22.28	0.31	4.19	3.29	61	0.89	17	82.3131	0.244	0.038	0.133	0.073	2.15	−0.23
854	203334.53+412136.6	20:33:34.53	41:21:36.61	0.48	7.82	4.71	346	0.84	34	95.8665	0.434	0.096	0.195	0.143	2.17	−0.08
855	203334.55+411622.2	20:33:34.56	41:16:22.22	0.38	4.41	2.63	64	0.90	12	96.4068	0.147	0.019	0.076	0.052	2.15	−0.18
856	203334.62+412039.6	20:33:34.63	41:20:39.70	0.48	7.04	4.93	305	0.89	37	94.6604	0.441	0.137	0.162	0.142	2.32	−0.02
857	203334.74+412050.5	20:33:34.75	41:20:50.58	0.28	7.20	9.56	332	0.89	113	96.9910	1.316	0.333	0.553	0.430	2.20	−2.21
858	203334.74+411147.7	20:33:34.75	41:11:47.80	0.28	5.32	4.24	117	0.89	27	83.3810	0.374	0.154	0.142	0.078	1.83	−0.03
859	203334.79+411456.1	20:33:34.80	41:14:56.11	0.32	4.24	1.75	61	0.89	6	53.9121	0.144	0.077	0.016	0.051	1.63	−0.05
860	203334.80+410748.7	20:33:34.80	41:07:48.78	0.73	8.36	3.80	589	0.90	27	96.3973	0.313	0.086	0.111	0.116	2.20	−1.10
861	203334.92+410857.5	20:33:34.93	41:08:57.52	0.72	7.41	2.36	383	0.90	13	93.7966	0.159	0.077	0.040	0.042	1.59	−0.45
862	203335.05+411612.2	20:33:35.05	41:16:12.25	0.48	4.45	2.53	65	0.90	11	88.0957	0.150	0.084	0.034	0.032	1.64	−0.00
863	203335.22+411119.2	20:33:35.23	41:11:19.28	0.12	5.69	15.37	141	0.89	268	96.5858	3.118	0.736	1.108	1.274	2.37	−4.00 †
864	203335.33+412059.5	20:33:35.33	41:20:59.53	0.37	7.39	6.36	363	0.89	56	95.9607	0.655	0.032	0.080	0.543	3.91	−1.43
865	203335.33+411821.8	20:33:35.33	41:18:21.82	0.37	5.48	4.03	119	0.89	25	91.6544	0.310	0.078	0.057	0.175	2.90	−0.45
866	203335.28+410714.0	20:33:35.28	41:07:14.08	0.65	8.90	4.30	741	0.90	34	89.5562	0.434	0.106	0.181	0.146	2.37	−0.91
867	203335.57+411659.0	20:33:35.57	41:16:59.09	0.30	4.81	4.40	80	0.90	29	83.3653	0.392	0.101	0.100	0.190	2.75	−1.00
868	203335.61+411556.4	20:33:35.62	41:15:56.48	0.30	4.49	3.94	68	0.89	23	93.0585	0.287	0.104	0.117	0.066	2.26	−0.05
869	203335.66+411205.9	20:33:35.66	41:12: 5.91	0.46	5.28	2.30	115	0.90	10	85.1243	0.142	0.031	0.074	0.037	1.89	−0.28
870	203335.66+410630.5	20:33:35.66	41:06:30.56	0.60	9.58	4.98	939	0.89	42	95.4330	0.497	0.208	0.170	0.119	1.82	−0.63
871	203335.80+411519.5	20:33:35.81	41:15:19.52	0.42	4.44	2.35	76	0.91	10	56.1548	0.212	0.013	0.093	0.105	2.77	−1.22
872	203335.87+410649.5	20:33:35.87	41:06:49.54	0.31	9.32	12.60	858	0.90	192	85.7211	2.506	0.590	0.675	1.242	2.78	−4.00 †
873	203336.00+411834.5	20:33:36.01	41:18:34.52	0.53	5.71	2.64	156	0.90	13	89.7981	0.165	0.062	0.042	0.061	1.99	−0.01
874	203336.25+410812.7	20:33:36.25	41:08:12.76	0.44	8.16	5.03	548	0.90	42	92.6407	0.511	0.152	0.221	0.139	1.98	−0.14
875	203336.34+412050.7	20:33:36.34	41:20:50.78	0.64	7.39	3.34	391	0.90	20	96.9753	0.229	0.079	0.090	0.060	2.14	−0.31
876	203336.29+411034.3	20:33:36.30	41:10:34.32	0.29	6.34	6.36	217	0.90	56	97.0601	0.654	0.284	0.201	0.169	1.80	−1.57
877	203336.40+411818.4	20:33:36.41	41:18:18.43	0.26	5.61	4.86	128	0.89	34	84.0815	0.458	0.112	0.089	0.258	2.99	−4.00 †
878	203336.67+411543.1	20:33:36.68	41:15:43.16	0.18	4.65	5.75	87	0.91	45	92.6721	0.541	0.090	0.198	0.254	2.74	−1.37
879	203336.64+410846.5	20:33:36.64	41:08:46.51	0.41	7.75	6.61	456	0.90	62	93.8280	0.742	0.052	0.150	0.540	3.89	−0.42
880	203336.69+411509.4	20:33:36.69	41:15: 9.46	0.49	4.60	2.09	85	0.91	9	90.0619	0.114	0.008	0.032	0.073	4.12	−0.56
881	203336.98+411610.9	20:33:36.99	41:16:10.98	0.17	4.80	6.27	80	0.89	52	91.1299	0.649	0.365	0.267	0.017	1.60	−0.67
882	203337.00+411157.8	20:33:37.00	41:11:57.88	0.49	5.57	2.52	147	0.90	12	90.9634	0.153	0.077	0.066	0.010	1.67	−0.18
883	203337.41+412028.9	20:33:37.41	41:20:28.93	0.54	7.23	4.64	278	0.86	33	89.3081	0.433	−0.002	0.078	0.356	4.20	−0.26
884	203337.47+412101.6	20:33:37.48	41:21: 1.66	0.45	7.66	6.34	412	0.89	57	95.6246	0.670	0.038	0.227	0.405	3.34	−0.14
885	203337.58+412048.6	20:33:37.58	41:20:48.62	0.67	7.50	3.49	379	0.89	21	94.0196	0.258	0.059	0.140	0.060	2.21	−1.31
886	203337.80+411640.3	20:33:37.80	41:16:40.38	0.21	5.08	5.98	109	0.91	49	89.0191	0.614	0.151	0.316	0.147	2.12	−0.40
887	203338.01+412036.0	20:33:38.01	41:20:36.03	0.78	7.40	2.25	296	0.86	11	92.8543	0.141	0.051	0.021	0.069	1.76	−0.27
888	203338.24+411833.4	20:33:38.25	41:18:33.45	0.56	6.04	2.75	181	0.90	14	83.6543	0.194	0.052	0.072	0.070	2.12	−0.09
889	203338.37+411620.4	20:33:38.37	41:16:20.42	0.53	5.09	1.72	111	0.91	7	91.4660	0.086	0.100	−0.005	−0.010	1.06	−0.07
890	203338.56+411914.3	20:33:38.56	41:19:14.38	0.59	6.51	3.43	231	0.90	20	79.0810	0.288	0.071	0.099	0.118	2.30	−0.17
891	203338.62+412012.2	20:33:38.63	41:20:12.23	0.48	7.18	4.53	320	0.90	32	96.0958	0.382	0.061	0.147	0.174	2.27	−0.33
892	203338.67+411234.0	20:33:38.67	41:12:34.06	0.45	5.54	2.20	152	0.90	10	88.2967	0.134	0.051	0.051	0.032	1.80	−0.01

Table 1. continued.

N_x	NAME	RA	Dec	Error	θ	Sig.	Area	PSF	Cts	Exp.	Count Rates ($\times10^{-3}$ ctn s^{-1})				$\overline{E_x}$	Var.
#	CXOCYG J+	[h:m:s]	[d:m:s]	($''$)	($'$)	(σ)	(px.)	(%)	(ph.)	(ks)	Tot.	Soft	Med.	Hard	(keV)	log(P_{ks})
893	203338.98+411933.4	20:33:38.99	41:19:33.43	0.24	6.78	7.61	184	0.83	75	96.5764	0.936	0.266	0.338	0.332	2.15	−0.50
894	203339.05+411435.8	20:33:39.05	41:14:35.84	0.31	5.06	4.13	103	0.90	26	97.7323	0.300	0.132	0.098	0.070	1.77	−0.39
895	203339.07+411925.7	20:33:39.07	41:19:25.79	0.23	6.71	7.98	147	0.80	81	94.6038	1.075	0.643	0.391	0.041	1.63	−0.33
896	203339.02+410833.8	20:33:39.02	41:08:33.86	0.34	8.18	8.81	546	0.90	102	95.7220	1.194	0.307	0.449	0.437	2.15	−0.71
897	203339.15+411359.3	20:33:39.16	41:13:59.37	0.47	5.16	2.54	125	0.91	12	83.9872	0.170	0.027	0.109	0.034	1.98	−0.48
898	203339.22+410648.2	20:33:39.23	41:06:48.24	0.62	9.65	5.26	621	0.79	42	96.2214	0.561	0.180	0.196	0.185	2.16	−0.15
899	203339.30+411558.5	20:33:39.30	41:15:58.57	0.40	5.18	2.92	104	0.89	15	75.6793	0.226	−0.008	0.054	0.180	3.44	−0.30
900	203339.52+411513.3	20:33:39.53	41:15:13.32	0.33	5.14	1.87	104	0.90	8	84.9955	0.105	0.006	0.032	0.067	2.96	−0.13
901	203339.47+410634.2	20:33:39.48	41:06:34.20	0.56	9.88	5.51	667	0.79	46	94.6918	0.622	0.096	0.109	0.417	3.28	−0.57
902	203339.64+411923.3	20:33:39.65	41:19:23.34	0.37	6.76	4.64	150	0.79	31	81.7320	0.493	0.161	0.192	0.139	1.99	−0.29
903	203339.64+411706.5	20:33:39.65	41:17: 6.51	0.16	5.56	10.19	142	0.91	126	95.3985	1.467	0.395	0.627	0.446	2.11	−0.55
904	203339.71+411524.9	20:33:39.71	41:15:24.95	0.38	5.18	3.39	107	0.90	19	87.7941	0.244	0.045	0.120	0.079	2.08	−0.10
905	203339.79+411641.1	20:33:39.79	41:16:41.16	0.30	5.44	4.15	119	0.89	26	89.2453	0.338	0.142	0.132	0.064	1.85	−0.10
906	203339.90+411532.8	20:33:39.91	41:15:32.86	0.32	5.23	4.34	109	0.90	28	94.4782	0.335	0.090	0.112	0.133	2.15	−0.20
907	203340.42+411445.7	20:33:40.42	41:14:45.70	0.33	5.31	1.88	35	0.63	7	85.2468	0.138	0.109	0.034	−0.005	1.54	−0.59
908	203340.59+411630.3	20:33:40.59	41:16:30.32	0.49	5.54	1.59	126	0.89	6	86.8361	0.085	0.017	0.005	0.062	5.04	−0.04
909	203340.66+411442.8	20:33:40.66	41:14:42.86	0.31	5.35	2.50	36	0.63	11	71.2034	0.256	0.019	0.131	0.106	2.01	−0.89
910	203340.74+411931.0	20:33:40.74	41:19:31.00	0.70	7.00	3.02	291	0.89	17	88.1208	0.223	0.063	0.086	0.074	2.04	−0.16
911	203340.74+411415.2	20:33:40.74	41:14:15.22	0.20	5.41	7.39	145	0.90	71	77.6079	1.020	0.245	0.320	0.454	2.42	−4.00 †
912	203340.91+410935.5	20:33:40.91	41:09:35.58	0.58	7.65	3.24	437	0.90	20	92.4931	0.249	0.134	0.067	0.048	1.66	−1.46 †
913	203341.03+412115.5	20:33:41.04	41:21:15.58	0.38	8.27	7.94	319	0.78	82	95.1284	1.116	0.156	0.521	0.439	2.40	−0.63
914	203340.97+410849.8	20:33:40.97	41:08:49.82	0.30	8.21	11.36	555	0.90	160	96.8873	1.836	0.746	0.684	0.406	1.93	−2.53 †
915	203341.19+411432.5	20:33:41.19	41:14:32.54	0.50	5.46	3.45	147	0.90	19	92.1256	0.240	0.126	0.090	0.024	1.66	−0.07
916	203341.27+411455.0	20:33:41.27	41:14:55.00	0.18	5.46	8.08	142	0.90	82	93.9254	0.980	0.088	0.383	0.509	2.88	−2.65
917	203341.27+411454.9	20:33:41.27	41:14:55.00	0.18	5.46	8.09	142	0.90	82	93.9254	0.980	0.088	0.383	0.509	2.88	−2.65
918	203341.38+411513.1	20:33:41.38	41:15:13.17	0.30	5.48	5.39	143	0.90	41	92.9925	0.490	0.030	0.065	0.395	4.29	−2.70
919	203341.35+410732.0	20:33:41.35	41:07:32.04	0.68	9.27	3.81	922	0.91	29	96.5544	0.333	0.228	0.052	0.052	1.29	−0.65
920	203341.52+411858.8	20:33:41.52	41:18:58.83	0.28	6.79	7.08	264	0.90	68	96.7366	0.783	0.202	0.375	0.206	2.12	−0.10
921	203341.50+411321.9	20:33:41.51	41:13:21.93	0.54	5.75	3.20	179	0.90	17	89.9489	0.214	0.080	0.094	0.040	1.88	−1.35
922	203341.60+411234.5	20:33:41.60	41:12:34.60	0.33	6.04	4.99	204	0.91	37	97.3334	0.423	0.066	0.240	0.117	2.17	−0.49
923	203341.84+411019.9	20:33:41.84	41:10:19.92	0.34	7.27	7.68	369	0.90	78	92.9611	0.943	0.309	0.341	0.293	1.99	−1.16
924	203341.94+412116.1	20:33:41.95	41:21:16.20	0.41	8.39	6.45	331	0.77	57	94.5881	0.786	0.092	0.163	0.531	3.41	−0.22
925	203341.93+411128.7	20:33:41.94	41:11:28.72	0.33	6.61	5.58	254	0.90	44	90.9257	0.553	0.319	0.163	0.070	1.63	−2.25 †
926	203341.99+411055.1	20:33:42.00	41:10:55.17	0.46	6.93	3.10	289	0.89	17	91.4063	0.221	0.061	0.100	0.059	2.18	−1.07
927	203342.18+410753.8	20:33:42.18	41:07:53.83	0.23	9.08	16.98	782	0.90	332	97.4370	3.813	3.539	0.215	0.058	0.99	−0.29
928	203342.25+411503.2	20:33:42.25	41:15: 3.24	0.16	5.64	10.12	158	0.90	124	95.8068	1.442	0.421	0.629	0.393	2.08	−0.21
929	203342.28+411145.8	20:33:42.29	41:11:45.82	0.46	6.52	3.69	244	0.90	23	90.8440	0.285	0.209	0.052	0.023	1.50	−0.05
930	203342.52+411456.4	20:33:42.52	41:14:56.43	0.71	5.70	2.28	163	0.90	10	86.6257	0.137	0.069	0.031	0.038	1.70	−0.05
931	203342.68+411734.5	20:33:42.69	41:17:34.58	0.38	6.27	5.01	206	0.90	37	94.5222	0.444	0.162	0.152	0.129	1.95	−0.24
932	203342.97+411237.0	20:33:42.98	41:12:37.08	0.38	6.26	5.07	223	0.90	38	84.2134	0.506	0.384	0.069	0.052	1.19	−0.68
933	203343.00+411504.3	20:33:43.00	41:15: 4.40	0.46	5.78	3.20	171	0.90	17	71.9855	0.274	0.067	0.083	0.124	2.23	−1.24 †
934	203343.26+411033.6	20:33:43.26	41:10:33.64	0.43	7.34	6.10	386	0.90	53	89.6253	0.660	0.162	0.282	0.217	2.31	−1.30 †
935	203343.47+411718.3	20:33:43.48	41:17:18.32	0.42	6.30	3.61	208	0.90	22	86.1357	0.294	0.083	0.163	0.049	2.12	−0.69
936	203343.47+411101.1	20:33:43.48	41:11: 1.10	0.66	7.10	3.32	349	0.90	19	95.4645	0.231	0.056	0.073	0.102	2.28	−0.98
937	203343.66+411002.3	20:33:43.67	41:10: 2.35	0.58	7.73	3.37	404	0.88	21	89.6693	0.274	0.111	0.080	0.083	1.83	−1.86
938	203343.80+410917.7	20:33:43.81	41:09:17.71	0.52	8.24	4.50	572	0.90	34	93.7024	0.403	0.118	0.163	0.122	1.95	−4.00 †
939	203343.98+411611.9	20:33:43.98	41:16:11.93	0.62	6.08	2.30	193	0.90	11	90.0996	0.141	0.026	0.054	0.062	1.85	−0.20

Table 1. continued.

N_x	NAME	RA	Dec	Error	θ	Sig.	Area	PSF	Cts	Exp.	Count Rates ($\times 10^{-3}$ ctn s^{-1})				$\overline{E}_x$	Var.
#	CXOCYG J+	[h:m:s]	[d:m:s]	($''$)	($'$)	(σ)	(px.)	(%)	(ph.)	(ks)	Tot.	Soft	Med.	Hard	(keV)	log(P_{ks})
940	203344.14+411939.2	20:33:44.14	41:19:39.22	0.24	7.58	11.80	385	0.89	168	93.2343	2.029	0.420	0.792	0.817	2.28	−4.00 †
941	203344.34+410522.0	20:33:44.34	41:05:22.09	1.02	11.38	4.24	2070	0.91	38	96.4759	0.445	0.147	0.118	0.180	2.12	−0.48
942	203344.46+411052.5	20:33:44.47	41:10:52.58	0.41	7.34	5.88	392	0.91	49	95.2257	0.574	0.170	0.187	0.217	2.15	−0.08
943	203344.58+411444.6	20:33:44.59	41:14:44.66	0.34	6.09	5.29	201	0.91	40	91.3340	0.487	0.188	0.135	0.164	1.91	−0.05
944	203344.53+410821.3	20:33:44.54	41:08:21.33	0.71	9.01	4.10	758	0.89	31	93.9222	0.373	0.195	0.085	0.093	1.67	−0.18
945	203344.61+410906.2	20:33:44.62	41:09: 6.23	0.35	8.49	9.96	626	0.90	125	90.5017	1.546	0.355	0.627	0.564	2.34	−4.00 †
946	203344.69+411419.8	20:33:44.69	41:14:19.82	0.40	6.14	3.06	210	0.90	17	93.4888	0.202	0.040	0.084	0.078	2.65	−0.40
947	203344.67+411002.2	20:33:44.68	41:10: 2.28	0.39	7.87	7.74	435	0.88	80	91.6230	1.000	0.179	0.423	0.397	2.65	−0.25
948	203344.88+411344.6	20:33:44.88	41:13:44.69	0.48	6.27	3.46	225	0.89	21	93.1370	0.253	0.059	0.083	0.111	2.53	−0.03
949	203344.91+411331.4	20:33:44.91	41:13:31.48	0.33	6.32	6.23	232	0.89	54	94.1735	0.648	0.245	0.247	0.155	1.95	−0.04
950	203345.00+412114.7	20:33:45.00	41:21:14.76	0.76	8.76	4.20	772	0.90	31	95.2634	0.369	0.177	0.143	0.049	1.70	−0.24
951	203345.06+412132.6	20:33:45.07	41:21:32.61	0.79	8.98	4.76	893	0.90	37	93.8343	0.445	0.186	0.044	0.215	2.80	−0.48
952	203345.29+411503.8	20:33:45.29	41:15: 3.82	0.34	6.22	4.31	211	0.90	29	80.6107	0.410	0.096	0.133	0.181	2.63	−4.00 †
953	203345.38+411731.2	20:33:45.38	41:17:31.27	0.38	6.72	3.56	152	0.80	21	92.5056	0.288	0.123	0.085	0.080	1.80	−1.24 †
954	203345.41+411621.7	20:33:45.41	41:16:21.72	0.58	6.38	2.45	224	0.90	12	85.9598	0.161	0.063	0.081	0.017	1.82	−0.03
955	203345.40+411430.7	20:33:45.40	41:14:30.76	0.52	6.26	3.22	218	0.90	18	75.7829	0.269	0.021	0.074	0.173	3.00	−0.16
956	203345.47+412018.2	20:33:45.48	41:20:18.25	0.49	8.19	4.86	542	0.90	38	90.7749	0.469	0.206	0.140	0.123	1.91	−0.24
957	203345.38+410936.4	20:33:45.39	41:09:36.42	0.44	8.25	7.15	572	0.90	71	94.2646	0.838	0.178	0.330	0.331	2.21	−0.09
958	203345.64+411400.7	20:33:45.64	41:14: 0.74	0.47	6.36	3.66	234	0.89	22	94.4939	0.273	0.129	0.070	0.074	1.70	−0.69
959	203345.84+411726.1	20:33:45.84	41:17:26.12	0.28	6.77	6.70	155	0.80	60	92.1664	0.820	0.041	0.154	0.625	3.93	−0.55
960	203345.95+410850.5	20:33:45.96	41:08:50.57	0.68	8.85	4.30	720	0.89	33	96.4633	0.387	0.213	0.094	0.081	1.58	−0.47 †
961	203346.31+411629.9	20:33:46.32	41:16:29.92	0.61	6.58	2.65	244	0.90	14	91.3026	0.172	0.047	0.050	0.074	2.65	−0.31
962	203346.47+411609.9	20:33:46.48	41:16: 9.92	0.41	6.54	4.25	239	0.90	28	94.0636	0.339	0.094	0.096	0.148	2.59	−0.38
963	203346.50+411812.9	20:33:46.50	41:18:12.96	0.62	7.19	3.08	318	0.89	18	90.8566	0.233	0.113	0.108	0.012	1.77	−0.16
964	203346.83+411354.7	20:33:46.83	41:13:54.73	0.36	6.60	6.33	267	0.89	55	92.8009	0.668	0.241	0.183	0.244	1.96	−2.98
965	203346.79+410801.0	20:33:46.79	41:08: 1.06	0.55	9.55	6.44	1023	0.91	65	95.6938	0.756	0.400	0.147	0.209	1.64	−0.64 †
966	203346.84+411048.2	20:33:46.85	41:10:48.25	0.75	7.75	2.90	463	0.90	17	93.9411	0.202	0.025	0.058	0.119	3.07	−0.40
967	203346.97+411146.3	20:33:46.97	41:11:46.35	0.40	7.29	5.65	359	0.89	47	91.8869	0.579	0.188	0.210	0.181	2.18	−0.01
968	203347.04+412005.6	20:33:47.04	41:20: 5.64	0.48	8.28	6.83	561	0.90	64	97.3145	0.743	0.220	0.241	0.282	2.08	−2.01
969	203347.04+410952.6	20:33:47.04	41:09:52.67	0.76	8.32	2.14	586	0.90	13	95.7660	0.152	0.067	0.039	0.047	2.28	−0.90
970	203347.20+411316.7	20:33:47.20	41:13:16.72	0.57	6.80	2.69	303	0.90	14	93.6835	0.175	0.173	−0.002	0.004	1.34	−0.02
971	203347.77+412040.9	20:33:47.78	41:20:40.99	0.51	8.76	5.71	686	0.90	50	95.9702	0.588	0.198	0.270	0.120	1.96	−0.41
972	203347.92+411537.5	20:33:47.93	41:15:37.54	0.62	6.74	2.41	263	0.89	12	81.5153	0.174	0.082	0.078	0.014	1.70	−0.36
973	203347.98+411910.1	20:33:47.99	41:19:10.20	0.51	7.90	4.23	484	0.90	31	92.4994	0.373	0.114	0.148	0.111	2.05	−1.29
974	203348.10+411842.3	20:33:48.11	41:18:42.34	0.50	7.69	5.80	406	0.89	48	95.8445	0.570	0.143	0.199	0.228	2.17	−1.46
975	203348.20+411346.2	20:33:48.20	41:13:46.27	0.41	6.88	5.52	310	0.90	44	95.3608	0.526	0.003	0.139	0.384	3.57	−0.10
976	203348.24+411032.8	20:33:48.24	41:10:32.88	0.68	8.11	4.42	534	0.89	32	96.7240	0.371	0.304	0.036	0.031	0.99	−0.01
977	203348.63+411824.4	20:33:48.63	41:18:24.48	0.57	7.64	3.95	397	0.89	27	97.4496	0.311	0.130	0.125	0.056	1.80	−0.07
978	203348.84+412108.0	20:33:48.85	41:21: 8.10	0.77	9.21	3.44	929	0.90	25	96.3722	0.289	0.120	0.085	0.084	1.83	−1.19
979	203348.87+411940.2	20:33:48.87	41:19:40.26	0.40	8.31	7.49	572	0.90	77	94.4216	0.912	0.197	0.345	0.370	2.37	−4.00
980	203348.91+411410.4	20:33:48.91	41:14:10.46	0.58	6.95	1.96	316	0.90	9	89.4180	0.115	0.012	0.028	0.075	3.72	−0.60
981	203349.31+411634.3	20:33:49.31	41:16:34.32	0.63	7.14	3.64	344	0.90	23	95.1472	0.275	0.050	0.079	0.146	2.83	−0.06
982	203349.32+411021.8	20:33:49.33	41:10:21.87	0.80	8.38	3.85	608	0.90	27	88.2276	0.343	0.058	0.161	0.124	2.27	−0.06
983	203349.51+411148.6	20:33:49.52	41:11:48.62	0.54	7.71	5.50	470	0.90	46	91.1330	0.568	0.137	0.225	0.206	2.37	−1.02 †
984	203350.36+411416.3	20:33:50.37	41:14:16.33	0.60	7.21	3.33	376	0.90	19	94.6886	0.234	0.114	0.084	0.036	1.72	−0.00
985	203350.47+411803.1	20:33:50.47	41:18: 3.13	0.58	7.80	4.05	458	0.90	29	91.1739	0.360	0.068	0.142	0.150	2.34	−0.01
986	203350.82+411616.1	20:33:50.82	41:16:16.11	0.54	7.36	4.08	355	0.89	28	90.4891	0.350	0.092	0.103	0.155	2.33	−0.31

Table 1. continued.

N_x	NAME	RA	Dec	Error	θ	Sig.	Area	PSF	Cts	Exp.	Count Rates ($\times 10^{-3}$ ctn s^{-1})				$\overline{E}_x$	Var.
#	CXOCYG J+	[h:m:s]	[d:m:s]	($''$)	($'$)	(σ)	(px.)	(%)	(ph.)	(ks)	Tot.	Soft	Med.	Hard	(keV)	log(P_{ks})
987	203350.79+410857.4	20:33:50.79	41:08:57.44	0.85	9.45	3.48	1276	0.91	27	94.9022	0.319	0.079	0.151	0.090	2.07	−0.03
988	203351.21+412029.2	20:33:51.21	41:20:29.26	0.95	9.14	2.26	782	0.89	14	89.9803	0.178	0.050	0.070	0.058	1.98	−0.11
989	203351.48+411358.4	20:33:51.49	41:13:58.41	0.71	7.45	3.14	430	0.90	18	96.8088	0.217	0.150	0.021	0.046	1.44	−0.20
990	203351.65+411539.0	20:33:51.65	41:15:39.06	0.77	7.44	1.99	398	0.90	10	86.5220	0.134	0.046	0.062	0.026	2.18	−0.35
991	203352.84+411558.8	20:33:52.84	41:15:58.86	0.62	7.69	3.67	443	0.90	24	92.3454	0.296	0.115	0.124	0.056	1.77	−0.02
992	203353.10+411118.8	20:33:53.10	41:11:18.89	0.57	8.53	6.42	898	0.90	64	96.2371	0.743	0.672	0.066	0.005	1.03	−0.52
993	203353.58+411754.9	20:33:53.58	41:17:54.96	0.56	8.30	5.07	562	0.90	42	96.8622	0.485	0.189	0.156	0.140	1.85	−0.19
994	203353.89+412004.0	20:33:53.90	41:20: 4.09	0.85	9.32	2.85	920	0.91	20	87.1754	0.254	0.104	0.083	0.068	1.99	−0.04
995	203354.19+411340.1	20:33:54.20	41:13:40.18	0.82	8.00	3.13	527	0.89	19	90.2127	0.245	0.124	0.060	0.061	1.69	−1.41 †
996	203355.18+411419.7	20:33:55.19	41:14:19.72	0.59	8.10	4.59	598	0.90	34	91.1330	0.424	0.135	0.106	0.182	2.50	−0.16
997	203355.54+411851.4	20:33:55.55	41:18:51.41	0.55	9.00	6.42	812	0.91	60	91.7110	0.731	0.298	0.255	0.179	1.89	−0.08
998	203356.32+412038.9	20:33:56.32	41:20:38.94	0.85	10.02	3.99	1170	0.90	31	94.8206	0.370	0.184	0.089	0.097	1.77	−0.49
999	203357.91+411803.1	20:33:57.92	41:18: 3.13	0.42	9.11	8.41	781	0.89	96	95.3734	1.137	0.036	0.280	0.821	3.61	−0.29
1000	203358.41+412055.7	20:33:58.42	41:20:55.79	0.33	10.50	16.38	1465	0.89	321	97.2768	3.709	1.247	1.301	1.162	2.05	−4.00 †
1001	203359.65+411737.2	20:33:59.66	41:17:37.24	0.68	9.29	6.66	1132	0.90	67	93.7715	0.800	0.535	0.162	0.103	1.45	−0.22
1002	203401.23+412010.4	20:34: 1.24	41:20:10.43	0.46	10.55	10.87	1446	0.90	158	96.8591	1.808	1.610	0.098	0.101	1.01	−0.69
1003	203401.44+411905.4	20:34: 1.44	41:19: 5.49	0.67	10.11	6.56	1541	0.90	68	94.4593	0.801	0.348	0.268	0.185	1.79	−0.19

Table 2. Near-IR counterparts of Cygnus OB2 X-ray sources and near-IR stellar parameters.

N_x	X-ray - 2MASS counterpart		Off.	2MASS photometry				A_v
#	CXOAC J+	2MASS J+	(″)	J	H	K_s	Ph. qual	(mag)
1	203225.09+411019.6	–	–	–	–	–	–	–
2	203225.55+410847.3	20322545+4108473	1.56	14.76 ± 0.06	14.23 ± 0.07	13.95 ± 0.07	AAA	8.54
3	203225.97+411054.7	20322597+4110547	0.24	15.24 ± 0.05	13.65 ± 0.03	12.69 ± 0.03	AAA	7.71
4	203227.51+411358.3	20322756+4114001	1.61	16.00 ± 0.06	14.46 ± 0.04	13.90 ± 0.06	AAA	0.16
5	203227.62+410831.4	20322754+4108336	2.41	15.91 ± 0.06	14.39 ± 0.03	13.82 ± 0.05	AAA	N/A
6	203227.70+411317.0	20322768+4113169	0.58	14.96 ± 0.03	13.49 ± 0.02	12.88 ± 0.03	AAA	2.21
7	203228.88+410807.5	–	–	–	–	–	–	–
8	203229.12+411400.7	20322913+4114012	0.26	16.74 ± 0.16	15.36 ± 0.08	14.72 ± 0.11	CAB	9.01
9	203229.26+410850.1	20322928+4108494	1.03	12.26 ± 0.01	11.49 ± 0.01	11.07 ± 0.01	AAA	8.52
10	203229.84+411454.2	20322985+4114536	0.83	17.44	15.43 ± 0.10	14.37 ± 0.09	UAA	N/A
11	203229.91+411056.0	20322994+4110575	1.29	15.26 ± 0.05	14.04 ± 0.04	13.53 ± 0.04	AAA	N/A
12	203230.63+410829.1	20323051+4108284	2.19	15.47 ± 0.07	13.71	13.09	AUU	4.19
13	203230.63+410854.8	20323064+4108565	1.49	15.31 ± 0.05	13.68 ± 0.03	13.01 ± 0.03	AAA	5.43
14	203230.88+411029.5	–	–	–	–	–	–	–
15	203231.39+410955.9	20323143+4109558	0.58	14.52 ± 0.05	13.04	12.46	AUU	9.69
16	203231.42+411335.0	–	–	–	–	–	–	–
17	203231.53+411407.9	20323154+4114082	0.11	7.82 ± 0.01	7.09 ± 0.02	6.66 ± 0.01	AAA	4.66
18	203231.58+411712.5	–	–	–	–	–	–	–
19	203232.32+411507.3	20323242+4115082	1.70	16.41 ± 0.10	14.62 ± 0.05	13.69 ± 0.05	BAA	4.87
20	203232.44+411312.3	20323249+4113131	0.80	14.29 ± 0.02	13.25 ± 0.02	12.70 ± 0.03	AAA	9.17
21	203233.28+411058.8	20323346+4110594	2.65	11.70 ± 0.01	11.50 ± 0.02	11.44 ± 0.02	AAA	10.45
22	203233.47+411218.0	20323349+4112184	0.19	13.48 ± 0.02	12.49 ± 0.02	12.00 ± 0.02	AAA	8.33
23	203233.53+411405.7	20323351+4114056	0.63	13.28 ± 0.02	12.48 ± 0.01	12.09 ± 0.02	AAA	N/A
24	203234.33+411506.3	–	–	–	–	–	–	–
25	203234.45+411154.7	20323447+4111552	0.39	14.69 ± 0.03	13.26 ± 0.02	12.68 ± 0.03	AAA	7.21
26	203235.17+411143.4	20323518+4111432	0.45	14.85 ± 0.03	13.47 ± 0.02	12.97 ± 0.03	AAA	7.73
27	203235.65+411509.5	20323564+4115097	0.33	10.85 ± 0.02	10.19 ± 0.02	9.85 ± 0.03	AAA	N/A
28	203235.86+411248.4	20323592+4112505	2.08	15.81 ± 0.07	13.58	12.95	AUU	4.18
29	203235.96+412135.6	20323599+4121363	0.55	15.08 ± 0.03	13.99 ± 0.02	13.53 ± 0.04	AAA	N/A
30	203236.32+411900.7	20323641+4119010	1.32	15.96 ± 0.09	14.63 ± 0.08	14.12 ± 0.08	AAA	N/A
31	203236.38+411831.0	20323629+4118308	1.51	15.52 ± 0.06	14.35 ± 0.07	13.90 ± 0.05	AAA	N/A
32	203236.50+411810.3	20323643+4118103	1.13	16.24 ± 0.09	14.96 ± 0.07	14.77 ± 0.12	AAB	9.19
33	203236.62+412214.5	20323661+4122147	0.22	12.11 ± 0.02	11.34 ± 0.01	10.88 ± 0.02	AAA	N/A
34	203236.86+411944.6	20323680+4119447	1.00	15.45 ± 0.06	14.23 ± 0.05	13.76 ± 0.06	AAA	10.11
35	203236.84+412146.1	–	–	–	–	–	–	–
36	203237.55+411150.8	20323754+4111514	0.39	13.34 ± 0.02	12.82 ± 0.02	12.64 ± 0.03	AAA	9.77
37	203237.53+411712.4	20323751+4117121	0.65	17.36	15.86 ± 0.13	15.83	UBU	19.97
38	203237.71+411405.3	20323767+4114052	0.86	13.42 ± 0.02	12.16 ± 0.02	11.61 ± 0.02	AAA	6.76
39	203237.83+412208.7	20323784+4122087	0.20	15.16 ± 0.04	14.07 ± 0.04	13.65 ± 0.05	AAA	17.08
40	203237.87+412119.0	20323787+4121194	0.19	14.37 ± 0.02	13.21 ± 0.02	12.81 ± 0.03	AAA	6.26
41	203237.94+411502.7	20323781+4115026	2.11	15.05 ± 0.05	14.01 ± 0.04	13.47 ± 0.05	AAA	N/A
42	203238.10+410833.1	20323804+4108316	1.94	15.57 ± 0.05	14.08 ± 0.03	13.43 ± 0.04	AAA	N/A
43	203238.10+411244.4	20323810+4112442	0.49	15.45 ± 0.06	14.23 ± 0.03	13.64 ± 0.05	AAA	8.73
44	203238.07+412313.8	20323799+4123138	1.25	13.76	12.78 ± 0.03	12.35	UAU	17.96
45	203238.26+411141.7	20323830+4111422	0.49	16.04 ± 0.08	14.48 ± 0.04	13.96 ± 0.06	AAA	7.88
46	203238.43+411201.1	–	–	–	–	–	–	–
47	203238.56+411422.0	–	–	–	–	–	–	–
48	203239.41+411906.3	20323944+4119066	0.22	14.95 ± 0.04	13.86 ± 0.03	13.56 ± 0.04	AAA	2.94
49	203239.52+411112.5	20323951+4111129	0.17	14.98 ± 0.03	13.48 ± 0.03	12.90 ± 0.03	AAA	3.81
50	203239.82+412358.2	20323986+4123595	1.21	14.78 ± 0.03	13.58 ± 0.03	13.18 ± 0.03	AAA	10.87
51	203239.90+411348.1	20323989+4113488	0.52	16.49 ± 0.14	15.26 ± 0.09	15.05 ± 0.20	BAC	8.51
52	203240.12+411034.7	20324009+4110346	0.52	11.78 ± 0.02	11.04 ± 0.02	10.64 ± 0.01	AAA	N/A
53	203240.07+412201.7	20324004+4122015	0.74	16.10 ± 0.09	14.65 ± 0.05	14.26 ± 0.08	AAA	5.71
54	203240.22+412244.7	20324032+4122473	2.64	15.49	14.33	14.37 ± 0.09	UUA	8.10
55	203240.26+411740.9	20324026+4117408	0.29	15.63 ± 0.06	14.29 ± 0.04	13.86 ± 0.06	AAA	6.17
56	203240.59+411454.8	20324061+4114548	0.23	15.35 ± 0.18	12.73	11.92	CUU	6.59
57	203240.65+411111.6	20324063+4111113	0.69	16.58 ± 0.13	14.81 ± 0.06	14.23 ± 0.08	BAA	5.18
58	203240.72+412106.1	20324067+4121059	0.99	14.81 ± 0.04	13.73 ± 0.04	13.39 ± 0.04	AAA	5.91
59	203240.81+411720.2	20324077+4117208	0.86	15.41 ± 0.05	14.20 ± 0.06	13.82 ± 0.06	AAA	7.40
60	203240.94+411428.8	20324096+4114291	0.11	4.67 ± 0.32	3.51 ± 0.26	2.70 ± 0.36	DDD	N/A
61	203240.96+411551.0	20324094+4115511	0.47	13.47 ± 0.02	12.65 ± 0.02	12.18 ± 0.02	AAA	1.34
62	203240.97+411449.6	–	–	–	–	–	–	–
63	203241.06+411955.2	20324109+4119552	0.40	14.51 ± 0.03	13.54 ± 0.03	13.16 ± 0.04	AAA	12.07
64	203241.33+411849.9	20324133+4118501	0.23	12.95 ± 0.02	12.01 ± 0.02	11.60 ± 0.02	AAA	7.06

Table 2. continued.

N_x	X-ray - 2MASS counterpart		Off.	2MASS photometry				A_v
#	CXOAC J+	2MASS J+	(″)	J	H	K_s	Ph. qual	(mag)
65	203241.55+411154.7	–	–	–	–	–	–	–
66	203241.61+411549.0	20324158+4115486	0.78	15.89	14.73	14.96 ± 0.15	UUB	5.50
67	203241.66+411406.5	–	–	–	–	–	–	–
68	203241.87+411555.9	20324185+4115557	0.53	16.24 ± 0.10	14.82 ± 0.06	14.30 ± 0.09	AAA	N/A
69	203242.15+411712.2	20324210+4117122	0.91	16.69 ± 0.13	15.42 ± 0.09	14.81 ± 0.14	BAB	5.47
70	203242.18+411641.4	20324216+4116412	0.65	15.30 ± 0.05	14.02 ± 0.04	13.61 ± 0.05	AAA	6.83
71	203242.46+412236.6	20324235+4122360	1.94	14.58 ± 0.03	13.48 ± 0.03	13.10 ± 0.04	AAA	4.50
72	203242.88+412016.5	20324289+4120164	0.36	10.68 ± 0.02	10.21 ± 0.01	10.00 ± 0.01	AAA	N/A
73	203242.86+412343.1	20324290+4123437	0.55	13.01 ± 0.02	12.14 ± 0.02	11.82 ± 0.02	AAA	7.64
74	203242.91+411914.4	20324288+4119148	0.58	15.03 ± 0.04	13.82 ± 0.04	13.37 ± 0.04	AAA	6.01
75	203243.03+411741.1	20324313+4117417	1.39	15.65	14.66 ± 0.06	14.02	UAU	7.77
76	203243.01+412309.3	20324298+4123107	1.31	14.90 ± 0.03	13.74 ± 0.03	13.32 ± 0.04	AAA	N/A
77	203243.09+411359.3	20324307+4113594	0.35	15.26 ± 0.04	13.71 ± 0.04	13.39 ± 0.04	AAA	1.09
78	203243.10+411750.9	–	–	–	–	–	–	–
79	203243.34+411514.1	–	–	–	–	–	–	–
80	203243.34+411657.1	–	–	–	–	–	–	–
81	203243.40+411102.9	20324342+4111034	0.31	16.44 ± 0.11	14.78 ± 0.06	14.24 ± 0.08	BAA	8.43
82	203243.95+411709.9	20324393+4117101	0.33	16.61 ± 0.14	15.32 ± 0.09	14.70 ± 0.12	BAB	N/A
83	203244.22+411615.7	20324426+4116162	0.53	16.39 ± 0.10	15.03 ± 0.06	14.59 ± 0.11	BAA	12.29
84	203244.31+411743.8	20324427+4117436	0.78	16.02 ± 0.08	14.75 ± 0.08	14.18 ± 0.08	AAA	N/A
85	203244.35+411445.3	20324431+4114453	0.81	14.85 ± 0.03	13.45 ± 0.01	12.91 ± 0.03	AAA	1.97
86	203244.42+411122.9	20324443+4111236	0.51	12.56 ± 0.01	11.69 ± 0.01	11.25 ± 0.01	AAA	N/A
87	203244.71+410701.4	20324468+4106596	2.11	14.16 ± 0.02	12.89 ± 0.02	12.35 ± 0.02	AAA	5.27
88	203244.74+411305.4	20324475+4113057	0.02	12.10 ± 0.02	11.23 ± 0.01	10.81 ± 0.02	AAA	N/A
89	203244.81+411227.4	20324480+4112281	0.51	13.57 ± 0.02	12.27 ± 0.01	11.59 ± 0.02	AAA	8.51
90	203244.82+411549.0	20324480+4115484	0.98	15.79 ± 0.08	14.49 ± 0.07	14.06 ± 0.07	AAA	N/A
91	203244.85+411419.1	–	–	–	–	–	–	–
92	203244.83+411848.1	20324484+4118484	0.09	15.45 ± 0.06	14.16 ± 0.05	13.81 ± 0.05	AAA	8.30
93	203244.90+411519.8	20324492+4115203	0.33	14.08 ± 0.03	12.64 ± 0.02	12.00 ± 0.02	AAA	6.55
94	203244.86+412350.5	20324478+4123519	1.72	12.74 ± 0.02	12.05 ± 0.02	11.72 ± 0.02	AAA	N/A
95	203245.08+411247.3	20324510+4112485	0.99	16.29 ± 0.10	14.92 ± 0.06	14.15 ± 0.07	AAA	18.57
96	203245.08+411725.6	–	–	–	–	–	–	–
97	203245.24+411221.2	20324523+4112209	0.59	16.06 ± 0.08	14.51 ± 0.04	13.65 ± 0.05	AAA	7.34
98	203245.30+411721.1	20324529+4117209	0.51	16.77	15.41 ± 0.10	14.59	UAU	8.24
99	203245.49+411546.9	20324542+4115465	1.28	15.48 ± 0.05	14.16 ± 0.05	13.68 ± 0.05	AAA	9.18
100	203245.59+411659.2	–	–	–	–	–	–	–
101	203245.64+411647.1	20324569+4116473	0.65	16.05 ± 0.08	14.47 ± 0.04	13.66 ± 0.05	AAA	N/A
102	203245.76+411349.7	20324577+4113497	0.16	15.10 ± 0.05	13.66 ± 0.06	13.18 ± 0.05	AAA	9.22
103	203245.81+411502.9	20324583+4115028	0.36	15.75 ± 0.06	14.48 ± 0.05	14.13 ± 0.07	AAA	5.21
104	203245.79+412108.2	20324580+4121083	0.08	12.18 ± 0.02	11.53 ± 0.02	11.21 ± 0.01	AAA	3.24
105	203245.91+411238.7	20324589+4112383	0.76	15.41 ± 0.05	14.14 ± 0.03	13.70 ± 0.05	AAA	N/A
106	203246.14+411040.1	20324624+4110396	1.70	14.57 ± 0.04	12.91 ± 0.03	11.10	AAU	15.25
107	203246.27+410713.3	20324630+4107141	0.74	14.62 ± 0.03	13.42 ± 0.03	12.93 ± 0.03	AAA	N/A
108	203246.31+411107.8	20324634+4111076	0.53	11.74 ± 0.02	11.07 ± 0.02	10.71 ± 0.02	AAA	8.01
109	203246.36+411652.9	20324651+4116534	2.10	15.01 ± 0.04	14.35 ± 0.05	14.15 ± 0.08	AAA	4.54
110	203246.41+411301.8	–	–	–	–	–	–	–
111	203246.66+411808.5	20324666+4118085	0.23	16.34 ± 0.10	14.87 ± 0.06	14.47 ± 0.09	AAA	2.43
112	203246.70+411316.3	–	–	–	–	–	–	–
113	203246.86+411742.8	20324681+4117442	1.48	16.15 ± 0.11	13.84	13.30	BUU	6.14
114	203246.91+412118.7	20324678+4121197	2.24	16.16 ± 0.13	14.96 ± 0.10	14.55 ± 0.11	BAA	7.89
115	203247.40+411251.1	20324744+4112513	0.44	15.68 ± 0.05	14.13 ± 0.04	13.54 ± 0.04	AAA	1.29
116	203247.47+411211.7	–	–	–	–	–	–	–
117	203247.81+411334.8	20324778+4113363	1.37	16.38 ± 0.10	15.18 ± 0.09	14.73 ± 0.12	BAB	3.72
118	203247.87+411632.3	20324781+4116324	1.01	15.37 ± 0.04	14.11 ± 0.03	13.47 ± 0.04	AAA	5.52
119	203247.98+411653.9	20324801+4116542	0.33	16.10 ± 0.08	14.72 ± 0.06	14.36 ± 0.09	AAA	N/A
120	203248.18+411352.1	–	–	–	–	–	–	–
121	203248.25+411229.1	–	–	–	–	–	–	–
122	203248.43+411439.4	20324844+4114396	0.06	15.99 ± 0.10	14.55 ± 0.07	13.96 ± 0.06	AAA	4.81
123	203248.47+411608.2	20324845+4116080	0.57	12.25 ± 0.02	11.67 ± 0.02	11.32 ± 0.02	AAA	5.69
124	203248.53+412336.2	20324844+4123366	1.45	14.23 ± 0.02	13.14 ± 0.02	12.78 ± 0.03	AAA	N/A
125	203248.63+410811.6	20324860+4108117	0.45	15.34 ± 0.05	13.97 ± 0.03	13.51 ± 0.04	AAA	8.14
126	203248.87+411519.8	20324891+4115197	0.54	14.81 ± 0.03	13.55 ± 0.02	12.97 ± 0.03	AAA	8.46
127	203248.91+410930.4	–	–	–	–	–	–	–
128	203249.02+410746.8	20324901+4107462	0.88	15.81 ± 0.06	14.40 ± 0.05	13.85 ± 0.05	AAA	N/A
129	203249.39+411230.6	20324937+4112307	0.37	16.10 ± 0.09	14.99 ± 0.06	14.41 ± 0.09	AAA	6.50
130	203249.38+411606.8	20324938+4116072	0.23	16.62 ± 0.12	15.36 ± 0.10	14.66 ± 0.11	BAB	11.75

Table 2. continued.

N_x	X-ray - 2MASS counterpart		Off.	2MASS photometry				A_v
#	CXOAC J+	2MASS J+	(″)	J	H	K_s	Ph. qual	(mag)
131	203249.34+412224.5	20324939+4122247	0.66	14.98 ± 0.04	13.85 ± 0.04	13.40 ± 0.04	AAA	N/A
132	203249.51+411532.8	20324954+4115329	0.24	13.48 ± 0.02	12.67 ± 0.02	12.25 ± 0.02	AAA	7.43
133	203249.85+412342.2	–	–	–	–	–	–	–
134	203249.92+411511.1	20324998+4115117	0.83	16.04 ± 0.07	14.69 ± 0.04	14.11 ± 0.07	AAA	8.60
135	203250.08+411626.7	20325011+4116270	0.33	16.62 ± 0.12	15.31 ± 0.09	13.56	BAU	4.27
136	203250.11+411458.1	20325012+4114586	0.28	15.94 ± 0.17	14.39 ± 0.10	13.57 ± 0.06	CAA	N/A
137	203250.16+411836.1	20325014+4118362	0.45	15.46 ± 0.05	14.32 ± 0.04	13.80	AAU	3.45
138	203250.25+412216.6	–	–	–	–	–	–	–
139	203250.39+411038.2	20325037+4110378	0.67	16.21 ± 0.09	14.90 ± 0.06	14.41 ± 0.09	AAA	N/A
140	203250.41+411749.5	20325043+4117497	0.22	15.06 ± 0.04	13.61 ± 0.03	13.13 ± 0.04	AAA	N/A
141	203250.42+411629.6	20325039+4116296	0.58	14.77 ± 0.03	13.57 ± 0.03	13.01	AAU	N/A
142	203250.69+410825.3	20325069+4108258	0.34	10.62 ± 0.02	9.89 ± 0.01	9.52 ± 0.01	AAA	7.23
143	203250.69+411609.1	–	–	–	–	–	–	–
144	203250.87+411145.6	20325089+4111461	0.39	13.30	12.74 ± 0.04	12.34 ± 0.03	UAA	3.71
145	203250.98+411245.6	–	–	–	–	–	–	–
146	203251.13+411253.5	–	–	–	–	–	–	–
147	203251.14+411237.7	20325116+4112380	0.11	15.45 ± 0.04	14.15 ± 0.04	13.65 ± 0.05	AAA	9.33
148	203251.15+412026.1	20325114+4120253	1.08	14.94	13.80	13.43 ± 0.05	UUA	6.03
149	203251.15+412245.8	20325136+4122470	3.25	14.80	13.64 ± 0.04	13.32	UAU	N/A
150	203251.35+411123.7	–	–	–	–	–	–	–
151	203251.34+411617.2	–	–	–	–	–	–	–
152	203251.36+411409.0	20325136+4114092	0.06	12.77 ± 0.02	11.96 ± 0.02	11.58 ± 0.02	AAA	8.54
153	203251.55+411300.7	20325156+4113010	0.10	14.78 ± 0.03	13.97 ± 0.04	13.80 ± 0.05	AAA	N/A
154	203251.52+412037.7	20325156+4120379	0.44	16.06 ± 0.08	14.66 ± 0.06	13.90 ± 0.06	AAA	17.45
155	203251.70+411710.9	20325177+4117129	1.99	16.26 ± 0.09	15.19 ± 0.08	14.28	AAU	7.03
156	203252.00+411600.7	–	–	–	–	–	–	–
157	203252.11+411313.5	20325212+4113135	0.26	16.76 ± 0.14	15.35 ± 0.09	14.63 ± 0.11	CAB	3.30
158	203252.12+411828.6	20325210+4118289	0.46	15.51 ± 0.05	14.08 ± 0.04	13.63 ± 0.05	AAA	N/A
159	203252.17+411815.7	20325218+4118160	0.16	13.13 ± 0.02	12.41 ± 0.02	12.05 ± 0.02	AAA	6.28
160	203252.41+411029.8	20325244+4110296	0.48	13.51 ± 0.02	12.59 ± 0.02	12.20 ± 0.02	AAA	N/A
161	203252.47+411541.3	20325249+4115426	1.14	16.57 ± 0.13	15.12 ± 0.07	14.57 ± 0.10	BAA	N/A
162	203252.52+411736.5	–	–	–	–	–	–	–
163	203252.59+411255.2	–	–	–	–	–	–	–
164	203252.60+412102.5	20325261+4121027	0.12	15.35 ± 0.05	14.20 ± 0.03	13.70 ± 0.05	AAA	N/A
165	203252.69+411019.4	20325266+4110193	0.74	14.05 ± 0.03	12.83 ± 0.02	12.40 ± 0.02	AAA	4.74
166	203252.84+411955.0	20325283+4119550	0.27	13.23 ± 0.02	12.56 ± 0.02	12.23 ± 0.02	AAA	7.75
167	203253.12+411559.0	20325310+4115589	0.50	12.93 ± 0.02	12.51 ± 0.02	12.32 ± 0.02	AAA	8.50
168	203253.37+411927.7	20325342+4119284	0.79	15.26 ± 0.05	14.15 ± 0.05	13.71 ± 0.05	AAA	7.09
169	203253.55+410714.1	–	–	–	–	–	–	–
170	203253.53+411545.3	20325354+4115455	0.12	16.27 ± 0.11	14.96 ± 0.07	14.62 ± 0.11	AAB	16.07
171	203253.56+412019.4	20325351+4120195	1.01	16.36	15.32 ± 0.10	14.70 ± 0.12	UAB	7.54
172	203253.77+411513.3	20325377+4115134	0.18	14.12 ± 0.03	12.96 ± 0.03	12.49 ± 0.03	AAA	8.20
173	203253.88+411216.0	20325385+4112151	1.27	17.04	15.62 ± 0.12	14.57 ± 0.10	UBA	5.19
174	203253.90+411536.7	20325388+4115366	0.59	13.37 ± 0.02	12.61 ± 0.02	12.32 ± 0.02	AAA	N/A
175	203253.95+411702.7	20325393+4117030	0.35	16.13 ± 0.08	14.87 ± 0.06	14.24 ± 0.07	AAA	9.31
176	203254.09+411726.5	20325419+4117257	1.69	16.82 ± 0.15	15.81 ± 0.14	15.60	CBU	N/A
177	203254.17+411128.1	–	–	–	–	–	–	–
178	203254.22+410818.2	20325412+4108185	1.55	13.15 ± 0.03	12.06 ± 0.02	11.63 ± 0.02	AAA	5.95
179	203254.19+411242.4	20325421+4112426	0.11	15.28 ± 0.04	13.96 ± 0.03	13.39 ± 0.04	AAA	N/A
180	203254.21+411025.4	20325422+4110256	0.12	13.11	12.30 ± 0.03	12.02	UAU	9.21
181	203254.28+411433.5	20325431+4114341	0.45	16.56	15.79 ± 0.14	15.11 ± 0.18	UBC	6.40
182	203254.28+412333.2	20325435+4123342	1.12	15.55 ± 0.06	14.44 ± 0.05	14.03 ± 0.07	AAA	10.78
183	203254.33+411458.5	20325432+4114586	0.27	14.88 ± 0.04	13.69 ± 0.04	13.22 ± 0.04	AAA	12.78
184	203254.39+410640.9	20325438+4106412	0.34	14.54 ± 0.03	13.26 ± 0.03	12.83 ± 0.03	AAA	6.96
185	203254.43+411550.0	20325439+4115499	0.73	14.43	14.88 ± 0.09	14.44 ± 0.10	UAA	2.57
186	203254.56+410840.2	20325469+4108396	2.04	15.91 ± 0.07	14.15 ± 0.05	13.42 ± 0.04	AAA	1.25
187	203254.55+411446.5	20325457+4114468	0.16	12.69 ± 0.02	11.79 ± 0.02	11.37 ± 0.02	AAA	N/A
188	203254.61+411341.4	20325461+4113416	0.23	15.87 ± 0.07	14.52 ± 0.05	13.86 ± 0.06	AAA	9.95
189	203254.60+411932.8	20325464+4119321	1.01	13.28 ± 0.03	12.54 ± 0.02	12.21 ± 0.02	AAA	7.03
190	203254.79+411203.0	20325480+4112034	0.12	15.58 ± 0.05	14.10 ± 0.03	13.58 ± 0.04	AAA	4.91
191	203254.89+411517.8	20325486+4115180	0.56	15.91 ± 0.14	14.60 ± 0.11	12.64	BBU	18.77
192	203255.02+411038.8	20325498+4110384	0.96	16.50	15.71 ± 0.12	14.59	UBU	N/A
193	203255.12+411314.8	20325514+4113148	0.24	15.35	13.95 ± 0.04	13.44 ± 0.04	UAA	N/A
194	203255.15+411651.9	–	–	–	–	–	–	–
195	203255.27+410832.0	20325525+4108321	0.46	15.83 ± 0.06	14.49 ± 0.04	13.99 ± 0.06	AAA	N/A

Table 2. continued.

N_x	X-ray - 2MASS counterpart		Off.	2MASS photometry				A_v
#	CXOAC J+	2MASS J+	(″)	J	H	K_s	Ph. qual	(mag)
196	203255.26+411747.5	–	–	–	–	–	–	–
197	203255.33+411821.9	20325536+4118216	0.66	16.44	15.51 ± 0.10	14.63	UAU	8.83
198	203255.34+411852.5	20325536+4118529	0.19	13.26 ± 0.02	12.25 ± 0.02	11.89 ± 0.02	AAA	0.21
199	203255.67+411519.0	20325570+4115194	0.50	16.14 ± 0.09	14.89 ± 0.06	14.40 ± 0.09	AAA	6.31
200	203255.78+411012.2	20325574+4110120	0.77	15.07 ± 0.04	13.82 ± 0.04	13.20 ± 0.04	AAA	6.34
201	203255.72+412246.6	20325572+4122475	0.69	15.53 ± 0.06	14.51 ± 0.04	14.01 ± 0.06	AAA	3.78
202	203255.86+412233.4	20325597+4122343	1.56	15.45 ± 0.07	14.28 ± 0.06	13.80 ± 0.06	AAA	N/A
203	203256.28+411317.6	20325632+4113180	0.47	16.62 ± 0.12	15.15 ± 0.07	14.55 ± 0.10	BAA	5.55
204	203256.35+411436.7	20325633+4114366	0.66	15.36 ± 0.04	14.15 ± 0.04	13.55 ± 0.04	AAA	11.00
205	203256.40+411206.6	20325647+4112075	1.20	11.07 ± 0.02	10.43 ± 0.01	10.09 ± 0.01	AAA	N/A
206	203256.49+411053.1	20325648+4110531	0.26	14.73 ± 0.03	13.32 ± 0.03	12.67 ± 0.03	AAA	8.75
207	203256.55+411314.8	–	–	–	–	–	–	–
208	203256.61+411401.9	20325661+4114017	0.43	16.47 ± 0.11	15.09 ± 0.08	14.67 ± 0.12	BAB	9.30
209	203256.66+412015.9	20325669+4120161	0.44	15.44 ± 0.05	14.21 ± 0.04	13.69 ± 0.05	AAA	N/A
210	203256.71+411044.8	–	–	–	–	–	–	–
211	203256.69+412025.4	20325666+4120255	0.56	15.89 ± 0.06	14.52 ± 0.05	14.09 ± 0.07	AAA	2.88
212	203256.74+411215.8	20325677+4112162	0.45	16.30 ± 0.11	14.94 ± 0.08	14.29 ± 0.08	AAA	N/A
213	203256.85+411441.0	20325683+4114412	0.33	16.64 ± 0.12	15.19 ± 0.08	14.75 ± 0.12	BAB	8.42
214	203257.07+410903.8	–	–	–	–	–	–	–
215	203257.06+411313.9	–	–	–	–	–	–	–
216	203257.17+412123.3	20325721+4121260	2.51	12.78 ± 0.02	11.55 ± 0.02	11.07 ± 0.02	AAA	5.84
217	203257.25+411445.4	20325729+4114461	0.72	15.65 ± 0.05	14.48 ± 0.04	14.06 ± 0.07	AAA	N/A
218	203257.32+412047.5	–	–	–	–	–	–	–
219	203257.36+411333.3	20325736+4113334	0.15	15.33 ± 0.05	14.00 ± 0.04	13.49 ± 0.05	AAA	8.25
220	203257.56+411234.7	20325758+4112352	0.38	15.26 ± 0.04	13.97 ± 0.04	13.51 ± 0.05	AAA	0.25
221	203257.73+411029.4	–	–	–	–	–	–	–
222	203257.80+410937.9	–	–	–	–	–	–	–
223	203257.82+411359.1	20325781+4113593	0.23	15.94 ± 0.07	14.61 ± 0.05	13.88 ± 0.06	AAA	6.13
224	203257.91+411619.0	20325792+4116190	0.23	15.05 ± 0.05	13.93 ± 0.05	13.34	AAU	N/A
225	203257.94+412156.9	–	–	–	–	–	–	–
226	203258.03+411058.1	20325803+4110582	0.13	15.14 ± 0.04	13.99 ± 0.03	13.48 ± 0.04	AAA	6.01
227	203258.09+410713.6	20325802+4107138	1.21	17.00 ± 0.17	15.83 ± 0.13	15.07 ± 0.15	CBC	12.54
228	203258.16+411735.0	20325816+4117347	0.53	16.82 ± 0.14	15.64 ± 0.11	14.34 ± 0.09	CBA	8.37
229	203258.22+411250.6	20325828+4112511	0.83	17.00 ± 0.18	15.68 ± 0.11	15.12	CBU	6.93
230	203258.27+411617.8	20325825+4116177	0.44	16.13 ± 0.09	14.86 ± 0.06	13.67	AAU	8.72
231	203258.27+412147.8	20325825+4121471	0.96	15.90 ± 0.07	14.50 ± 0.05	14.12 ± 0.07	AAA	16.30
232	203258.37+412000.9	–	–	–	–	–	–	–
233	203258.39+411543.2	–	–	–	–	–	–	–
234	203258.44+411105.4	–	–	–	–	–	–	–
235	203258.45+411403.9	20325845+4114042	0.26	15.82 ± 0.07	14.53 ± 0.06	13.99 ± 0.07	AAA	12.50
236	203258.52+411234.8	20325853+4112353	0.37	16.38 ± 0.11	15.04 ± 0.09	14.53 ± 0.10	BAA	N/A
237	203258.54+411525.2	20325859+4115253	0.56	16.53	15.23 ± 0.08	14.72 ± 0.12	UAB	17.45
238	203258.73+411226.6	20325874+4112266	0.23	16.29 ± 0.10	14.81 ± 0.07	14.33 ± 0.08	AAA	N/A
239	203258.74+411110.0	20325883+4111095	1.38	16.25 ± 0.10	14.60 ± 0.08	13.98 ± 0.08	AAA	5.08
240	203258.93+411202.8	–	–	–	–	–	–	–
241	203258.93+411840.7	20325896+4118410	0.33	16.64	15.42 ± 0.10	14.46 ± 0.09	UAA	27.48
242	203259.00+411051.8	20325899+4110518	0.36	13.06 ± 0.02	12.22 ± 0.02	11.78 ± 0.02	AAA	8.47
243	203259.04+411758.7	20325904+4117589	0.11	12.12 ± 0.02	11.50 ± 0.01	11.26 ± 0.02	AAA	7.13
244	203259.17+411937.4	20325916+4119376	0.22	10.55 ± 0.02	10.35 ± 0.02	10.30 ± 0.02	AAA	N/A
245	203259.20+411229.5	–	–	–	–	–	–	–
246	203259.21+412049.0	20325925+4120512	2.10	15.75 ± 0.06	14.75 ± 0.06	14.06 ± 0.07	AAA	N/A
247	203259.24+412137.4	20325933+4121379	1.23	11.40 ± 0.02	10.70 ± 0.01	10.23 ± 0.01	AAA	N/A
248	203259.24+412238.4	20325916+4122386	1.32	15.70 ± 0.06	14.35 ± 0.05	13.96 ± 0.06	AAA	7.54
249	203259.31+411037.4	20325932+4110376	0.12	16.20 ± 0.09	14.88 ± 0.06	14.32 ± 0.08	AAA	0.56
250	203259.38+411223.5	–	–	–	–	–	–	–
251	203259.45+410941.4	20325954+4109434	2.14	16.84	15.31	14.85 ± 0.14	UUB	13.89
252	203259.57+411055.1	20325955+4110560	0.78	16.52	15.46 ± 0.12	14.79	UBU	6.02
253	203259.63+411514.6	20325964+4115146	0.17	9.05 ± 0.02	8.45 ± 0.01	8.14 ± 0.01	AAA	8.97
254	203259.63+411941.0	20325959+4119409	0.77	15.16 ± 0.17	13.90 ± 0.09	13.48 ± 0.06	CAA	N/A
255	203259.75+411300.0	20325972+4112599	0.65	14.92 ± 0.04	13.87 ± 0.03	13.32 ± 0.04	AAA	7.58
256	203259.75+411419.4	20325976+4114196	0.01	10.78 ± 0.02	10.18 ± 0.02	9.87 ± 0.02	AAA	0.79
257	203259.77+411345.4	–	–	–	–	–	–	–
258	203259.85+412036.5	–	–	–	–	–	–	–
259	203259.94+411027.9	20325995+4110280	0.16	16.79 ± 0.14	15.24 ± 0.08	14.71 ± 0.11	CAB	5.64
260	203259.98+410848.6	20325987+4108488	1.76	15.22	14.32 ± 0.06	13.88 ± 0.06	UAA	N/A

Table 2. continued.

N_x	X-ray - 2MASS counterpart		Off.	2MASS photometry				A_v
#	CXOAC J+	2MASS J+	(″)	J	H	K_s	Ph. qual	(mag)
261	203300.01+411107.2	20330000+4111073	0.35	15.72 ± 0.06	14.98 ± 0.07	14.76 ± 0.13	AAB	N/A
262	203300.16+411217.6	20330015+4112178	0.23	16.40 ± 0.11	15.06 ± 0.09	14.49 ± 0.09	BAA	12.50
263	203300.29+411656.6	–	–	–	–	–	–	–
264	203300.38+411730.6	20330041+4117308	0.44	16.32 ± 0.10	14.89 ± 0.07	14.34 ± 0.09	AAA	8.49
265	203300.38+411651.7	20330038+4116520	0.22	16.46 ± 0.12	15.20 ± 0.08	14.58 ± 0.11	BAB	6.64
266	203300.42+411124.4	20330035+4111252	1.34	15.06 ± 0.04	13.49 ± 0.03	12.65 ± 0.03	AAA	4.00
267	203300.41+412030.8	–	–	–	–	–	–	–
268	203300.46+411147.5	20330050+4111476	0.46	13.33	12.29 ± 0.02	11.90 ± 0.02	UAA	1.85
269	203300.52+411550.1	–	–	–	–	–	–	–
270	203300.52+412214.0	20330032+4122141	3.08	15.45 ± 0.04	14.22 ± 0.04	13.74 ± 0.05	AAA	N/A
271	203300.59+411859.3	20330058+4118594	0.36	15.87 ± 0.08	14.39	13.86	AUU	8.67
272	203300.73+410929.4	20330070+4109299	0.65	12.21 ± 0.02	11.48 ± 0.01	11.11 ± 0.01	AAA	14.31
273	203300.77+411627.1	20330078+4116275	0.10	15.54 ± 0.05	14.15 ± 0.04	13.64 ± 0.05	AAA	23.09
274	203300.77+412032.1	–	–	–	–	–	–	–
275	203300.84+412133.8	20330091+4121339	0.98	16.09	14.92 ± 0.07	14.59	UAU	1.87
276	203300.88+411115.6	20330088+4111157	0.29	14.65 ± 0.04	13.20 ± 0.04	12.70 ± 0.03	AAA	9.81
277	203300.90+411736.7	20330091+4117367	0.28	15.91 ± 0.06	14.62 ± 0.05	14.02 ± 0.06	AAA	N/A
278	203300.95+411423.8	20330097+4114241	0.13	15.27 ± 0.05	13.92 ± 0.03	13.50 ± 0.04	AAA	9.89
279	203300.95+412119.9	20330103+4121201	1.10	16.08 ± 0.08	15.13 ± 0.07	14.55 ± 0.10	AAA	8.77
280	203301.09+411755.7	20330106+4117564	0.65	13.54 ± 0.02	12.53 ± 0.02	12.09 ± 0.02	AAA	7.62
281	203301.15+411321.8	20330116+4113218	0.20	16.97	15.84 ± 0.13	15.06 ± 0.16	UBC	6.10
282	203301.16+411152.7	20330118+4111525	0.50	16.78	15.68 ± 0.12	14.78	UBU	N/A
283	203301.20+410918.2	20330119+4109182	0.30	13.96 ± 0.03	12.79 ± 0.03	12.30 ± 0.03	AAA	5.71
284	203301.21+410858.0	20330124+4108580	0.27	15.15 ± 0.04	13.82 ± 0.04	13.31 ± 0.04	AAA	7.81
285	203301.25+411459.5	20330127+4114596	0.22	14.91	13.61	13.62 ± 0.05	UUA	7.94
286	203301.26+411256.8	–	–	–	–	–	–	–
287	203301.35+411055.5	20330133+4110562	0.62	16.87	15.50 ± 0.11	15.34 ± 0.21	UBC	5.94
288	203301.35+411223.6	–	–	–	–	–	–	–
289	203301.35+411331.2	20330133+4113316	0.46	16.44	15.72 ± 0.14	15.17	UBU	9.69
290	203301.38+412158.5	20330156+4121579	2.77	15.35 ± 0.05	14.14 ± 0.05	13.63 ± 0.05	AAA	8.11
291	203301.43+411200.2	20330142+4112000	0.51	16.29 ± 0.10	15.02 ± 0.07	14.38 ± 0.08	AAA	N/A
292	203301.49+411211.5	20330150+4112115	0.10	16.69 ± 0.14	15.42 ± 0.11	14.42	BAU	5.99
293	203301.49+411211.6	20330150+4112116	0.19	16.79 ± 0.11	15.32 ± 0.12	14.49	BAU	N/A
294	203301.58+412302.9	–	–	–	–	–	–	–
295	203301.67+411248.2	20330168+4112486	0.10	15.03 ± 0.05	13.62 ± 0.04	13.22 ± 0.04	AAA	9.08
296	203301.66+411959.0	20330155+4119591	1.77	16.39 ± 0.10	15.11 ± 0.07	14.47 ± 0.09	BAA	N/A
297	203301.68+411751.4	20330169+4117513	0.24	14.71 ± 0.03	13.58 ± 0.03	13.11 ± 0.03	AAA	10.36
298	203301.72+411147.0	20330170+4111475	0.43	13.41 ± 0.02	12.61 ± 0.02	12.22 ± 0.02	AAA	14.35
299	203301.72+411500.5	20330173+4115007	0.15	14.26 ± 0.03	12.98 ± 0.05	12.48 ± 0.03	AAA	7.54
300	203301.77+411110.5	20330176+4111107	0.11	16.42 ± 0.12	14.92	14.48	BUU	N/A
301	203301.80+411103.9	20330182+4111037	0.36	16.25 ± 0.10	14.76 ± 0.06	14.36 ± 0.09	AAA	N/A
302	203301.83+411317.3	20330182+4113174	0.24	16.19 ± 0.09	14.97 ± 0.06	14.39 ± 0.09	AAA	10.17
303	203301.94+411059.0	20330198+4110593	0.55	15.05 ± 0.04	13.81 ± 0.04	13.26 ± 0.04	AAA	7.64
304	203301.93+411739.3	20330193+4117400	0.50	14.99 ± 0.09	13.84 ± 0.08	13.43 ± 0.06	AAA	N/A
305	203301.97+410644.4	20330191+4106457	1.44	16.80 ± 0.15	15.32 ± 0.08	14.75 ± 0.12	CAB	7.43
306	203301.95+411946.8	20330197+4119466	0.52	15.44 ± 0.05	14.21 ± 0.05	13.74 ± 0.06	AAA	5.07
307	203302.18+411848.8	20330224+4118489	0.66	13.29 ± 0.02	12.60 ± 0.02	12.22 ± 0.02	AAA	8.17
308	203302.26+411533.4	20330226+4115336	0.11	14.44 ± 0.03	13.23 ± 0.04	12.72 ± 0.03	AAA	7.54
309	203302.31+411324.2	20330231+4113245	0.14	15.27 ± 0.06	13.84 ± 0.09	13.36 ± 0.04	AAA	7.31
310	203302.35+411828.1	20330231+4118285	0.79	12.04 ± 0.02	11.26 ± 0.02	10.88 ± 0.01	AAA	N/A
311	203302.40+411738.4	20330249+4117393	1.44	14.74 ± 0.14	11.42	10.84	BUU	1.50
312	203302.63+411355.7	20330259+4113563	0.85	16.83 ± 0.14	15.44 ± 0.10	14.84 ± 0.13	CAB	3.20
313	203302.87+410705.9	20330285+4107068	0.80	16.18 ± 0.09	14.89 ± 0.07	14.30 ± 0.08	AAA	N/A
314	203302.87+411514.0	–	–	–	–	–	–	–
315	203302.90+411742.9	20330292+4117431	0.12	8.72 ± 0.02	8.16 ± 0.01	7.87 ± 0.01	AAA	N/A
316	203303.03+411329.2	–	–	–	–	–	–	–
317	203303.03+411740.1	–	–	–	–	–	–	–
318	203303.07+411243.4	20330308+4112435	0.12	14.83 ± 0.04	13.54 ± 0.03	12.94 ± 0.03	AAA	N/A
319	203303.22+411629.4	20330322+4116297	0.08	15.77 ± 0.06	14.84 ± 0.06	14.29 ± 0.08	AAA	21.26
320	203303.53+411253.6	20330356+4112539	0.34	15.63 ± 0.06	14.00 ± 0.04	13.26 ± 0.04	AAA	8.97
321	203303.64+411236.6	–	–	–	–	–	–	–
322	203303.66+411334.2	–	–	–	–	–	–	–
323	203303.66+411218.2	20330368+4112188	0.42	15.87 ± 0.10	14.48 ± 0.06	13.87 ± 0.06	AAA	6.53
324	203303.88+411736.2	20330390+4117367	0.26	13.05 ± 0.02	12.45 ± 0.02	12.10 ± 0.02	AAA	5.76
325	203304.06+411124.5	20330410+4111250	0.62	16.13 ± 0.09	14.79 ± 0.08	14.19 ± 0.08	AAA	N/A

Table 2. continued.

N_x	X-ray - 2MASS counterpart		Off.	2MASS photometry				A_v
#	CXOAC J+	2MASS J+	(″)	J	H	K_s	Ph. qual	(mag)
326	203304.10+410755.3	20330408+4107542	1.40	14.45 ± 0.05	13.26 ± 0.08	12.76 ± 0.03	AAA	9.16
327	203304.16+410651.5	20330423+4106514	1.14	13.94 ± 0.02	12.74 ± 0.02	12.29 ± 0.02	AAA	N/A
328	203304.22+411411.7	–	–	–	–	–	–	–
329	203304.26+410723.1	20330435+4107237	1.38	15.80 ± 0.07	14.42 ± 0.04	14.05 ± 0.07	AAA	N/A
330	203304.24+411254.6	20330425+4112548	0.04	15.12 ± 0.04	13.81 ± 0.03	13.46 ± 0.04	AAA	N/A
331	203304.28+411235.2	20330428+4112354	0.03	16.94	15.85 ± 0.15	14.98 ± 0.15	UBB	23.62
332	203304.30+411613.4	20330427+4116138	0.56	15.75 ± 0.07	14.37 ± 0.06	13.71 ± 0.06	AAA	7.08
333	203304.32+411420.4	20330433+4114209	0.27	15.87	14.37 ± 0.04	13.91	UAU	37.03
334	203304.38+411405.3	20330437+4114056	0.33	16.11 ± 0.08	14.56 ± 0.04	14.04 ± 0.06	AAA	12.13
335	203304.42+411830.8	20330442+4118311	0.13	13.82 ± 0.02	12.84 ± 0.02	12.41 ± 0.02	AAA	N/A
336	203304.48+411128.1	20330447+4111282	0.25	16.44 ± 0.12	15.31 ± 0.09	14.98 ± 0.15	BAB	N/A
337	203304.49+411157.6	20330447+4111580	0.48	16.22 ± 0.10	14.90 ± 0.07	14.48 ± 0.10	AAA	4.79
338	203304.57+411612.9	–	–	–	–	–	–	–
339	203304.67+411205.9	20330466+4112058	0.48	16.00 ± 0.08	14.68 ± 0.05	13.98 ± 0.06	AAA	8.08
340	203304.70+411506.2	20330475+4115064	0.66	16.31 ± 0.10	14.95 ± 0.07	14.36 ± 0.09	AAA	9.49
341	203304.75+411312.4	20330476+4113130	0.39	15.79 ± 0.09	14.35 ± 0.09	13.91 ± 0.08	AAA	5.47
342	203304.75+411650.4	–	–	–	–	–	–	–
343	203304.78+410857.2	–	–	–	–	–	–	–
344	203304.86+411238.7	20330487+4112389	0.06	15.52	14.23 ± 0.08	13.77 ± 0.06	UAA	11.20
345	203304.95+411129.5	20330495+4111291	0.55	16.27 ± 0.09	14.81 ± 0.07	14.38 ± 0.09	AAA	3.32
346	203305.01+411256.2	20330500+4112566	0.37	16.66 ± 0.17	15.03 ± 0.07	14.50 ± 0.09	CAA	10.59
347	203305.03+411421.5	20330505+4114219	0.17	15.61 ± 0.06	14.08 ± 0.03	13.33 ± 0.05	AAA	7.86
348	203305.03+411831.4	20330502+4118317	0.24	15.95 ± 0.08	14.66 ± 0.06	14.02 ± 0.07	AAA	5.06
349	203305.04+411146.6	–	–	–	–	–	–	–
350	203305.03+411421.4	20330505+4114219	0.26	15.61 ± 0.06	14.08 ± 0.03	13.33 ± 0.05	AAA	N/A
351	203305.05+411144.8	20330503+4111452	0.38	15.20 ± 0.06	13.74 ± 0.05	13.19 ± 0.05	AAA	N/A
352	203305.17+411233.2	20330519+4112336	0.25	15.82 ± 0.07	14.25 ± 0.05	13.84 ± 0.06	AAA	8.31
353	203305.20+411335.6	20330519+4113360	0.36	14.88 ± 0.12	13.90 ± 0.09	13.34 ± 0.07	EAA	6.78
354	203305.25+411604.5	20330525+4116047	0.05	14.62 ± 0.03	13.86 ± 0.03	13.55 ± 0.04	AAA	0.40
355	203305.26+412138.7	20330526+4121391	0.22	14.32 ± 0.03	13.15 ± 0.03	12.54 ± 0.02	AAA	N/A
356	203305.28+411258.6	20330528+4112591	0.29	15.58 ± 0.08	14.23 ± 0.10	13.75 ± 0.07	AAA	N/A
357	203305.30+411303.6	20330529+4113038	0.24	13.29 ± 0.03	12.56 ± 0.03	12.24 ± 0.03	AAA	7.98
358	203305.36+411311.8	–	–	–	–	–	–	–
359	203305.41+411153.6	20330541+4111538	0.01	15.23	13.87 ± 0.05	13.37 ± 0.05	UAA	2.48
360	203305.47+411610.5	20330549+4116109	0.27	16.29 ± 0.10	15.24 ± 0.08	14.55 ± 0.11	AAA	N/A
361	203305.59+411348.2	20330561+4113486	0.15	14.45 ± 0.02	13.17 ± 0.02	12.75 ± 0.03	AAA	3.61
362	203305.72+411136.7	–	–	–	–	–	–	–
363	203305.79+411634.7	20330579+4116352	0.28	16.62 ± 0.13	13.96 ± 0.03	12.30 ± 0.02	BAA	4.88
364	203305.89+411905.0	20330587+4119048	0.54	16.85	15.60 ± 0.12	15.44	UBU	N/A
365	203305.92+412057.5	20330594+4120573	0.42	16.10 ± 0.09	14.79 ± 0.06	14.40 ± 0.09	AAA	N/A
366	203306.07+411256.7	–	–	–	–	–	–	–
367	203306.13+411012.6	20330615+4110140	1.26	15.82	15.37 ± 0.09	13.94	UAU	N/A
368	203306.19+411453.8	–	–	–	–	–	–	–
369	203306.21+411715.3	20330616+4117158	0.82	16.19	14.78	14.59 ± 0.12	UUB	N/A
370	203306.20+412242.9	20330611+4122434	1.46	16.03 ± 0.09	14.90 ± 0.07	14.19 ± 0.08	AAA	6.96
371	203306.24+410948.3	20330621+4109495	1.10	15.16 ± 0.05	13.80 ± 0.04	13.26 ± 0.04	AAA	1.12
372	203306.26+411235.1	20330626+4112354	0.17	14.19 ± 0.02	12.94 ± 0.02	12.44 ± 0.02	AAA	6.78
373	203306.27+411100.4	–	–	–	–	–	–	–
374	203306.27+412019.0	20330629+4120188	0.44	14.81 ± 0.03	13.61 ± 0.02	13.10 ± 0.03	AAA	3.16
375	203306.32+412215.2	20330622+4122138	2.32	16.15 ± 0.10	15.02 ± 0.08	14.45 ± 0.10	AAA	6.82
376	203306.35+411353.1	20330635+4113536	0.30	16.03 ± 0.08	14.75 ± 0.07	14.25 ± 0.09	AAA	4.50
377	203306.38+411330.7	20330641+4113310	0.22	14.77 ± 0.04	13.41 ± 0.04	13.01 ± 0.04	AAA	2.20
378	203306.47+411206.8	20330646+4112071	0.23	13.97 ± 0.03	12.77 ± 0.04	12.30 ± 0.03	AAA	10.37
379	203306.61+412158.3	–	–	–	–	–	–	–
380	203306.64+411817.7	–	–	–	–	–	–	–
381	203306.71+411200.0	20330671+4112002	0.12	14.50	13.14 ± 0.02	12.72	UAU	7.02
382	203306.73+411527.5	–	–	–	–	–	–	–
383	203306.79+411727.8	20330681+4117283	0.25	15.61 ± 0.06	14.30 ± 0.04	13.89 ± 0.07	AAA	N/A
384	203306.84+411224.3	20330684+4112245	0.11	15.99 ± 0.08	14.47 ± 0.05	13.90 ± 0.06	AAA	N/A
385	203306.85+411503.4	–	–	–	–	–	–	–
386	203306.91+411647.2	–	–	–	–	–	–	–
387	203306.93+411858.9	20330697+4118592	0.44	15.06 ± 0.05	13.84 ± 0.04	13.42 ± 0.05	AAA	5.49
388	203307.00+411649.6	20330702+4116499	0.11	14.84 ± 0.03	13.48 ± 0.02	12.80 ± 0.03	AAA	N/A
389	203307.06+411300.1	20330711+4113002	0.56	15.30 ± 0.06	13.94 ± 0.05	13.41 ± 0.05	AAA	16.66
390	203307.07+411604.3	–	–	–	–	–	–	–

Table 2. continued.

N_x	X-ray - 2MASS counterpart		Off.	2MASS photometry				A_v
#	CXOAC J+	2MASS J+	(″)	J	H	K_s	Ph. qual	(mag)
391	203307.13+411625.7	20330713+4116263	0.38	17.16	15.55 ± 0.10	14.93 ± 0.15	UBB	4.92
392	203307.14+411141.2	–	–	–	–	–	–	–
393	203307.14+412006.9	20330712+4120072	0.45	14.24 ± 0.02	13.03 ± 0.02	12.52 ± 0.02	AAA	N/A
394	203307.15+411318.7	–	–	–	–	–	–	–
395	203307.16+411730.4	–	–	–	–	–	–	–
396	203307.17+411520.2	20330718+4115206	0.26	16.15 ± 0.09	14.83 ± 0.06	14.18 ± 0.08	AAA	4.51
397	203307.25+411000.4	20330736+4110014	1.60	16.48	15.49 ± 0.10	14.86 ± 0.13	UAB	N/A
398	203307.32+411214.6	20330733+4112148	0.05	14.67 ± 0.11	13.28 ± 0.03	12.74 ± 0.03	BAA	6.72
399	203307.34+411341.5	–	–	–	–	–	–	–
400	203307.36+411800.0	20330737+4118000	0.23	16.32 ± 0.10	15.06 ± 0.08	14.57 ± 0.11	AAA	4.87
401	203307.40+411151.3	20330739+4111505	1.09	16.02 ± 0.08	14.40 ± 0.06	13.75 ± 0.06	AAA	6.35
402	203307.45+411226.4	20330746+4112266	0.06	13.16 ± 0.02	12.02 ± 0.02	11.50 ± 0.02	AAA	N/A
403	203307.47+411254.5	–	–	–	–	–	–	–
404	203307.50+412032.3	20330747+4120324	0.57	17.38	15.64 ± 0.12	15.31	UBU	7.39
405	203307.55+411821.2	20330751+4118214	0.66	16.18 ± 0.09	14.85 ± 0.05	14.42 ± 0.09	AAA	11.82
406	203307.57+411947.6	20330758+4119478	0.01	14.18 ± 0.03	13.12 ± 0.03	12.68 ± 0.02	AAA	5.51
407	203307.59+411300.7	20330759+4113010	0.04	14.05 ± 0.06	12.60	12.39 ± 0.05	AUA	N/A
408	203307.73+410828.5	20330768+4108291	0.97	13.75 ± 0.04	12.73 ± 0.03	12.31 ± 0.03	AAA	4.66
409	203307.83+411243.0	20330783+4112435	0.23	16.27 ± 0.12	15.09 ± 0.09	14.68 ± 0.15	BAB	4.81
410	203307.86+411216.3	20330786+4112161	0.45	12.84 ± 0.03	11.91 ± 0.05	11.44 ± 0.04	AAA	N/A
411	203307.91+411254.3	–	–	–	–	–	–	–
412	203307.91+411606.9	20330791+4116074	0.33	16.68	15.46 ± 0.13	14.79	UBU	N/A
413	203307.97+411257.7	20330792+4112571	1.12	15.41 ± 0.08	13.03	13.48 ± 0.07	AUA	7.59
414	203307.98+411300.7	20330798+4113007	0.18	15.02 ± 0.07	12.73	13.23 ± 0.05	AUA	9.77
415	203307.99+411659.4	20330801+4116597	0.11	15.81 ± 0.07	14.55 ± 0.05	14.05 ± 0.07	AAA	3.74
416	203308.02+411801.5	20330806+4118016	0.48	13.93 ± 0.02	13.28 ± 0.03	12.99 ± 0.03	AAA	N/A
417	203308.03+411436.9	–	–	–	–	–	–	–
418	203308.04+411642.9	–	–	–	–	–	–	–
419	203308.05+412217.4	20330808+4122180	0.44	15.30 ± 0.05	14.11 ± 0.04	13.63 ± 0.05	AAA	N/A
420	203308.09+411109.6	20330808+4111091	0.66	13.37	12.52 ± 0.04	12.09	UAU	9.78
421	203308.09+411526.9	20330809+4115270	0.16	16.24 ± 0.11	15.22 ± 0.08	14.45	BAU	5.62
422	203308.21+410626.4	20330817+4106265	0.57	13.28 ± 0.02	12.12 ± 0.04	11.70 ± 0.02	AAA	8.89
423	203308.21+411304.0	20330821+4113045	0.23	14.45 ± 0.05	15.34 ± 0.21	14.72 ± 0.18	ECC	5.03
424	203308.23+411823.1	20330824+4118235	0.20	15.41 ± 0.06	14.26 ± 0.06	13.71 ± 0.05	AAA	N/A
425	203308.25+411513.1	–	–	–	–	–	–	–
426	203308.29+411543.0	20330833+4115432	0.55	13.68 ± 0.03	13.10 ± 0.03	12.85 ± 0.04	AAA	0.18
427	203308.33+411421.1	20330834+4114214	0.06	15.72 ± 0.06	14.28 ± 0.03	13.76 ± 0.05	AAA	8.52
428	203308.50+411734.6	20330848+4117347	0.36	16.37 ± 0.11	15.12 ± 0.08	14.61 ± 0.11	BAB	4.98
429	203308.53+411328.1	–	–	–	–	–	–	–
430	203308.56+411435.9	–	–	–	–	–	–	–
431	203308.59+411915.1	20330859+4119154	0.02	13.17 ± 0.02	11.97 ± 0.01	10.93 ± 0.01	AAA	N/A
432	203308.63+411514.4	20330865+4115146	0.22	14.15 ± 0.04	12.76 ± 0.03	12.20 ± 0.02	AAA	N/A
433	203308.76+411318.5	20330879+4113182	0.66	7.11 ± 0.01	6.54 ± 0.01	6.23 ± 0.01	AAA	N/A
434	203308.80+411257.4	–	–	–	–	–	–	–
435	203308.84+411214.8	20330880+4112151	0.66	15.72	14.99 ± 0.10	13.08	UAU	11.35
436	203308.84+411317.1	–	–	–	–	–	–	–
437	203308.89+411327.7	–	–	–	–	–	–	–
438	203308.90+411243.5	–	–	–	–	–	–	–
439	203308.91+412227.3	20330892+4122276	0.06	15.73 ± 0.06	14.60 ± 0.05	14.31 ± 0.09	AAA	4.36
440	203308.95+411705.7	–	–	–	–	–	–	–
441	203308.96+411101.9	20330896+4111024	0.35	15.84 ± 0.07	14.56 ± 0.05	14.01 ± 0.06	AAA	3.03
442	203308.97+411537.5	–	–	–	–	–	–	–
443	203309.01+411331.0	–	–	–	–	–	–	–
444	203309.06+411227.8	–	–	–	–	–	–	–
445	203309.12+411308.6	20330911+4113094	0.68	14.24 ± 0.16	13.11 ± 0.13	11.93	CBU	N/A
446	203309.15+411343.2	20330915+4113434	0.11	10.83 ± 0.03	10.22 ± 0.03	9.88 ± 0.02	AAA	5.87
447	203309.26+411302.1	–	–	–	–	–	–	–
448	203309.30+411618.6	20330929+4116188	0.34	16.14	14.54	14.24 ± 0.09	UUA	5.28
449	203309.32+411250.6	20330944+4112510	1.76	11.87	11.14	12.88 ± 0.06	UUA	35.41
450	203309.32+411428.9	20330936+4114290	0.44	11.88 ± 0.02	11.17 ± 0.02	10.81 ± 0.02	AAA	13.50
451	203309.38+411347.0	–	–	–	–	–	–	–
452	203309.42+411320.3	–	–	–	–	–	–	–
453	203309.45+411258.3	–	–	–	–	–	–	–
454	203309.53+412109.9	20330954+4121102	0.16	15.61 ± 0.05	14.25 ± 0.04	13.72 ± 0.05	AAA	N/A
455	203309.59+411308.0	–	–	–	–	–	–	–

Table 2. continued.

N_x	X-ray - 2MASS counterpart		Off.	2MASS photometry				A_v
#	CXOAC J+	2MASS J+	(″)	J	H	K_s	Ph. qual	(mag)
456	203309.60+411300.4	20330960+4113005	0.20	8.65 ± 0.01	8.14 ± 0.01	7.76 ± 0.01	AAE	9.20
457	203309.60+411429.9	–	–	–	–	–	–	–
458	203309.63+412130.4	–	–	–	–	–	–	–
459	203309.67+412214.3	20330984+4122143	2.53	15.87 ± 0.09	14.55 ± 0.06	14.22 ± 0.08	AAA	8.06
460	203309.73+411250.6	20330965+4112508	1.21	13.06	14.06 ± 0.13	11.80	UBU	9.80
461	203309.78+410902.2	20330978+4109029	0.52	15.71 ± 0.07	14.30 ± 0.06	13.76 ± 0.06	AAA	14.58
462	203309.85+411247.8	–	–	–	–	–	–	–
463	203309.92+411139.5	–	–	–	–	–	–	–
464	203309.92+411756.2	20330992+4117563	0.17	14.83 ± 0.03	13.54 ± 0.03	12.79 ± 0.02	AAA	10.20
465	203309.93+411325.9	20330994+4113260	0.20	15.66 ± 0.09	13.10	12.68	AUU	5.40
466	203309.95+410856.9	20330996+4108571	0.03	16.55 ± 0.14	15.16 ± 0.08	14.50 ± 0.10	BAA	7.70
467	203310.02+412042.2	–	–	–	–	–	–	–
468	203310.03+411429.6	–	–	–	–	–	–	–
469	203310.04+411743.2	–	–	–	–	–	–	–
470	203310.05+411301.6	–	–	–	–	–	–	–
471	203310.07+411000.8	20331014+4110026	1.88	10.49 ± 0.02	9.71 ± 0.01	9.37 ± 0.01	AAE	3.06
472	203310.10+411414.4	–	–	–	–	–	–	–
473	203310.11+411337.1	–	–	–	–	–	–	–
474	203310.12+411239.7	20331014+4112398	0.19	14.90 ± 0.04	13.75 ± 0.04	13.26 ± 0.04	AAA	4.49
475	203310.17+411545.3	20331018+4115455	0.11	14.10 ± 0.03	12.90 ± 0.04	12.37 ± 0.03	AAA	7.64
476	203310.18+411339.4	20331016+4113394	0.39	14.49 ± 0.02	13.26 ± 0.05	12.78 ± 0.04	AAA	6.17
477	203310.21+411322.4	–	–	–	–	–	–	–
478	203310.23+411533.1	–	–	–	–	–	–	–
479	203310.26+411413.3	20331027+4114136	0.04	14.99 ± 0.03	13.59 ± 0.03	13.06 ± 0.03	AAA	7.48
480	203310.29+412205.1	20331029+4122055	0.10	13.46 ± 0.03	12.52 ± 0.02	12.12 ± 0.02	AAA	14.32
481	203310.45+410925.5	20331047+4109257	0.11	16.52	15.52 ± 0.12	14.68 ± 0.12	UBB	7.45
482	203310.56+411328.4	20331059+4113285	0.24	14.98 ± 0.03	13.62 ± 0.03	13.05 ± 0.04	AAA	N/A
483	203310.57+412102.3	20331060+4121041	1.61	15.39 ± 0.08	14.31 ± 0.09	13.97 ± 0.06	AAA	N/A
484	203310.58+411538.7	–	–	–	–	–	–	–
485	203310.60+411323.8	–	–	–	–	–	–	–
486	203310.64+411748.8	–	–	–	–	–	–	–
487	203310.71+411339.6	–	–	–	–	–	–	–
488	203310.72+411507.9	20331074+4115081	0.33	6.47 ± 0.01	5.90 ± 0.01	5.57±N/A	AAA	N/A
489	203310.73+411502.2	–	–	–	–	–	–	–
490	203310.81+411256.4	20331084+4112568	0.42	15.78 ± 0.09	14.45 ± 0.08	13.61	AAU	6.49
491	203310.93+410953.3	20331095+4109537	0.16	16.38 ± 0.12	14.90 ± 0.07	14.42 ± 0.09	BAA	N/A
492	203310.99+411241.8	–	–	–	–	–	–	–
493	203311.05+411032.0	20331106+4110321	0.16	10.17 ± 0.02	9.60 ± 0.01	9.28 ± 0.01	AAA	N/A
494	203311.07+411318.0	–	–	–	–	–	–	–
495	203311.09+411445.4	20331108+4114457	0.25	13.93 ± 0.01	13.34 ± 0.03	13.24 ± 0.05	AAA	9.77
496	203311.13+411640.6	–	–	–	–	–	–	–
497	203311.22+410833.9	20331123+4108338	0.39	15.27 ± 0.04	13.98 ± 0.02	13.44 ± 0.04	AAA	N/A
498	203311.29+411711.4	–	–	–	–	–	–	–
499	203311.32+411729.0	20331134+4117294	0.24	15.31 ± 0.05	14.06 ± 0.04	13.55 ± 0.05	AAA	8.17
500	203311.44+411256.7	20331145+4112568	0.10	14.87 ± 0.05	13.60 ± 0.05	12.97	AAU	9.39
501	203311.47+411348.0	20331148+4113481	0.14	16.11 ± 0.09	14.40 ± 0.05	13.98 ± 0.06	AAA	9.16
502	203311.51+411238.8	–	–	–	–	–	–	–
503	203311.52+410718.9	20331151+4107197	0.63	15.71 ± 0.06	14.53 ± 0.06	14.28 ± 0.08	AAA	5.52
504	203311.59+411243.0	–	–	–	–	–	–	–
505	203311.60+411615.8	20331157+4116169	0.96	16.94 ± 0.19	15.43 ± 0.09	14.94 ± 0.16	CAC	8.29
506	203311.63+411646.4	20331162+4116468	0.29	14.94 ± 0.05	13.49 ± 0.05	12.77	AAU	N/A
507	203311.79+411149.9	20331180+4111502	0.16	16.25 ± 0.13	14.89 ± 0.11	14.33 ± 0.10	BAA	11.08
508	203311.87+411245.3	20331183+4112455	0.66	15.06 ± 0.16	13.66 ± 0.08	13.25 ± 0.07	CAA	N/A
509	203311.89+411213.9	20331189+4112139	0.24	15.11 ± 0.04	13.86 ± 0.03	13.47 ± 0.04	AAA	6.84
510	203312.04+412023.1	20331204+4120235	0.15	12.73 ± 0.03	11.96 ± 0.03	11.56 ± 0.02	AAA	6.83
511	203312.05+411649.2	20331206+4116495	0.11	15.53 ± 0.05	14.19 ± 0.04	13.51	AAU	N/A
512	203312.20+411014.2	–	–	–	–	–	–	–
513	203312.25+411104.6	–	–	–	–	–	–	–
514	203312.50+411502.0	20331252+4115021	0.22	12.28 ± 0.02	11.21 ± 0.02	10.43 ± 0.01	AAA	2.45
515	203312.50+411150.1	–	–	–	–	–	–	–
516	203312.57+411453.3	20331259+4114532	0.39	16.15 ± 0.11	14.40 ± 0.04	13.53 ± 0.06	BAA	10.13
517	203312.60+411539.4	20331261+4115395	0.09	16.01 ± 0.09	14.57 ± 0.05	14.21 ± 0.08	AAA	10.72
518	203312.62+411635.1	20331265+4116353	0.33	16.77	15.25 ± 0.08	14.49 ± 0.10	UAA	1.28
519	203312.66+411913.6	–	–	–	–	–	–	–
520	203312.73+411132.6	20331273+4111330	0.16	13.98 ± 0.02	12.67 ± 0.02	11.99 ± 0.02	AAA	12.31

Table 2. continued.

N_x	X-ray - 2MASS counterpart		Off.	2MASS photometry				A_v
#	CXOACJ+	2MASS J+	(″)	J	H	K_s	Ph. qual	(mag)
521	203312.74+411439.3	–	–	–	–	–	–	–
522	203312.86+412115.8	20331289+4121171	1.06	16.00 ± 0.08	14.66 ± 0.05	14.31 ± 0.09	AAA	N/A
523	203312.87+411154.4	–	–	–	–	–	–	–
524	203312.97+411257.5	20331287+4112575	1.56	13.91	14.72 ± 0.08	12.67	UAU	0.93
525	203313.03+411539.0	20331304+4115393	0.09	15.58 ± 0.05	14.20 ± 0.04	13.62 ± 0.05	AAA	7.65
526	203313.04+411311.5	20331307+4113119	0.40	15.20 ± 0.17	14.04 ± 0.10	13.73 ± 0.08	CAA	N/A
527	203313.08+411030.1	20331305+4110311	0.92	16.44 ± 0.12	15.01 ± 0.07	14.49 ± 0.10	BAA	7.86
528	203313.16+411338.6	20331320+4113389	0.45	15.25 ± 0.12	13.98 ± 0.08	13.56 ± 0.05	BAA	11.21
529	203313.23+411319.1	–	–	–	–	–	–	–
530	203313.24+411328.4	20331326+4113287	0.12	8.98 ± 0.03	8.35 ± 0.01	8.01 ± 0.01	AAA	7.43
531	203313.25+411727.2	20331327+4117275	0.22	16.26	15.19 ± 0.09	14.70 ± 0.12	UAB	N/A
532	203313.38+411110.8	20331334+4111111	0.77	15.97 ± 0.09	14.54 ± 0.06	14.10 ± 0.07	AAA	6.85
533	203313.40+411233.6	20331339+4112337	0.37	16.59 ± 0.13	15.01 ± 0.07	14.70 ± 0.13	BAB	14.74
534	203313.54+411948.8	20331362+4119494	1.06	14.84 ± 0.03	13.70 ± 0.02	13.26 ± 0.04	AAA	N/A
535	203313.60+412004.8	20331366+4120052	0.78	15.66 ± 0.07	14.61 ± 0.05	13.96 ± 0.07	AAA	N/A
536	203313.62+411749.2	20331359+4117497	0.63	15.10 ± 0.04	14.20 ± 0.04	13.95 ± 0.07	AAA	N/A
537	203313.67+411305.4	20331369+4113057	0.15	9.03 ± 0.02	8.56 ± 0.02	8.28 ± 0.01	AAA	N/A
538	203313.78+411028.0	20331377+4110294	1.22	16.12 ± 0.09	14.77 ± 0.07	14.15 ± 0.08	AAA	6.11
539	203313.85+411715.1	20331385+4117154	0.23	16.02 ± 0.08	15.01 ± 0.07	14.62 ± 0.11	AAA	N/A
540	203313.87+411259.0	20331382+4113001	1.22	11.83	13.47 ± 0.11	11.01	UBU	9.91
541	203313.88+411345.4	20331387+4113458	0.26	16.49	15.48 ± 0.11	14.35 ± 0.09	UBA	9.67
542	203314.05+411626.9	20331406+4116270	0.08	16.41 ± 0.12	14.68 ± 0.05	13.65 ± 0.05	BAA	5.91
543	203314.09+410925.6	20331411+4109264	0.51	15.90 ± 0.07	14.55 ± 0.05	14.06 ± 0.07	AAA	5.17
544	203314.11+412021.6	20331411+4120218	0.15	7.25 ± 0.01	6.82 ± 0.01	6.61 ± 0.01	AAA	N/A
545	203314.13+411446.6	–	–	–	–	–	–	–
546	203314.15+411450.2	20331416+4114504	0.01	13.27 ± 0.02	12.24 ± 0.02	11.83 ± 0.02	AAA	1.12
547	203314.16+412054.9	–	–	–	–	–	–	–
548	203314.22+410852.7	20331419+4108523	0.83	16.69 ± 0.15	15.49 ± 0.10	15.19 ± 0.18	BAC	N/A
549	203314.24+411227.8	20331428+4112283	0.48	15.04 ± 0.06	13.61 ± 0.06	13.14 ± 0.06	AAA	N/A
550	203314.25+411236.7	20331421+4112372	0.69	15.47 ± 0.06	14.21 ± 0.05	13.70 ± 0.06	AAA	7.87
551	203314.31+411221.2	20331434+4112218	0.51	15.39 ± 0.06	13.91 ± 0.04	13.08 ± 0.04	AAA	N/A
552	203314.32+411932.8	20331433+4119331	0.11	10.19 ± 0.02	9.57 ± 0.02	9.24 ± 0.02	AAA	6.98
553	203314.38+411223.5	–	–	–	–	–	–	–
554	203314.39+411901.0	–	–	–	–	–	–	–
555	203314.42+411923.5	20331443+4119238	0.06	11.66 ± 0.02	10.83 ± 0.02	10.26 ± 0.01	AAA	8.99
556	203314.44+410633.3	20331442+4106320	1.56	15.61	14.60 ± 0.08	14.02	UAU	N/A
557	203314.47+411856.2	–	–	–	–	–	–	–
558	203314.50+411253.9	20331451+4112542	0.08	15.92 ± 0.08	14.50 ± 0.06	14.19 ± 0.08	AAA	N/A
559	203314.58+411837.1	–	–	–	–	–	–	–
560	203314.69+410944.1	–	–	–	–	–	–	–
561	203314.76+412012.5	–	–	–	–	–	–	–
562	203314.76+411841.4	20331476+4118416	0.23	7.21 ± 0.02	6.76 ± 0.01	6.57 ± 0.01	AAA	4.93
563	203314.81+411421.0	20331480+4114215	0.42	16.78 ± 0.16	15.34 ± 0.10	14.84 ± 0.15	CAB	4.95
564	203314.84+410831.4	20331492+4108317	0.99	15.08 ± 0.04	13.81 ± 0.03	13.42 ± 0.04	AAA	8.56
565	203314.87+410957.6	20331487+4109572	0.66	16.82 ± 0.16	14.93 ± 0.07	14.25 ± 0.07	CAA	6.46
566	203314.92+411719.4	–	–	–	–	–	–	–
567	203314.97+411556.8	20331500+4115572	0.26	15.57 ± 0.05	14.09 ± 0.03	13.48 ± 0.04	AAA	N/A
568	203315.07+411850.3	20331508+4118504	0.15	6.12 ± 0.01	5.72 ± 0.01	5.50 ± 0.01	AAA	12.75
569	203315.11+411310.5	20331513+4113106	0.28	16.03 ± 0.11	14.46 ± 0.06	13.77 ± 0.07	BAA	9.97
570	203315.12+411903.3	–	–	–	–	–	–	–
571	203315.18+411530.8	20331519+4115311	0.12	14.80 ± 0.04	13.46 ± 0.03	12.95 ± 0.03	AAA	N/A
572	203315.21+411327.5	20331523+4113277	0.22	15.72 ± 0.09	14.28 ± 0.08	13.66 ± 0.06	AAA	N/A
573	203315.28+411522.6	20331529+4115229	0.11	15.36 ± 0.04	13.85 ± 0.01	13.34 ± 0.03	AAA	N/A
574	203315.31+411855.6	–	–	–	–	–	–	–
575	203315.33+411029.9	20331532+4110297	0.58	15.26 ± 0.05	13.93 ± 0.04	13.52 ± 0.04	AAA	N/A
576	203315.38+411751.5	20331541+4117518	0.35	15.37 ± 0.05	14.18 ± 0.04	13.82 ± 0.06	AAA	N/A
577	203315.39+411338.4	20331539+4113389	0.25	15.19 ± 0.04	13.88 ± 0.03	13.40 ± 0.04	AAA	4.15
578	203315.40+411329.6	–	–	–	–	–	–	–
579	203315.43+411816.0	20331546+4118162	0.33	15.50 ± 0.07	14.31 ± 0.07	13.80 ± 0.06	AAA	N/A
580	203315.45+411856.7	–	–	–	–	–	–	–
581	203315.55+412133.3	–	–	–	–	–	–	–
582	203315.63+411851.4	–	–	–	–	–	–	–
583	203315.68+411319.4	–	–	–	–	–	–	–
584	203315.70+412017.0	20331571+4120172	0.08	9.33 ± 0.02	8.94 ± 0.01	8.73 ± 0.02	AAA	6.99
585	203315.76+410633.1	20331562+4106322	2.59	15.81 ± 0.07	14.71 ± 0.08	14.15 ± 0.07	AAA	7.48

Table 2. continued.

N_x	X-ray - 2MASS counterpart		Off.	2MASS photometry				A_v
#	CXOAC J+	2MASS J+	(″)	J	H	K_s	Ph. qual	(mag)
586	203315.80+411510.2	20331579+4115107	0.29	15.32	14.21	14.27 ± 0.10	UUA	N/A
587	203315.82+411225.8	20331584+4112264	0.44	16.33 ± 0.11	15.04 ± 0.07	14.44 ± 0.09	AAA	10.41
588	203315.84+412115.0	–	–	–	–	–	–	–
589	203315.89+411623.3	20331589+4116239	0.41	15.95 ± 0.08	14.72 ± 0.05	14.21 ± 0.08	AAA	18.23
590	203315.90+412025.3	20331589+4120254	0.35	12.60 ± 0.04	11.99 ± 0.02	11.73	AAU	6.55
591	203316.17+411245.3	20331619+4112459	0.34	14.08 ± 0.04	13.10 ± 0.04	12.77 ± 0.03	AAA	N/A
592	203316.21+411721.8	20331622+4117220	0.01	15.19 ± 0.05	13.82 ± 0.04	13.37 ± 0.05	AAA	7.35
593	203316.21+411440.3	20331624+4114406	0.44	14.35 ± 0.05	12.90 ± 0.08	12.48 ± 0.04	AAA	7.06
594	203316.22+412015.5	20331623+4120158	0.13	14.48 ± 0.07	13.51 ± 0.06	13.03 ± 0.05	AAA	7.48
595	203316.29+412143.7	–	–	–	–	–	–	–
596	203316.34+411858.9	–	–	–	–	–	–	–
597	203316.36+411902.1	20331634+4119017	0.72	8.84 ± 0.01	8.42 ± 0.04	8.24 ± 0.01	AAA	10.15
598	203316.44+411659.2	20331645+4116597	0.23	15.16 ± 0.06	13.85 ± 0.07	13.27 ± 0.05	AAA	7.19
599	203316.45+410924.9	20331647+4109245	0.62	16.99	15.32 ± 0.09	14.80 ± 0.12	UAB	4.88
600	203316.50+411653.9	–	–	–	–	–	–	–
601	203316.52+410703.7	20331653+4107036	0.41	14.81 ± 0.04	13.77 ± 0.03	13.42 ± 0.04	AAA	6.62
602	203316.57+411703.9	20331658+4117039	0.25	12.47 ± 0.03	11.60 ± 0.03	11.25 ± 0.04	AAA	7.45
603	203316.60+411258.8	20331660+4112589	0.17	14.88 ± 0.08	13.60 ± 0.06	13.18 ± 0.05	AAA	4.36
604	203316.64+411542.2	20331667+4115423	0.35	16.39	15.15 ± 0.08	14.70 ± 0.13	UAB	N/A
605	203316.66+411404.4	20331663+4114053	0.92	16.50 ± 0.12	14.77 ± 0.07	14.31 ± 0.09	BAA	0.64
606	203316.72+411833.1	–	–	–	–	–	–	–
607	203316.73+411129.3	20331675+4111298	0.26	16.60 ± 0.14	15.03	14.44	BUU	N/A
608	203316.83+411056.8	20331682+4110575	0.53	14.54 ± 0.04	13.27 ± 0.03	12.72 ± 0.03	AAA	3.34
609	203317.08+411659.7	20331712+4116599	0.44	14.86 ± 0.09	13.72 ± 0.09	13.46 ± 0.06	AAA	41.63
610	203317.12+411506.6	20331714+4115067	0.23	16.36 ± 0.11	15.00 ± 0.07	14.27 ± 0.08	BAA	N/A
611	203317.31+411342.0	20331733+4113421	0.25	15.69 ± 0.06	14.74 ± 0.07	14.21 ± 0.08	AAA	5.90
612	203317.38+411653.9	–	–	–	–	–	–	–
613	203317.40+411453.8	20331740+4114541	0.01	11.35 ± 0.02	10.78 ± 0.01	10.48 ± 0.01	AAA	6.41
614	203317.40+411238.4	20331740+4112387	0.26	10.23 ± 0.02	9.68 ± 0.01	9.43 ± 0.01	AAA	9.41
615	203317.47+411709.0	20331748+4117093	0.02	8.35 ± 0.02	7.89 ± 0.01	7.65 ± 0.01	AAA	7.23
616	203317.51+410724.3	20331744+4107242	1.27	16.63 ± 0.14	15.39 ± 0.11	14.52	BBU	11.43
617	203317.53+411800.7	–	–	–	–	–	–	–
618	203317.55+412041.1	20331754+4120416	0.41	16.25 ± 0.10	14.98 ± 0.07	14.36 ± 0.10	AAA	9.41
619	203317.63+412022.0	20331767+4120221	0.46	15.43 ± 0.06	14.39 ± 0.05	14.02 ± 0.07	AAA	45.95
620	203317.74+411304.7	20331774+4113047	0.23	13.44 ± 0.01	12.23 ± 0.01	11.42 ± 0.02	AAA	8.69
621	203317.76+411753.0	20331777+4117532	0.06	17.36	15.53 ± 0.12	15.47	UBU	0.62
622	203317.83+411323.3	20331787+4113240	0.60	13.52 ± 0.03	12.58 ± 0.03	12.20 ± 0.03	AAA	6.86
623	203317.95+411917.9	20331800+4119181	0.76	14.22 ± 0.02	13.30 ± 0.02	12.93 ± 0.03	AAA	N/A
624	203317.97+410749.6	20331807+4107499	1.43	16.74 ± 0.15	15.19 ± 0.08	14.73 ± 0.12	BAB	39.70
625	203317.99+411830.9	20331798+4118311	0.23	7.16 ± 0.01	6.79 ± 0.01	6.58 ± 0.01	AAA	7.22
626	203318.06+412136.3	20331803+4121366	0.55	8.74 ± 0.01	8.31 ± 0.01	8.11 ± 0.01	AAA	N/A
627	203318.06+412136.4	20331803+4121366	0.55	8.74 ± 0.01	8.31 ± 0.01	8.11 ± 0.01	AAA	5.19
628	203318.06+411714.4	20331809+4117146	0.45	15.58 ± 0.37	14.29 ± 0.17	14.23 ± 0.12	DCB	5.24
629	203318.08+411731.1	20331811+4117315	0.35	12.26 ± 0.02	11.44 ± 0.02	11.06 ± 0.01	AAA	14.35
630	203318.08+411731.2	20331811+4117315	0.35	12.26 ± 0.02	11.44 ± 0.02	11.06 ± 0.01	AAA	7.03
631	203318.14+411101.1	20331817+4111010	0.43	16.56 ± 0.13	15.04 ± 0.08	14.74 ± 0.12	BAB	11.38
632	203318.17+410920.5	20331821+4109201	0.77	15.76 ± 0.07	14.52 ± 0.05	14.03 ± 0.07	AAA	4.11
633	203318.28+411739.0	20331828+4117394	0.13	11.52 ± 0.02	10.97 ± 0.02	10.66 ± 0.01	AAA	6.68
634	203318.30+412209.5	20331837+4122106	1.30	15.47 ± 0.09	11.27	10.50	AUU	20.34
635	203318.42+411240.4	–	–	–	–	–	–	–
636	203318.46+411452.9	20331846+4114533	0.17	14.91 ± 0.03	13.69 ± 0.02	13.22 ± 0.03	AAA	2.03
637	203318.46+411119.2	20331848+4111195	0.26	15.52 ± 0.06	14.21 ± 0.04	13.67 ± 0.05	AAA	N/A
638	203318.52+411534.9	20331853+4115351	0.11	9.41 ± 0.02	8.58 ± 0.02	7.98 ± 0.01	AAA	2.80
639	203318.66+411912.0	20331862+4119122	0.77	16.76 ± 0.17	15.30 ± 0.10	15.15	CAU	8.05
640	203318.66+411723.6	20331865+4117243	0.61	17.01 ± 0.27	15.11 ± 0.09	14.61 ± 0.12	DAB	N/A
641	203318.74+411704.1	20331872+4117044	0.45	16.28 ± 0.19	14.64	14.19	CUU	1.23
642	203318.77+412130.5	20331873+4121313	1.00	15.19 ± 0.07	14.13 ± 0.07	13.71 ± 0.06	AAA	3.27
643	203318.87+411436.8	20331888+4114371	0.15	14.97 ± 0.05	13.17 ± 0.03	12.01 ± 0.02	AAA	N/A
644	203318.91+411319.2	–	–	–	–	–	–	–
645	203318.94+411332.6	20331892+4113328	0.55	15.92	14.68 ± 0.05	14.15 ± 0.08	UAA	1.12
646	203319.01+412134.8	20331906+4121350	0.66	14.17 ± 0.04	13.12 ± 0.03	12.66 ± 0.03	AAA	2.27
647	203318.99+410759.1	20331903+4107589	0.68	15.85 ± 0.07	14.51 ± 0.07	14.18 ± 0.08	AAA	7.41
648	203319.06+411354.1	20331909+4113542	0.35	15.74 ± 0.06	14.45 ± 0.11	13.95 ± 0.07	AAA	N/A
649	203319.11+410658.4	20331907+4106585	0.68	15.65 ± 0.06	14.41 ± 0.05	13.93 ± 0.07	AAA	0.31
650	203319.13+411659.2	20331914+4116598	0.33	14.03 ± 0.04	13.34 ± 0.05	13.09 ± 0.05	AEA	6.80

Table 2. continued.

N_x	X-ray - 2MASS counterpart		Off.	2MASS photometry				A_v
#	CXOAC J+	2MASS J+	(″)	J	H	K_s	Ph. qual	(mag)
651	203319.16+411906.7	–	–	–	–	–	–	–
652	203319.21+411756.4	20331924+4117567	0.23	14.84 ± 0.02	13.79 ± 0.02	13.30 ± 0.04	AAA	6.78
653	203319.29+411702.1	–	–	–	–	–	–	–
654	203319.42+411741.4	–	–	–	–	–	–	–
655	203319.44+411349.8	20331943+4113495	0.65	15.18 ± 0.08	14.11 ± 0.07	13.69 ± 0.06	AAA	9.68
656	203319.46+412008.5	20331945+4120088	0.13	16.07 ± 0.08	14.65 ± 0.05	14.14 ± 0.08	AAA	0.26
657	203319.48+411517.6	20331948+4115173	0.49	16.13 ± 0.10	14.32	13.66	AUU	14.93
658	203319.48+411225.7	20331950+4112259	0.22	15.53 ± 0.06	14.35 ± 0.06	13.73	AAU	2.97
659	203319.48+410737.0	20331948+4107373	0.09	12.81 ± 0.02	12.03 ± 0.01	11.60 ± 0.02	AAA	7.49
660	203319.52+412127.0	20331963+4121270	1.44	15.11 ± 0.04	13.79 ± 0.05	13.23 ± 0.04	AAA	N/A
661	203319.58+411906.4	20331959+4119064	0.29	11.95 ± 0.02	11.47 ± 0.01	11.20 ± 0.01	AAA	1.31
662	203319.59+411803.9	20331962+4118043	0.29	16.05	15.01	14.17 ± 0.08	UUA	N/A
663	203319.59+411042.3	20331959+4110425	0.12	14.79 ± 0.03	13.69 ± 0.03	13.24 ± 0.03	AAA	10.94
664	203319.73+412103.1	20331968+4121025	1.32	15.61 ± 0.06	14.40 ± 0.05	13.99 ± 0.07	AAA	6.69
665	203319.88+411124.6	20331986+4111250	0.42	16.44 ± 0.12	15.43 ± 0.10	14.71 ± 0.11	BAB	6.72
666	203319.91+410716.8	20331982+4107179	1.70	13.49	14.10 ± 0.11	11.33	UBU	7.62
667	203320.02+412011.6	20332000+4120117	0.47	15.72 ± 0.08	14.46 ± 0.05	13.95 ± 0.07	AAA	1.55
668	203320.03+411831.6	–	–	–	–	–	–	–
669	203320.09+411632.8	–	–	–	–	–	–	–
670	203320.12+411943.2	20332016+4119432	0.47	13.94 ± 0.02	12.82 ± 0.02	12.41 ± 0.02	AAA	4.49
671	203320.19+411716.4	–	–	–	–	–	–	–
672	203320.23+411432.3	20332024+4114326	0.12	15.24 ± 0.04	14.04 ± 0.03	13.62 ± 0.05	AAA	6.21
673	203320.31+411647.1	20332028+4116478	0.68	16.51 ± 0.12	15.19 ± 0.09	14.53 ± 0.11	BAB	5.36
674	203320.39+411840.8	20332040+4118412	0.12	13.08 ± 0.02	12.48 ± 0.02	12.37 ± 0.02	AAA	3.66
675	203320.40+411929.0	–	–	–	–	–	–	–
676	203320.47+412033.0	20332044+4120334	0.59	12.89 ± 0.02	12.22 ± 0.03	12.03 ± 0.02	AAA	6.95
677	203320.49+412144.8	20332047+4121447	0.56	16.15 ± 0.09	15.15 ± 0.08	14.62 ± 0.12	AAB	5.88
678	203320.55+411815.6	–	–	–	–	–	–	–
679	203320.58+411451.3	20332058+4114518	0.25	16.83 ± 0.19	15.16 ± 0.08	14.13 ± 0.07	CAA	4.72
680	203320.58+411704.4	20332057+4117048	0.36	14.52 ± 0.03	13.64 ± 0.03	13.28 ± 0.04	AAA	8.51
681	203320.58+411653.6	20332057+4116539	0.23	16.65 ± 0.14	14.95 ± 0.08	14.15 ± 0.08	BAA	N/A
682	203320.68+411418.4	–	–	–	–	–	–	–
683	203320.76+411723.1	20332076+4117235	0.17	12.40	11.79	12.60 ± 0.03	UUA	N/A
684	203320.83+411013.4	–	–	–	–	–	–	–
685	203320.93+411207.9	20332093+4112080	0.15	17.34	15.83	14.81 ± 0.14	UUB	N/A
686	203321.01+411739.8	20332101+4117401	0.03	9.30 ± 0.02	8.90 ± 0.01	8.67 ± 0.01	AAA	11.12
687	203321.04+411708.8	–	–	–	–	–	–	–
688	203321.04+410647.3	20332108+4106483	0.88	16.19 ± 0.09	14.82 ± 0.06	14.42 ± 0.09	AAA	38.89
689	203321.10+411659.2	–	–	–	–	–	–	–
690	203321.11+411756.6	20332112+4117570	0.23	14.54 ± 0.03	13.26 ± 0.05	12.40 ± 0.04	AAA	N/A
691	203321.14+411242.1	20332112+4112436	1.37	16.18 ± 0.10	14.85 ± 0.07	14.56 ± 0.10	AAA	N/A
692	203321.15+411325.4	20332116+4113257	0.07	13.94 ± 0.02	13.07 ± 0.02	12.64 ± 0.03	AAA	5.92
693	203321.21+411845.9	20332123+4118462	0.23	15.88 ± 0.08	14.77 ± 0.06	14.50 ± 0.10	AAA	12.40
694	203321.25+411839.4	20332126+4118395	0.19	13.03 ± 0.02	12.45 ± 0.02	12.16 ± 0.02	AAA	N/A
695	203321.27+411250.3	20332128+4112507	0.17	13.38	12.58	12.13 ± 0.02	UUA	7.11
696	203321.29+411312.8	–	–	–	–	–	–	–
697	203321.59+411229.1	20332161+4112296	0.29	15.76 ± 0.07	14.43 ± 0.06	13.95 ± 0.06	AAA	N/A
698	203321.64+411127.0	–	–	–	–	–	–	–
699	203321.69+412026.3	20332169+4120262	0.34	14.98 ± 0.04	14.17 ± 0.03	13.77 ± 0.05	AAA	N/A
700	203321.73+411511.1	–	–	–	–	–	–	–
701	203321.81+411332.2	20332182+4113325	0.01	12.51 ± 0.02	11.75 ± 0.01	11.34 ± 0.02	AAA	N/A
702	203321.85+412136.1	20332184+4121367	0.46	14.90 ± 0.04	13.55 ± 0.03	13.12 ± 0.04	AAA	11.02
703	203321.83+410944.6	20332184+4109445	0.30	15.14 ± 0.05	13.68 ± 0.03	12.98 ± 0.06	AAA	N/A
704	203321.90+411316.5	20332193+4113167	0.22	15.33 ± 0.04	14.00 ± 0.03	13.47 ± 0.04	AAA	7.27
705	203321.92+411731.3	20332194+4117317	0.20	15.14 ± 0.05	14.11 ± 0.04	13.63 ± 0.05	AAA	20.23
706	203321.97+412037.2	20332191+4120371	0.93	15.94 ± 0.08	14.65 ± 0.06	14.23 ± 0.09	AAA	10.17
707	203322.00+411431.3	20332201+4114314	0.08	16.59 ± 0.14	15.44 ± 0.12	14.65 ± 0.12	BBB	N/A
708	203322.01+411217.5	20332202+4112179	0.17	15.02 ± 0.04	13.76 ± 0.04	13.29 ± 0.04	AAA	N/A
709	203322.06+412153.8	–	–	–	–	–	–	–
710	203322.06+411003.9	20332206+4110044	0.29	16.35	15.18 ± 0.08	14.24	UAU	8.69
711	203322.12+411245.1	20332214+4112453	0.11	15.40 ± 0.05	14.11 ± 0.03	13.64 ± 0.05	AAA	1.68
712	203322.25+411744.3	20332224+4117446	0.23	13.04 ± 0.02	12.01 ± 0.03	11.60 ± 0.02	AAA	7.99
713	203322.34+411815.8	–	–	–	–	–	–	–
714	203322.37+411551.4	20332236+4115518	0.29	16.48 ± 0.12	14.87 ± 0.07	14.28 ± 0.08	BAA	7.63
715	203322.40+411551.4	20332236+4115518	0.70	16.48 ± 0.12	14.87 ± 0.07	14.28 ± 0.08	BAA	5.13

Table 2. continued.

N_x	X-ray - 2MASS counterpart		Off.	2MASS photometry				A_v
#	CXOAC J+	2MASS J+	(″)	J	H	K_s	Ph. qual	(mag)
716	203322.44+411736.5	20332247+4117368	0.44	16.36 ± 0.12	14.96 ± 0.09	14.38 ± 0.11	BAA	N/A
717	203322.57+411340.2	20332260+4113403	0.37	15.62 ± 0.09	14.44 ± 0.13	13.88 ± 0.08	ABA	7.10
718	203322.91+411859.8	20332290+4119002	0.25	15.29 ± 0.04	14.13 ± 0.06	13.59 ± 0.05	AAA	N/A
719	203323.02+411612.0	–	–	–	–	–	–	–
720	203323.02+410932.5	20332294+4109324	1.25	16.42 ± 0.15	14.81 ± 0.10	14.23 ± 0.09	BAA	5.84
721	203323.02+411222.0	20332300+4112218	0.58	12.77 ± 0.02	12.01 ± 0.02	11.82 ± 0.02	AAA	N/A
722	203323.02+411222.1	20332300+4112218	0.58	12.77 ± 0.02	12.01 ± 0.02	11.82 ± 0.02	AAA	9.35
723	203323.22+411909.2	–	–	–	–	–	–	–
724	203323.34+411236.2	20332335+4112364	0.05	14.73 ± 0.04	13.52 ± 0.04	13.01 ± 0.03	AAA	12.66
725	203323.38+411912.1	20332336+4119126	0.51	14.81 ± 0.04	13.75 ± 0.04	13.35 ± 0.04	AAA	10.53
726	203323.37+411347.3	20332337+4113478	0.21	13.09	13.99 ± 0.12	13.67 ± 0.07	UBA	5.51
727	203323.38+411747.8	–	–	–	–	–	–	–
728	203323.43+412039.8	20332345+4120398	0.29	13.84 ± 0.02	13.23 ± 0.02	12.88 ± 0.03	AAA	7.59
729	203323.48+410912.2	20332346+4109130	0.68	7.03 ± 0.01	6.38 ± 0.01	6.05 ± 0.01	AAA	0.97
730	203323.57+411746.8	20332354+4117475	0.84	15.12	14.14 ± 0.06	13.65 ± 0.05	UAA	N/A
731	203323.67+412151.0	20332364+4121511	0.67	12.93 ± 0.02	12.04 ± 0.02	11.64 ± 0.02	AAA	8.08
732	203323.73+411537.3	20332377+4115375	0.44	15.47 ± 0.08	14.27 ± 0.03	13.59 ± 0.07	AAA	14.46
733	203323.77+412006.4	20332378+4120068	0.13	14.97 ± 0.05	13.84 ± 0.04	13.34 ± 0.04	AAA	2.24
734	203323.84+411310.6	20332384+4113111	0.27	14.34 ± 0.03	13.14 ± 0.03	12.69 ± 0.03	AAA	0.01
735	203323.83+411106.4	–	–	–	–	–	–	–
736	203323.89+412207.8	20332391+4122083	0.31	15.43 ± 0.06	14.24 ± 0.05	13.88 ± 0.06	AAA	12.64
737	203323.94+411640.2	20332398+4116405	0.45	15.65 ± 0.06	14.40 ± 0.06	13.94 ± 0.07	AAA	1.31
738	203324.01+412145.9	20332409+4121449	1.59	16.17 ± 0.11	14.98 ± 0.08	14.62 ± 0.13	BAB	N/A
739	203324.25+411700.1	20332426+4117004	0.13	14.45 ± 0.03	13.33 ± 0.02	12.88 ± 0.03	AAA	11.61
740	203324.31+412106.7	–	–	–	–	–	–	–
741	203324.32+411752.5	20332434+4117515	1.21	11.00 ± 0.02	10.39 ± 0.02	10.27 ± 0.01	AAA	6.91
742	203324.38+411416.6	20332442+4114164	0.62	16.65 ± 0.15	15.49 ± 0.10	15.11 ± 0.17	BAC	N/A
743	203324.41+412032.8	20332440+4120330	0.12	15.53 ± 0.06	14.18 ± 0.07	13.80 ± 0.07	AAA	8.84
744	203324.39+410812.3	20332439+4108131	0.62	15.65 ± 0.05	14.19 ± 0.04	13.69 ± 0.05	AAA	N/A
745	203324.48+411532.7	20332453+4115339	1.16	13.31 ± 0.02	12.17 ± 0.02	11.70 ± 0.02	AAA	10.25
746	203324.53+411534.0	20332453+4115339	0.29	13.31 ± 0.02	12.17 ± 0.02	11.70 ± 0.02	AAA	N/A
747	203324.55+411046.3	20332461+4110451	1.60	16.86	15.80 ± 0.14	14.67	UBU	6.52
748	203324.58+411907.9	20332463+4119081	0.54	15.51 ± 0.05	14.26 ± 0.04	14.04	AAU	N/A
749	203324.60+411553.8	20332461+4115542	0.17	16.62 ± 0.13	15.22 ± 0.08	14.55 ± 0.12	BAB	N/A
750	203324.62+411059.4	20332464+4110596	0.22	16.02 ± 0.08	14.72 ± 0.05	14.32 ± 0.09	AAA	15.96
751	203324.77+412223.1	20332481+4122235	0.59	15.32 ± 0.05	14.19 ± 0.04	13.70 ± 0.05	AAA	3.27
752	203324.89+412001.6	–	–	–	–	–	–	–
753	203324.96+410836.3	20332497+4108366	0.12	16.37 ± 0.17	14.30	13.80	CUU	3.90
754	203325.01+411537.0	20332503+4115375	0.22	16.06 ± 0.10	14.57 ± 0.06	14.05 ± 0.07	AAA	N/A
755	203325.12+411818.6	20332513+4118187	0.17	13.20 ± 0.02	12.71 ± 0.02	12.43 ± 0.02	AAA	N/A
756	203325.10+411050.1	20332509+4110515	1.17	16.71 ± 0.15	15.18 ± 0.08	15.04 ± 0.15	BAC	8.01
757	203325.10+410724.8	20332511+4107248	0.25	15.98 ± 0.08	14.62 ± 0.05	13.97 ± 0.06	AAA	0.89
758	203325.23+411146.1	–	–	–	–	–	–	–
759	203325.27+410918.4	–	–	–	–	–	–	–
760	203325.42+411039.4	20332541+4110400	0.41	14.92 ± 0.05	13.57 ± 0.05	13.18 ± 0.04	AAA	11.96
761	203325.50+410932.1	20332548+4109314	1.05	15.74 ± 0.06	14.40 ± 0.04	13.74 ± 0.05	AAA	N/A
762	203325.66+411555.6	20332563+4115557	0.58	16.60 ± 0.16	15.17 ± 0.10	14.44 ± 0.11	CAA	N/A
763	203325.82+411853.6	20332584+4118536	0.33	15.12 ± 0.06	14.00 ± 0.05	13.46 ± 0.05	AAA	N/A
764	203325.91+411322.2	20332594+4113222	0.50	15.02 ± 0.04	13.79 ± 0.04	13.46 ± 0.05	AAA	N/A
765	203325.92+411333.2	20332592+4113332	0.17	15.86 ± 0.08	14.40 ± 0.05	13.70 ± 0.06	AAA	6.69
766	203325.93+411718.6	20332597+4117191	0.52	17.07	15.30 ± 0.09	15.14 ± 0.19	UAC	8.57
767	203325.94+411316.5	–	–	–	–	–	–	–
768	203326.03+411901.1	20332601+4119014	0.56	16.57 ± 0.16	14.99 ± 0.10	14.58 ± 0.12	CAB	N/A
769	203326.08+411229.6	20332611+4112298	0.33	13.74 ± 0.02	12.74 ± 0.02	12.32 ± 0.02	AAA	N/A
770	203326.11+411549.0	20332608+4115497	0.76	11.66 ± 0.02	10.98 ± 0.02	10.62 ± 0.02	AAA	5.73
771	203326.28+412146.7	–	–	–	–	–	–	–
772	203326.33+411806.0	20332632+4118059	0.39	15.97 ± 0.07	14.67 ± 0.06	14.18 ± 0.08	AAA	11.84
773	203326.33+411238.4	20332633+4112388	0.24	14.42 ± 0.03	13.38 ± 0.03	12.91 ± 0.03	AAA	8.89
774	203326.33+410819.1	20332629+4108174	1.97	15.51 ± 0.05	14.90 ± 0.07	14.83 ± 0.14	AAB	10.07
775	203326.44+411048.5	–	–	–	–	–	–	–
776	203326.55+411503.6	20332654+4115041	0.45	16.18 ± 0.09	14.60 ± 0.05	13.46 ± 0.04	AAA	3.96
777	203326.60+411547.3	20332661+4115475	0.12	14.05 ± 0.04	12.89 ± 0.03	12.40 ± 0.02	AAA	5.47
778	203326.68+411555.4	20332665+4115560	0.69	16.61 ± 0.14	15.22 ± 0.12	14.72 ± 0.13	BBB	N/A
779	203326.74+411059.3	20332674+4110595	0.11	8.97 ± 0.02	8.43 ± 0.01	8.16 ± 0.01	AAA	9.77
780	203326.81+412046.9	20332679+4120471	0.33	15.75 ± 0.07	14.64 ± 0.06	14.50 ± 0.11	AAB	N/A

Table 2. continued.

N_x	X-ray - 2MASS counterpart		Off.	2MASS photometry				A_v
#	CXOAC J+	2MASS J+	(″)	J	H	K_s	Ph. qual	(mag)
781	203326.79+411217.6	–	–	–	–	–	–	–
782	203326.85+411741.3	20332686+4117415	0.11	15.16 ± 0.04	13.95 ± 0.03	13.40 ± 0.04	AAA	18.25
783	203326.87+411319.1	20332685+4113199	0.65	16.62 ± 0.14	14.93 ± 0.07	14.25 ± 0.08	BAA	5.25
784	203327.11+411822.5	20332713+4118225	0.24	14.17 ± 0.02	13.09 ± 0.02	12.63 ± 0.02	AAA	N/A
785	203327.19+411709.8	20332723+4117106	0.71	13.02 ± 0.02	12.29 ± 0.03	11.91 ± 0.02	AAA	8.41
786	203327.23+412008.8	20332724+4120088	0.23	13.97 ± 0.03	13.00 ± 0.03	12.59 ± 0.03	AAA	9.71
787	203327.30+411525.6	20332733+4115254	0.55	16.63 ± 0.16	15.11 ± 0.10	14.43 ± 0.12	CAB	5.61
788	203327.31+410751.3	20332731+4107534	1.88	16.63 ± 0.14	15.33 ± 0.10	15.05 ± 0.16	BAC	8.57
789	203327.45+411626.5	20332742+4116263	0.68	16.65 ± 0.14	15.40 ± 0.10	14.96	BAU	N/A
790	203327.59+411507.0	20332761+4115064	0.86	16.23 ± 0.13	14.64 ± 0.08	13.82 ± 0.06	BAA	N/A
791	203327.61+412015.7	20332754+4120158	1.22	14.37	13.47 ± 0.04	13.04	UAU	0.67
792	203327.91+411509.4	20332793+4115097	0.12	15.89 ± 0.07	14.84 ± 0.07	14.31 ± 0.09	AAA	7.13
793	203328.32+412126.7	20332828+4121276	0.95	16.55	15.14 ± 0.08	14.64	UAU	N/A
794	203328.32+410933.9	20332833+4109341	0.11	14.18 ± 0.03	12.81 ± 0.03	12.14 ± 0.02	AAA	N/A
795	203328.36+411501.3	20332836+4115015	0.23	15.71 ± 0.06	14.43 ± 0.04	13.85 ± 0.06	AAA	7.30
796	203328.43+411937.1	20332845+4119373	0.23	14.00 ± 0.03	12.96 ± 0.02	12.59 ± 0.02	AAA	13.34
797	203328.49+411915.4	20332851+4119152	0.43	15.19 ± 0.05	14.04 ± 0.03	13.47 ± 0.05	AAA	8.11
798	203328.54+410716.7	20332853+4107172	0.34	15.38 ± 0.05	13.94 ± 0.04	13.48 ± 0.04	AAA	N/A
799	203328.58+411409.4	20332848+4114097	1.76	14.64 ± 0.04	12.80 ± 0.03	12.01 ± 0.02	AAA	11.67
800	203328.74+411611.3	–	–	–	–	–	–	–
801	203328.74+411424.0	20332876+4114240	0.28	15.04 ± 0.05	13.65 ± 0.05	13.22 ± 0.04	AAA	4.58
802	203329.20+411425.8	20332917+4114263	0.65	15.19 ± 0.05	14.14 ± 0.05	13.75 ± 0.06	AAA	3.28
803	203329.26+412138.2	20332922+4121387	0.81	15.63 ± 0.06	14.56 ± 0.06	14.03 ± 0.07	AAA	N/A
804	203329.31+411605.8	20332933+4116058	0.31	16.64 ± 0.14	15.38 ± 0.10	14.38	BAU	N/A
805	203329.41+411806.2	20332944+4118062	0.39	17.06 ± 0.22	15.52 ± 0.11	15.81	CBU	5.57
806	203329.45+412034.8	20332948+4120344	0.68	13.07 ± 0.02	12.61 ± 0.02	12.32 ± 0.02	AAA	6.68
807	203329.48+411858.7	20332950+4118589	0.12	15.90 ± 0.07	14.64 ± 0.07	14.13 ± 0.08	AAA	15.80
808	203329.57+412005.5	20332962+4120060	0.75	14.57 ± 0.05	13.36 ± 0.03	12.85 ± 0.03	AAA	N/A
809	203329.72+411557.2	20332973+4115577	0.24	14.10 ± 0.04	12.98 ± 0.03	12.54 ± 0.03	AAA	N/A
810	203329.95+411218.5	20332994+4112185	0.39	15.65 ± 0.06	14.60 ± 0.06	14.17 ± 0.07	AAA	7.13
811	203330.25+411608.5	20333027+4116087	0.22	15.29 ± 0.05	14.00 ± 0.04	13.51 ± 0.04	AAA	N/A
812	203330.32+411406.2	20333036+4114064	0.34	13.91 ± 0.02	12.97 ± 0.02	12.49 ± 0.03	AAA	N/A
813	203330.47+412016.4	20333052+4120171	0.68	11.03 ± 0.02	10.53 ± 0.01	10.30 ± 0.01	AAA	6.90
814	203330.47+410935.7	20333043+4109368	1.19	14.88 ± 0.04	13.86 ± 0.04	13.44 ± 0.04	AAA	7.24
815	203330.51+411722.0	20333053+4117219	0.37	15.14 ± 0.04	13.89 ± 0.03	13.31 ± 0.04	AAA	12.21
816	203330.57+411012.0	20333061+4110119	0.53	15.27 ± 0.04	14.03 ± 0.04	13.49 ± 0.04	AAA	N/A
817	203330.74+411522.7	20333078+4115226	0.56	6.49 ± 0.02	5.89 ± 0.01	5.54 ± 0.01	AAA	N/A
818	203331.06+412025.5	20333104+4120258	0.45	15.09 ± 0.05	14.01 ± 0.04	13.56 ± 0.05	AAA	N/A
819	203331.14+411317.4	20333108+4113180	0.98	15.75	15.49 ± 0.11	14.25	UAU	N/A
820	203331.20+411610.4	20333122+4116105	0.25	14.97 ± 0.05	14.07 ± 0.07	13.63 ± 0.05	AAA	17.86
821	203331.27+412131.4	20333147+4121311	2.90	15.19 ± 0.05	14.16 ± 0.04	13.66 ± 0.05	AAA	8.24
822	203331.33+411602.8	20333136+4116028	0.54	15.89 ± 0.08	14.73 ± 0.06	14.31 ± 0.09	AAA	8.51
823	203331.36+411609.6	–	–	–	–	–	–	–
824	203331.36+411529.3	–	–	–	–	–	–	–
825	203331.35+410912.5	20333137+4109123	0.55	15.21 ± 0.05	14.12 ± 0.04	13.64 ± 0.05	AAA	15.63
826	203331.35+410912.6	20333137+4109123	0.55	15.21 ± 0.05	14.12 ± 0.04	13.64 ± 0.05	AAA	N/A
827	203331.72+411532.9	20333169+4115336	0.80	15.14 ± 0.11	14.15 ± 0.10	13.78 ± 0.07	AAA	N/A
828	203331.77+412047.2	20333177+4120473	0.17	13.27 ± 0.03	12.36 ± 0.04	12.04 ± 0.03	AAA	8.16
829	203331.87+411003.3	20333190+4110041	0.62	15.99 ± 0.08	14.60 ± 0.05	14.11 ± 0.07	AAA	14.06
830	203331.91+411642.9	20333194+4116432	0.45	15.30	14.17 ± 0.08	13.11	UAU	6.22
831	203332.11+412122.2	20333215+4121233	1.02	12.94 ± 0.02	12.28 ± 0.02	11.95 ± 0.02	AAA	N/A
832	203332.11+412019.7	–	–	–	–	–	–	–
833	203332.05+410558.7	–	–	–	–	–	–	–
834	203332.16+411801.9	20333215+4118023	0.28	16.87	15.69	14.95 ± 0.16	UUC	N/A
835	203332.28+411639.2	20333229+4116397	0.27	15.40	14.50 ± 0.06	13.39	UAU	0.08
836	203332.38+411155.8	20333229+4111566	1.56	15.36	14.64 ± 0.08	14.01 ± 0.08	UAA	24.08
837	203332.47+411543.1	20333248+4115434	0.06	15.19 ± 0.04	13.98 ± 0.03	13.37 ± 0.04	AAA	4.33
838	203332.68+411100.1	20333265+4110596	0.89	15.82 ± 0.07	14.22	13.73	AUU	N/A
839	203332.74+411251.8	20333271+4112522	0.58	16.26 ± 0.09	14.74 ± 0.06	13.97 ± 0.07	AAA	N/A
840	203332.81+410519.6	20333278+4105202	0.58	12.93 ± 0.03	12.16 ± 0.02	11.73 ± 0.02	EAA	N/A
841	203332.92+412147.2	–	–	–	–	–	–	–
842	203332.93+411040.4	20333293+4110405	0.24	15.70 ± 0.06	14.42 ± 0.05	13.91 ± 0.06	AAA	7.27
843	203333.01+411428.5	20333304+4114287	0.22	14.68 ± 0.04	13.56 ± 0.03	13.09 ± 0.04	AAA	N/A
844	203333.09+411730.0	20333308+4117298	0.46	15.90 ± 0.07	14.61 ± 0.05	14.27 ± 0.08	AAA	0.20
845	203333.09+411132.4	20333294+4111321	2.36	15.33 ± 0.06	14.30 ± 0.06	13.78 ± 0.06	AAA	8.03

Table 2. continued.

N_x	X-ray - 2MASS counterpart		Off.	2MASS photometry				A_v
#	CXOAC J+	2MASS J+	(″)	J	H	K_s	Ph. qual	(mag)
846	203333.43+411917.2	20333351+4119166	1.41	15.38 ± 0.05	14.52 ± 0.05	14.02 ± 0.07	AAA	11.25
847	203333.44+410803.1	20333343+4108031	0.31	15.50 ± 0.05	14.12 ± 0.04	13.73 ± 0.05	AAA	7.78
848	203333.72+412152.1	20333357+4121521	2.43	11.94 ± 0.02	11.45 ± 0.02	11.19 ± 0.01	AAA	5.48
849	203333.78+411937.0	20333393+4119382	2.40	10.27 ± 0.02	9.66 ± 0.01	9.42 ± 0.01	AEE	10.14
850	203333.96+411129.5	20333399+4111292	0.61	16.49 ± 0.11	14.99 ± 0.07	14.67 ± 0.12	BAB	N/A
851	203334.06+412145.9	–	–	–	–	–	–	–
852	203334.26+411851.4	20333427+4118520	0.36	15.90	15.00 ± 0.12	13.60	UBU	7.30
853	203334.27+411422.2	20333429+4114222	0.30	15.97 ± 0.07	14.84 ± 0.06	14.33 ± 0.09	AAA	N/A
854	203334.53+412136.6	20333456+4121372	0.53	11.59 ± 0.02	11.18 ± 0.01	10.93 ± 0.01	AAA	1.31
855	203334.55+411622.2	–	–	–	–	–	–	–
856	203334.62+412039.6	20333479+4120382	2.92	15.27 ± 0.05	14.08 ± 0.04	13.66 ± 0.05	AAA	13.89
857	203334.74+412050.5	20333478+4120502	0.77	16.62	15.65 ± 0.12	14.92 ± 0.15	UBB	N/A
858	203334.74+411147.7	20333474+4111481	0.15	15.64 ± 0.05	14.64 ± 0.05	14.13 ± 0.07	AAA	6.78
859	203334.79+411456.1	20333471+4114574	1.79	15.93 ± 0.08	14.85 ± 0.06	14.13 ± 0.08	AAA	N/A
860	203334.80+410748.7	20333481+4107473	1.68	15.99 ± 0.08	14.84 ± 0.07	14.27 ± 0.09	AAA	5.73
861	203334.92+410857.5	20333494+4108577	0.11	13.75 ± 0.02	13.14 ± 0.02	12.82 ± 0.03	AAA	7.76
862	203335.05+411612.2	–	–	–	–	–	–	–
863	203335.22+411119.2	20333523+4111195	0.11	15.45 ± 0.07	14.19 ± 0.08	13.69 ± 0.05	AAA	7.81
864	203335.33+412059.5	–	–	–	–	–	–	–
865	203335.33+411821.8	20333535+4118221	0.24	16.11 ± 0.10	15.05 ± 0.09	14.64 ± 0.12	AAB	6.17
866	203335.28+410714.0	–	–	–	–	–	–	–
867	203335.57+411659.0	20333541+4116584	2.69	12.94 ± 0.02	12.24 ± 0.02	11.88 ± 0.02	AAA	N/A
868	203335.61+411556.4	–	–	–	–	–	–	–
869	203335.66+411205.9	20333572+4112068	1.13	16.76 ± 0.16	15.58 ± 0.13	15.19 ± 0.18	CBC	7.11
870	203335.66+410630.5	20333565+4106303	0.54	15.34 ± 0.06	14.21 ± 0.05	13.67 ± 0.05	AAA	7.18
871	203335.80+411519.5	20333584+4115192	0.67	16.35	15.60 ± 0.14	14.39	UBU	5.55
872	203335.87+410649.5	20333585+4106506	0.97	15.78 ± 0.07	14.57 ± 0.05	14.23 ± 0.08	AAA	33.68
873	203336.00+411834.5	20333602+4118344	0.29	15.93 ± 0.08	14.55 ± 0.05	14.14 ± 0.08	AAA	N/A
874	203336.25+410812.7	20333626+4108116	1.37	13.98 ± 0.03	12.79 ± 0.03	12.40 ± 0.03	AAA	7.59
875	203336.34+412050.7	20333638+4120503	0.79	14.85 ± 0.03	13.48 ± 0.03	12.82 ± 0.03	AAA	4.73
876	203336.29+411034.3	20333631+4110345	0.22	13.12 ± 0.02	12.52 ± 0.01	12.20 ± 0.02	AAA	1.34
877	203336.40+411818.4	20333640+4118189	0.37	15.82 ± 0.07	14.72 ± 0.07	14.31 ± 0.09	AAA	N/A
878	203336.67+411543.1	20333669+4115429	0.41	15.58 ± 0.06	14.21 ± 0.05	13.58 ± 0.05	AAA	7.51
879	203336.64+410846.5	–	–	–	–	–	–	–
880	203336.69+411509.4	20333682+4115096	1.86	16.13	14.95 ± 0.09	14.04 ± 0.07	UAA	N/A
881	203336.98+411610.9	20333700+4116113	0.14	8.68 ± 0.01	8.17 ± 0.01	7.93 ± 0.01	AAA	6.14
882	203337.00+411157.8	20333705+4111580	0.77	16.30 ± 0.10	15.28 ± 0.09	14.77 ± 0.12	AAB	N/A
883	203337.41+412028.9	–	–	–	–	–	–	–
884	203337.47+412101.6	–	–	–	–	–	–	–
885	203337.58+412048.6	20333755+4120490	0.48	16.47	15.31 ± 0.11	14.78 ± 0.13	UAB	N/A
886	203337.80+411640.3	20333783+4116403	0.50	13.94 ± 0.02	12.82 ± 0.02	12.34 ± 0.02	AAA	7.15
887	203338.01+412036.0	20333815+4120355	2.20	16.01 ± 0.08	14.92 ± 0.06	14.48 ± 0.10	AAA	N/A
888	203338.24+411833.4	20333823+4118334	0.29	15.96 ± 0.08	14.87 ± 0.06	14.30 ± 0.09	AAA	N/A
889	203338.37+411620.4	20333840+4116200	0.69	12.91 ± 0.02	12.55 ± 0.02	12.47 ± 0.02	AAA	N/A
890	203338.56+411914.3	20333860+4119140	0.80	14.29 ± 0.10	13.69 ± 0.13	11.65	EBU	7.26
891	203338.62+412012.2	20333862+4120119	0.56	15.94 ± 0.08	14.70 ± 0.06	14.35 ± 0.09	AAA	2.60
892	203338.67+411234.0	20333868+4112334	0.81	15.88 ± 0.07	14.77 ± 0.06	14.32 ± 0.09	AAA	N/A
893	203338.98+411933.4	20333906+4119331	1.11	11.22	12.52 ± 0.06	10.70	UAU	11.86
894	203339.05+411435.8	20333903+4114362	0.46	15.35	14.10 ± 0.05	13.61 ± 0.05	UAA	23.71
895	203339.07+411925.7	20333910+4119258	0.47	7.23 ± 0.01	6.74 ± 0.01	6.48 ± 0.01	AAA	4.26
896	203339.02+410833.8	20333902+4108340	0.03	14.24 ± 0.03	12.90 ± 0.02	12.19 ± 0.02	AAA	6.74
897	203339.15+411359.3	20333920+4113586	1.12	15.47 ± 0.05	14.45 ± 0.05	13.83 ± 0.05	AAA	8.40
898	203339.22+410648.2	20333928+4106470	1.59	15.01 ± 0.05	13.56 ± 0.05	12.96 ± 0.04	AAA	10.66
899	203339.30+411558.5	–	–	–	–	–	–	–
900	203339.52+411513.3	20333955+4115133	0.40	16.05	15.34	14.81 ± 0.14	UUB	7.92
901	203339.47+410634.2	20333954+4106334	1.37	16.80 ± 0.17	15.63 ± 0.13	15.15	CBU	3.50
902	203339.64+411923.3	–	–	–	–	–	–	–
903	203339.64+411706.5	20333967+4117066	0.34	12.42 ± 0.02	11.69 ± 0.02	11.30 ± 0.01	AAA	N/A
904	203339.71+411524.9	–	–	–	–	–	–	–
905	203339.79+411641.1	20333986+4116411	1.01	13.36 ± 0.04	12.49 ± 0.04	12.04 ± 0.03	AAA	6.15
906	203339.90+411532.8	20333987+4115328	0.72	15.44 ± 0.06	13.71	13.19	AUU	9.65
907	203340.42+411445.7	–	–	–	–	–	–	–
908	203340.59+411630.3	–	–	–	–	–	–	–
909	203340.66+411442.8	20334060+4114438	1.28	12.27	11.44	10.93 ± 0.03	UUA	N/A
910	203340.74+411931.0	20334077+4119308	0.53	14.97 ± 0.08	13.75 ± 0.04	13.25 ± 0.05	AAA	9.69

Table 2. continued.

N_x	X-ray - 2MASS counterpart		Off.	2MASS photometry				A_v
#	CXOACJ+	2MASS J+	(″)	J	H	K_s	Ph. qual	(mag)
911	203340.74+411415.2	–	–	–	–	–	–	–
912	203340.91+410935.5	20334092+4109362	0.50	16.13 ± 0.09	14.90 ± 0.09	14.24 ± 0.09	AAA	2.09
913	203341.03+412115.5	–	–	–	–	–	–	–
914	203340.97+410849.8	–	–	–	–	–	–	–
915	203341.19+411432.5	20334106+4114334	2.09	16.18 ± 0.11	14.74 ± 0.08	13.90 ± 0.08	BAA	15.77
916	203341.27+411455.0	20334124+4114540	1.28	16.20 ± 0.14	14.60 ± 0.08	13.13	BAU	14.53
917	203341.27+411454.9	20334124+4114540	1.28	16.20 ± 0.14	14.60 ± 0.08	13.13	BAU	N/A
918	203341.38+411513.1	20334143+4115130	0.83	16.19 ± 0.09	14.26 ± 0.03	12.87 ± 0.03	AAA	6.13
919	203341.35+410732.0	20334128+4107342	2.30	15.14 ± 0.04	14.60 ± 0.06	14.45 ± 0.12	AAB	7.21
920	203341.52+411858.8	20334158+4118590	0.77	12.98 ± 0.02	12.32 ± 0.02	11.94 ± 0.02	AAA	6.32
921	203341.50+411321.9	20334151+4113225	0.39	15.10 ± 0.07	13.62 ± 0.18	12.65 ± 0.03	ACE	5.44
922	203341.60+411234.5	–	–	–	–	–	–	–
923	203341.84+411019.9	–	–	–	–	–	–	–
924	203341.94+412116.1	–	–	–	–	–	–	–
925	203341.93+411128.7	–	–	–	–	–	–	–
926	203341.99+411055.1	20334204+4110549	0.80	16.36 ± 0.12	15.24 ± 0.10	14.53 ± 0.11	BAB	N/A
927	203342.18+410753.8	–	–	–	–	–	–	–
928	203342.25+411503.2	20334228+4115034	0.33	13.87 ± 0.03	12.85 ± 0.04	12.33 ± 0.03	AAA	6.75
929	203342.28+411145.8	20334234+4111456	0.75	9.89 ± 0.02	9.38 ± 0.02	9.10 ± 0.01	AAA	N/A
930	203342.52+411456.4	20334254+4114566	0.11	10.74 ± 0.02	10.23 ± 0.02	9.89 ± 0.01	AAA	5.98
931	203342.68+411734.5	20334268+4117350	0.34	12.52 ± 0.02	11.99 ± 0.02	11.59 ± 0.01	AAA	7.27
932	203342.97+411237.0	20334307+4112376	1.37	14.66 ± 0.04	13.88 ± 0.05	13.27	AAU	3.08
933	203343.00+411504.3	–	–	–	–	–	–	–
934	203343.26+411033.6	20334329+4110343	0.62	14.95 ± 0.04	13.64 ± 0.02	13.19 ± 0.04	AAA	4.84
935	203343.47+411718.3	20334347+4117185	0.12	15.76 ± 0.07	14.54 ± 0.05	13.98 ± 0.07	AAA	N/A
936	203343.47+411101.1	20334333+4111005	2.32	13.86 ± 0.03	13.02 ± 0.04	12.53 ± 0.03	AAA	6.73
937	203343.66+411002.3	20334369+4110032	0.72	15.72 ± 0.07	14.43 ± 0.04	13.97 ± 0.06	AAA	N/A
938	203343.80+410917.7	20334383+4109185	0.73	14.13 ± 0.02	12.97 ± 0.02	12.39 ± 0.02	AAA	3.80
939	203343.98+411611.9	–	–	–	–	–	–	–
940	203344.14+411939.2	20334414+4119396	0.19	15.77 ± 0.07	14.50 ± 0.05	13.72 ± 0.05	AAA	4.61
941	203344.34+410522.0	20334435+4105199	2.35	11.97 ± 0.01	11.34 ± 0.01	10.95 ± 0.01	AAA	N/A
942	203344.46+411052.5	20334448+4110529	0.18	13.27 ± 0.02	12.33 ± 0.03	11.91 ± 0.02	AAA	0.27
943	203344.58+411444.6	–	–	–	–	–	–	–
944	203344.53+410821.3	20334448+4108218	0.93	15.60 ± 0.06	14.48 ± 0.07	14.07 ± 0.08	AAA	N/A
945	203344.61+410906.2	20334461+4109067	0.29	14.51 ± 0.03	13.28 ± 0.02	12.92 ± 0.03	AAA	16.69
946	203344.69+411419.8	–	–	–	–	–	–	–
947	203344.67+411002.2	20334465+4110025	0.45	15.95	14.95 ± 0.07	14.25	UAU	6.73
948	203344.88+411344.6	20334492+4113445	0.65	15.75	14.49	14.23 ± 0.09	UUA	N/A
949	203344.91+411331.4	20334492+4113321	0.44	14.63 ± 0.03	13.45 ± 0.03	12.94 ± 0.03	AAA	5.96
950	203345.00+412114.7	20334503+4121151	0.46	13.55 ± 0.02	12.70 ± 0.02	12.28 ± 0.02	AAA	N/A
951	203345.06+412132.6	20334504+4121326	0.48	14.47 ± 0.03	13.19 ± 0.03	12.40 ± 0.03	AAA	8.84
952	203345.29+411503.8	–	–	–	–	–	–	–
953	203345.38+411731.2	20334542+4117310	0.71	14.91 ± 0.04	13.77 ± 0.05	13.16 ± 0.04	AAA	12.71
954	203345.41+411621.7	20334543+4116214	0.57	16.29 ± 0.10	15.07 ± 0.07	14.47 ± 0.10	AAA	1.78
955	203345.40+411430.7	20334544+4114301	0.96	16.31	14.81 ± 0.09	13.16 ± 0.05	UAA	N/A
956	203345.47+412018.2	20334546+4120178	0.65	14.78 ± 0.04	13.70 ± 0.04	13.12 ± 0.04	AAA	9.19
957	203345.38+410936.4	20334544+4109382	1.74	12.60 ± 0.02	11.86 ± 0.02	11.57 ± 0.02	AAA	5.31
958	203345.64+411400.7	20334563+4114006	0.42	15.33 ± 0.05	14.17 ± 0.04	13.57 ± 0.05	AAA	4.61
959	203345.84+411726.1	–	–	–	–	–	–	–
960	203345.95+410850.5	20334599+4108500	0.83	13.87 ± 0.03	12.96 ± 0.03	12.57 ± 0.03	AAA	12.38
961	203346.31+411629.9	20334635+4116303	0.49	16.00 ± 0.09	14.93 ± 0.06	14.49 ± 0.10	AAA	N/A
962	203346.47+411609.9	20334650+4116102	0.23	15.90 ± 0.08	14.73 ± 0.06	14.04 ± 0.07	AAA	8.57
963	203346.50+411812.9	20334649+4118136	0.48	15.15 ± 0.04	13.93 ± 0.04	13.54 ± 0.05	AAA	3.23
964	203346.83+411354.7	–	–	–	–	–	–	–
965	203346.79+410801.0	20334680+4108019	0.66	10.15 ± 0.01	9.68 ± 0.01	9.40 ± 0.01	AAA	N/A
966	203346.84+411048.2	20334672+4110495	2.16	16.00 ± 0.08	14.65 ± 0.06	14.36 ± 0.09	AAA	N/A
967	203346.97+411146.3	20334704+4111455	1.50	14.91 ± 0.04	13.63 ± 0.03	13.17 ± 0.04	AAA	11.29
968	203347.04+412005.6	20334710+4120061	0.81	16.31 ± 0.11	15.28 ± 0.12	14.65 ± 0.13	BBB	2.10
969	203347.04+410952.6	20334709+4109524	0.81	15.11	13.82 ± 0.03	13.38 ± 0.04	UAA	N/A
970	203347.20+411316.7	20334713+4113165	1.26	14.26 ± 0.04	13.73 ± 0.04	13.57 ± 0.06	AAA	5.98
971	203347.77+412040.9	20334783+4120415	0.83	7.99 ± 0.01	7.49 ± 0.02	7.21 ± 0.01	AAA	N/A
972	203347.92+411537.5	20334794+4115382	0.45	15.40 ± 0.05	14.20 ± 0.04	13.79 ± 0.05	AAA	N/A
973	203347.98+411910.1	20334804+4119105	0.67	15.50 ± 0.04	14.27 ± 0.04	13.75 ± 0.06	AAA	9.68
974	203348.10+411842.3	–	–	–	–	–	–	–
975	203348.20+411346.2	–	–	–	–	–	–	–

Table 2. continued.

N_x	X-ray - 2MASS counterpart		Off.	2MASS photometry				A_v
#	CXOAC J+	2MASS J+	(″)	J	H	K_s	Ph. qual	(mag)
976	203348.24+411032.8	20334822+4110330	0.33	10.05 ± 0.01	9.87 ± 0.01	9.79 ± 0.01	AAA	4.01
977	203348.63+411824.4	20334868+4118243	0.83	14.86 ± 0.07	13.76 ± 0.07	13.36 ± 0.05	AAA	10.28
978	203348.84+412108.0	20334894+4121071	1.82	15.54 ± 0.05	14.25 ± 0.04	13.72 ± 0.06	AAA	N/A
979	203348.87+411940.2	20334884+4119406	0.57	10.03 ± 0.02	9.62 ± 0.02	9.37 ± 0.01	AAA	7.28
980	203348.91+411410.4	20334899+4114089	2.02	12.63 ± 0.02	11.74 ± 0.02	11.16 ± 0.01	AAA	16.15
981	203349.31+411634.3	20334930+4116358	1.36	16.19 ± 0.09	14.66 ± 0.06	13.48 ± 0.05	AAA	8.88
982	203349.32+411021.8	20334944+4110220	1.53	15.55 ± 0.06	14.13 ± 0.06	13.68 ± 0.06	AAA	N/A
983	203349.51+411148.6	20334948+4111480	1.07	15.92 ± 0.07	14.68 ± 0.06	14.21 ± 0.08	AAA	7.44
984	203350.36+411416.3	20335035+4114170	0.50	15.05 ± 0.04	14.07 ± 0.03	13.64 ± 0.05	AAA	N/A
985	203350.47+411803.1	20335050+4118027	0.73	15.86 ± 0.07	14.83 ± 0.07	14.29 ± 0.09	AAA	N/A
986	203350.82+411616.1	20335078+4116149	1.49	13.13 ± 0.03	12.35 ± 0.04	11.93 ± 0.02	AAA	4.23
987	203350.79+410857.4	20335081+4108567	0.88	16.19 ± 0.11	15.08 ± 0.10	14.56 ± 0.13	BAB	3.47
988	203351.21+412029.2	20335127+4120288	1.06	15.54 ± 0.05	14.42 ± 0.04	13.97 ± 0.06	AAA	8.70
989	203351.48+411358.4	20335151+4113584	0.27	15.45 ± 0.07	14.41 ± 0.07	14.09 ± 0.09	AAA	N/A
990	203351.65+411539.0	20335172+4115397	1.09	16.75 ± 0.16	15.65 ± 0.12	14.89 ± 0.15	CBB	5.47
991	203352.84+411558.8	20335287+4115590	0.44	16.05 ± 0.09	14.87 ± 0.06	14.25 ± 0.08	AAA	7.44
992	203353.10+411118.8	20335310+4111193	0.30	13.82 ± 0.02	13.24 ± 0.02	13.07 ± 0.03	AAA	5.81
993	203353.58+411754.9	20335360+4117560	0.89	14.58 ± 0.03	13.45 ± 0.04	12.90 ± 0.04	AAA	10.46
994	203353.89+412004.0	20335381+4120042	1.32	15.11 ± 0.05	14.30 ± 0.04	13.80 ± 0.06	AAA	7.20
995	203354.19+411340.1	20335426+4113397	1.10	15.27	14.26 ± 0.05	13.64 ± 0.05	UAA	2.13
996	203355.18+411419.7	20335519+4114202	0.27	13.17 ± 0.03	12.73 ± 0.02	12.50 ± 0.03	AAA	N/A
997	203355.54+411851.4	20335552+4118514	0.37	14.09 ± 0.10	13.03 ± 0.07	12.58 ± 0.04	AAA	N/A
998	203356.32+412038.9	20335633+4120391	0.11	15.18 ± 0.05	14.08 ± 0.06	13.44 ± 0.05	AAA	N/A
999	203357.91+411803.1	–	–	–	–	–	–	–
1000	203358.41+412055.7	20335834+4120562	1.23	13.62 ± 0.03	12.67 ± 0.03	12.30	AAU	N/A
1001	203359.65+411737.2	20335952+4117354	2.80	8.53 ± 0.01	8.14 ± 0.03	7.89 ± 0.01	AAA	0.58
1002	203401.23+412010.4	20340128+4120106	0.66	13.18 ± 0.02	12.59 ± 0.02	12.31 ± 0.02	AAA	N/A
1003	203401.44+411905.4	20340141+4119058	0.56	14.78 ± 0.04	13.66 ± 0.04	13.17 ± 0.05	AAA	7.69

Table 3. X-ray source spectroscopy.

N_x #	NetCnts (ph.)	$\log(N_H)$ (cm^{-2})	kT (keV)	log(EM) (cm^{-3})	Stat. (χ^2_ν)	d.o.f.
1	67	22.13 ± 0.26	9.99	53.70	0.34	17
2	72	21.05 ± 0.34	0.74 ± 0.12	53.40	1.54	17
3	35	21.75 ± 0.03	9.99	53.40	0.38	9
5	55	22.15 ± 0.27	6.05 ± 8.52	53.40	0.81	14
6	216	22.13 ± 0.68	5.52 ± 3.06	54.10	0.96	19
7	49	21.86 ± 0.04	9.99	53.40	0.78	15
8	33	21.70 ± 0.08	9.99	53.40	0.51	9
9	64	21.44 ± 0.03	9.99	53.40	0.76	14
10	50	21.60 ± 0.10	1.04 ± 0.23	53.40	1.00	12
12	99	22.14 ± 0.47	2.19 ± 0.91	53.88	1.02	24
13	44	22.42 ± 0.29	3.74 ± 3.87	53.70	1.20	10
14	75	22.51 ± 0.30	9.99	53.70	1.10	19
15	60	21.90 ± 0.24	6.85 ± 8.19	53.40	0.66	14
16	30	22.53 ± 0.10	2.72 ± 2.67	53.70	0.82	7
17	3173	22.16 ± 0.25	1.34 ± 0.64	55.65	1.57	252
19	25	22.48 ± 0.15	3.43 ± 4.19	53.40	0.56	6
20	49	22.26 ± 0.30	3.04 ± 1.86	53.70	0.72	11
22	34	21.83 ± 0.03	3.15 ± 3.35	53.40	1.24	7
23	50	21.73 ± 0.11	6.04 ± 6.96	53.40	0.96	12
24	26	21.98 ± 0.05	9.99	53.40	0.56	6
25	27	22.59 ± 0.39	0.69 ± 0.28	54.51	0.85	5
26	39	21.63 ± 0.03	5.76 ± 8.14	52.40	0.93	8
27	70	22.27 ± 0.51	1.85 ± 0.63	53.88	0.90	15
28	43	22.27 ± 0.27	2.16 ± 1.33	53.40	1.58	10
29	33	22.20 ± 0.75	9.99	52.40	1.06	6
30	41	21.96 ± 0.28	1.04 ± 0.43	53.40	1.04	10
31	26	22.13 ± 0.35	0.54 ± 0.45	54.00	0.35	5
32	26	22.74 ± 1.22	9.99	52.40	0.42	4
33	232	21.82 ± 0.60	4.59 ± 1.58	54.10	0.79	20
34	74	22.16 ± 0.41	2.01 ± 0.78	53.70	1.23	16
35	46	21.70 ± 0.16	2.79 ± 1.84	53.40	0.87	9
36	45	21.19 ± 0.18	1.37 ± 0.36	53.40	0.52	8
37	55	22.27 ± 0.32	4.76 ± 4.84	53.40	0.74	12
38	29	22.42 ± 0.25	1.27 ± 0.67	53.88	0.49	6
39	91	21.79 ± 0.32	9.99	53.70	0.62	19
40	109	21.84 ± 0.35	2.10 ± 0.68	53.70	0.86	25
41	31	22.34 ± 0.28	1.22 ± 0.61	53.70	0.93	7
42	23	21.59 ± 0.30	9.99	52.40	0.75	7
43	53	22.24 ± 0.26	8.61	53.40	0.74	11
44	83	22.02 ± 0.28	1.63 ± 0.66	53.88	0.66	22
46	20	22.46 ± 0.19	1.24 ± 0.84	53.70	1.19	3
47	42	22.17 ± 0.28	1.88 ± 0.90	53.70	0.46	10
48	45	21.74 ± 0.16	5.09 ± 4.48	53.40	0.57	10
49	53	22.47 ± 0.45	2.05 ± 0.99	53.88	1.25	11
50	78	22.00 ± 0.33	1.23 ± 0.38	53.88	0.90	23
51	32	22.06 ± 0.01	8.62	52.40	1.48	7
52	156	22.39 ± 0.71	3.02 ± 0.99	54.25	1.00	19
53	43	22.11 ± 0.39	1.14 ± 0.38	53.70	0.48	10
54	73	21.85 ± 0.19	9.99	53.40	0.54	18
55	33	22.11 ± 0.29	1.39 ± 0.63	53.40	1.32	5
56	62	22.44 ± 0.53	1.48 ± 0.42	54.18	0.39	14
57	30	22.61 ± 0.39	1.40 ± 0.51	54.10	0.25	5
58	49	22.08 ± 0.27	2.73 ± 1.60	53.40	0.53	11
60	14913	22.30 ± 0.82	1.24 ± 0.19	56.49	1.40	141
61	40	22.12 ± 0.24	4.80 ± 5.04	53.40	0.53	8
62	23	21.97 ± 0.04	4.00 ± 5.57	52.40	1.05	5
63	24	21.78 ± 0.14	9.99	52.40	1.07	5
64	77	22.03 ± 0.36	9.99	53.40	0.72	17
67	40	22.02 ± 0.15	3.92 ± 3.64	53.40	1.06	10
68	27	22.52 ± 0.39	0.90 ± 0.33	54.10	0.91	4
69	22	22.22 ± 0.16	3.29 ± 3.19	53.40	0.30	3
71	68	22.07 ± 0.32	1.59 ± 0.60	53.88	0.60	15
72	107	21.75 ± 0.38	3.16 ± 1.29	53.70	1.50	12
73	138	22.08 ± 0.45	2.72 ± 1.16	54.00	1.33	18
74	89	22.26 ± 0.59	1.43 ± 0.35	54.00	1.01	19

Table 3. continued.

N_x #	NetCnts (ph.)	$\log(N_H)$ (cm^{-2})	kT (keV)	log(EM) (cm^{-3})	Stat. (χ^2_ν)	d.o.f.
76	38	21.98 ± 0.11	3.15 ± 3.19	53.40	0.81	10
77	38	22.12 ± 0.22	2.11 ± 1.27	53.40	1.04	8
81	47	22.14 ± 0.32	2.72 ± 1.68	53.40	0.67	10
82	27	21.20 ± 0.29	9.99	52.40	0.20	4
84	22	22.65 ± 0.20	0.54 ± 0.50	54.85	0.97	3
85	29	22.30 ± 0.35	1.15 ± 0.44	53.70	0.40	5
87	52	22.16 ± 0.25	5.97 ± 9.26	53.40	1.00	13
88	37	22.29 ± 0.27	4.49 ± 5.18	53.40	0.60	7
92	21	22.86 ± 1.38	9.99	52.40	0.64	3
93	45	22.11 ± 0.33	2.53 ± 1.40	54.00	0.41	8
94	80	21.78 ± 0.16	2.66 ± 1.08	53.40	0.68	21
97	22	21.74 ± 0.07	6.33	52.40	0.97	3
100	28	22.35 ± 0.29	1.36 ± 0.67	53.70	0.20	4
102	37	22.18 ± 0.26	2.72 ± 1.66	53.40	0.34	7
104	77	21.64 ± 0.26	5.17 ± 3.06	53.40	0.57	17
105	24	22.60 ± 0.43	0.43 ± 0.15	55.08	0.50	3
106	53	22.59 ± 0.41	1.56 ± 0.66	54.10	1.41	11
107	33	21.99 ± 0.06	4.04 ± 5.07	53.40	0.72	9
114	43	21.42 ± 0.14	9.99	53.40	0.82	9
121	24	21.95 ± 0.09	5.77 ± 9.05	52.40	0.30	3
122	66	22.30 ± 0.46	3.86 ± 2.46	53.70	0.99	13
123	41	21.78 ± 0.16	9.56	53.40	0.51	7
124	63	22.04 ± 0.32	1.20 ± 0.43	53.70	1.22	15
125	121	22.13 ± 0.54	4.02 ± 2.05	53.88	1.10	15
128	63	22.36 ± 0.46	1.84 ± 0.78	53.88	0.87	15
131	31	21.76 ± 0.01	2.61 ± 2.03	53.40	0.73	6
132	87	22.21 ± 0.52	2.64 ± 1.06	53.70	1.35	18
133	72	22.09 ± 0.79	0.62 ± 0.17	54.35	1.10	15
137	24	22.00 ± 0.07	2.03 ± 1.51	53.40	0.64	3
140	42	22.07 ± 0.29	6.10 ± 6.99	53.40	0.67	8
141	55	21.97 ± 0.32	3.08 ± 1.76	53.40	1.07	11
142	186	22.15 ± 0.72	2.44 ± 0.61	54.18	1.26	22
143	28	22.25 ± 0.32	1.89 ± 0.94	53.40	0.38	4
146	27	22.08 ± 0.08	9.99	53.40	0.34	4
147	22	22.03 ± 0.13	6.30	52.40	2.00	3
148	29	22.12 ± 0.23	1.76 ± 0.99	53.40	0.59	5
149	33	21.68 ± 0.02	8.04	53.40	0.27	7
152	53	22.23 ± 0.34	2.08 ± 1.11	53.70	0.92	10
156	22	22.36 ± 0.21	1.88 ± 1.27	53.40	0.41	2
158	21	22.55 ± 0.31	1.17 ± 0.57	54.00	0.21	2
159	21	22.15 ± 0.07	1.67 ± 1.33	53.40	0.42	3
160	22	22.26 ± 0.22	2.19 ± 1.54	53.40	0.29	3
161	33	22.51 ± 0.21	9.99	53.40	0.92	5
164	85	22.08 ± 0.51	1.74 ± 0.53	53.88	0.82	19
165	106	22.20 ± 0.56	1.91 ± 0.57	54.00	1.53	11
166	35	22.52 ± 0.49	0.93 ± 0.33	54.25	1.03	6
169	41	22.53 ± 0.15	9.99	53.40	0.89	11
170	39	22.17 ± 0.30	2.47 ± 1.48	53.40	1.22	6
172	219	22.22 ± 0.75	3.81 ± 1.27	54.30	1.21	18
177	51	22.51 ± 0.33	9.99	53.70	1.12	10
178	103	22.26 ± 0.64	2.31 ± 0.70	54.00	0.77	12
179	44	22.29 ± 0.34	2.16 ± 1.09	53.70	1.00	8
180	25	21.48 ± 0.10	7.19	52.40	0.25	4
182	42	22.10 ± 0.20	2.17 ± 1.43	53.70	0.71	10
183	28	22.36 ± 0.33	1.21 ± 0.53	54.25	0.29	4
184	65	21.95 ± 0.22	9.99	53.40	0.74	17
187	49	22.10 ± 0.31	3.69 ± 2.62	53.40	0.87	9
188	27	22.65 ± 0.47	0.78 ± 0.31	54.51	0.32	4
189	24	21.74 ± 0.05	8.31	52.40	0.73	3
190	64	22.16 ± 0.43	3.56 ± 2.05	53.40	0.83	13
193	58	22.27 ± 0.51	2.41 ± 1.02	53.70	0.60	11
194	23	22.50 ± 0.30	1.16 ± 0.62	53.88	1.40	3
195	59	22.29 ± 0.40	6.84 ± 8.06	53.40	0.87	12
199	21	22.18 ± 0.14	2.31 ± 2.02	53.40	1.08	2
200	27	21.98 ± 0.09	3.43 ± 3.04	53.40	0.62	4

Table 3. continued.

N_x #	NetCnts (ph.)	log(N_H) (cm^{-2})	kT (keV)	log(EM) (cm^{-3})	Stat. (χ^2_ν)	d.o.f.
202	24	22.14 ± 0.15	2.31 ± 2.19	53.40	0.51	5
206	71	22.31 ± 0.54	2.21 ± 0.77	53.88	0.90	14
209	23	22.22 ± 0.08	1.52 ± 1.12	53.40	1.65	3
218	52	22.30 ± 0.46	2.38 ± 1.03	53.70	1.57	10
219	83	22.32 ± 0.60	2.59 ± 0.88	53.88	0.83	16
220	42	22.23 ± 0.39	2.31 ± 1.13	53.40	1.18	7
224	26	22.24 ± 0.25	1.41 ± 0.69	53.40	0.84	3
225	25	22.11 ± 0.10	9.99	53.40	1.82	4
226	70	22.21 ± 0.10	2.85 ± 3.07	53.70	0.76	14
227	39	22.13 ± 0.19	8.28	53.40	0.50	9
229	21	21.99 ± 0.04	7.56	52.40	0.20	2
231	24	22.44 ± 0.33	1.05 ± 0.64	53.88	1.18	4
233	67	22.51 ± 0.41	9.99	53.70	0.62	13
238	67	22.05 ± 0.39	6.85 ± 7.25	53.40	0.55	13
239	74	22.32 ± 0.53	2.64 ± 1.12	53.88	0.74	15
242	93	22.29 ± 0.61	2.28 ± 0.77	53.88	1.31	19
243	54	22.09 ± 0.34	6.84 ± 7.70	53.40	0.88	10
244	68	22.23 ± 0.69	0.11 ± 0.63	57.70	1.12	12
245	21	22.43 ± 0.33	0.59 ± 0.30	54.30	0.24	2
246	32	21.69 ± 0.02	9.99	53.40	0.36	5
247	22	21.99 ± 0.10	4.46 ± 6.06	52.40	2.00	3
248	42	21.60 ± 0.07	9.99	53.40	1.31	9
251	22	22.17 ± 0.02	9.99	52.40	1.17	3
253	37	22.59 ± 0.50	0.43 ± 0.13	55.12	1.00	6
254	83	22.38 ± 0.65	1.43 ± 0.30	54.18	0.92	17
256	53	22.46 ± 0.59	1.09 ± 0.27	54.25	0.63	10
259	21	22.09 ± 0.09	2.00 ± 1.58	53.40	0.63	2
260	289	22.39 ± 0.86	4.76 ± 1.60	54.40	0.66	25
270	71	22.11 ± 0.41	2.61 ± 1.25	53.70	0.64	16
271	186	22.22 ± 0.70	4.66 ± 2.06	54.00	1.23	22
272	39	22.25 ± 0.31	1.97 ± 1.12	53.40	0.90	8
273	23	22.33 ± 0.27	1.94 ± 1.24	53.40	0.50	3
277	21	22.43 ± 0.18	1.56 ± 1.01	53.70	0.47	2
279	24	22.11 ± 0.09	2.71 ± 2.90	53.40	0.99	4
280	106	22.29 ± 0.58	2.66 ± 1.04	54.00	1.33	12
283	346	22.30 ± 0.86	3.85 ± 1.02	54.40	1.11	30
284	25	22.09 ± 0.12	4.02 ± 4.57	53.40	0.65	4
290	21	22.55 ± 0.19	1.25 ± 0.84	53.88	0.20	3
294	40	22.26 ± 0.27	1.47 ± 0.80	53.70	1.00	10
297	25	22.49 ± 0.45	0.76 ± 0.31	54.18	1.25	3
299	65	22.24 ± 0.55	1.92 ± 0.59	53.70	0.78	14
300	270	21.81 ± 0.70	2.27 ± 0.44	54.10	1.98	21
301	27	22.19 ± 0.04	9.99	53.40	1.84	4
302	22	22.36 ± 0.19	1.24 ± 0.79	53.70	0.20	2
303	21	22.43 ± 0.15	5.10 ± 8.15	53.40	0.57	2
305	33	22.34 ± 0.26	1.46 ± 0.93	53.70	0.90	8
306	22	22.53 ± 0.43	0.88 ± 0.32	54.10	0.97	3
307	22	22.19 ± 0.15	1.25 ± 0.77	53.40	1.02	3
308	37	22.19 ± 0.33	1.97 ± 1.02	53.40	0.37	6
309	36	22.31 ± 0.38	1.37 ± 0.54	53.70	0.70	5
313	41	21.97 ± 0.06	9.99	53.40	1.18	9
315	107	22.34 ± 0.86	0.70 ± 1.00	54.63	0.80	11
316	27	22.38 ± 0.32	1.36 ± 0.65	53.70	0.51	4
317	20	21.50 ± 0.27	9.99	52.40	1.84	2
319	20	23.18 ± 0.32	0.87 ± 0.30	55.16	1.82	2
320	27	21.99 ± 0.05	9.99	52.40	0.79	4
324	47	22.33 ± 0.44	1.99 ± 0.90	53.70	0.86	8
326	47	22.23 ± 0.33	1.39 ± 0.63	53.70	1.10	11
327	97	22.19 ± 0.49	3.19 ± 1.34	54.00	1.09	22
329	23	22.13 ± 0.04	8.20	52.40	0.88	5
330	67	22.21 ± 0.46	4.10 ± 2.53	53.70	0.80	13
335	141	22.20 ± 0.60	4.18 ± 2.06	53.88	1.37	17
336	74	22.41 ± 0.54	3.87 ± 2.41	53.70	1.11	15
341	31	22.49 ± 0.37	1.49 ± 0.66	53.88	1.15	4
345	22	22.08 ± 0.10	9.32	52.40	0.23	3

Table 3. continued.

N_x #	NetCnts (ph.)	$\log(N_H)$ (cm^{-2})	kT (keV)	log(EM) (cm^{-3})	Stat. (χ^2_ν)	d.o.f.
351	36	22.58 ± 0.53	0.82 ± 0.32	54.72	0.66	5
352	68	22.23 ± 0.48	3.12 ± 1.42	53.70	0.73	13
354	31	21.84 ± 0.10	3.33 ± 2.74	52.40	1.20	4
355	30	22.21 ± 0.24	2.17 ± 1.37	53.40	0.78	6
356	33	22.54 ± 0.40	1.38 ± 0.47	53.88	0.99	5
358	24	22.38 ± 0.23	1.30 ± 0.77	53.70	0.49	3
359	62	22.43 ± 0.57	2.76 ± 1.16	53.88	0.67	12
361	59	22.40 ± 0.51	1.29 ± 0.43	54.10	0.48	11
366	123	22.20 ± 0.68	2.77 ± 0.89	54.00	0.55	14
372	66	22.32 ± 0.47	1.71 ± 0.64	53.88	1.08	13
375	21	21.25 ± 0.41	9.99	52.40	0.20	3
378	105	22.43 ± 0.70	1.89 ± 0.46	54.25	0.58	11
379	69	22.44 ± 0.33	9.99	53.70	1.63	15
381	89	22.49 ± 0.65	1.48 ± 0.39	54.30	1.07	17
383	27	22.09 ± 0.15	4.98 ± 6.55	53.40	1.18	3
384	36	22.59 ± 0.42	1.99 ± 0.99	53.88	0.69	6
387	31	22.48 ± 0.53	0.57 ± 0.15	54.66	0.39	5
388	38	21.79 ± 0.06	9.99	52.40	1.90	6
389	59	22.37 ± 0.51	1.85 ± 0.59	53.88	0.85	11
390	26	22.28 ± 0.13	8.63	53.40	1.41	3
392	45	22.50 ± 0.47	1.73 ± 0.64	53.88	1.08	8
393	65	22.20 ± 0.53	1.41 ± 0.40	53.88	1.29	12
396	43	22.11 ± 0.26	9.99	53.40	1.20	7
398	60	22.40 ± 0.46	1.71 ± 0.63	54.00	0.41	11
399	21	22.20 ± 0.02	9.99	53.40	0.54	2
400	32	21.96 ± 0.11	9.99	52.40	1.50	5
402	182	22.28 ± 0.69	7.44 ± 5.20	54.10	0.52	21
404	216	22.37 ± 0.76	4.89 ± 2.05	54.25	1.03	18
406	110	22.27 ± 0.62	1.94 ± 0.56	54.10	1.06	13
407	103	22.44 ± 0.65	1.57 ± 0.39	54.25	1.22	11
408	46	22.63 ± 0.49	1.18 ± 0.38	54.40	0.95	9
410	65	22.17 ± 0.30	9.99	53.40	1.50	13
413	25	22.49 ± 0.22	1.09 ± 0.60	53.88	1.39	3
414	139	22.35 ± 0.73	2.38 ± 0.61	54.18	1.04	16
415	25	22.29 ± 0.22	4.99 ± 6.40	53.40	0.62	3
419	36	22.28 ± 0.38	2.25 ± 1.26	53.70	0.54	7
420	37	22.28 ± 0.35	3.75 ± 2.96	53.40	1.02	6
422	76	22.41 ± 0.61	1.00 ± 0.30	54.51	0.99	18
423	26	22.57 ± 0.37	1.83 ± 0.93	53.70	0.41	3
424	70	22.16 ± 0.51	2.89 ± 1.24	53.70	0.78	14
429	21	22.52 ± 0.24	1.54 ± 0.95	53.70	1.00	2
430	20	22.31 ± 0.15	3.10 ± 3.56	53.40	1.44	2
432	113	22.44 ± 0.67	2.48 ± 0.78	54.10	1.23	12
433	1240	22.34 ± 1.28	1.05 ± 0.76	55.08	1.40	15
434	47	22.41 ± 0.07	2.32 ± 1.04	53.70	0.97	8
435	23	22.30 ± 0.24	2.05 ± 1.35	53.40	0.20	3
436	366	22.31 ± 1.13	0.60 ± 0.53	55.29	2.00	27
438	28	22.48 ± 0.28	1.62 ± 1.05	53.70	0.74	4
439	148	22.35 ± 0.66	2.59 ± 0.84	54.18	1.36	17
440	21	22.24 ± 0.15	5.19 ± 7.13	53.40	0.20	2
443	26	22.35 ± 0.25	1.60 ± 0.94	53.70	0.65	3
445	83	22.36 ± 0.61	3.00 ± 1.21	53.88	0.83	17
446	54	22.32 ± 0.46	2.04 ± 0.83	53.88	0.61	10
447	51	22.23 ± 0.45	3.55 ± 2.20	53.40	1.09	9
448	24	22.52 ± 0.41	0.97 ± 0.43	54.00	0.53	3
449	42	22.19 ± 0.38	2.40 ± 1.16	53.40	0.96	6
454	37	22.42 ± 0.39	1.74 ± 0.81	53.70	0.66	7
455	47	22.25 ± 0.45	2.56 ± 1.13	53.70	0.51	8
456	106	22.32 ± 0.81	0.85 ± 0.21	54.44	1.40	11
458	34	22.15 ± 0.22	1.45 ± 0.80	53.70	0.85	6
459	40	22.11 ± 0.17	8.62	53.40	1.08	8
460	21	21.81 ± 0.13	9.99	52.40	1.75	2
461	54	22.41 ± 0.57	1.73 ± 0.56	54.10	0.82	10
464	30	22.51 ± 0.31	1.66 ± 0.96	53.88	0.36	5
466	24	22.53 ± 0.16	1.72 ± 1.34	53.70	1.45	3

Table 3. continued.

N_x #	NetCnts (ph.)	$\log(N_H)$ (cm^{-2})	kT (keV)	log(EM) (cm^{-3})	Stat. (χ^2_ν)	d.o.f.
467	41	22.28 ± 0.22	9.99	53.40	0.40	8
471	147	22.19 ± 0.63	3.91 ± 1.56	53.88	1.74	17
472	24	23.00 ± 0.04	6.83	53.70	0.21	3
475	61	22.33 ± 0.48	1.53 ± 0.50	53.88	0.84	12
476	41	22.63 ± 0.63	0.89 ± 0.19	54.51	0.82	7
478	32	22.29 ± 0.30	3.31 ± 2.57	53.40	0.87	5
479	57	22.75 ± 0.51	1.30 ± 0.49	54.51	1.25	11
480	158	22.36 ± 0.48	1.62 ± 0.79	53.88	0.96	682
481	176	22.33 ± 0.70	3.37 ± 1.09	54.18	1.09	21
482	21	22.46 ± 0.33	1.05 ± 0.66	54.00	0.20	2
483	48	22.43 ± 0.40	2.50 ± 1.49	53.70	0.90	10
484	46	22.34 ± 0.43	1.37 ± 0.51	53.88	1.08	8
485	25	22.36 ± 0.19	6.57	53.40	0.96	3
488	9736	22.30 ± 0.66	2.39 ± 0.77	55.96	1.30	121
490	37	22.65 ± 0.51	0.92 ± 0.25	54.80	0.56	6
492	30	22.16 ± 0.29	1.82 ± 1.00	53.70	1.32	4
495	81	22.19 ± 0.80	0.44 ± 0.74	54.66	1.12	13
497	143	22.31 ± 0.61	6.84 ± 5.75	53.88	1.44	17
499	29	22.62 ± 0.46	1.01 ± 0.47	54.25	0.77	4
500	34	22.54 ± 0.49	1.78 ± 0.67	54.35	0.27	5
501	32	22.42 ± 0.35	2.81 ± 2.13	53.70	1.71	5
502	51	22.49 ± 0.49	1.61 ± 0.59	54.35	0.34	9
503	58	22.24 ± 0.42	2.00 ± 0.96	53.70	0.79	13
506	22	22.46 ± 0.32	0.91 ± 0.46	53.88	1.40	2
507	105	22.31 ± 0.60	3.78 ± 1.79	53.88	1.12	11
508	23	21.98 ± 0.15	2.78 ± 2.60	53.40	0.76	3
509	26	22.63 ± 0.24	0.90 ± 0.45	54.25	1.70	3
510	85	22.44 ± 0.58	1.47 ± 0.42	54.18	1.02	18
511	40	21.94 ± 0.09	8.62	52.40	2.00	7
513	26	22.58 ± 0.09	9.99	53.40	0.31	4
515	30	22.68 ± 0.48	0.91 ± 0.29	54.40	1.23	4
519	20	22.10 ± 0.05	1.49 ± 1.16	53.40	0.54	3
520	78	22.44 ± 0.57	1.29 ± 0.37	54.18	1.07	16
523	50	22.37 ± 0.48	2.36 ± 1.07	53.70	0.79	9
525	33	22.37 ± 0.32	1.64 ± 0.88	53.88	0.73	5
526	22	22.62 ± 0.39	0.93 ± 0.40	54.18	1.10	2
527	24	22.07 ± 0.12	4.29 ± 4.89	53.40	0.71	3
529	25	22.20 ± 0.22	2.17 ± 1.54	53.40	1.06	3
530	137	22.27 ± 0.96	0.70 ± 0.77	54.60	1.10	14
534	23	22.50 ± 0.31	0.85 ± 0.60	54.10	0.90	3
535	29	22.57 ± 0.41	0.93 ± 0.34	54.25	0.33	5
536	28	22.35 ± 0.36	1.17 ± 0.46	53.70	0.25	4
537	111	22.28 ± 0.87	0.75 ± 0.12	54.51	1.10	11
539	50	22.61 ± 0.46	2.54 ± 1.50	53.88	1.47	9
544	1834	22.48 ± 1.46	0.59 ± 0.21	56.30	1.30	24
547	42	22.63 ± 0.50	1.15 ± 0.38	54.35	0.58	9
549	26	22.23 ± 0.24	3.66 ± 3.63	53.40	0.79	3
552	58	22.43 ± 0.56	0.60 ± 0.18	54.60	1.36	11
554	21	22.59 ± 0.33	0.58 ± 0.24	54.66	0.20	3
555	343	22.34 ± 0.87	2.60 ± 0.56	54.51	2.00	29
556	60	22.10 ± 0.31	2.63 ± 1.48	53.70	0.47	14
557	130	22.14 ± 0.61	2.76 ± 0.90	54.00	1.41	15
559	108	22.26 ± 0.57	1.07 ± 0.33	54.00	1.14	12
561	27	22.25 ± 0.19	2.52 ± 2.03	53.40	0.99	4
562	290	22.34 ± 1.10	0.55 ± 0.38	55.37	1.00	22
564	25	22.30 ± 0.24	1.44 ± 0.79	53.40	0.98	5
567	22	22.39 ± 0.19	1.68 ± 1.21	53.88	0.39	2
568	13138	22.31 ± 0.72	1.92 ± 0.45	56.29	1.40	152
569	26	22.31 ± 0.90	8.81	53.40	0.85	3
570	36	22.76 ± 0.47	0.46 ± 0.12	55.54	0.58	7
571	34	22.29 ± 0.36	1.98 ± 0.94	53.70	0.42	5
572	24	22.39 ± 0.26	2.03 ± 1.30	53.40	0.20	3
575	20	22.01 ± 0.01	5.68	52.40	2.00	2
577	20	22.17 ± 0.13	2.75 ± 2.60	53.40	0.79	2
579	94	22.22 ± 0.52	2.63 ± 0.93	53.88	0.74	20

Table 3. continued.

N_x #	NetCnts (ph.)	$\log(N_H)$ (cm^{-2})	kT (keV)	log(EM) (cm^{-3})	Stat. (χ^2_ν)	d.o.f.
581	50	22.23 ± 0.64	0.22 ± 0.47	55.54	0.69	10
582	75	22.30 ± 0.47	1.60 ± 0.60	54.00	1.36	16
584	53	22.43 ± 0.59	0.39 ± 0.15	55.13	0.80	11
585	31	21.40 ± 0.24	9.99	52.40	0.89	7
586	40	22.37 ± 0.37	1.48 ± 0.72	53.70	1.08	7
588	26	22.54 ± 0.47	0.70 ± 0.20	54.40	0.73	5
590	58	22.35 ± 0.39	2.37 ± 1.30	53.70	1.34	12
593	65	22.16 ± 0.48	3.55 ± 2.16	53.40	0.74	13
594	74	22.29 ± 0.52	1.88 ± 0.67	53.88	1.26	16
595	60	22.70 ± 0.58	0.59 ± 0.15	55.23	0.78	13
596	327	22.17 ± 0.37	2.54 ± 3.91	54.44	1.76	28
597	66	22.36 ± 0.65	0.51 ± 0.18	54.92	1.00	13
599	50	22.30 ± 0.37	4.96 ± 4.58	53.40	1.01	10
600	428	22.19 ± 0.96	1.23 ± 0.13	54.83	0.90	35
601	48	21.32 ± 0.18	9.99	53.40	1.33	11
603	53	22.37 ± 0.54	1.47 ± 0.40	54.00	0.64	9
606	55	22.30 ± 0.29	1.10 ± 0.70	54.35	0.90	11
608	36	22.48 ± 0.37	1.34 ± 0.66	54.00	0.33	6
610	22	22.42 ± 0.17	1.67 ± 1.28	53.40	0.82	2
612	118	22.47 ± 0.78	1.38 ± 0.24	54.48	1.03	12
615	135	22.43 ± 0.86	0.55 ± 0.62	55.11	1.00	14
616	55	22.25 ± 0.36	5.43 ± 4.86	53.40	0.59	12
618	41	22.38 ± 0.09	2.91	54.00	0.94	8
619	24	21.99 ± 0.00	4.11 ± 6.28	52.40	1.21	4
620	68	22.14 ± 0.51	3.52 ± 1.79	53.70	0.52	13
622	139	22.22 ± 0.69	2.88 ± 0.87	54.00	0.98	15
623	33	22.17 ± 0.29	2.50 ± 1.62	53.70	0.63	6
624	25	22.31 ± 0.18	1.45 ± 0.90	53.40	1.64	4
625	430	22.11 ± 1.03	0.48 ± 0.52	55.37	1.00	32
626	120	22.05 ± 0.44	1.37 ± 0.36	54.00	1.00	14
627	120	22.05 ± 0.45	1.37 ± 0.37	54.00	1.50	14
629	44	22.30 ± 0.46	1.39 ± 0.46	53.70	1.10	8
632	25	22.30 ± 0.25	2.04 ± 1.33	53.40	0.43	4
633	144	22.37 ± 0.63	1.69 ± 0.47	54.30	1.51	16
634	36	22.11 ± 0.14	9.99	53.40	1.12	7
635	33	21.76 ± 0.01	9.99	52.40	1.22	5
637	31	22.28 ± 0.25	3.22 ± 2.86	53.40	0.76	5
643	93	22.53 ± 0.66	1.97 ± 0.60	54.18	0.70	19
646	27	22.35 ± 0.36	1.45 ± 0.62	53.88	0.38	4
649	41	21.68 ± 0.00	9.29	52.40	1.25	9
650	119	22.02 ± 0.77	0.86 ± 0.15	54.10	0.92	13
652	212	22.44 ± 0.79	3.25 ± 0.97	54.35	2.00	17
656	27	22.39 ± 0.37	1.15 ± 0.79	53.70	1.13	4
659	67	22.29 ± 0.46	1.37 ± 0.45	54.00	1.28	14
660	21	22.15 ± 0.05	9.99	53.40	1.92	3
661	31	22.53 ± 0.44	0.89 ± 0.28	54.25	0.98	5
664	33	21.88 ± 0.01	9.99	53.40	1.41	6
666	34	22.23 ± 0.24	1.86 ± 1.12	53.70	0.55	7
667	35	22.30 ± 0.34	2.01 ± 1.13	53.70	0.56	7
668	34	21.87 ± 0.13	3.23 ± 2.37	53.40	0.58	6
670	82	22.49 ± 0.61	1.52 ± 0.42	54.30	0.77	17
671	46	22.28 ± 0.46	1.93 ± 0.79	53.70	0.69	8
672	86	22.36 ± 0.64	2.32 ± 0.72	54.00	0.58	18
675	64	23.15 ± 0.21	9.99	54.00	1.20	14
676	186	22.12 ± 0.95	0.79 ± 0.12	54.51	0.81	21
683	30	22.38 ± 0.36	2.35 ± 1.45	53.40	0.67	4
685	35	22.06 ± 0.27	4.61 ± 4.76	53.40	0.54	6
686	36	22.39 ± 0.49	0.35 ± 0.97	55.02	1.10	5
687	91	22.26 ± 0.52	4.95 ± 3.37	53.70	0.89	17
688	39	21.94 ± 0.12	4.29 ± 4.71	53.40	0.74	9
690	21	22.56 ± 0.00	1.71 ± 1.87	53.70	1.87	3
693	23	22.13 ± 0.08	9.99	52.40	2.00	3
694	46	22.29 ± 0.45	1.95 ± 0.85	53.88	0.39	9
695	32	22.18 ± 0.33	2.30 ± 1.27	53.40	0.49	5
700	57	22.57 ± 0.61	1.13 ± 0.26	54.40	0.71	11

Table 3. continued.

N_x #	NetCnts (ph.)	log(N_H) (cm^{-2})	kT (keV)	log(EM) (cm^{-3})	Stat. (χ^2_ν)	d.o.f.
701	65	22.05 ± 0.34	8.22	53.40	1.12	13
702	42	22.32 ± 0.36	1.72 ± 0.78	53.70	0.55	9
703	20	21.95 ± 0.14	6.85	52.40	1.54	2
705	49	22.56 ± 0.59	1.40 ± 0.34	54.18	0.62	9
708	97	22.19 ± 0.58	2.27 ± 0.71	53.88	0.63	20
709	28	22.76 ± 0.31	1.14 ± 0.48	54.30	1.43	5
710	81	22.42 ± 0.61	1.98 ± 0.65	54.00	0.92	17
711	28	22.18 ± 0.22	1.37 ± 0.67	53.40	0.45	4
712	209	22.34 ± 0.79	2.31 ± 0.54	54.35	2.00	16
718	37	22.43 ± 0.38	1.64 ± 0.76	53.88	0.34	6
721	389	22.01 ± 0.17	0.61 ± 0.49	54.78	2.00	28
722	161	21.04 ± 0.56	1.00 ± 0.13	54.51	0.68	26
724	165	22.23 ± 0.74	2.74 ± 0.77	54.10	0.68	20
725	32	21.95 ± 0.12	9.99	53.40	0.46	5
727	22	22.11 ± 0.04	9.99	53.40	0.37	2
728	28	22.17 ± 0.46	0.20 ± 0.12	55.44	0.20	4
729	3731	22.15 ± 0.40	1.89 ± 0.80	55.55	1.10	49
731	25	22.51 ± 0.49	0.73 ± 0.23	54.51	2.00	3
732	33	22.28 ± 0.27	2.31 ± 1.45	53.40	1.13	5
733	61	22.37 ± 0.40	1.63 ± 0.72	53.88	1.37	12
734	57	22.35 ± 0.59	1.37 ± 0.33	54.00	0.77	11
736	59	22.24 ± 0.43	2.52 ± 1.22	53.70	0.63	13
738	21	22.74 ± 0.22	0.62 ± 0.47	55.01	2.00	2
739	37	22.46 ± 0.50	0.93 ± 0.33	54.18	0.71	6
740	28	22.18 ± 0.08	7.17	53.40	1.35	5
743	417	22.26 ± 0.89	5.75 ± 2.26	54.48	1.18	36
744	35	22.27 ± 0.30	1.57 ± 0.80	53.70	0.73	7
745	29	22.21 ± 0.25	2.12 ± 1.27	53.70	0.78	4
746	92	22.22 ± 0.55	4.28 ± 2.27	54.00	0.72	19
750	102	22.20 ± 0.55	4.78 ± 3.11	53.70	1.43	11
751	50	21.93 ± 0.21	5.94 ± 7.90	53.40	1.25	10
753	1416	22.20 ± 1.08	9.99	54.91	2.00	20
754	35	22.19 ± 0.24	9.83	53.40	0.31	6
759	24	22.47 ± 0.28	1.46 ± 0.76	53.70	0.71	4
760	29	22.44 ± 0.40	1.03 ± 0.52	54.00	0.82	4
761	32	21.94 ± 0.16	2.57 ± 1.75	53.40	0.75	6
762	36	22.40 ± 0.42	2.95 ± 1.87	53.40	0.61	6
763	117	22.46 ± 0.69	2.03 ± 0.54	54.25	1.10	13
764	51	22.38 ± 0.51	1.17 ± 0.32	54.00	0.99	9
769	30	22.25 ± 0.28	1.86 ± 0.98	53.40	0.59	4
770	64	22.31 ± 0.51	2.58 ± 1.07	53.70	0.84	12
771	22	22.61 ± 0.01	9.99	53.40	1.15	4
772	24	22.32 ± 0.17	3.36 ± 3.66	53.40	1.95	3
773	38	22.27 ± 0.37	1.37 ± 0.54	53.70	0.77	6
774	23	22.65 ± 0.87	3.83 ± 5.41	52.40	1.28	5
775	29	22.22 ± 0.22	4.66 ± 6.36	53.40	1.07	5
777	121	22.39 ± 0.74	1.39 ± 0.26	54.35	1.48	13
779	331	22.03 ± 0.79	2.44 ± 0.48	54.30	1.20	25
781	28	22.43 ± 0.39	1.16 ± 0.44	53.88	0.35	4
784	44	22.47 ± 0.52	1.16 ± 0.32	54.18	0.36	8
785	26	22.56 ± 0.37	1.17 ± 0.51	54.00	1.20	3
786	153	22.31 ± 0.74	1.89 ± 0.44	54.25	1.20	18
787	22	22.22 ± 0.12	4.98 ± 7.58	53.40	0.86	2
791	28	22.02 ± 0.09	1.93 ± 1.57	53.40	0.91	5
794	46	22.07 ± 0.19	1.96 ± 1.11	53.40	1.64	9
795	23	21.83 ± 0.05	9.99	52.40	0.85	3
796	370	22.29 ± 0.88	4.22 ± 1.09	54.44	2.00	31
797	38	22.15 ± 0.28	3.29 ± 2.61	53.40	1.30	7
798	139	22.12 ± 0.53	5.24 ± 3.04	53.88	1.36	17
801	31	22.48 ± 0.42	1.03 ± 0.48	54.00	1.23	4
803	27	22.20 ± 0.23	1.95 ± 1.21	53.40	0.34	4
806	21	21.88 ± 0.13	9.99	52.40	1.14	3
808	31	22.30 ± 0.34	1.89 ± 1.02	53.70	0.48	5
809	52	22.30 ± 0.44	1.66 ± 0.65	53.88	0.82	9
811	33	22.50 ± 0.56	0.86 ± 0.27	54.25	0.26	5

Table 3. continued.

N_x #	NetCnts (ph.)	$\log(N_H)$ (cm^{-2})	kT (keV)	log(EM) (cm^{-3})	Stat. (χ^2_ν)	d.o.f.
813	63	22.00 ± 0.36	3.07 ± 1.71	53.40	1.02	13
818	168	22.19 ± 0.68	4.91 ± 2.10	54.00	1.00	20
821	30	21.73 ± 0.01	9.99	53.40	0.52	5
822	21	22.37 ± 0.22	1.11 ± 0.54	53.70	1.46	2
824	34	22.66 ± 0.44	0.31 ± 0.15	55.75	2.00	5
828	228	22.35 ± 0.81	1.57 ± 0.27	54.58	1.90	18
830	26	22.37 ± 0.31	2.01 ± 1.23	53.40	0.68	4
831	72	22.55 ± 0.63	1.12 ± 0.23	54.55	0.52	15
833	36	23.22 ± 0.06	9.99	53.88	0.79	10
834	173	22.22 ± 0.64	7.78 ± 6.21	54.00	1.68	21
837	33	22.35 ± 0.33	2.73 ± 2.01	53.40	1.33	5
838	23	21.99 ± 0.09	4.01 ± 4.46	52.40	0.63	3
840	59	21.38 ± 0.04	9.99	53.40	0.41	16
842	53	22.26 ± 0.42	2.11 ± 0.93	53.70	0.51	11
847	34	22.31 ± 0.28	2.01 ± 1.15	53.70	0.41	7
848	25	22.09 ± 0.16	1.77 ± 1.12	53.40	0.66	3
849	59	22.21 ± 0.39	2.48 ± 1.26	53.70	1.00	11
851	24	22.83 ± 0.08	9.99	53.70	1.43	3
854	34	22.27 ± 0.26	2.16 ± 1.42	53.70	0.64	7
856	37	22.14 ± 0.33	2.87 ± 1.84	53.40	0.45	7
857	113	22.33 ± 0.65	2.03 ± 0.55	54.18	0.99	13
858	27	22.27 ± 0.43	0.92 ± 0.36	53.88	0.43	4
860	27	21.43 ± 0.24	9.99	52.40	0.30	6
863	268	22.25 ± 0.87	2.81 ± 0.57	54.40	0.83	22
864	56	22.64 ± 0.29	9.99	53.70	0.56	12
865	25	22.00 ± 0.03	9.99	53.40	1.25	3
866	34	21.77 ± 0.05	9.39	52.40	1.10	8
867	29	21.91 ± 0.09	9.99	53.40	0.20	4
868	23	21.64 ± 0.08	9.23	52.40	0.78	3
870	42	22.93 ± 1.21	9.99	52.40	1.19	9
872	192	22.07 ± 0.60	9.99	54.00	0.61	24
874	42	22.23 ± 0.22	1.70 ± 1.03	53.70	0.22	9
875	20	21.81 ± 0.06	3.95 ± 5.10	52.40	0.41	3
876	56	21.88 ± 0.27	4.13 ± 3.08	53.40	0.91	12
877	34	22.34 ± 0.30	3.49 ± 2.87	53.40	0.71	5
878	45	22.16 ± 0.32	6.84 ± 8.91	53.40	0.65	8
879	62	22.43 ± 0.32	9.99	53.70	0.85	14
881	52	22.29 ± 0.65	0.55 ± 0.13	54.44	0.90	10
883	33	22.56 ± 0.14	9.99	53.70	0.90	6
884	57	22.30 ± 0.31	9.99	53.70	0.67	12
885	21	21.08 ± 0.68	9.99	52.40	2.00	3
886	49	22.46 ± 0.54	1.12 ± 0.28	54.18	0.47	9
890	20	21.93 ± 0.07	6.11	52.40	0.89	2
891	32	22.11 ± 0.19	6.69 ± 8.97	53.40	0.40	6
893	75	22.11 ± 0.49	3.43 ± 1.73	53.70	0.47	15
894	26	22.29 ± 0.17	1.24 ± 0.87	53.70	1.30	4
895	81	22.16 ± 0.77	0.75 ± 0.16	54.30	1.00	15
896	102	22.11 ± 0.53	2.99 ± 1.25	53.88	1.04	12
898	42	22.08 ± 0.26	2.89 ± 2.22	53.40	0.50	9
901	46	22.27 ± 0.11	9.99	53.40	0.97	10
902	31	22.25 ± 0.27	1.60 ± 0.88	53.70	1.00	5
903	126	22.19 ± 0.61	2.48 ± 0.76	54.00	1.45	14
905	26	22.65 ± 0.12	0.43 ± 0.56	55.11	0.61	1
906	28	22.10 ± 0.18	2.72 ± 2.18	53.40	1.27	4
911	71	22.16 ± 0.40	5.44 ± 5.05	53.40	0.82	14
912	20	22.21 ± 0.28	0.48 ± 0.36	54.10	0.98	4
913	82	22.15 ± 0.29	5.23 ± 4.74	53.70	1.32	17
914	160	21.99 ± 0.56	2.31 ± 0.63	54.10	1.01	19
916	82	22.50 ± 0.61	2.33 ± 0.80	54.10	0.75	18
917	82	22.50 ± 0.63	2.23 ± 0.70	54.10	0.75	18
918	41	22.78 ± 0.17	9.99	53.70	0.83	7
919	29	21.72 ± 0.20	0.69 ± 0.24	53.40	0.45	7
920	68	22.35 ± 0.51	1.26 ± 0.41	54.10	0.99	14
922	37	22.49 ± 0.51	1.09 ± 0.32	54.10	0.45	7
923	78	22.30 ± 0.56	1.56 ± 0.44	54.00	0.82	16

Table 3. continued.

N_x #	NetCnts (ph.)	log(N_H) (cm^{-2})	kT (keV)	log(EM) (cm^{-3})	Stat. (χ^2_ν)	d.o.f.
924	57	22.42 ± 0.31	9.99	53.70	0.82	11
925	44	22.11 ± 0.41	1.14 ± 0.38	53.70	0.79	8
927	332	22.90 ± 1.12	0.68 ± 0.39	54.00	0.91	24
928	124	22.33 ± 0.66	1.57 ± 0.34	54.30	0.87	14
929	23	22.02 ± 0.21	0.99 ± 1.49	53.40	1.54	3
931	37	21.88 ± 0.06	6.50 ± 9.80	53.40	1.15	7
932	38	21.73 ± 0.31	0.76 ± 0.19	53.40	1.05	7
934	53	22.27 ± 0.37	2.64 ± 1.54	53.70	0.72	11
935	22	22.53 ± 0.32	0.74 ± 0.36	54.25	1.05	3
937	21	22.20 ± 0.05	1.24 ± 1.12	53.40	0.97	4
938	34	21.79 ± 0.05	5.10 ± 6.05	53.40	0.52	7
940	168	22.27 ± 0.74	2.92 ± 0.85	54.25	0.39	21
941	38	21.69 ± 0.06	2.94 ± 3.65	53.40	1.05	11
942	49	22.25 ± 0.41	1.73 ± 0.64	53.70	0.74	10
943	40	22.07 ± 0.34	2.96 ± 1.73	53.40	0.39	7
944	31	21.72 ± 0.00	3.87 ± 4.67	53.40	0.41	7
945	125	22.18 ± 0.54	3.43 ± 1.47	54.00	1.00	15
947	80	22.28 ± 0.44	5.07 ± 4.09	53.70	1.28	18
948	21	21.74 ± 0.19	9.99	52.40	0.39	2
949	54	21.86 ± 0.29	3.18 ± 1.77	53.40	0.38	11
950	31	22.17 ± 0.36	1.08 ± 0.48	53.70	0.45	7
951	37	21.73 ± 0.05	0.84 ± 0.64	52.40	2.00	8
952	29	22.11 ± 0.12	9.70	53.40	1.07	5
953	21	22.11 ± 0.15	2.20 ± 1.77	53.40	1.09	3
956	38	21.90 ± 0.16	3.34 ± 2.58	53.40	0.50	8
957	71	21.87 ± 0.25	9.99	53.40	0.57	16
958	22	21.40 ± 0.20	5.61 ± 9.43	52.40	0.45	3
959	60	22.58 ± 0.34	9.99	53.88	0.34	12
960	33	22.75 ± 1.29	9.99	52.40	0.80	7
962	28	21.71 ± 0.01	9.99	52.40	0.62	5
964	55	21.85 ± 0.24	8.82	53.40	0.93	11
965	65	21.74 ± 0.20	3.43 ± 2.61	53.40	0.80	16
967	47	22.14 ± 0.27	2.01 ± 1.02	53.40	0.95	10
968	64	22.02 ± 0.35	4.78 ± 3.77	53.70	0.36	14
971	50	22.23 ± 0.31	1.28 ± 0.63	53.88	0.90	11
973	31	22.08 ± 0.20	2.83 ± 2.39	53.40	0.76	6
974	48	21.85 ± 0.11	9.99	53.40	1.30	10
975	44	22.63 ± 0.28	9.99	53.70	0.79	9
976	32	22.83 ± 1.29	0.69 ± 0.26	52.40	0.93	6
977	27	22.33 ± 0.38	1.10 ± 0.43	53.88	0.53	5
978	25	22.22 ± 0.23	1.42 ± 0.87	53.70	0.33	6
979	77	22.39 ± 0.53	2.16 ± 0.80	54.00	1.50	17
981	23	22.02 ± 0.04	9.99	52.40	0.40	4
982	27	22.52 ± 0.28	1.24 ± 0.67	54.00	0.71	5
983	46	21.62 ± 0.04	9.99	53.40	0.85	10
985	29	21.84 ± 0.04	9.99	53.40	0.66	6
986	28	21.83 ± 0.02	9.99	52.40	0.38	5
987	27	22.60 ± 0.26	0.34 ± 0.16	55.26	1.27	7
991	24	22.33 ± 0.40	0.73 ± 0.38	54.00	0.76	4
992	64	21.28 ± 0.12	0.57 ± 0.73	53.40	0.56	14
993	42	21.85 ± 0.12	2.84 ± 2.23	53.40	0.70	9
994	20	21.60 ± 0.28	9.99	52.40	0.62	5
996	34	21.21 ± 0.29	9.99	53.40	0.50	7
997	60	22.26 ± 0.57	1.14 ± 0.30	54.00	0.51	13
998	31	22.15 ± 0.68	9.99	52.40	0.82	8
999	96	22.66 ± 0.49	6.85 ± 8.53	54.00	0.78	23
1000	321	21.93 ± 0.69	4.20 ± 1.12	54.25	1.18	28
1001	67	22.08 ± 0.75	0.55 ± 0.11	54.30	0.80	15
1002	158	22.18 ± 0.86	0.72 ± 0.64	53.70	0.78	18
1003	68	21.72 ± 0.17	2.40 ± 1.23	53.40	0.70	17